UNIVERSITÀ DEGLI STUDI DI TRIESTE

XXX. CICLO DEL DOTTORATO DI RICERCA IN CHIMICA

NOVEL ANALYTICAL METHODS FOR IMPROVING THE QUALITY CONTROL OF COFFEE

Settore scientifico-disciplinare: **CHIM/06**

Ph.D STUDENT
ANA OREŠKI

Ph.D PROGRAM DIRECTOR
PROF. BARBARA MILANI

THESIS SUPERVISOR
PROF. FEDERICO BERTI

THESIS CO-SUPERVISOR
PROF. CRISTINA FORZATO

ANNO ACCADEMICO 2016/2017

UNIVERSITÀ DEGLI STUDI DI TRIESTE

XXX. CICLO DEL DOTTORATO DI RICERCA IN CHIMICA

Funded by the European Union's Horizon 2020 research and innovation programme under the
Marie Sklodowska-Curie grant agreement No. 642014

NOVEL ANALYTICAL METHODS FOR IMPROVING THE QUALITY CONTROL OF COFFEE

Settore scientifico-disciplinare: **CHIM/06**

Ph.D STUDENT
ANA OREŠKI

Ph.D PROGRAM DIRECTOR
PROF. BARBARA MILANI

THESIS SUPERVISOR
PROF. FEDERICO BERTI

THESIS CO-SUPERVISOR
PROF. CRISTINA FORZATO

ANNO ACCADEMICO 2016/2017

To whomever might stumble upon it.

Also, to mom, dad, Loki, Tina and Carlo.

Who now kinda have to read it.

“WHAT IS SUPPOSED TO HAPPEN?"

“How many coffees have you had?”

"FORTY-SEVEN."

“Just about anything, then,” said the barman.

~ Adapted from: Terry Pratchett, Mort

Table of Contents

University of Trieste

PhD School in Chemistry

Novel Analytical methods for Improving the Quality Control of Coffee

Ph.D. Thesis

Ph.D. Candidate: Ana Oreški

Supervisor: Prof. Federico Berti
Co-upervisor: Prof. Cristina Forzato

Abstract

The degree to which the consumption of coffee expanded over the centuries is rather surprising. Although the traditional preparation of coffee beverages differs around the world, the common factors of their popularity remain their intriguing sensory properties, together with psycho-psychical effects of caffeine. Due to wide spread use of coffee, monitoring of its quality is of vast importance and has to be done on all the steps of the coffee supply chain.

The main purpose of this thesis is to present our contribution to improvement of two aspects of quality control of coffee: monitoring of fraudulence and monitoring of the quantity of a potentially carcinogenic compound in coffee. Specifically, we focused on improvements in the topic of differentiation between two mostly known species on the market, *Coffea arabica* (Arabica) and *Coffea canephora* (Robusta), and on quantification of acrylamide, a 2A classified carcinogen, in coffee (IARC). Half of the research work was done in an industrial environment, in illycaffè's Aroma Lab and Demus Lab S.r.L, and the other half in an academical environment, in the Department of Chemical and Pharmaceutical sciences at the University of Trieste and School of Biological and Chemical Sciences at the Queen Mary University of London.

To reach differentiation between the beans of Arabica and Robusta, two non-related approaches were attempted: synthesis of molecularly imprinted polymers for selective recognition of 16-O-methylcafestol (16-OMC) with a possible application into a sensing system, and development of a colorimetric assay with an antimony(III) chloride reagent. For quantification of acrylamide in roasted coffee an HPLC-UV method was developed.

The search for ways of differentiation between Arabica and Robusta is gaining attention since Arabica, giving a beverage with a superior taste, is far more popular than Robusta. It occupies more than 75% of the global coffee market ans is about twice as expensive as Robusta, often leading to fraudulence. Green beans of both species by eye or under a microscope are distinguishable, but the methods are biased and deemed unpractical on the large scale of coffee production. Search for chemical markers of authenticity of Arabica is on the rise, as their analysis would give far more reliable results. Currently developed methods, however, often require tedious and time-consuming sample preparation techniques and analysis using expensive laboratory equipment.

One of such analytical methods is the DIN 10779 method for quantification of 16f-OMC in roasted coffee, a diterpene alcohol, found in 10 to 50 mg/kg in Robusta beans. The method consists of Soxhlet extraction and saponification of coffee oil, followed by HPLC-UV analysis. By creating a selective molecularly imprinted polymer for 16-OMC, we wanted to simplify its extraction from the coffee matrix, and possibly try to integrate the imprinted material into a sensing device in the future. Namely, imprinted polymers are essentially highly selective porous materials, cross-linked around the template molecule. Thus, molecular memory is introduced into the structure. Upon the removal of the template selective rebinding of the target molecule is possible.

As a significant amount of cafestol (50-100 mg/kg), a diterpene alcohol with one methoxy group of difference in the structure, is present in the beans of Arabica and Robusta as well, we decided upon synthesis of imprinted polymers for both diterpenes. Having the information on their content in the coffee extract could give us a more precise information on the degree of contamination of Arabica with Robusta.

First, a larger amount of diterpenes was isolated from roasted and ground Robusta coffee beans. Appropriate functional monomers were selected to gain optimal molecular recognition for each diterpene. Upon synthesizing the polymerizable derivatives for both, a palette of imprinted polymers was synthesized via high dilution radical polymerisation. Covalent imprinting was attempted, as thusly synthesized polymers usually exhibit a more specific rebinding. The polymers were characterized and based on the results of the rebinding studies, the most perspective ones were determined. It is important to consider, that this method due to a recently published finding of 16-OMC in Arabica coffee will not be capable of detecting less than 1% of contamination of Arabica with Robusta Arabica due to the masking effect.[1]

A simpler way to differentiate the roasted beans of Arabica from the roasted beans of Robusta was found in an antimony(III) chloride reagent. A 30% chloroform solution of the Lewis acid has been reported to give colour reactions with various terpenes, sterols and oils. Upon preliminary studies, chloroform and dichloromethane extracts of Robusta and Arabica have been found to give each a characteristic colour when treated with it as well, thus offering a possibility to create a separate colorimetric method for quantification of the contamination of Arabica with Robusta coffee. In the UV-Vis spectra of the treated extracts, peaks at 726 nm and 819 nm were found, characteristic for Robusta and Arabica, respectively. With further optimisation of the preparation of coffee extracts, composition of the antimony(III) chloride solution, kinetic studies and selection of a working wavelength, another simple, fast and reliable method for quantification of contamination of Arabica with Robusta coffee was developed.

Our final contribution to the improvement of quality control of coffee was development of an HPLC-UV method for quantification of acrylamide in roasted coffee, in collaboration with Demus Lab S.r.l., a quality assurance laboratory. Namely, acrylamide was classified as a probable carcinogen (2A, IARC), whose presence in food was found and made public in 2002. Formed mostly through Maillard reaction in foodstuffs exposed to temperatures above 100°C, it also occurs during the coffee roasting process. Due to an EU regulation, coffee roasting companies have been required to report the amount of acrylamide in their roasted coffee products since the 11th of April of this year.

1. INTRODUCTION

1.1 The world of coffee

In a world of millions of café's and 225 billion cups of coffee consumed per day[2], it is absolutely fascinating to think of the humble beginnings of the beverage. An old Ethiopian legend exists, dating to the 9th century, according to which a young goat herder of the name Kaldi noticed, that his goats become very energetic when eating berries from a nearby bush. Upon reporting his observances to the abbot of the local monastery, the story of the existence of the berries soon began to spread. First among the monks, who came up with the first version of the beverage from roasted coffee beans.[3]

By the 14th of century it was cultivated on the Arabian peninsula, and by the 16th century, it had already reached Persia, Egypt, Syria and Turkey. It entered Europe through Italy and the Balkans, and in the 17th century found its way to the newly discovered world and finally reached the tropic areas, where it is nowadays massively cultivated.[3,4]

Due to its sensory properties and physiological effects of coffee beverages, the popularity of coffee heavily increased to this day, making it the second most traded commodity on a global scale. This way it has secured a strong economic, social and cultural impact.[5]

1.1.1 Different types of coffee beverages and habits of consuming

With the long history of coffee and its popularity around the globe, several techniques of preparation of coffee beverages have been developed. They are mostly based on roasted coffee beans of Arabica and Robusta coffees, due to their availability and pleasant organoleptic properties. The methods of preparation can be divided between decoctions, infusions and pressure methods. Depending on the method of choice, coffee grind, proportion between coffee and water, time and temperature of brewing need to be adapted for the optimal result.[5]

Methods of preparation of coffee are geographically clustered, meaning that certain areas of Europe adopted and developed primarily one of them. The preparation methods can be roughly divided between decoction methods, infusion methods and pressure methods.[6] Coffee beverages prepared by decoction are boiled and Turkish coffee, very common in Turkey, Greece and known in most of the south-Eastern European countries. An often present type of coffee, prepared by the infusion method is french press (**Figure 1.1**).[7]

Figure 1.1: Espresso coffee, French press and Turkish coffee.

In Italy, espresso and moka are very popular ways of preparation of coffee and have been implemented in many varieties of coffee beverages. Preparation of both follows the pressure method. This preparation is known to result in the richest taste, as the ratio between coffee and water is very close. With the high-pressure preparation, a relatively big amount of lipids, responsible for the richness of the taste, can be extracted. Beverages are often prepared with the addition of milk and sugar, which ameliorate their bitter taste.[7]

Another widespread form of preparation of a coffee beverage is the use of soluble coffee, a dry beverage, which requires solubilization in water.[6]

1.1.2 Chemical composition of coffee

Green coffee has a rich chemical composition, consisting roughly in the most part of carbohydrates, over 50%, 8-18% of lipids, around 10% of total amino acids and about 5% of minerals. Additionally, significant amounts of trigonelline, minerals and potassium can be found. Very vital for the popularity of coffee is the alkaloid caffeine, present in about 1 to 2 wt.% of green coffee beans (**Table 1.1**).[8]

	Arabica (%)	**Robusta (%)**
Caffeine	1.2	2.2
Lipids	16	10
Chlorogenic acids	6.5	10
Total amino acids	10.3	10.3
Free amino acids	0.5	0.8
Trigonelline	1.0	0.7
Glycosides	0.2	Traces
Minerals	4.2	4.4
→ Potassium	1.7	1.8
Carbohydrates	58.9	60.8

Table 1.1: Simplified chemical composition of Arabica and Robusta.

Coffee lipids are, due to their high representation, a very important fraction of the coffee bean. In most part, they are composed of triacylglycerols, which can be found as about 75 wt.% of the dry matter. The second biggest group are esters of diterpene alcohols with fatty acids, which combined with diterpene alcohols compose 19 wt.% of the coffee dry matter. Other classes of coumpounds, found in coffee, are esters of sterols and fatty acids, free sterols, tocopherols, phosphatides and triptamyl derivatives. 18.5 wt.% of the unsaponifiable fraction has been found in coffee, the main constituents of which are diterpenes, together with sterols, tocopherols, phosphatides, waxes in a form of tryptamine derivatives and even caffeine. The composition of the unsaponifiable and the lipid fraction of the coffee bean are often used for coffee authentication and traceability and have been found to have biologic activities.[9,10]

Diterpene compounds

Even though coffee oil has a relatively similar composition to the other vegetable oils, diterpene compounds are what makes it unique. They are lipophilic pentacyclic alcohols, whose kaurene structure includes a furan ring.[9] Cafestol and kahweol were the first two to be identified and can be found in coffee beans of Arabica and Robusta. They are unstable in light, heat and presence of acids, and are affected by the coffee roasting process, leading to approximately 75% of their degradation in Arabica and 60% of their degradation in Robusta beans after 2-10 min roasting at 230°C.[11]

They both undergo dehydration at usual roasting temperatures, and form dehydrocafestol and dehydrokahweol. The degree of degradation of cafestol and kahweol depends greatly on the intensity of the roasting procedure. Dehydrocafestol and dehydrokahweol are capable to degrade further, thus forming cafestal and kahweal (**Figure 1.2**).

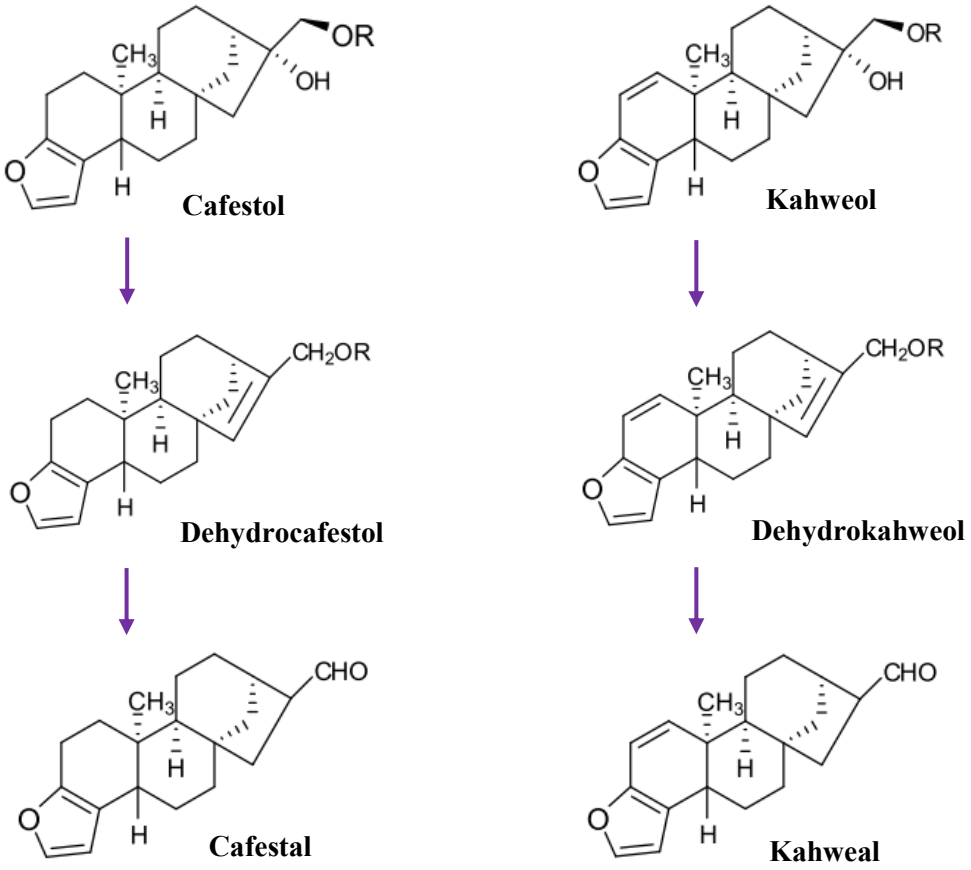

Figure 1.2: Degradation of cafestol and kahweol during roasting, R=H in free diterpene and R=fatty acid in diterpene esters.[9]

Along with both compounds having anticarcinog enic, antioxidant, antiinflamatory and hepatoprotective effects, cafestol has been recognized as the most hypercholesterolemic compound in human diet, as it is suspected to raise total cholesterol, serum concentrations of triglycerides and low density lipoprotein levels in human blood.[12]

In significant amounts in Robusta coffee, methylated derivatives of cafestol and kahweol have been found as well, 16-O-methylcafestol (16-OMC) and 16-O-methylkahweol (**Figure 1.3**). Especially 16-OMC is a very interesting compound, as it has been detected only in minor amounts in Arabica coffee. As such, it has been early on considered as the marker for authenticity of Arabica and a tool for determination the degree of contamination of Arabica with Robusta coffee. For the purpose, a German standard method DIN 10779[13] has been developed and has been actively in use.

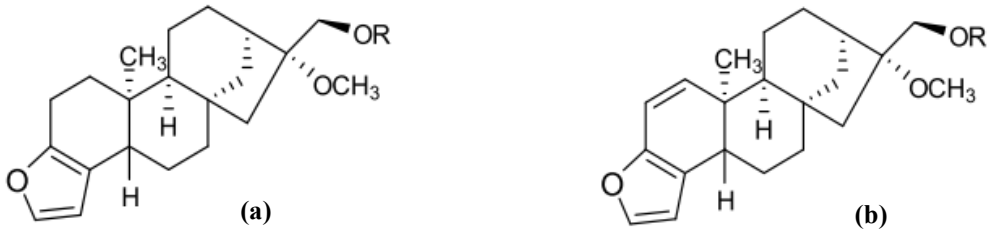

Figure 1.3: 16-O-methylcafestol (a) and 16-O-methylkahweol (b), R=H in free diterpene and R=fatty acid in diterpene esters.[9]

The composition of both, the unsaponifiable fraction and the lipid fraction of the coffee bean, are often used for coffee authentication and traceability, while they have at the same time been found to have biologic activities. [10,14]

Relationship between preparation of beverages and chemical composition

As different ratios between water and coffee used in different coffee beverage preparations, the set of compounds, extracted from coffee, varies greatly based on the way the beverage was prepared. Its intake has been correlated to raising serum cholesterol level where mostly boiled coffee is consumed (Scandinavian countries), in comparison to the studies performed in the countries where only filtered coffee is consumed.[15]

The lipid content in a coffee beverage depends on the preparation of coffee. According to a study, paper filtered coffee beverages contain about 7 mg of lipids, beverages prepared by boiling or perculation even 60 to 160 mg, while coffee beverages prepared by filtering through a metal screener about 50 mg of lipids per a cup. Interestingly, although with filtration a large degree of lipids is retained on the filter, it was reported that the filter paper does not influence the profile of lipids in the beverage. The biggest group of lipids found in coffee beverages were triacylglycerides, representing 92.9% and 6.5 to 12.5% of lipids, respectively.[7]

Several factors influence the amount of lipids in coffee beverages: geographical origin of the coffee beans, blends of various types of coffee beans, different roasting processes and the chosen brewing method. It was found that Arabica contains more lipids than Robusta, yet that the lipid profiles of the two are similar. The duration of boiling of coffee does not appear to change the amount of lipids in the coffee brew, while the amount of lipids in espresso is usually higher due to pressure and steam in the preparation.[7]

Upon decaffeination, the amount of lipids does not significantly change, when the same source is used. Levels of caffeine and other methylxanthines were found to differ in different coffee preparations as well.[7] Different coffee beverages also contain different levels of polyphenols. Thud their antioxidant capacity differs as well and is in compliance with the total phenol content and the content of chlorogenic acid derivatives. In instant coffee the highest content of total phenols, chlorogenic acid derivates and caffeine as found, and consequently the highest antioxidant capacity. Milk was found to noticeably decrease the antioxidant capacity of coffee and the physiological effects of caffeine.[5]

Health effects of coffee

Through the history, coffee has been reported to have both, positive and negative effects on health. Numerous components of coffee exhibit a wide variety of health effects, but perhaps the most known ones are a result of injestion of caffeine. Newer studies have shown, that regular consumption of coffee can result in positive psychoactive responses in the form of enhanced alertness, increased perception and levels of concentration when performing simple tasks, when low caffeine doses are used.[16]

Additionally, effects of coffee beverages have been found to be beneficial in Parkinson's disease. It has been found to positively influence metabolic disorders such as diabetes, in development of gallstone disease, as well as on the gonad and liver function.[17] Those effects have been attributed to polyphenols and other bioactive compounds with strong antioxidant and radical scavenging effects,[18,19] especially polyphenols,[5,20,21] among which chlorogenic acids (quinyl esters of hydroxycinnamic acids)[21], caffeic, ferulic, p-coumaric acid[12] and proanthocyanidins[22] are the most important.[5]

Diterpenes have been found to act anti-inflammatory, anticarcinogenic and as antioxidants. They have been found to induce degradation of toxic substances and protect against aflatoxin B1.[14,23,24,25]

A large number of studies reported adverse effects of coffee consumption: coronary heart disease, insomnia, anxiety, osteoporosis, anemia, hypertension, depression, iron and zinc absorption during pregnancy, adverse effect on fetus, newborn and nursing infant.[5,26,27]

The effects of caffeine and coffee beverages on the human body depends on the frequency of coffee consumption, daily coffee intake and metabolism rates. With frequent coffee consumption a tolerance to caffeine related health effects is usually developed. Dependence to caffeine has been reported with mild withdrawal symptoms. Overdose with coffee is possible and is as well the result of overinjestion of caffeine. It can lead to caffeinism with consumption

of 1-1.5 g of caffeine per day and death at a massive overdose of 150-200 mg of caffeine per kg of body mass (75-100 cups of coffee for a 70 kg adult).[16,28]

1.1.3 Coffee market today

Coffee is one of the most widely traded global commodities (ICO, 2017b). Thus far 104 species have been reported,[29,30] yet only two are commercially important: Coffea arabica L. (Arabica coffee) and C. canephora Pierre ex A. Froehner (Robusta, or conilon).[31] Due to more difficult cultivation and superior organoleptic properties of roasted beans in comparison to Robusta, Arabica coffee costs twice as much as Robusta and still represents the majority of the global production.[32]

The obvious price difference leads to a higher possibility of fraudulence by adulteration of pure Arabica coffee, most often by at least partially replacing it with Robusta, and consequential economic gain[33]. Due to both species belonging to the same botanical genus Coffea, differences, enabling detection and quantification of the added Robusta to Arabica coffee are sparse.[14] Before processed, it is possible to differ their beans by visual inspection,[34] however with roasting and grinding, chemical analysis becomes necessary.[1]

Several other species are known, among those *C. stenophylla*, *C. liberica*, *C. stenophylla, C. salvatrix* and *C. pseudozanguebariae*, with little commercial value.[35] In an attempt to develop a species, which would provide good cup quality and high disease resistance, variety Carabusta was developed.[8]

1.1.4 Quality of coffee

The term food quality has been in development for centuries and will continue to do so even in the future. It is a concept of vast importance in food industry and is a sum of hygienic quality, nutritional quality, sensorial quality, general food law quality and geographical origin quality. All these factors contribute to the "total quality" of the foodstuffs and are regulated by a local or global food authority. Well known organisations, monitoring the quality of foodstuffs are World Health Organization (WHO), Food and Agricultural Organization of United Nations, European Food Safety Authority (EFSA), U.S. Food and Drug Administration (FDA) and International Organization for Standardization (ISO).

Additionally, several organizations focusing on more specific food groups are known. A vital organisation in the coffee world is the International Coffee Organization (ICO). It was formed by coffee producing and coffee consuming countries and closely cooperates with the United Nations.[8] The organization deals with monitoring of the behaviour and sustainability of the coffee market, and gives guidelines for the quality of coffee. The concept of quality of coffee, of course, can have a different meaning for coffee producers, consumers of coffee and regulating organisations themselves.[36]

From the grower to consumer

Coffee beverages are in most cases prepared from roasted coffee beans. To reach the step of a roasted coffee bean, however, a long supply chain needs to be followed (**Figure 1.4**). It all starts with coffee cultivation. The main point of this step is protection of the crop from insect, diseases and bad weather, as all of those factors can lower the yield and quality of harvested beans. Several protective treatments can be applied but using them often changes the cup quality of the final product.[37]

The coffee cherries are ripe when red to dark red in colour. They are then harvested manually or automatically, depending on the size of the coffee plantation and the geographical location of coffee cultivation. As the coffee cherries consist of a pericarp, pulp and coffee beans, the beans need to be released. This can be done wet procedure, followed by fermentation and then washing with water and drying, or via the dry procedure, by drying the berries on the sun and then mechanically removing the pericarp.[4,8] The coffee beans are then dried and sold to coffee roasters. It is of utter importance, that the amount of moisture in the coffee beans upon drying does not exceed 13 wt.%, to avoid development of mold.

Figure 1.4: the journey of a coffee bean from the producer to the consumer.[4]

Roasting is a crucial treatment of coffee beans before they can be used in preparation of coffee beverages. It is usually done at around 200°C for different amounts of time to result in an appropriate degree of roasting. Moisture and gases are released from the beans during roasting (CO, CO_2), resulting in brittler coffee beans. Several reactions occur inside of the coffee bean during the process, but probably the most obvious ones are the browning reactions, visible as the coffee beans turn to light and darker brown. Flavour of roasted coffee develops at that stage and compounds, responsible for the aroma of coffee are formed: pyrroles, pyrazines, pyridines, furans, sulphur containing compounds and several others. Other than that, decarboxilations, dehydrations (quinic acid), lactonizations, isomerisations, polymerisations and several other reactions occur as well.[8] The content of chlorogenic acid has been found to be indicative of the degree of the roast due to its degradation to phenols during the process.[8,38]

Quality checkpoints

Quality of coffee can mean different things through different levels of the supply chain. In the first stages, during cultivation, the quality is greatly influenced by the level of production of coffee, its selling price and easiness of culture. When exporting the product, coffee beans come into focus, more specifically the bean size and their physical characteristics. Lack of defects, regularities, provisioning and available tonnage are of great importance.[37]

As coffee is then passed on to coffee roasters, during transport, storage and roasting itself, adequate level of moisture in coffee is of great importance, together with the origin of coffee and its price. Before roasting, grading of coffee beans is usually done, very often with an electronic approach with a monochromatic light to sort out the black beans and bichromatic light to remove brown and bleached beans, finishing with fluorometrics to remove "sinker beans".[8]

Upon roasting of the coffee beans, then neutral and clean notes of coffee are expected for a good quality of coffee beans.[8] They are strongly connected to the biochemical composition of coffee, stability of its characteristics and its organoleptic quality. Cupping is a method, often used to determine them based on specific taste they are supposed to cause when tasted (**Figure 1.5**). As the coffee arrives to consumers, price, taste, flavour, physiological effects, geographical origin, and environmental and sociological aspects become important.[39]

Figure 1.5: Taster's wheel is a set of expressions to best describe the tasting sensations during cupping.

Although cupping is a method of choice to describe organoleptic properties of coffee, science streams to a more objective way of evaluation of coffee beans in via simpler and faster analytical methods, which in comparison can be far more reproducible. For the purpose, markers of quality of coffee are searched for. For the purpose chlorogenic acids, carbohydrates, proteins, trigonelline and caffeine have been reported.[36]

Fraudulence

Substitutions and adulterations of coffee have been present ever since coffee has entered the market. While substitutions exist for the sake of customers' preference, religion and health issues, adulterations can cause serious financial issues.[8]

Substituents of coffee still have an aroma similar to the one of coffee, when roasted. A very popular substitution, is chicory (*Chicorium intybus,* **Figure 1.6**), popular for its pleasant taste in beverages as well as positive health effects. Other known substitutions are dandelion roots, carrots, parsnips, turnips and mangold wurzel.[40] Cereals, such as barley, malt, rye and wheat, and leguminous seeds, such as chickpeas, peanuts, soybeans, other beans and lupins, have also been reported to have been in use. They are usually roasted, ground and brewed alone or in mixtures with coffee. An interesting example is "Viennese coffee", a blend of roasted coffee, roasted figs, dates, cocoa beans, acorns, cola nuts, sweet potatoes, sugar canes, cashew nuts, carobs and beetroots.[8]

Figure 1.6: Chicicory (*Chicorium intybus*).

Adulteration, on the other hand, is substitution of coffee with a material of a lesser value. Amongst the most often appearing ones are husk, coats and stems, sugar, soil, hulls, sand and spent coffee (lopez 1974). Sometimes chemicals are used as adulterating agents, such as soft forms of lead and inedible fat as bean polishers. The international standard organization defines the impurities in coffee as "defects", and lists them as wood, sticks, husks, parchment or whole cherries found in between the coffee beans.[8] Recently, an issue of adulterations of Arabica with Robusta has occurred. The main reason for it is a superior quality of Arabica, which is nowadays sold in the market for twice the price of Robusta. Ways to detect contaminations of Arabica coffee with Robusta are of great interest to coffee producers, coffee industry and regulatory authorities.[14,41]

Detection of adulterants

In many cases it is possible to detect adulteration of coffee merely by investigating its organoleptic properties. The more significant the adulteration, the more noticeable is the change in organoleptic properties. Some of the known adulterants in coffee are coffee berry skins, coffee berry parchment, other cellulose material (twigs), and can be well observed through oranoleptic analysis. Others are more challenging to pick up, especially contaminations of Arabica with coffee or other substituent of a lesser value. For such cases, numerous methods for detection and quantification of adulterants in coffee have been described thus far:

- Percent of total solids in a 4% w/v extract of coffee.
- Content of volatile matter.
- Level of caffeine.
- Soluble and insoluble fixed mineral residues.
- Alkalinity of the water-soluble ash.
- Ash content.
- Ferric chloride test to quantify phenolic compounds.
- Chloramine number.
- Fehling solution for determination of reducing sugars.
- Testing with iodide solution and lead acetate to teste the presence of lead in the environment.
- Monitoring of caffeoylquinic, dicaffeoylquinic and 5-hydroxymethyl furfural acid.
- Low power microscopy.[8]

Existing methods of differentiation between Arabica and Robusta

Although both species belong to the family Coffea, there are several interesting differences between them (**Figure 1.7**). Thanks to substantial differences in their genome and different environment of their cultivation, non-equal contents of several compounds in their beans have been found. This results in a noticeably different taste of the beverages. As the coffee beverages, prepared from the beans of Arabica are generally more popular due to their more pleasant taste, the market value of the species by far overgrew the market value of Robusta, giving rise to adulterations of Arabica coffee with contaminations of Robusta.

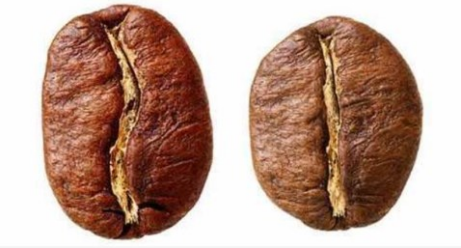

Figure 1.7: Roasted beans of Arabica (left) and Robusta (right).

The contaminations are hard to notice, as the beans of Arabica and Robusta are generally very similar. Small differences can be found when observing their beans up close. Namely, the beans of Arabica are elongated, split by an S-shaped line, while beans of Robusta being rounder and split with a straight line. Those differences, however, are not significant enough to make visual analysis of the beans sufficient in determination of the degree of contamination of one coffee species with another, chemical analysis is a much more efficient approach to it.

Techniques, which are in use for differentiation nowadays, very often require laboratory equipment. Use of infrared spectroscopy, Raman spectroscopy, NMR, mass spectrometry and chromatographic methods, such as gas chromatography or high-pressure liquid chromatography, coupled with a UV or MS detector, is usually reported. Due to differences in their genome, DNA analysis via polymerase chain reaction is possible as well. [42] Several types of compounds can be monitored to allow differentiation between Arabica and Robusta:

- The amount of the **lipid fraction** of the coffee bean is much higher in the beans of Arabica. Similar differences can be found in the amounts of the components representing it:
    - **16-OMC** is better represented in Robusta and is believed to be a good marker for contaminations of Arabica beans with Robusta beans.
    - **α-avenasterol** is as well predominant in Robusta.
    - **Kahweol** has been found in higher amounts in Arabica beans.
- **Reducing sugars** are generally found in higher amounts in the beans of Robusta, while **sucrose** occurs in higher percentages in Arabica.[38]
- **Butanedione, 2,3-pentanedione, and 3-methylbutanal** can be found in bigger amounts in the beans of Arabica, while **2-methylbutanal, 3-methylbutanal** are better represented in Robusta.

- **Furfurylpyrroles and 2-furaldehyde** have been found in larger amounts in Arabica, while **alkylated pyrroles, 2-methylfuran and furyl acetate** are better represented in Robusta.
- Among sulfur compounds **dimethyl sulphide** can be found in bigger amounts in the beans of Arabica, while **thiophene** is a better representative of Robusta.
- **Phenol, toluene, 1-methylpyrrole, 2-hydroxyphenol, 2,s-dimethylpyrazine and** are better representatives of Robusta.
- **Caffeine and chlorogenic acids** content is reported higher for Robusta coffee.[43]
- Average **trigonelline** contents have been found higher in Arabica.[38]

An on-line LC-GC method can be used for analysis of 16-OMC and total sterols from green beans of Robusta and Arabica. The analysis results in a simultaneous determination of, the two markers for authentication of coffee.[42,25] For the sterols a multivariate analysis needs to be applied.[44]

Gas chromatography (GC) with the headspace technique was reported for the characterization of aroma compounds and sulphur compounds.[45] In the case of aroma compounds, a multivariable analysis can give a reliable information when detecting the degree of contamination of Arabica with Robusta.[8] For sulphur compounds a correlation between their profile in coffee and sensory evaluation of coffee can allow even 1% of contamination of Arabica with Robusta.[8,46]

Mid-infrared spectroscopy is used for observing the polysaccharide composition and lipid contet of coffee. The regions 1100 cm−1 and 1744 cm−1 are usually observed. The region 1100 cm−1 is associated with carbohydrates and varies upon different polysaccharide composition of Arabica and Robusta varieties, while the region 1744 cm−1 is associated with the lipid content of the beans and is usually more intense in Arabica than Robusta. [8,41]

Fourier Transform Infrared Spectroscopy (FTIR) and **HPLC-UV** are suitable for discrimination between the two species based on the content of chlorogenic acid and caffeine. [8,41]

HPLC-UV is also a good method of choice for detection of 16-OMC, kahweol, cafestol and other diterpenes in coffee. Specifically for quantification of 16-OMC, DIN 10779 method was developed, to be of use in determination of the degree of contamination of Arabica with Robusta coffee.[13]

Interestingly, **petroleum ether extracts of green and roasted coffee beans**, specifically the double bond of kahweol, **react with potassium iodide and hydrochloric acid in glacial acetic acid**. The reaction yields formation of blue colour. Difference between the absorbance measurements at 290 nm, the maximum wavelength for kahweol, and 620 nm, the maximum wavelength for the reaction products can be used to distinguish between the two species of coffee.[14] Although chromatographical and IR methods are more precise, the colorimetric quantification of kahweol is interesting due to a much simpler sample preparation.

Another solution in authentication of coffee was reported from the field of molecular biology. Namely, **polymerase chain reaction – restriction fragment length polymorphism (PCR-RFLP)** was used and single nucleotide polymorphism was observed in the chloroplastic genome. Analysis was performed with a lab-on-a-chip capillary electrophoresis system.[47]

Upon reading more into colour reactions as a possible method for differentiation of Arabica from Robusta, we stumbled upon antimony(III) chloride.

Colour reactions with antimony(III) chloride

Antimony(III) chloride is mainly known as a TLC staining agent and as a reagent in the Carr-price test for determination of vitamin A.[48] As a staining agent it is useful for visualization of vitamins A and D, as well as carotenoids, steroids, sapogenins, steroid glycosides and terpenes. Its speciality is, that it often visualizes different compounds on a TLC plate with different colours.[49]

In the Carr-Price reaction (**Figure 1.8**) it is used in the form of a saturated solution in chloroform. As such it reacts with vitamin A forming a relatively unstable blue product with a maximum absorbance at the wavelength 550 nm. As the absorbance of the product is very variable, the method is not very precise. Attempts to improve the saturated antimony(III) chloride solution have been reported, with the best results obtained after the addition of elementary Zn, Sn or Sb to limit the conversion of the reactive trivalent antimony to its unreactive pentavalent relative.[50]

An interesting application of this method is its incorporation into a simple portable device to use it in quantification of vitamin A in palm oil, as a substitution for the more complicated and more expensive HPLC method.[51]

Differentiation of two species of cardamoms with antimony(III) chloride

The seeds of true cardamoms are often adulterated with seeds of *Amomum aromaticum, A. subulatum, A. cardamomum*, fruits with orange seeds, unroasted coffee seeds and small pebbles. A thin layer chromatography (TLC) method has been found to distinguish between true cardamoms (*Elettoria cardamomum Maton*) and large cardamoms (*Amomum subulatum Roxb*.). A TLC of their volatile oils is developed in a mixture of n-hexane-diethylether (80+20) solvent system and visualized with a saturated solution of antimony trichloride in chloroform.

Camphor is used as a marker to find if a mixture is present. The chromatographic pattern allows detection of adulteration to 5%.[8]

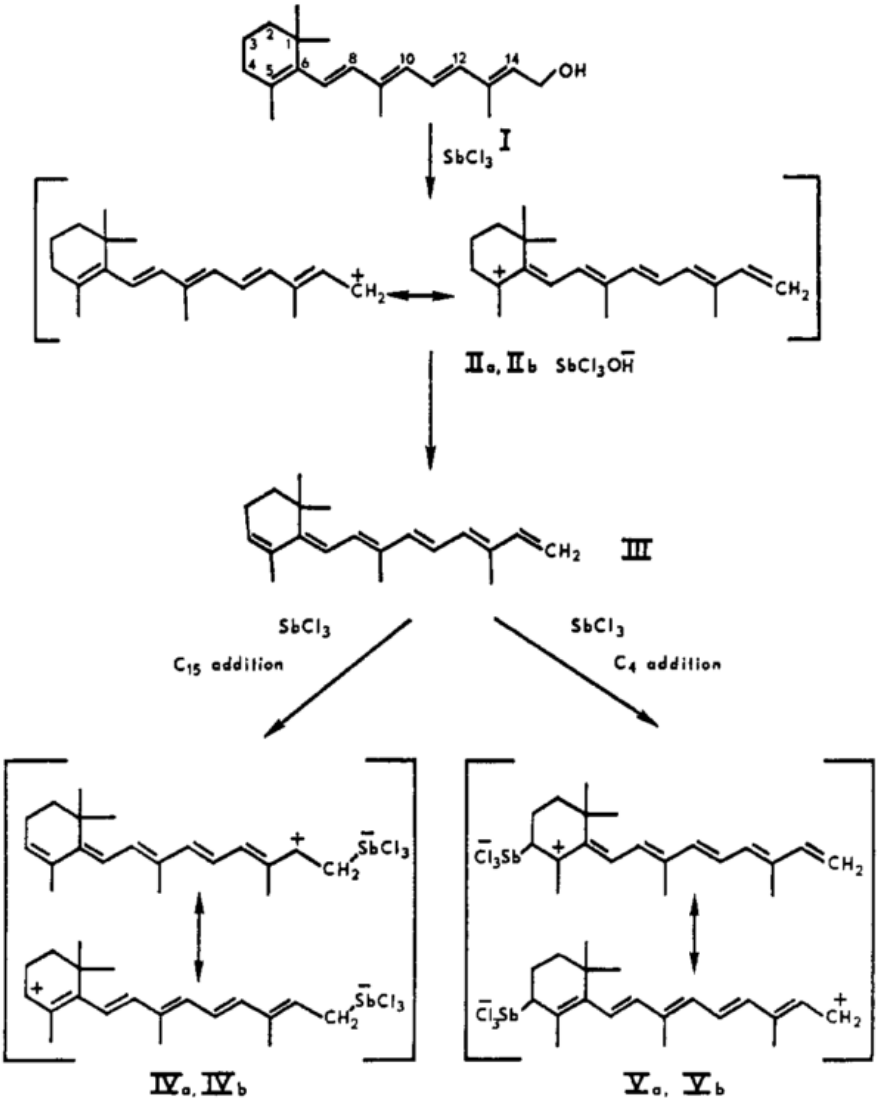

Figure 1.8: Retinol (I) is dehydroxylated to give the retinylic cation (IIa, IIb. λ_{max}= 586 nm). II deprotonates to give anhydroretinol (III, λ_{max} = 386 nm). III can add $SbCl_3$ at C_4 to yield the new retinylic cation (Va, Vb, λ_{max}= 619 nm) or at C_{15} to give the anhydroretinylic cation (Iva, IVb, 586 nm).[52]

1.2 Molecular imprinting

Molecularly imprinted polymers (MIPs) are synthesized porous materials. Their speciality is the capability of selectively rebinding a single molecule or several related molecules into their cavities. This is possible due to established molecular recognition between the target molecules and the binding sites of the polymer.

The idea of molecular imprinting has been on the rise ever since Polyakov and his group in 1931 prepared silica particles with a novel synthetical procedure.[53] Upon examination of the product, they found an unusually high capability of the material to adsorb benzene and toluene, which was soon after assigned to a template induced formation of binding sites. Not long after, in 1972, first imprinted polymers were reported by Wulff.[54] In his case, a covalently imprinted organic polymer for differentiation between two enantiomers of glyceric acid has been synthesized. Followed has discovery of a non-covalent approach to molecular imprinting by Mosbach in 1981. [55] The approach was much simpler to perform and soon led to an expansion in the imprinting technology.

The process of molecular imprinting (**Figure 1.9**) has since been described to consist of four critical steps. First, interactions between the template and the monomer need to be formed in a covalent or non-covalent manner. Thusly formed polymerizable derivatives are then polymerized with one or more cross-linkers to form a polymer matrix. Upon removal of the template from the matrix by disrupting its interaction with the polymer, the template itself or its analogues can be selectively rebound to the imprints in the polymer. Additionally, the matrix itself can improve the rebinding by introducing steric, van der Walls and even electrostatic interactions.[56]

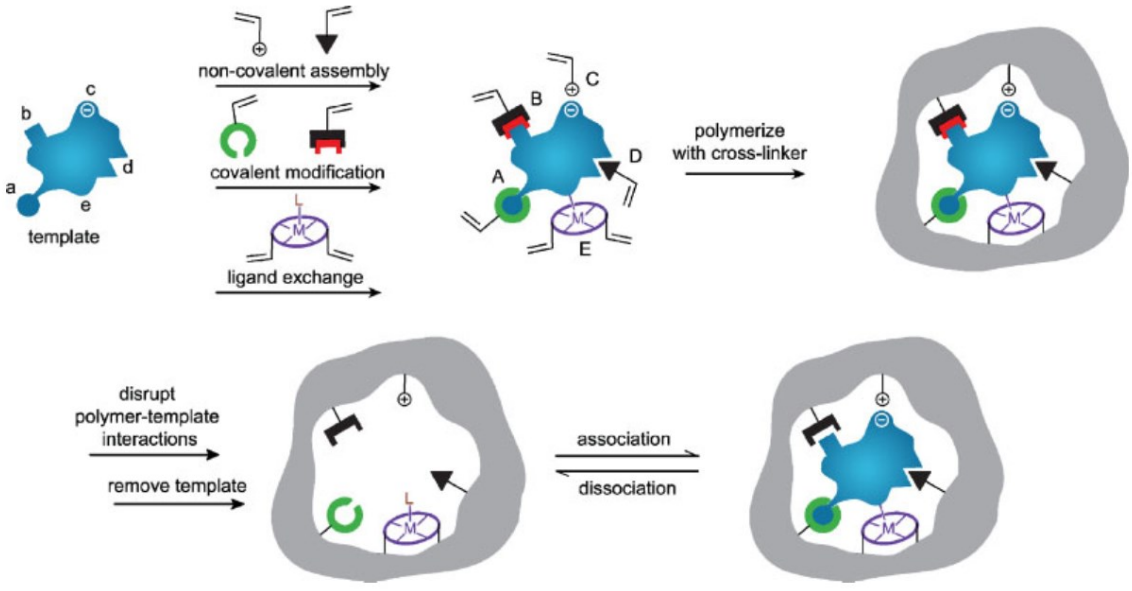

Figure 1.9: Scheme, representing the process of molecular imprinting.[56]

Before imprinting, however, proper functional monomers need to be selected to establish molecular recognition.[57] The phenomena of molecular recognition occurs, when a specific interaction is formed between two molecules. They can interact via non-covalent bonding, through formation of hydrogen bonding, metal coordination, hydrophobic forces, van der Waals forces, π-π interactions, halogen bonding, electrostatic and electromagnetic effects. Several approaches to molecular imprinting exist, less specifically we can group them as covalent imprinting and the non-covalent imprinting approaches.[56,58,59]

Covalent imprinting

An obvious characteristic of covalent imprinting is, that templates need to be covalently bound to monomers of choice prior to polymerisation. This way, when the reaction finishes, the template remains connected to the polymer via a covalent bond. To release the template, the bond needs to be broken and re-established, when rebinding of the template is necessary. In this way formed binding sites are located only in the pores of the polymers and are as such limited in number. This method generally works well for imprinting of diols, aldehydes, ketones, amines and carboxylic acids.[60]

The rebinding kinetics of this group of polymers is often relatively slow as a covalent bond needs to be re-established, and the binding sites in most cases need to be activated prior to rebinding. The situation is improved when diols and diamines are imprinted via ketal bonds. Especially interesting is the formation of boronic esters in between boronic acids and diols.[61]

Non-covalent imprinting

The non-covalent approach, on the other hand, is based on the formation of non-covalent interactions between the template and the monomer prior to imprinting and during polymerisation. This way, upon the termination of the reaction of polymerisation, the template is less strongly bound to a polymer, thus milder conditions of template removal can be used. The formed binding sites in the polymer are generally less homogenously distributed than when covalently imprinted and are rarely positioned only inside of the imprinted pores.[62]

Several types of compounds can be imprinted in this way and due to broad utility of the method, numerous functional monomers are commercially available. Many interesting applications of this method have been presented, such as the use of modified cyclodextrins[63] for hydrophobic analytes in polar solvents and crown ethers for charged compounds. Imprinting of dummy templates has been attempted, where the original template could not have been used for polymerisation due to instability under polymerisation conditions.[64]

The method also allows the use of more than one functional monomer or one functional monomer with several functional groups for improved molecular recognition. Particularly interesting is the use of fluorescent monomers, which can yield imprinted polymers, suitable for sensing purposes. Additionally, “bait and switch” concept can be applied by introducing functional groups in the binding site by non-covalent imprinting, which upon rebinding form covalent bonds with the template.[65]

Other approaches

A combination of covalent imprinting and non-covalent imprinting is the semi-covalent approach. It can be accomplished by initially imprinting a template, covalently bound to the functional monomer. Upon cleaving the covalent bond, non-covalent interactions between the template and the polymer are formed during rebinding. Sacrificial spacers are often used in this approach.[66]

Metal-ion mediated imprinting and imprinting of ionic species are nowadays also finding their way in the world of imprinted polymers.[67]

1.2.1 Synthesis of imprinted polymers

The most often used method for molecular imprinting is free radical initiated vinyl polymerisation in bulk[64] or in the solution.[68] There are several critical points in the formation of an imprinted polymer. Considering the structure, purpose and the degree of selectivity of the polymer we wish to obtain, the correct imprinting approach needs to be chosen. The template for imprinting needs to be stable during the reaction of polymerisation and needs not to contain functional groups, which could prevent polymerisation or be capable of polymerising with the rest of the monomers.[67]

Polymerizable derivatives

An appropriate functional monomer or a combination of them needs to be chosen, to allow for optimal molecular recognition of the template molecule.[69] Depending on the imprinting approach, the monomers should be able to form covalent or non-covalent interactions with the template, resistant enough to survive the conditions of the polymerisation. If the chosen approach is covalent imprinting, the polymerizable derivative of the template needs to be synthesized prior to polymerisation.[70] With non-covalent imprinting an additional synthetic step is not required as self-assembly of the template and the monomers occurs.[71]

Often the molar ratio between one or more functional monomers and the template needs to be adjusted, to achieve better affinity and improve selectivity of the final product. Namely, too low of an amount of the monomer results in a lower number of binding sites in the polymer, while too high of an amount of the functional monomer can lead to a high degree of non-specific binding and thus lower selectivity.[72]

Solvents

Polymerisation usually takes place by using an aprotic porogenic solvent, a structural monomer and a cross-linker. The choice of the solvent has a very big influence on the strength of non-covalent interactions between the template and the functional monomer. The volume of the solvent is closely related to the size of the synthesized polymeric particles. Generally, with increase of the amount of the solvent, the size of the synthesized particles is decreasing.[73]

Formation of the polymeric network

The structural monomer and the cross-linker allow formation of the polymer matrix around the template, thus allowing incorporation of molecular memory into the material and maintaining a sufficient stability and physico-chemical characteristics of the material to hold its shape even after the template is removed. Therefore, an optimal amount of a cross-linker needs to be determined, as too much added cross-linker can lead to a decrease of recognition sites in a polymer, while too little of it can result in lower selectivity of the imprinted polymer.[74]

Mechanism of the reaction

Radical polymerisations can usually be described in three steps: initiation, propagation and termination. For the reaction to take place, an initiator has to be included in the reaction mixture. During initiation (**Figure 1.10**), which can follow an increase of temperature, exposure to light a redox reaction, ionizing radiation or electromechanically, free radicals are formed from the initiator by homological dissociation. The radical then reacts with a molecule of the monomer to produce a monomer radical, initiating the reaction.[75]

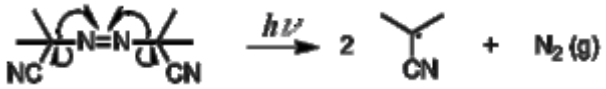

Figure 1.10: Initiation of radical polymerisation by formation of two free radicals from AIBN upon its exposure to light.[76]

Propagation occurs next and it comprises of a chain of radical additions of the monomers, forming new monomer radicals upon every addition. Prolongation of the polymer chain occurs in this phase.

The reaction finishes with a termination step, where a covalent bond is formed between two radical chains, forming the product. Knowing this, we can regulate the amount of the initiator in the reaction mixture. Increasing its amount generally leads to shorter polymer chains and an increased number of particles, while decreasing its amount forms longer polymer chains with a decreased number of the particles.[76]

Existing types of polymerisation

Depending on the amounts of components in the polymerisation mixture, several versions of polymerisations can be executed, resulting in polymer particles of different dimensions, which can be used for different purposes. A very popular method is bulk polymerisation, where a polymeric monolith is formed and needs to be ground before use.[77] By increasing the amount of the solvent, a high dilution polymerisation can be performed, interesting especially because it yields polymer particles in nanometer dimensions with a high surface to volume ratio.

Suspension[78] and emulsion[79] polymerisation have been reported, as well as seed polymerisation[80] and precipitation[81] polymerisation. Additionally, surface imprinting[82], controlled/living free radical polymerisation (CLRP)[83], polymerisation with block copolymer self-assembly[84], microwave-assistant heating polymerisation[85] and polymerisation with an ionic liquid as a porogen[86] have been described.

1.2.2 Applications of the MIPs

Due to their mechanical and chemical stability, low preparation costs and high selectivity, imprinted polymers can be found in a wide variety of applications, albeit for environmental and bioanalytical uses or in food and pharmaceutical sciences.[87,88,89,90]

Initially the goal of their application was to form a stationary phase for HPLC separation of enantiomers. From there, their use has expanded to analytical chemistry for sample preparations via imprinted solid phase extractions and solid phase micro extractions (**Figure 1.11**). An interesting application of a solid phase extraction has been the one for isolation of acrylamide from complex matrices. A dummy template was used, which is essentially a compound with a structure similar enough to the one of the original template, to yield binding sites in the polymers, capable of recognizing the original template.[64]

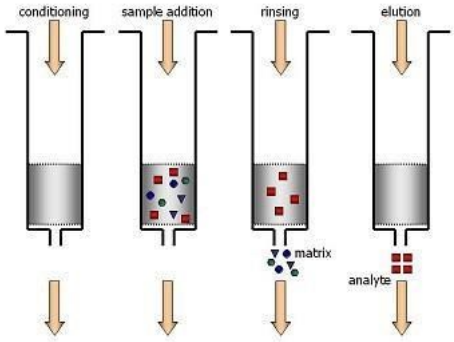

Figure 1.11: Synthesis of MIPs for solid phase extraction is usually attempted via bulk polymerisation.

With the concept of a dummy template, also the issue "bleeding" of the template was resolved. Namely, when the template is not sufficiently removed from the polymer, its release during an analytical procedure and give false results of the analysis.[56]

Another very useful direction of application of imprinted polymers is their use in sensing elements, as artificial antibodies and as artificial catalysts. As such, imprinted polymers have been incorporated into Quartz Crystal Microbalance sensors,[91] optical sensors[92] and electrode sensors[93], where they have aided with detection of several types of compounds (epinephrine, phenobarbital, …).

Due to the affinity of the MIPs for templates, their use in immunoassays is not surprising. Their affinity and specificity has been shown to be very similar to the one of actual antibodies

in several cases, according to the literature. Additionally, due to their selectivity and affinity for the target compound, they can be synthesized to have a role of artificial enzymes.[94] Namely, it has been shown, that it is possible to locate a catalytic and a substrate binding site of in the polymer in such a way, that effective catalysis is achieved. Additionally, their properties have been demonstrated as beneficial in in drug delivery systems.[95]

1.3 Acrylamide

Acrylamide (**Figure 1.12**) is an amide of acrylic acid. It has been recognized as a probable carcinogen (2A) by the International Agency for research on cancer, meaning its carcinogenicity has been proved on rodents while assumed on humans.[96] Additionally, with subchronic exposure it has neurotoxic effects mostly on the peripheral nervous system of humans and laboratory animals, leading to neuropathies, muscle weakness, ataxia, numbness and hands and feet and cerebellar alterations.[97]

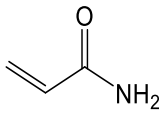

Figure 1.12: Structure of acrylamide.

In human body, its assumingly oxidized by cytochrome P450 2E1 to form an epoxide, 2,3-epoxypropionamide (glycidamide).[98] Both, acrylamide and the oxidized product, have been found to form adducts with haemoglobin, thus forming N-(2-carbamoylethyl)valine on the N-terminal valine of the globin chain (**Figure 1.13**). Analysing the amount of adducts allows monitoring of occupational exposure to acrylamide and exposure by smoking. Additionally, glycidamide and higher levels of acrylamide are capable to form adducts with the amino groups in the DNA chain.[99]

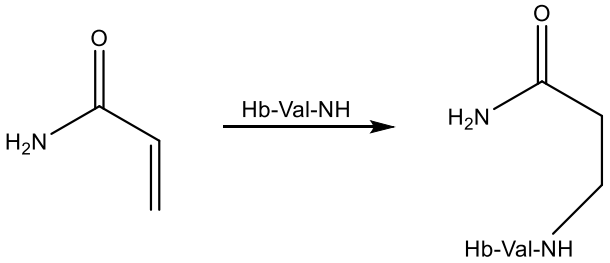

Figure 1.13: Formation of N-(2-carbamoylethyl)valine on the N-termini of haemoglobin (Hb).

In most part, acrylamide is metabolised to N-acetyl-S-(3-amino-3-oxopropyl)cysteine (72%), and less as glyceramide (11%), glycidamide (2.6%), N-acetyl-S-(3-amino-2-hydroxy-3-oxopropyl)cysteine and N-acetyl-S-carbamoylethylcysteine-S-oxide (14%) with either hydrolysis, glutathione conjugation or combination of both and then excreted with urine.[100]

1.3.1 Uses of acrylamide

It is a versatile compound, most often used as a precursor for water-soluble polyacrylamides, which are used in enhanced oil recovery, additives for oil well drilling fluids, floculants for waste water treatment, dye acceptors, additives for textiles, paint and cement, and so on. Acrylamide alone is directly used in photopolymerisation systems and in cross-linking agents. Occupationally, exposure is possible during its production from acrylonitrile, during production of polyacrylamides, during adhesive and grout manufacture and in biotechnological laboratories.[96]

1.3.2 Discovery in food

In 1997 Swedish scientists discovered an unusually high level of haemoglobin adducts of acrylamide in the blood of the control group, when its level was investigated in people occupationally exposed to acrylamide and smokers.[99] Namely, acrylamide is undergoes a 1,4-addition to the N-terminal valine in the said chain. With that a N-(2-carbamoylethyl)valine group is formed.[101]

Questioning the source of exposure of the control group, researchers soon after started working on a hypothesis, that the main source of acrylamide in this case could be fried food. Their observance was formed on the fact, that the levels of the adduct appear to be lower in the blood of wild animals when compared to their levels in the blood of a human. Additionally, they found a relatively low variation of the amounts of the adducts in the blood of smokers.[99]

Based on that, a theory was established, that the source of acrylamide could be food. Due to the low variability of acryl amide found in the smokers and in the blood of the control group, not occupationally exposed to acrylamide, it was assumed that the source apparently needs to be burnt to yield acrylamide. By feeding rats fried food and monitoring the blood levels of adducts to the N-termini of globin chains, this theory was confirmed.[101]

1.3.3 Ways of formation

Several pathways of acrylamide formation mechanisms have been proposed: the Maillard reaction, lipid degradation, decarboxylation and deamination of asparagine, and Strecker reaction, all assuming formation of acrylamide from different precursors.[100]

The Maillard reaction has been found to be a major pathway in formation of acrylamide. It occurs between amino acids and carbohydrates at temperatures above 100°C. Carbonyl groups in carbohydrates condense with the amino group of the amino acids, resulting in formation of a Schiff base. Upon acid-catalysed rearrangement unstable Amadori products are formed.[102]

Through enolization, deamination, dehydration, sugar dehydration and fragmentation products are formed (furfurals, furanones, pyranones), while amino acids also undergo deamination and decarboxylation through Strecker degradation. This leads to the last stage of reaction, where melanoidins are formed through a reaction of condensation (**Figure 1.14**).[103]

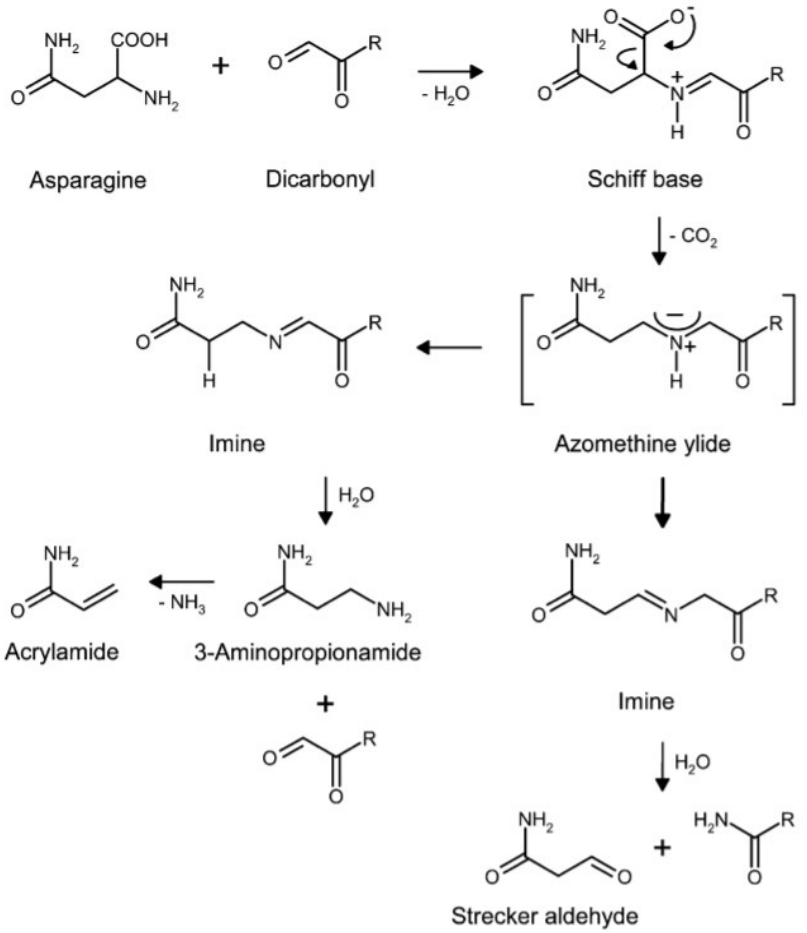

Figure 1.14: Formation of acrylamide by Maillard reaction.

Oxidative lipid degradation is another possible acrylamide formation pathway and has been described to occur during deep frying, hence occurring during roasting of coffee in a far lesser degree than the Mailard reaction. During the degradation acrolein and acrylic acid are formed. The latter then reacts with ammonia to form acrylamide. Ammonia is derived from free amino acids, mostly asparagine, glutamine, cysteine and aspartic acid (**Figure 1.15**).[104]

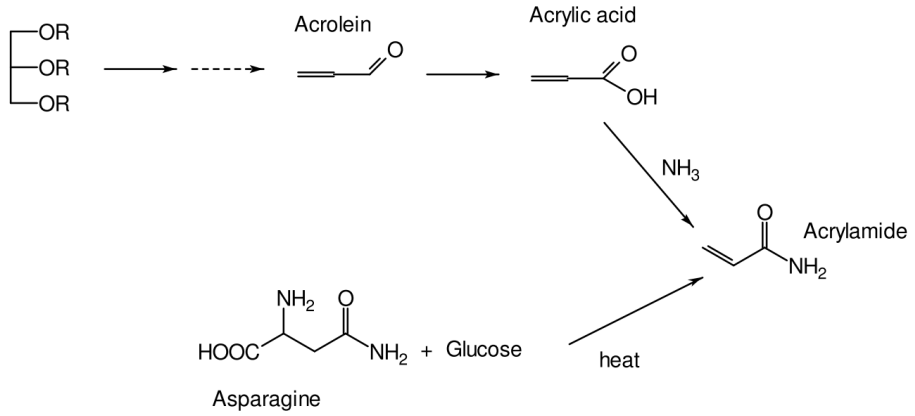

Figure 1.15: Formation of acrylamide with oxidative lipid degradation.

Another possibility, the least represented during roasting of coffee, is formation of acrylamide with decarboxylation and deamination of asparagine at temperatures higher than 170 °C. In this case presence of a reducing sugar is not necessary, and acrylamide is essentially just a side-product of cyclisation of asparagine into maleimide (**Figure 1.16**).[105]

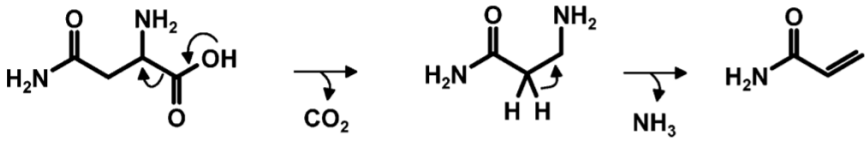

Figure 1.16: Formation of acrylamide from asparagine alone.

The conversion of 3-aminopropionamide, a precursor for acrylamide generally starts at higher temperatures, around 140°C, and the formation of 3-aminopropionamide itself usually occurs in presence of a reducing sugar. In aqueous systems, however, there is a possibility for 3-aminopropionamide to be synthesized even without it. Namely, as seen in **Figure 1.16**, acrylamide can be formed with decarboxylation and deamination of asparagine. It has been found, that 3-aminopropionamide can also be formed enzymatically directly from asparagine at 10 to 40°C.[105]

1.3.4 Chemistry of acrylamide

Acrylamide is an amide of acrylic acid. The compound contains an amide group and is of low molecular weight, which makes it very well soluble in water and polar organic solvents. The double bond in its structure is conjugated with the double bond in the carbonyl group, thus making acrylamide a Michael acceptor. It has a relatively low melting point, at 84.5°C and is slightly volatile. Its absorbance at 202 nm and 210 nm has been described, allowing UV detection of the compound.[106] Derivatization of the compound is possible, to improve its UV, MS or fluorescent signal.[107]

Containing a double bond, conjugated with the double bond in the carbonyl group, it is a Michael acceptor, capable of partaking in 1,4- additions. Due to the amide group it has acidic and basic properties and can be protonated in presence of medium to strong acids. An interesting property of the compound to form complexes with M^{2+} transition metal chlorides (Ni^{2+}, Cu^{2+}) (**Figure 1.17**).[108]

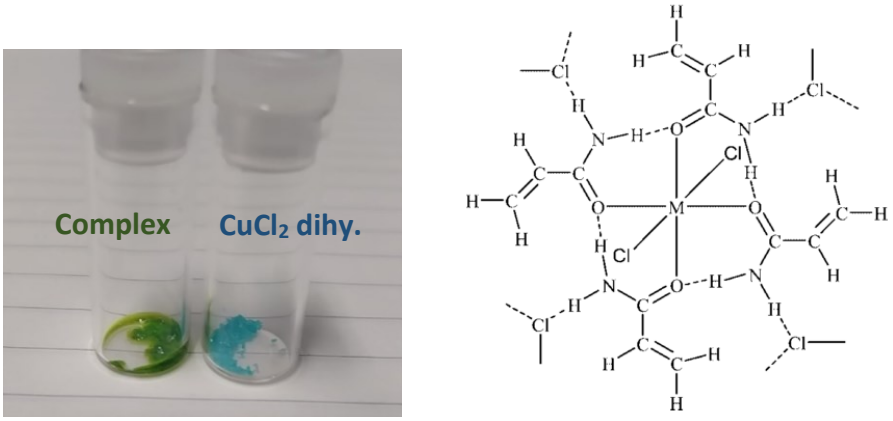

Figure 1.17: Complex of acrylamide with $CuCl_2$ dihydrate (left) and scheme of the general structure of M^{2+} chloride complexes with acrylamide (right).[108]

1.3.5 Existing analytical methods

Nowadays, several approaches to quantification of acrylamide in foodstuffs have been reported. Most often, the reports have been given for deep-fried food[109–111], heated food[111,112] and coffee[113–115], the later especially being a particularly complicated matrix for analysis. Most often used methods of quantifications are various chromatographic methods. GC-MS[115–118] with or without pre-colum derivatization[116,119] and with MS or MS/MS detection has been reported to work very well.

Additionally, with the rise of SPE extractions[115,120–123], liquid chromatography has been more and more often reported[121,124,125], as it is a far less time consuming and expensive technique, very adaptable for industrial use. The detection of choice can be done with UV[110,111,126,127], MS[64,107,121,128,129], or MS/MS detectors[118,121,130–133]. Reports have been given on capillary electrophoresis.[134]fii

Due to the properties of acrylamide, the sample preparation usually consists of defatting of the sample prior to extraction, if necessary (fried food),[116,122,135] then extraction into water[110,116,122,135] or other polar solvent[126] at room temperature. Proteins are usually removed from the extract with Carrez solutions[114,115,125,128,136]. SPE filtration is usually a crucial step in removal of the sample matrix, and is, in some cases, followed by a bromination step, where acrylamide is converted into 2-bromopropeneamide, to improve detection of the GC-MS analysis.

Choice of a proper chromatographic column is crucial in detection of acrylamide. The use of several types of stationary phases has been reported, most often C18[126,137] or a hydrophilic ones[122] have been reported to work well.

Indicative values of acrylamide in food

In **Table 1.2**, values of acrylamide in foods, rich in acrylamide, are presented, as those are the ones with the highest amounts of acrylamide formed upon exposing them to high temperatures. Tha highest level of acrylamide was found in potato chips, at 627 ng/g and the lowest in breakfast cereals, at 95 ng/g. Considering the hypotheses of formation of acrylamide, the high level in potato chips is not surprising. As frying occurs at temperatures above 170°C in presence of lipids, along with the Maillard reaction, acrylamide is most probably additionally formed from oxidative lipid degradation and decarboxylation and deamination of asparagine. In roasted coffee a substantially lower, yet still significant level of acrylamide occurs.[138]

Median values of acrylamide in the specified food groups

Food group	Mean (ng/g)	Median (ng/g)	Number of samples analysed
Potato crisps	627	499	44
Cookies	275	99	30
Crisp bread	153	69	38
Breakfast cereals	95	0	28
Popcorn and rice products	106	97	15
Potato chips	152	161	7
Coffee	204	169	7

For statistical analysis, the values below the LOQ (30 ng/g) were assigned as 0.

Table 1.2: Indicative values of acrylamide in food, rich with carbohydrates.[138]

Bibliography

1. Gunning, Y. *et al.* 16-O-methylcafestol is present in ground roast Arabica coffees: Implications for authenticity testing. *Food Chem.* **248,** 52–60 (2018).
2. Ponte, S. The latte revolution? Winners and losers in the re-structuring of the global coffee marketing chain. *CDR Work. Pap.* **1,** 1–35 (2001).
3. National Coffee Association. No Title.
4. Illy company website.
5. Niseteo, T., Komes, D., Belščak-Cvitanović, A., Horžić, D. & Budeč, M. Bioactive composition and antioxidant potential of different commonly consumed coffee brews affected by their preparation technique and milk addition. *Food Chem.* **134,** 1870–1877 (2012).
6. Petracco, M. Products of Chemistry Our Everyday Cup of Coffee : The Chemistry behind Its Magic. **82,** (2005).
7. Ratnayake, W. M. N., Hollywood, R., O'Grady, E. & Stavric, B. Lipid content and composition of coffee brews prepared by different methods. *Food Chem. Toxicol.* **31,** 263–269 (1993).
8. Singhal, R. S., Kulkarni, P. R. & Rege, D. V. Handbook of Indices of Food Quality and Authenticity. *Handb. Indices Food Qual. Authent.* 209–299 (1997). doi:10.1533/9781855736474.209
9. Speer, K. & Kölling-Speer, I. The lipid fraction of the coffee bean. *Braz. J. Plant Physiol* **18,** 201–216 (2006).
10. D'Amelio, N., De Angelis, E., Navarini, L., Schievano, E. & Mammi, S. Green coffee oil analysis by high-resolution nuclear magnetic resonance spectroscopy. *Talanta* **110,** 118–127 (2013).
11. Carlos, R., Dias, E., Ferreira, A. & Machado, D. F. Roasting process affects the profile of diterpenes in coffee. 961–970 (2014). doi:10.1007/s00217-014-2293-x
12. Richelle, M., Tavazzi, I. & Offord, E. Comparison of the antioxidant activity of commonly consumed polyphenolic beverages (coffee, cocoa, and tea) prepared per cup serving. *J. Agric. Food Chem.* **49,** 3438–3442 (2001).
13. Naegele, E. Determination of Methylcafestol in Roasted Coffee Products According to DIN 10779. *Agil. Technol.* (2016).
14. Dias, R. C. E., Alves, S. T. & Benassi, M. de T. Spectrophotometric method for quantification of kahweol in coffee. *J. Food Compos. Anal.* **31,** 137–143 (2013).
15. Urged, R. *et al.* Levels of the Cholesterol-Elevating Diterpenes Cafestol and Kahweol in Various Coffee Brews. (1995).
16. Panel, E. & Nda, A. Scientific Opinion on the safety of caffeine. *EFSA J.* **13,** 4102 (2015).
17. Dórea, J. G. & da Costa, T. H. M. Is coffee a functional food? *Br. J. Nutr.* **93,** 773 (2005).
18. Cämmerer, B. & Kroh, L. W. Antioxidant activity of coffee brews. *Eur. Food Res.*

Technol. **223,** 469–474 (2006).

19. Parras, P., Martínez-Tomé, M., Jiménez, A. M. & Murcia, M. A. Antioxidant capacity of coffees of several origins brewed following three different procedures. *Food Chem.* **102,** 582–592 (2007).

20. Charurin, P., Ames, J. M. & Del Castillo, M. D. Antioxidant activity of coffee model systems. *J. Agric. Food Chem.* **50,** 3751–3756 (2002).

21. Olthof, M. R., Hollman, P. C., Zock, P. L. & Katan, M. B. Consumption of high doses of chlorogenic acid, present in coffee, or of black tea increases plasma total homocysteine concentrations in humans. **73,** 532–538 (2001).

22. Arts, I. C. W., Van De Putte, B. & Hollman, P. C. H. Catechin contents of foods commonly consumed in The Netherlands. 2. Tea, wine, fruit juices, and chocolate milk. *J. Agric. Food Chem.* **48,** 1752–1757 (2000).

23. Muriel, P. & Arauz, J. Review Coffee and liver diseases. *Fitoterapia* **81,** 297–305 (2010).

24. Nkondjock, A. Coffee consumption and the risk of cancer: An overview. *Cancer Lett.* **277,** 121–125 (2009).

25. Cavin, C. *et al.* Cafestol and kahweol, two coffee specific diterpenes with anticarcinogenic activity. *Food Chem. Toxicol.* **40,** 1155–1163 (2002).

26. Nawrot, P. *et al.* Effects of caffeine on human health. *Food Addit. Contam.* **20,** 1–30 (2003).

27. Smith, P. F., Smith, A., Miners, J., McNeil, J. & Proudfoot, A. Report from the expert working group on the safety aspects of dietary caffeine. (2000).

28. Benowitz, N. L. Clinical Pharmacology of Caffeine. *Annu. Rev. Med.* **41,** 277–288 (1990).

29. Davis, A. P., Govaerts, R., Bridson, D. M. & Stoffelen, P. An annotatated taxonomic of the genus coffea (Rubiaceae). *Bot. J. Linn. Soc.* **152,** 465–512 (2006).

30. Tran, H. T., Lee, L. S., Furtado, A., Smyth, H. & Henry, R. J. Advances in genomics for the improvement of quality in coffee. *J. Sci. Food Agric.* **96,** 3300–3312 (2016).

31. Belitz HD, Grosch W, S. *Food Chemistry*. (2009).

32. Pacetti, D., Boselli, E., Balzano, M. & Frega, N. G. Authentication of Italian Espresso coffee blends through the GC peak ratio between kahweol and 16- O -methylcafestol. *Food Chem.* **135,** 1569–1574 (2012).

33. Toci, A. T., Farah, A., Pezza, H. R. & Pezza, L. Coffee Adulteration: More than Two Decades of Research. *Crit. Rev. Anal. Chem.* **46,** 83–92 (2016).

34. Craig, A. P., Franca, A. S. & Oliveira, L. S. Discrimination between defective and non-defective roasted coffees by diffuse reflectance infrared Fourier transform spectroscopy. *LWT - Food Sci. Technol.* **47,** 505–511 (2012).

35. Roos, B. De, Weg, G. Van Der, Urgert, R., Bovenkamp, P. Van De & Katan, M. B. Levels of Cafestol , Kahweol , and Related Diterpenoids in Wild Species of the Coffee Plant Coffea. (1997).

36. Ribeiro, J. S., Ferreira, M. M. C. & Salva, T. J. G. Chemometric models for the quantitative descriptive sensory analysis of Arabica coffee beverages using near infrared spectroscopy. *Talanta* **83,** 1352–1358 (2011).

37. Murthy, P. S. & Madhava Naidu, M. Sustainable management of coffee industry by-products and value addition - A review. *Resour. Conserv. Recycl.* **66,** 45–58 (2012).

38. Ky, C. L. *et al.* Caffeine, trigonelline, chlorogenic acids and sucrose diversity in wild Coffea arabica L. and C. canephora P. accessions. *Food Chem.* **75,** 223–230 (2001).

39. Leroy, T. *et al.* Genetics of coffee quality. *Brazilian J. Plant Physiol.* **18,** 229–242 (2006).

40. JR, N. AID TO THE ANALYSIS OF FOOD AND DRUGS. (1952).

41. Briandet, R., Kemsley, E. K. & Wilson, R. H. Discrimination of Arabica and Robusta in Instant Coffee by Fourier Transform Infrared Spectroscopy and Chemometrics. 170–174 (1996).

42. Kamm, W. *et al.* Rapid and simultaneous analysis of 16-O-methylcafestol and sterols as markers for assessment of green coffee bean authenticity by on-line LC-GC. *J. Am. Oil Chem. Soc.* **79,** 1109–1113 (2002).

43. Jeszka-Skowron, M., Sentkowska, A., Pyrzyńska, K. & De Peña, M. P. Chlorogenic acids, caffeine content and antioxidant properties of green coffee extracts: influence of green coffee bean preparation. *Eur. Food Res. Technol.* **242,** 1403–1409 (2016).

44. G Consiglieri, G Fonseca, F. A.-R. C. Multivariate analysis for the classification of coffee blends. *Rass. Chim.* **43,** 171–77 (1991).

45. J Koszinowski, O. P. THE IMPORTANCE OF OXIDATION-PRODUCTS OF UNSATURATED-HYDROCARBONS IN THE SENSORIAL PROPERTIES OF FOOD PACKING. 1. OXYGEN DERIVATIVES OF THE ALKENES. *Dtsch. Leb.* **79,** 179–183 (1983).

46. Leino, M., Kaitaranta, J. & Kallio, H. Comparison of changes in headspace volatiles of some coffee blends during storage. *Food Chem.* **43,** 35–40 (1992).

47. Spaniolas, S., May, S. T., Bennett, M. J. & Tucker, G. A. Authentication of coffee by means of PCR-RFLP analysis and lab-on-a-chip capillary electrophoresis. *J. Agric. Food Chem.* **54,** 7466–7470 (2006).

48. Corbet, E. & Geisinger, H. TEST FOR VITAMIN Antimony Trichloride Color Test. (1933).

49. Sarpong, R. *Dyeing Reagents for Thin-Layer and Paper Chromatography*. *Amines Amino acids Amino acids* **7624729820,** (1962).

50. Nikolić, J. A. Letters to the Editors Letters to the Editors. *Br. J. Nutr.* **63,** 669–671 (1990).

51. Hutchinson, M. S., Figenschau, Y., Almås, B., Njølstad, I. & Jorde, R. Serum 25-Hydroxyvitamin D Levels in Subjects with Reduced Glucose Tolerance and Type 2 Diabetes – The Tromsø OGTT-Study. *Int. J. Vitam. Nutr. Res.* **81,** 317–327 (2011).

52. Blatz, P. E., Estrada, A. & Estrada, A. Investigation of the Molecular Behavior of the

Carr-Price Reaction. *Anal. Chem.* **44,** 570–573 (1972).

53. MV, P. Adsorption properties and structure of silica gel. *Zhurnal Fizieskoj Khimii/Akademiya SSSR* **2,** 799–805 (1931).

54. Wulff G, S. A. Uber die Anwendung von Enzymanalog gebauten Polymeren zur Racemattrennung. *Angew Chem* **84,** 364 (1972).

55. Arshady, R. & Mosbach, K. Synthesis of Substrate-selective Polymers by Host-Guest Polymerizatioa. **692,** 687–692 (1981).

56. Alexander, C. *et al.* Molecular imprinting science and technology: A survey of the literature for the years up to and including 2003. *J. Mol. Recognit.* **19,** 106–180 (2006).

57. Aoyama, Y., Tanaka, Y. & Sugahara, S. Molecular Recognition. 5. Molecular Recognition. **68,** 5397–5404 (1989).

58. Kenny, P. W. Hydrogen bonding, electrostatic potential, and molecular design. *J. Chem. Inf. Model.* **49,** 1234–1244 (2009).

59. Karim, K. *et al.* How to find effective functional monomers for effective molecularly imprinted polymers ? B. **57,** 1795–1808 (2005).

60. Whitcombe, M. J., Kirsch, N. & Nicholls, I. A. *Molecular imprinting science and technology: A survey of the literature for the years 2004-2011*. *Journal of Molecular Recognition* **27,** (2014).

61. Wulff, G. & Poll, H.-G. Enzyme-analogue built polymers, 23. Influence of the structure of the binding sites on the selectivity for racemic resolution. *Die Makromol. Chemie* **188,** 741–748 (1987).

62. Vasapollo, G. *et al.* Molecularly imprinted polymers: Present and future prospective. *Int. J. Mol. Sci.* **12,** 5908–5945 (2011).

63. Ng, S. M. & Narayanaswamy, R. Sensors and Actuators B : Chemical Molecularly imprinted □ -cyclodextrin polymer as potential optical receptor for the detection of organic compound. **139,** 156–165 (2009).

64. Arabi, M., Ghaedi, M. & Ostovan, A. Development of dummy molecularly imprinted based on functionalized silica nanoparticles for determination of acrylamide in processed food by matrix solid phase dispersion. *Food Chem.* **210,** 78–84 (2016).

65. Subrahmanyam, S. *et al.* 'Bite-and-Switch' approach using computationally designed molecularly imprinted polymers for sensing of creatinine. *Biosens. Bioelectron.* **16,** 631–637 (2001).

66. Kirsch, N., Alexander, C., Davies, S. & Whitcombe, M. J. Sacrificial spacer and non-covalent routes toward the molecular imprinting of 'poorly-functionalized' N-heterocycles. *Anal. Chim. Acta* **504,** 63–71 (2004).

67. Yan, H. & Ho Row, K. Characteristic and Synthetic Approach of Molecularly Imprinted Polymer. *Int. J. Mol. Sci* **7,** 155–178 (2006).

68. Haupt, K. & Mosbach, K. Molecularly imprinted polymers and their use in biomimetic sensors. *Chem. Rev.* **100,** 2495–2504 (2000).

69. Flavin, K. & Resmini, M. Imprinted nanomaterials : a new class of synthetic receptors.

437–444 (2009). doi:10.1007/s00216-008-2496-8

70. Percival, C. J., Stanley, S., Braithwaite, A., Newton, M. I. & McHale, G. Molecular imprinted polymer coated QCM for the detection of nandrolone. *Analyst* **127,** 1024–1026 (2002).

71. Mosbach, K. & Haupt, K. Some new developments and challenges in non- covalent molecular imprinting technology. **11,** 62–68 (1998).

72. Luliński, P. & Maciejewska, D. Examination of imprinting process with molsidomine as a template. *Molecules* **14,** 2212–2225 (2009).

73. Pérez-Moral, N. & Mayes, A. G. Comparative study of imprinted polymer particles prepared by different polymerisation methods. *Anal. Chim. Acta* **504,** 15–21 (2004).

74. Wulff, G. Molecular Imprinting in Cross-Linked Materials with the Aid of Molecular. (1972).

75. Odian, G. *Principles of Polymerisation*. (Wiley-Interscience, 2004).

76. Cowie JMG, A. V. *Polymers: Chemistry and Physics of Modern Materials*. (CRC Press, 2008).

77. Taylor, P. & Say, R. Separation Science and Technology Comparison of Adsorption and Selectivity Characteristics for 4 - Nitrophenol Imprinted Polymers Prepared via Bulk and Suspension Polymerization. 37–41 (2005). doi:10.1081/SS-200028939

78. Jing, T. *et al.* Determination of trace tetracycline antibiotics in foodstuffs by liquid chromatography – tandem mass spectrometry coupled with selective molecular-imprinted solid-phase extraction. 2009–2018 (2018). doi:10.1007/s00216-009-2641-z

79. Tan CJ, T. Y. Preparation of superparamagnetic ribonuclease A surface-imprinted submicrometer particls for protein recognition in aqueous media. *Anal. Chem.* (2007).

80. Hoshina, K., Horiyama, S., Matsunaga, H. & Haginaka, J. Molecularly imprinted polymers for simultaneous determination of antiepileptics in river water samples by liquid chromatography – tandem mass spectrometry. **1216,** 4957–4962 (2009).

81. Tamayo, F. G., Casillas, J. L. & Martin-esteban, A. Evaluation of new selective molecularly imprinted polymers prepared by precipitation polymerisation for the extraction of phenylurea herbicides. **1069,** 173–181 (2005).

82. Emir, S., Say, R. & Sibel, B. Quantum dot nanocrystals having guanosine imprinted nanoshell for DNA recognition. **75,** 890–896 (2008).

83. Boonpangrak, S., Whitcombe, M. J., Prachayasittikul, V., Mosbach, K. & Ye, L. Preparation of molecularly imprinted polymers using nitroxide-mediated living radical polymerization. **22,** 349–354 (2006).

84. Chen, Z. *et al.* Unique Toroidal Morphology from Composition and Sequence Control of Triblock Copolymers. **3,** 8592–8593 (2005).

85. Zhang, X., Jiao, K., Liu, S. & Hu, Y. Hybridization Biosensor Based on the Interaction of DNA with Single-Walled Carbon Nanotubes. **81,** 6006–6012 (2009).

86. Ghilane, J., Martin, P., Fontaine, O., Lacroix, J. & Randriamahazaka, H. Electrochemistry Communications Modification of carbon electrode in ionic liquid

through the reduction of phenyl diazonium salt . Electrochemical evidence in ionic liquid. **10,** 1060–1063 (2008).

87. Ton, X., Acha, V., Haupt, K., Tse, B. & Bui, S. Biosensors and Bioelectronics Direct fluorimetric sensing of UV-excited analytes in biological and environmental samples using molecularly imprinted polymer nanoparticles and fluorescence polarization. *Biosens. Bioelectron.* **36,** 22–28 (2012).

88. Rezaei, B., Mallakpour, S. & Majidi, N. Talanta Solid-phase molecularly imprinted pre-concentration and spectrophotometric determination of isoxicam in pharmaceuticals and human serum. **78,** 418–423 (2009).

89. Regal, P., Díaz-bao, M., Barreiro, R., Cepeda, A. & Fente, C. Application of molecularly imprinted polymers in food analysis : clean-up and chromatographic improvements. **10,** (2012).

90. Allender, C. ., Richardson, C., Woodhouse, B., Heard, C. . & Brain, K. . Pharmaceutical applications for molecularly imprinted polymers. *Int. J. Pharm.* **195,** 39–43 (2000).

91. Reimhult, K. *et al.* Biosensors and Bioelectronics Characterization of QCM sensor surfaces coated with molecularly imprinted nanoparticles. **23,** 1908–1914 (2008).

92. Fang, Y. *et al.* Biosensors and Bioelectronics Flow injection chemiluminescence sensor using molecularly imprinted polymers as recognition element for determination of maleic hydrazide. **24,** 2323–2327 (2009).

93. Fang, C., Yi, C., Wang, Y., Cao, Y. & Liu, X. Biosensors and Bioelectronics Electrochemical sensor based on molecular imprinting by photo-sensitive polymers. **24,** 3164–3169 (2009).

94. Liu, J. Jun-qiu Liu and Günter Wulff*. 1287–1290 (2004). doi:10.1002/anie.200352770

95. Cunliffe, D., Kirby, A. & Alexander, C. Molecularly imprinted drug delivery systems B. **57,** 1836–1853 (2005).

96. IARC. Acrylamide. *IARC Monogr.* **60,** 389–433 (1994).

97. Friedman, M. Chemistry, biochemistry, and safety of acrylamide. A review. *J. Agric. Food Chem.* **51,** 4504–4526 (2003).

98. Dybing, E., Farmer, P. B., Andersen, M., Fennell, T. R. & Lalljie, S. P. D. Human exposure and internal dose assessments of acrylamide in food. **43,** 365–410 (2005).

99. Bergmark, E. Hemoglobin Adducts of Acrylamide and Acrylonitrile in Laboratory Workers , Smokers and Nonsmokers. 78–84 (2000).

100. Fennell, T. R. *et al.* Metabolism and Hemoglobin Adduct Formation of Acrylamide in Humans. **85,** 447–459 (2005).

101. Tareke, E., Rydberg, P., Karlsson, P., Eriksson, S. & To, M. Acrylamide : A Cooking Carcinogen ? 517–522 (2000).

102. Keramat, J., LeBail, A., Prost, C. & Soltanizadeh, N. Acrylamide in Foods: Chemistry and Analysis. A Review. *Food Bioprocess Technol.* **4,** 340–363 (2011).

103. Blank, I. *et al.* Mechanisms of acrylamide formation: Maillard-induced transformation of asparagine. *Adv. Exp. Med. Biol.* **561,** 171–189 (2005).

104. Capuano, E. Lipid Oxidation Promotes Acrylamide Formation in Fat-Rich Systems. *Acrylamide Food Anal. Content Potential Heal. Eff.* **43,** 309–324 (2015).

105. Chieberle, P. E. S. Thermally Generated 3-Aminopropionamide as a Transient Intermediate in the Formation of Acrylamide AND. 5933–5938 (2006).

106. Sigma Aldrich. *Acrylamide, Specification sheet*.

107. Bagdonaite, K., Derler, K. & Murkovic, M. Determination of acrylamide during roasting of coffee. *J. Agric. Food Chem.* **56,** 6081–6086 (2008).

108. Girma, K. B., Lorenz, V., Blaurock, S. & Edelmann, F. T. Coordination Chemistry of Acrylamide 2 . Classical Complexes of Acrylamide with Manganese (II), Iron (II) and Nickel (II) Chlorides : Syntheses and Crystal Structures. 2763–2769 (2005). doi:10.1002/zaac.200500132

109. Gertz, C. & Klostermann, S. Analysis of acrylamide and mechanisms of its formation in deep-fried products. *Eur. J. Lipid Sci. Technol.* **104,** 762–771 (2002).

110. Wang, H., Lee, A. W. M., Shuang, S. & Choi, M. M. F. SPE/HPLC/UV studies on acrylamide in deep-fried flour-based indigenous Chinese foods. *Microchem. J.* **89,** 90–97 (2008).

111. Wang, H., Feng, F., Guo, Y., Shuang, S. & Choi, M. M. F. HPLC-UV quantitative analysis of acrylamide in baked and deep-fried Chinese foods. *J. Food Compos. Anal.* **31,** 7–11 (2013).

112. Ahn, J. S. *et al.* Verification of the findings of acrylamide in heated foods. *Food Addit. Contam.* **19,** 1116–1124 (2002).

113. Lantz, I. *et al.* Studies on acrylamide levels in roasting, storage and brewing of coffee. *Mol. Nutr. Food Res.* **50,** 1039–1046 (2006).

114. Arisseto, A. P. *et al.* A Modified Sample Preparation for Acrylamide Determination in Cocoa and Coffee Products. *Food Anal. Methods* **1,** 49–55 (2008).

115. Soares, C., Cunha, S. & Fernandes, J. Determination of acrylamide in coffee and coffee products by GC-MS using an improved SPE clean-up. *Food Addit. Contam.* **23,** 1276–1282 (2006).

116. Fernandes, J. O. & Soares, C. Application of matrix solid-phase dispersion in the determination of acrylamide in potato chips. *J. Chromatogr. A* **1175,** 1–6 (2007).

117. Zhang, Y., Zhang, G. & Zhang, Y. Occurrence and analytical methods of acrylamide in heat-treated foods: Review and recent developments. *J. Chromatogr. A* **1075,** 1–21 (2005).

118. Ehotay, S. T. J. L. Rapid Sample Preparation Method for LC − MS / MS or GC − MS Analysis of Acrylamide in Various Food Matrices AND. (2006).

119. Nemoto, S., Takatsuki, S., Sasaki, K. & Maitani, T. Determination of acrylamide in foods by GC/MS using 13C-labeled acrylamide as an internal standard. *Shokuhin Eiseigaku Zasshi.* **43,** 371–376 (2002).

120. Xu, L., Zhang, L., Qiao, X., Xu, Z. & Song, J. Determination of trace acrylamide in potato chip and bread crust based on SPE and HPLC. *Chromatographia* **75,** 269–274

(2012).

121. Bortolomeazzi, R., Munari, M., Anese, M. & Verardo, G. Rapid mixed mode solid phase extraction method for the determination of acrylamide in roasted coffee by HPLC-MS/MS. *Food Chem.* **135,** 2687–2693 (2012).

122. Michalak, J., Gujska, E. & Kuncewicz, A. RP-HPLC-DAD studies on acrylamide in cereal-based baby foods. *J. Food Compos. Anal.* **32,** 68–73 (2013).

123. Soares, C. M. D., Alves, R. C., Casal, S., Oliveira, M. B. P. P. & Fernandes, J. O. Development and validation of a matrix solid-phase dispersion method to determine acrylamide in coffee and coffee substitutes. *J. Food Sci.* **75,** (2010).

124. Eaman, S. T. W. S. Acrylamide in Foods : Occurrence , Sources , and Modeling. 802–808 (2003).

125. Şenyuva, H. Z. & Gökmen, V. Study of acrylamide in coffee using an improved liquid chromatography mass spectrometry method: Investigation of colour changes and acrylamide formation in coffee during roasting. *Food Addit. Contam.* **22,** 214–220 (2005).

126. Khoshnam, F., Zargar, B., Pourreza, N. & Parham, H. Acetone Extraction and HPLC Determination of Acrylamide in Potato Chips. *J. Iran. Chem. Soc.* **7,** 853–858 (2010).

127. Paleologos, E. K. & Kontominas, M. G. Determination of acrylamide and methacrylamide by normal phase high performance liquid chromatography and UV detection. *J. Chromatogr. A* **1077,** 128–135 (2005).

128. HPLC assay for determination of acrylamide in roasted cooee.

129. Gianni, S. *et al.* HPLC-MS validation of QualisaFoo?? biosensor kit for cost-effective control of acrylamide levels in Italian coffee. *Food Control* **18,** 1267–1271 (2007).

130. Ndrzejewski, D. E. A., Oach, J. O. H. N. A. G. R., Ay, M. A. L. G. & Usser, S. T. M. M. Analysis of Coffee for the Presence of Acrylamide by LC-MS / MS. 1996–2002 (2004).

131. Go, V. Survey of acrylamide in Turkish foods by an in-house validated LC-MS method. **22,** 204–209 (2005).

132. Taylor, P. *et al.* Analysis of acrylamide by LC-MS / MS and GC-MS in processed Japanese foods Analysis of acrylamide by LC-MS / MS and GC-MS in processed Japanese foods. 37–41 doi:10.1080/0265203021000060887

133. Roach, J. A. G., Andrzejewski, D., Gay, M. L., Nortrup, D. & Musser, S. M. Rugged LC-MS/MS Survey Analysis for Acrylamide in Foods. *J. Agric. Food Chem.* **51,** 7547–7554 (2003).

134. Puignou, L., Galceran, M. T., Bermudo, E. & Oscar, N. Analysis of acrylamide in food products by in-line preconcentration capillary zone electrophoresis. **1129,** 129–134 (2006).

135. Geng, Z., Wang, P. & Liu, A. Determination of acrylamide in starch-based foods by HPLC with pre-column ultraviolet derivatization. *J. Chromatogr. Sci.* **49,** 818–824 (2011).

136. Delatour, T., Périsset, A., Goldmann, T., Riediker, S. & Stadler, R. H. Improved Sample Preparation to Determine Acrylamide in Difficult Matrixes Such as Chocolate Powder, Cocoa, and Coffee by Liquid Chromatography Tandem Mass Spectroscopy. *J. Agric. Food Chem.* **52,** 4625–4631 (2004).

137. Albishri, H. M. & El-Hady, D. A. Eco-friendly ionic liquid based ultrasonic assisted selective extraction coupled with a simple liquid chromatography for the reliable determination of acrylamide in food samples. *Talanta* **118,** 129–136 (2014).

138. Murkovic, M. Acrylamide in Austrian foods. *J. Biochem. Biophys. Methods* **61,** 161–167 (2004).

2. AIM OF THE PROJECT

My work was done in the scope of the IPCOS project – imprinted polymers as coffee sensors, a part of the MSCA financed Innovative Training Networks, allowing me to do half of the research in an industrial environment, and the other half in an academic environment. The industrial part of the project was executed at illycaffè's Aroma Lab and Demus Lab S.r.l., and the academical part at the Department of Chemical and Pharmaceutical Sciences at the University of Trieste and School of Biological and Chemical Siences at Queen Mary University of London. The main focuses of this thesis were:

1. Synthesis of molecularly imprinted polymers for selective recognition of 16-OMC and possible application to a sensing device.
2. Development of a colorimetric assay for quantification of Robusta in a mixture with Arabica.
3. Development of an HPLC-UV method for quantification of acrylamide in roasted coffee.

With the synthesis of molecularly imprinted polymers of cafestol and 16-O-methylcafestol, finding a simpler and less time-consuming way of extraction of the two diterpenes from the coffee matrix, compared to the one in the DIN 10779 method, with a possible future applicability for sensing purposes was attempted. To obtain the polymers, first cafestol and 16-OMC were isolated from commercially available roasted Robusta beans.

Next, functional monomers for cafestol and 16-OMC were chosen. The difference in the substitution on the carbon 16 between the molecules was explored for specific molecular recognition. In its polymerizable derivative, formation of a boronic ester was attempted with the vicinal diol of cafestol. In the polymerizable derivative of 16-OMC, formation of a carboxylic ester with the hydroxyl group and a π-methyl interaction with the remaining methoxy group was attempted. The polymerizable derivatives were used in polymerisations.

Polymers with different ratios of monomer to cross-linker to co-polymer were synthesized and upon the results of their characterisation and rebinding studies, the most optimal ones were selected for further testing. It is important to consider, that this method due to a recently published finding of 16-OMC in Arabica coffee it theoretically will not be capable of detecting less than 1% of Robusta in the mixture with Arabica due to the masking effect.[1]

Additionally, a colorimetric method for quantification of contamination of Arabica with Robusta was developed. Namely, preliminary studies have shown, that chloroform and dichloromethane extracts of Robusta and Arabica gave a characteristic colour upon treatment with a 30% solution of antimony(III) chloride in chloroform. In the UV-Vis spectra of the treated samples, interesting peaks at 726 nm and 819 nm were found, the first being characteristic for Robusta and the second for Arabica. With further optimisation of the preparation of coffee extracts, composition of the antimony(III) chloride solution, kinetic studies and selection of a working wavelength, development of a simple, fast and reliable method for quantification of contamination of Arabica with Robusta coffee was attempted.

Our final contribution to the improvement of quality control of coffee was development of an HPLC-UV method for quantification of acrylamide in coffee. By collaborating with Demus Lab S.r.l, and starting from their already developed GC-MS method for quantification of acrylamide, proper chromatographic conditions, detection wavelength and sample preparation were developed.

3. RESULTS AND DISCUSSION:

MIPs for cafestol and 16-OMC

3.1 Isolation of cafestol and 16-OMC

As commercially available cafestol and 16-O-methylcafestol hold a very high price, we have decided to isolate them on our own. For the isolation, a slightly adapted DIN 10779 method[13] was applied, consisting of three main steps. Extraction of coffee oil and saponification thereof were performed in illycaffe's AromaLab. Isolation of cafestol and 16-OMC was then performed. Several exractions were done to obtain enough or cafestol and 16-OMC for the following experiments..

For the extractions a commercial brand of ground roasted beans of *C. canephora* was always used sold under the brand Amigos, as the species contains cafestol and 16-O-methylcafestol in usable amounts[9]. *C. arabica*, on the other hand, contains cafestol in significant amounts and 16-OMC in minor amounts and is thus not as practical for the purpose of extraction.[1] Roasted beans were used, as coffee products available in the market are either roasted whole or ground beans or soluble coffee, made from roasted coffee beans.

3.1.1 Extraction of coffee oil

Soxhlet extraction of coffee oil has been performed in the first step, with methyl t-butyl ether as a solvent of choice. The type of extraction requires an assembly of a Soxhlet apparatus (**Figure 3.18**). For the purpose, coffee was weighed into a cellulose thimble and placed inside of the Soxhlet extractor, which was then connected to a round-bottom flask below and a condenser above it.

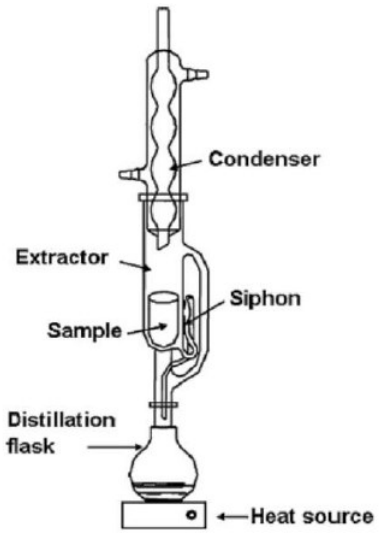

Figure 3.18: Soxhlet apparatus.[139]

The round-bottom flask, filled with solvent, was heated to reflux during the process, to allow for the circulation of the solvent and subsequent extraction of the coffee oil. Although the use of a cellulose thimble for our purpose could be debatable upon, considering that diterpenes have been reported to adsorb to cellulose coffee filters,[140] the continuous washing of the filter allowed for good yields upon isolation.

For the extractions, a water bath or an oil bath have been used as a heating source. The circulation of the solvent was greatly improved if the round-bottom flask was equipped with a stirring bar. The temperature of the heating source was maintained at 80°C and the extraction went on for 6 h. The time limit allows a compromise between the amount of coffee oil extracted and the degradation of the compounds present in it, as throughout the whole time of extraction the extract is collected in the round-bottom flask, most exposed to the heating.

Afterwards, the Soxhlet apparatus was disassembled and the solvent was removed under vacuum, leaving behind a brown oily residue with a pronounced smell of coffee. The obtained weights of coffee oil were in the range of 6 to 7 g, with an average of 6.30 g from about 60 g of coffee used per extraction. Extractions were performed to obtain a large enough amount of coffee oil and the weights of coffee oil after each of 15 extractions are presented in **Figure 3.2**.

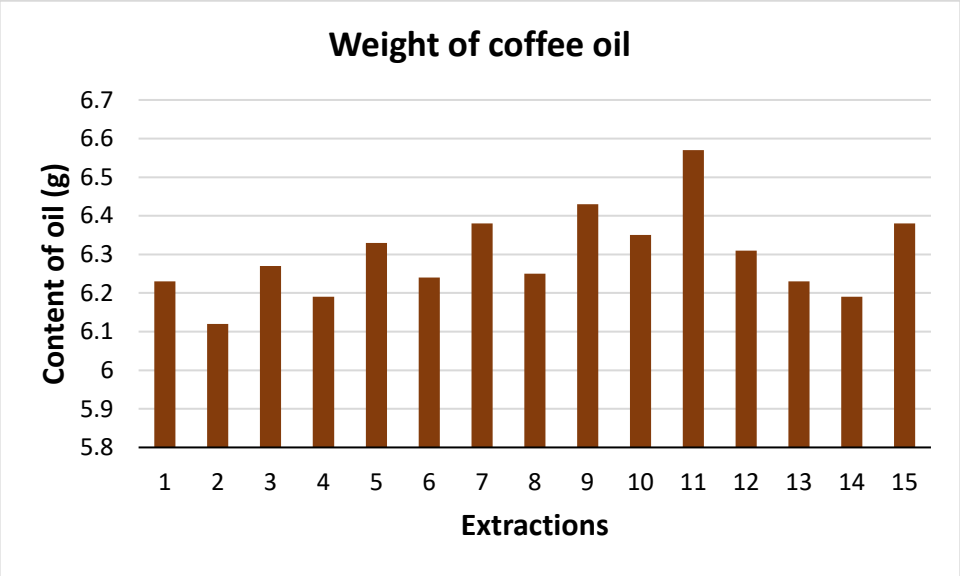

Figure 3.2: Weights of coffee oil, obtained through 15 extractions.

The yields of the extractions were between 10 and 11 %, with an average of 10.5 % and were calculated to the precise amount of coffee used in each case. Yields of 15 extractions are presented in **Figure 3.3**.

The yields of the extractions were in accordance with the literature.[9] The variability of the obtained amounts of coffee oil in our case depends on the amount of coffee used for the extraction, as we were always using the same brand of coffee. If different brands of Robusta would be used, the average particle size of the batch of coffee used could influence the yield of the extraction as well. The company reports a fine grind, proper for a Turkish preparation of coffee.[141]

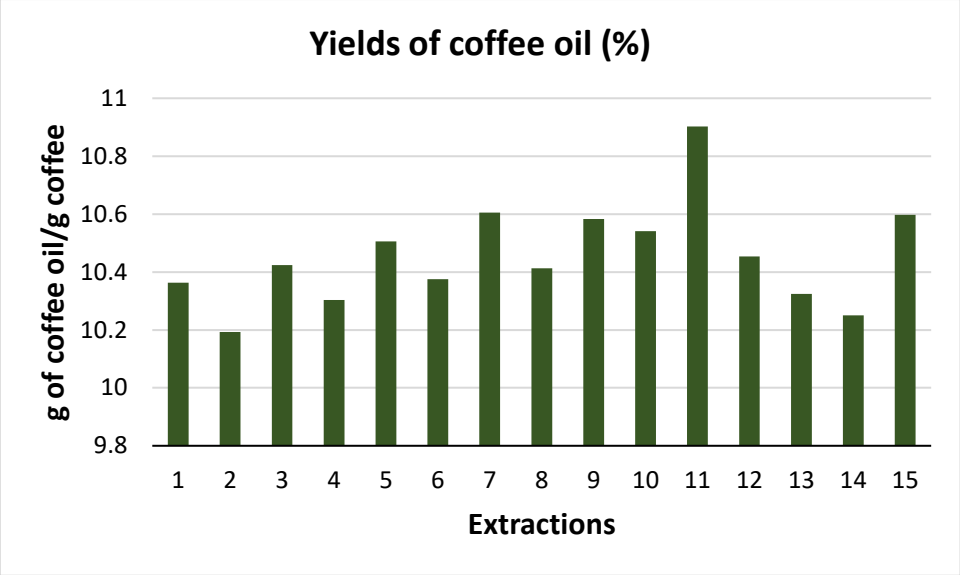

Figure 3.3: Yields of coffee oil, obtained through 15 extractions.

3.1.2 Isolation of the unsaponifiable fraction

As nearly all of cafestol and 16-O-methylcafestol in coffee are in the form of esters with fatty acids,[142] the next step in their isolation was saponification of coffee oil in a 10 % ethanolic solution of KOH. An ethanolic solution of KOH was used to allow dissolution of all components of the coffee oil. Upon the isolation of the unsaponifiable fraction, the issue we met was formation of a hardly separable emulsion during extraction in the separating funnel, suspected to form because of the presence of saponins and ethanol in the mixture. To avoid it, moderate shaking was applied. If the emulsion was already formed, addition of a small amount of NaCl usually aided in the separation of phases.

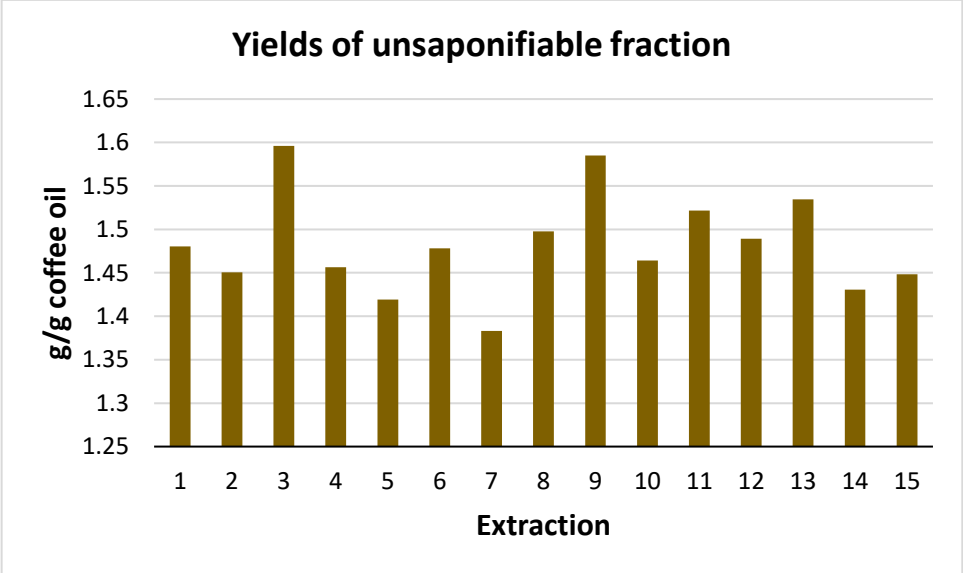

Figure 3.4: Yields of the unsaponifiable fraction per extraction, for 15 extractions.

On average, 0.893 g of unsaponifiable fraction was obtained, corresponding to 1.48 % (**Figure 3.4**). The variations of the obtained amounts of the unsaponifiable fraction are mostly connected to the loses of the organic material during imperfect separation of the phases in the separating funnel.

3.1.3 Isolation of cafestol and 16-O-methylcafestol

Cafestol and 16−OMC were isolated from the unsaponifiable fractions via "flash" column chromatography on silica gel. With gradient elution, using mixtures of petroleum ether and ethyl acetate from 4:1 to 1:1 as a mobile phase, cafestol and 16-OMC were in most cases successfully separated from impurities. The elution was monitored with thin layer chromatography, staining the chromatograms with an aqueous permanganate solution. On average, 62 mg of cafestol and 28 mg of 16-OMC were isolated, corresponding to 7.0 % and 3.2 % of the unsaponifiable fraction (**Figure 3.5**). The amounts of isolated cafestol and 16-OMC are consistent with the literature.[9]

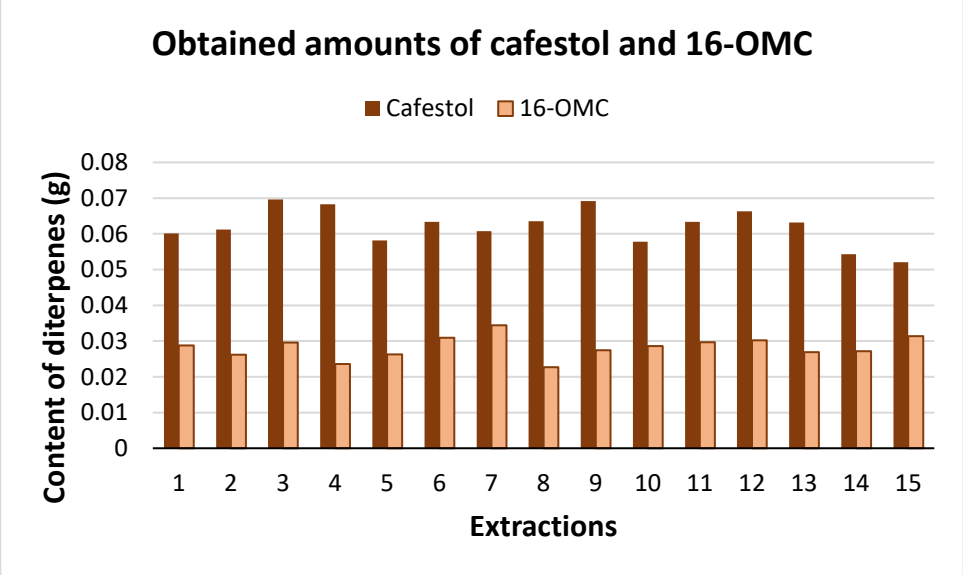

Figure 3.5: Contents of cafestol and 16-OMC in each extraction, for 15 extractions.

The contents of cafestol and 16-OMC throughout the extractions were variable, with lower levels of 16-OMC extracted, compared to the contents reported in literature.[10,42] A part of the variability originates in the losses of material during the coffee oil extraction step, the saponification step and column chromatography.

Should we have been using different brands of coffee, additional reasons as to why such differences may occur, are the geographical origin of coffee and different roasting procedures, causing different degrees of deterioration of the two diterpenes. This occurs because mostly the levels of cafestol depend greatly on the time of roasting and the temperatures used in the roasting processs.[9]

3.1.4 Further purification

When cafestol and 16−OMC were not isolated completely pure, additional purification was necessary. Usually another round of “flash” column chromatography on silica with isocratic elution was performed, using a mixture of acetonitrile and dichloromethane as a mobile phase sufficed for both diterpenes. The solvents were used in a ratio 95:5. 5% of methanol were initially considered instead of the 5% of acetonitrile, however the system with acetonitrile resulted in a better resolution of the peaks on the TLC, especially if the ratio of both diterpenes in the mixture was closer to 1:1.

The use of a mixture of petroleum ether and ethyl acetate was attempted but was less successful in dissolution and consequently application of 16-OMC to the column. When pure diterpenes were obtained, they were characterized with ^{1}H NMR, ^{13}C NMR, IR and mass spectroscopy.

3.2 Selection of functional monomers for cafestol and 16-OMC

Before the synthesis of molecularly imprinted polymers for cafestol and 16-OMC was attempted, functional monomers for both diterpenes needed to be selected, capable of selective molecular recognition. Cafestol and 16-OMC are both pentacyclic alcohols, in which a furane ring is fused to a kaurene skeleton.[9] The only difference between them occurs at carbon 16. In cafestol carbon 16 bears a hydroxy and a hydroxymethyl functional group, forming a vicinal diol. In 16-OMC, on the other hand, a hydroxymethyl and a methoxy group can be found (**Figure 3.6**).

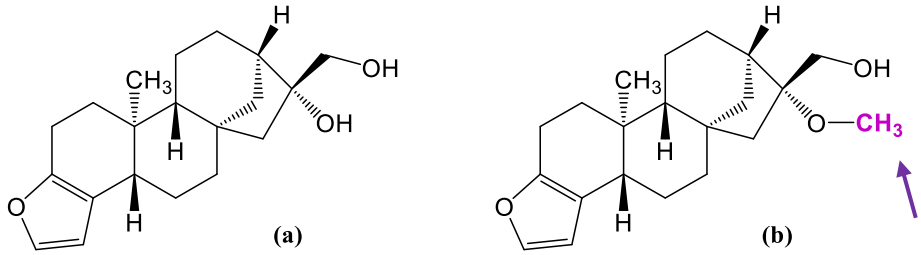

Figure 3.6: A difference between cafestol (a) and 16-OMC (b).

This minor, yet significant difference allows us to form different interactions towards a monomer for each compound, giving an opportunity to build a molecularly imprinted polymer selective for either cafestol or 16-OMC. Due to a high degree of similarity between the two molecules, we found that covalent imprinting would be the best approach for the formation of the imprinted polymers for the two diterpenes. This approach is believed to offer more specific interactions and more homogeneous binding sites for the templates, and requires synthesis of polymerizable derivatives of the template with a chosen functional monomer before the reaction of polymerization takes place[143].

In literature, two remarkably different approaches for molecular recognition of the groups present in each diterpene were found. Highly selective formation of boronic esters between boronic acids and vicinal diols were reported[144] and as such represent a very good opportunity for differentiation of cafestol from 16-OMC, since only cafestol of the two is a vicinal diol. On the other hand, π-methyl interactions could be an excellent solution for molecular recognition of 16-OMC due to the presence of a methoxy group in the structure.[145] As a covalent interaction, an ester bond between the remaining hydroxyl group of the diterpene and a carboxyl group of a functional monomer could be used.

The decision was a crucial criterion in the choice of functional monomers, as they should contain functionalities, capable of forming covalent interactions with the two diterpenes in vastly different ways. Additionally, although capable of surviving the reaction of polymerization, the formed covalent bonds should be able to break in mild enough conditions to allow removal of the templates from their corresponding polymers without damage to the polymeric skeleton.

Another important thing to consider was the size of the monomer and the position of the double bond and functional groups in its structure. Namely, with molecular weights of 316.44 and 330.16, respectively, cafestol and 16-OMC are relatively large structures. As we were attempting to import molecular recognition of just small parts of the two diterpenes into the polymers, choosing a big enough molecule of a monomer with an optimal arrangement of the double bond and the desired functional groups could greatly improve the selectivity of the molecularly imprinted polymer.

We focused mainly on derivatives of cinnamic acid, as the most appropriate functional monomers for both diterpenes. Containing a phenyl ring in the structure, they allow for a better control over the arrangement of the functional groups in the monomer and give an opportunity to form a π-methyl interaction with the methoxy group of 16-OMC. When the most suitable functional monomers have been chosen, polymerizable derivatives of cafestol and 16-OMC were synthesized.

3.2.1 Selection of functional monomers for cafestol

Due to the fact, that isolation of cafestol from coffee is a time-consuming and tedious process, and at the same time commercially available cafestol is very expensive, we decided to begin the process of selection by synthesizing a model molecule for cafestol. For the purpose, we chose (1-hydroxymethyl)-cyclohexanol (**1**, **Figure 3.7**).

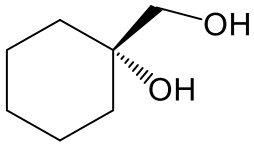

Figure 3.7: Structure of (1-hydroxymethyl)-cyclohexanol.

The vicinal diol moiety in its structure is positioned on a quarternary carbon, the same way it is found in the molecule of cafestol. Its skeleton, on the other hand, is a cyclohexane ring and is as such smaller than the kaurane skeleton of cafestol. This allows us to monitor the formation of a boronic acid in a less hindered environment.

Synthesis of the model molecule for cafestol

1 was synthesized from methylenecyclohexane via Sharpless dihydroxylation, using osmium(VIII) oxide as an oxidant and N-methyl morpholine as a co-oxidant[146]. The medium for the reaction was a mixture of acetone and water, and osmium(III) oxide was added in the form of a 2.5% solution in t-butanol.

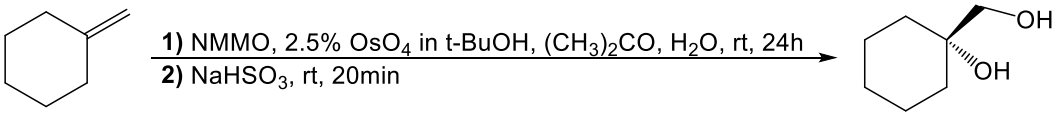

The work-up for the procedure was the addition of sodium bisulfite to stop the oxidation, dilution of the reaction mixture with water and extraction with the excess amount of ethyl acetate. As the yield of the reaction was very high at 96%, no additional purification was necessary, and the compound was used as such in the following experiments.

Selection of functional monomers for cafestol

The key characteristic of an optimal functional monomer for cafestol is a boronic acid moiety for the formation of a boronic ester via the vicinal diol. Namely, boronic esters can be formed in aqueous[147] and anhydrous[148] conditions and have been described as stable under the conditions of dilution radical polymerization[61]. Additionally, an appropriate size of the monomer molecule and a double bond, suitably positioned in its structure, are of high importance.

Considering those, an overlook on potentially useful commercially available monomers was done. Several structures were taken into account, however, the two satisfying our criteria the most were 2-[(E)-2-cyanoethenyl]phenylboronic acid (**3a**) and 4-(trans-2-carboxyvinyl)phenylboronic acid (**3b**, **Figure 3.8**).

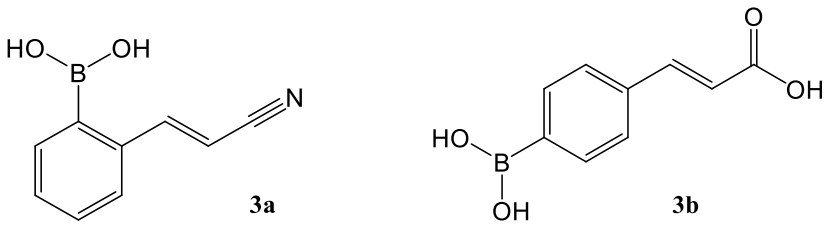

Figure 3.8: Structures of 2-[(E)-2-cyanoethenyl]phenylboronic acid (3a) and 4-(trans-2-carboxyvinyl)phenylboronic acid (3b).

Both phenylboronic acids contain an additional substituent in their structures. In the orto position of **3a,** (E)-2-cyanoethenyl substituent can be found, while in the para position of **3b** a trans-2-carboxyvinyl substituent. The double bond in both monomers resides in a conjugated system, in proximity of two different substituents. In **3a**, it is located near to a ciano group, known to be an electron acceptor with a substantial negative inductive effect. In **3b**, on the other hand, it is located near to a carboxylic group, as well known for its electron withdrawing properties and exhibiting a moderately negative inductive effect.

Due to being positioned close to the double bond, the ciano group, as well as the carboxylic group, should increase its reactivity during the synthesis of imprinted polymers. Both groups should also be able to create additional binding sites in the imprinted polymer, thus possibly aiding with the rebinding capability of the synthesized MIPs.

Additionally, the geometry of both monomers is different. The para substitution of **3b** is especially interesting, as it allows for a more elongated structure of the compound. This could have a beneficial effect in the process of imprinting cafestol, a relatively big structure, to which an elongated structure of **3b** could fit better. We therefore chose **3b** as a suitable functional monomer.

Synthesis of the polymerizable derivatives for the model molecule

To see if the chosen reaction works, before synthesizing a functional monomer for cafestol, a boronic ester for its model molecule (**1**) was synthesized. The reaction between **1** and **3b** was relatively simple, requiring a 1 to 1 molar ratio of both compounds. As a solvent, THF was used as a substitution of hexane, as none of the compounds was well soluble in the later:[148]

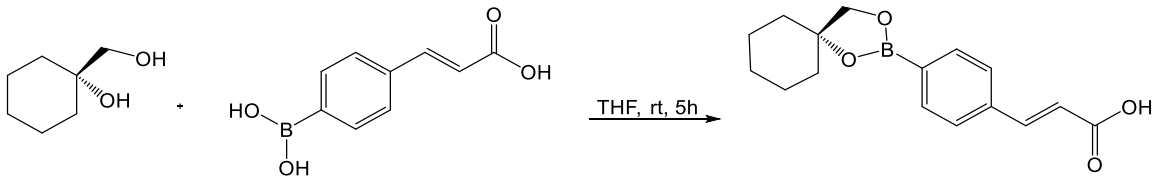

Monitoring of the reaction with TLC was sufficient, with the chromatogram stained with aqueous permanganate solution, to allow observing the formation of the product. The reaction finished after 5 h at room temperature and the yield of 53% was calculated from the ^{1}H NMR spectra. Due to the relative instability of the product, further purification was avoided. The same protocol was used for the synthesis of the polymerizable derivative of cafestol:

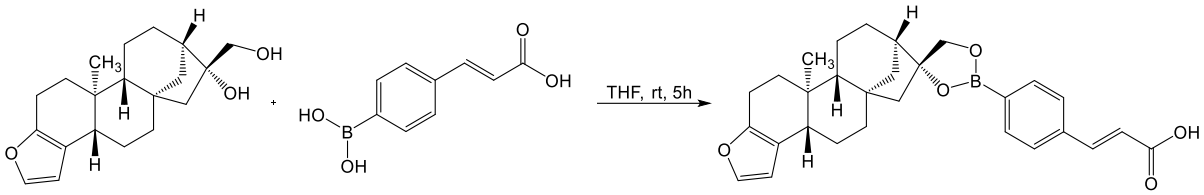

The reaction was comparably successful, with a slightly lower yield of 49%, again calculated from the ^{1}H NMR spectra. Further purification of the product was again avoided and the compound, as prepared, was used for the synthesis of molecularly imprinted polymers.

3.2.2 Selection of functional monomers for 16-OMC

For the same reasons of a tedious process of isolation of 16-O-methylcafestol from coffee, as met in the case of cafestol, and its high commercial price, a model molecule for 16-OMC was synthesized. A cyclohexane skeleton was again chosen to simplify the kaurene structure of 16-OMC and the substituents of interest on the quaternary C_{16} atom of the diterpene were transferred to the model, forming a (1-methoxycyclohexyl)-methanol (**5, Figure 3.9**).

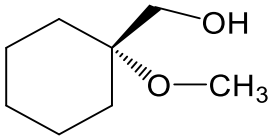

5

Figure 3.9: Structure of (1-methoxycyclohexyl)-methanol (5).

In the molecule, a modified vicinal diol is present, with one hydroxy group methoxylated. This substitution is the only thing kept from the original structure of 16-OMC, as it represents the only part of the molecule different from cafestol. The methoxylation of one hydroxy group gives us an opportunity to consider vastly different interactions between the template and the functional molecule.

Synthesis of the model molecule for 16-O-methylcafestol

5 was synthesized from cyclohexanone in two steps. First, through a Corey Chaykovsky epoxidation, 1-oxaspiro[2.5] octane (**4**) was formed:[149]

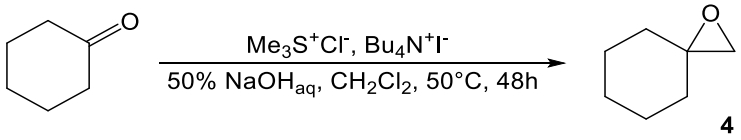

4

A bi-phase reaction was performed, with a phase of dichloromethane and a phase of 50% aqueous NaOH solution. Trimethylsulfonium bromide was deprotonated in basic medium, thus forming the corresponding ylide. The ylide then reacted as a nucleophile with the carbonyl group of the cyclohexanone. An oxygen anion forms during the reaction, attacking the now electrophylic ylide carbon, a good leaving goup, as an intramolecular nucleophile. Thus an epoxide (**4**) is formed and a side product of dimethylsulfide[150].

As trimethylsulfonium bromide was insoluble in dichloromethane, tetrabutylammonium iodide was used as a phase-transfer catalyst. Vigorous mixing was applied throughout the reaction. Upon its completion, the organic phase was collected and dried over Na_2SO_4. The solvent was removed under vacuum and the residue was immediately used for reaction of opening of the epoxide ring, assuming 100% yield:

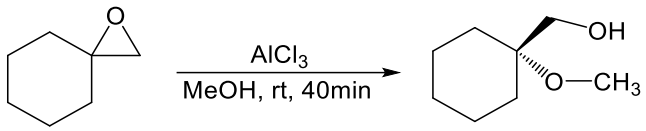

Methanol was used as a protic solvent and a nucleophile, and aluminium(III) chloride as a Lewis acid. The reaction is initiated by the formation of a complex epoxide-Lewis acid, which is then opened by an attack of the nucleophilic molecule of methanol on the more substituted carbon. The final product is **5**. The reaction was rapid and disappearance of the epoxide was monitored with TLC. Upon completion, the solvent was removed under vacuum and the residue was purified on via column chromatography.

Selection of functional monomers for 16-OMC

Compared to cafestol, one hydroxy group of the vicinal diol of 16-OMC is methoxylated. This prevents us from forming a boronic ester as a mean of molecular recognition, however, it does bring us another approach. On one hand, we have a possibility to form an ester bond through the remaining hydroxy group with the functional monomer of choice. This, when synthesizing a MIP, would help us to keep the molecule of 16-OMC in place during polymerization. The methoxy group, on the other hand, can participate in a π-methyl interaction with an aromatic ring and serves as a recognition site. This way, the aspect of molecular recognition is completely different from the one for cafestol and allows us a better attempt at increasing the selectivity of future MIPs.

The π-methyl interaction and the ester bond are suitable for the purpose, as they are cable to survive the polymerisation conditions, when the solvent of the polymerization is chosen well. At the same time, it is possible to break both types of interactions under mild conditions, by hydrolysis for the ester and by switching the solvent for the π-methyl interaction. This allows us to synthesize the molecularly imprinted polymer and remove the template afterwards. In the created MIP, the interactions formed when re-binding the template would be hydrogen bonds where hydrolysis of the ester took place, and π-methyl interactions where they were present during the synthesis of the MIP.

Based on that, our expectations of an optimal functional monomer for 16-O-methylcafestol were presence of a carboxylic group as a prerequisite for the formation of an ester bond, presence of an aromatic ring to allow the formation of a π-methyl interaction and possibly take place in π-π stacking with the furan ring of 16-OMC, and a properly positioned double bond. The size of the monomer was also of importance, to allow for the formation of big enough pores in the MIP to be able to re-bind the relatively big structure of the diterpene.

All the requirements were met in the structure of trans-cinnamic acid (**Figure 3.10**), consisting of a phenyl ring and a carboxylic group, connected with an ethenyl chain inside a conjugated system. With a double bond in between the phenyl ring and the carboxy group, it allows for the two substituents to be positioned optimally, although in a relatively rigid system. It is necessary to consider, that upon the polymerisation, the double bond in the monomer is transformed into a single bond, allowing rotation of the previously planar molecule and thus an even better adjustability of the position of the phenyl ring in respect to the position of the carboxylic group.

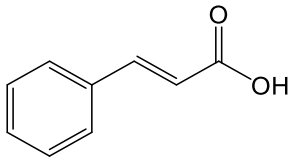

Figure 3.10: Structure of trans-cinnamic acid.

To expand our selection of possible monomers, several related compounds were considered. Among those, derivatives of cinnamic acid with a longer alkenyl chain between the phenyl ring and the carboxylic group, compounds with an additional phenyl substituent, and finally, derivatives with a heteroaromatic ring instead of the phenyl ring, as it was reported in literature that especially N-heteroaromatic compounds can give rise to an even greater π-methyl interaction (**Figure 3.11**).[151]

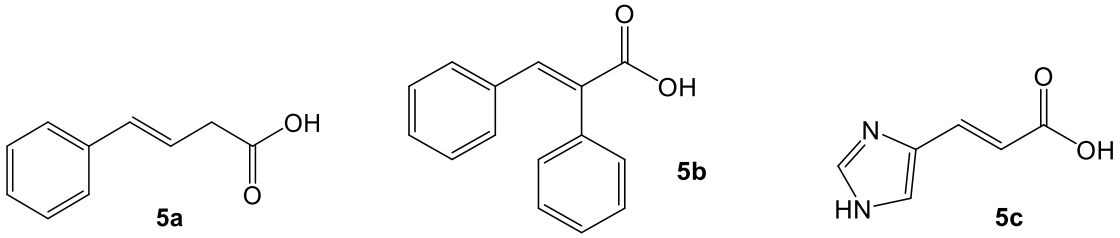

Figure 3.11: Derivatives of cinnamic acid with a longer alkenyl group (5a), with an additional phenyl substituent (5b) and an N-aromatic ring (5c).

Upon a search for commercially available compounds, theoretically most suitable functional monomers were chosen to be tested via NMR titrations, to observe interactions between the chosen functional monomer and **5** and choose the optimal one for the synthesis of the MIP.

3.2.3 NMR titrations

As the hydroxy group of **5** was already reserved for the formation of an ester bond with the carboxylic group of the monomer, the main focus of NMR titrations was observing the interactions between the methoxy group of **5** and the aromatic ring of the functional monomers. Using a model molecule for 16-OMC with a simple cyclohexane skeleton instead of the massive structure of the diterpene, was in this case advantageous as it allowed us to observe the interactions of interest with minor interferences.

To perform the titrations, a solution of the template molecule was prepared in $CDCl_3$ or DMSO-d_6, depending on the solubility of the tested functional monomer. Ideally, $CDCl_3$ was used, as it allows formation of a more intensive π-methyl interaction. To get information about the intensity of the π-methyl interaction in DMSO was also necessary, as it was the solvent of choice in the subsequent polymerisation process. First, spectra of the template molecule and the tested monomer were recorded for orientation, then several molar equivalents of a chosen monomer were added to the solution of the template. After every addition of the functional monomer, an ^1H NMR spectra was recorded. The shifts of the signal of the methoxy group of the template molecule were always observed, originally found as a singlet at 3.21 ppm in $CDCl_3$ and 3.08 ppm in DMSO-d_6.

The shifts of the signal after every addition were always deducted from the shift of the signal of the methoxy group of **5**, and the absolute differences between the shifts were plotted to added equivalents. The differences after the addition of the 12th equivalent of the monomer were compared between all the monomers tested. The one with the highest difference in the shift was selected as the most optimal monomer, in view of the biggest π-methyl effect.

NMR titration of MTBE with toluene

With the first titration the π-methyl effect was investigated on a simple model. As an aromatic system toluene was used, and as a template methyl t-butyl ether (**Figure 3.12**), containing several methyl groups and a methoxy group. By choosing this combination, we wanted to see to which extent the π-methyl effect generally affects the shift of the signal of protons of a methoxy group in an ^1H NMR spectrum.

Figure 3.12: Structures of methyl t-butyl ether (left) and toluene (right).

The titration was performed in $CDCl_3$ to allow optimal conditions for the formation of a π-methyl interaction. A 20 mM solution of methyl t-butyl ether was prepared, representing 8 µmol of the compound. First, twice 0.5 molar equivalents of toluene were added, each representing 4 µmol, then one by one molar equivalent of toluene, until there were 12 added molar equivalents in the mixture.

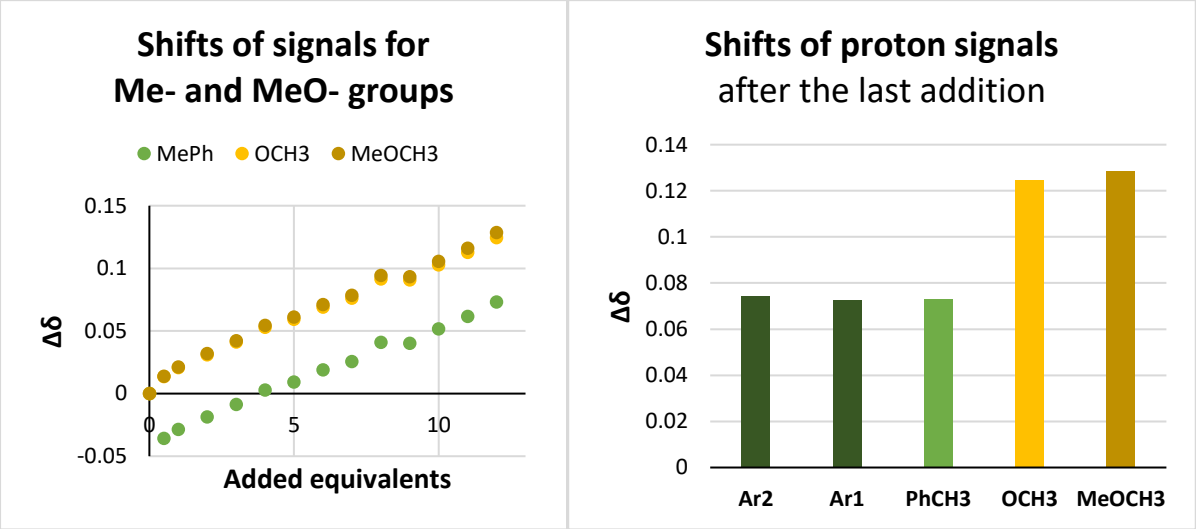

Figure 3.13: Graph of shifts of signals for Me- and MeO- groups (left) and graph of shifts of proton signals after the addition of 12 molar equivalents of toluene.

We can see a relatively big shift of the protons of the methoxy group of MTBE upon the twelfth added molar equivalent of toluene, at 0.125 ppm, leading us to believe a π-methyl interaction influences the environment of the protons greatly. Similarly, the shift of the protons of the methyl group of MTBE moves for 0.128 ppm, confirming the theory of the existing π-methyl interactions in the system. Interestingly, the signal of methyl groups in the molecules of toluene is affected by the interaction as well, causing a change in the shift of 0.073 ppm.

Finally, as a consequence of the π-methyl interaction, the signals of the aromatic protons are affected as well, causing their signals to move for 0.074 and 0.073 ppm. The changes of the shifts increase in a linear manner, making it impossible to calculate the binding constants. In **Figure 3.13**, plots of changes in the shift upon the additions of toluene are presented.

NMR Titrations of 5 with toluene and imidazole

As it has been reported in literature, that N-heteroaromates can cause an even more intensive π-methyl effect with methyl ethers, due to the dipole−dipole interactions between the C-O bond of the ether and the N- heterocyclic aromatic dipole.[152] We wanted to investigate, if this is valid also for our model molecule. **5** was therefore titrated with toluene and imidazole, to give us enough data to decide in which direction to continue our search for the optimal functional monomers (**Figure 3.14**).

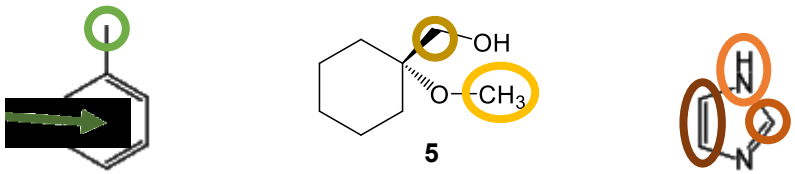

Figure 3.14: Toluene (left), (1-methoxycyclohexyl)methanol (5) and imidazole (right).

Up to 12 molar equivalents of each compound were added to 8 μmol of the two compounds in two separate experiments and the shifts of the substituents were calculated and plotted to the number of added molar equivalents, to observe the presence of interactions. The interactions we were expecting were of π-methyl nature and hydrogen bonds.

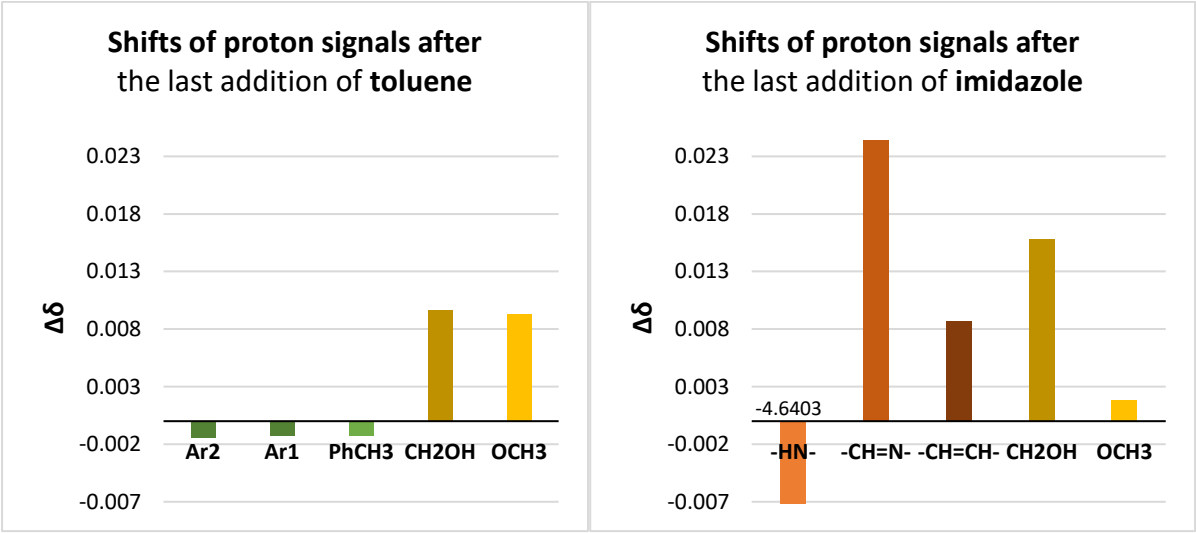

Figure 3.15: Graphs of shifts of proton signals in the template and monomers after the last addition of toluene (left) and imidazole (right).

In **Figure 3.15**, shifts of substituents involved in the observed interactions are presented. According to the results, we can clearly see, that the effect of hydrogen bonds is far more imposing, compared to the effect of π-methyl interactions in both experiments.

When titrated with any of the two aromaties, the signals of protons of the methoxy group and the protons on the carbon next to the hydroxy group of the template exhibit a shift in their corresponding spectrum. The shift of the protons on the carbon, next to the hydroxy group, is much bigger when the titrant is imidazole, as it gives many more opportunities for the formation of hydrogen bonds, not only intramolecularly in the molecule of the template itself, but also with–N= and –NH– groups of imidazole. This is well observed also in shifts of the protons on all atoms of the imidazole ring and explains a very big shift of the signal representing the –NH– group.

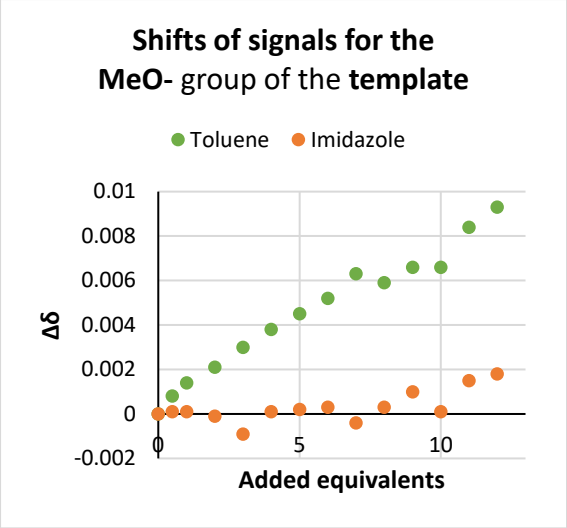

Figure 3.16: Shifts of signals for the MeO- group of the template after the final addition of toluene and imidazole.

On the other hand, when the titrant is toluene, the shift of the signal of the protons next to the hydroxy group is much smaller and similar to the shift of the signal of the methoxy group, as the only opportunity for the formation of hydrogen bonds is intramolecularly.

The signal representing the methoxy group of the template, is, in opposite, much bigger when the titrant is toluene. Considering that hydrogen interactions are not as prominent in this case, they leave room for more intensive π-methyl interactions. Their presence is confirmed by well observable shifts of aromatic protons in toluene upon increasing the number of added equivalents of the titrant.

The shift of the signal of the methoxy group is much smaller when the titrant is imidazole, due to more dominant hydrogen interactions. In case of both titrations, the signal shift to number of added equivalents relationship is linear (**Figure 3.16**).

NMR Titrations of 5 with derivatives of cinnamic acid

As our results confirmed the presence of a π-methyl interaction during the titration of the template molecule with toluene, we moved on to potential functional monomers. Hydrocinnamic, trans-cinnamic, phenylbutyric and phenylvaleric acid were tested. All of them contain a phenyl ring and a carboxylic group in their structure, connected with 2 to 4 carbon atoms (**Figure 3.17**).

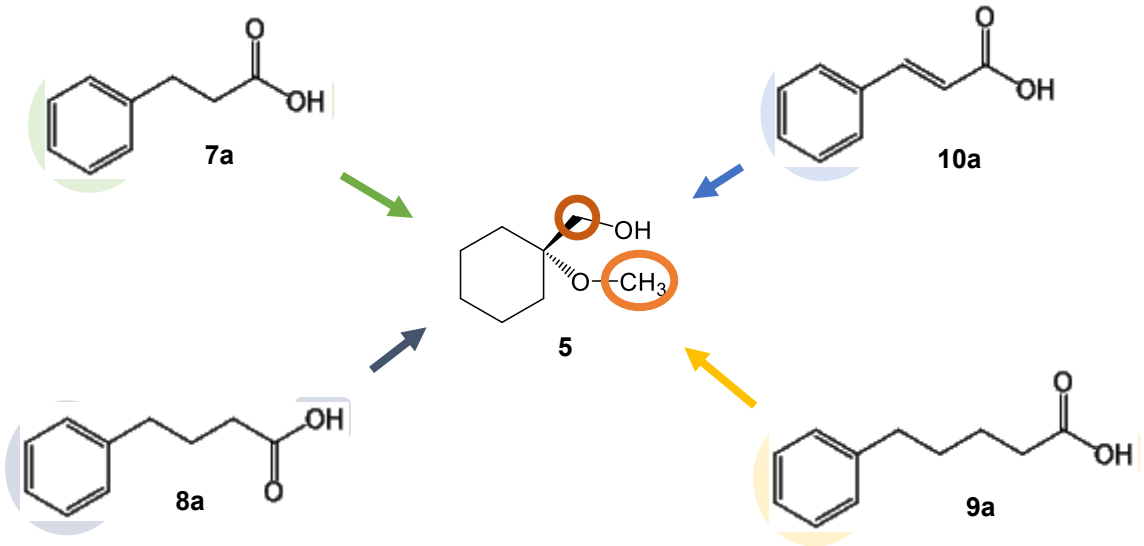

Figure 3.17: Structures of hydrocinnamic acid (7a), trans-cinnamic acid (8a), phenylbutyric acid (9a), phenylvaleric acid (10a).

Hydrocinnamic acid (**10a**) is in essence just hydrogenated trans-cinnamic acid, however with testing both we have gotten some insight on what happens to the interactions between the template and the functional monomer upon losing the double bond during polymerization. Up to 12 molar equivalents of each compound were added to 8 μmol of the template in two separate experiments to form a 10 mM solution. The shifts of the substituents were calculated and plotted to the number of added molar equivalents, to observe the present interactions. The interactions we were expecting were of π-methyl nature and hydrogen bonds (**Figure 3.18**).

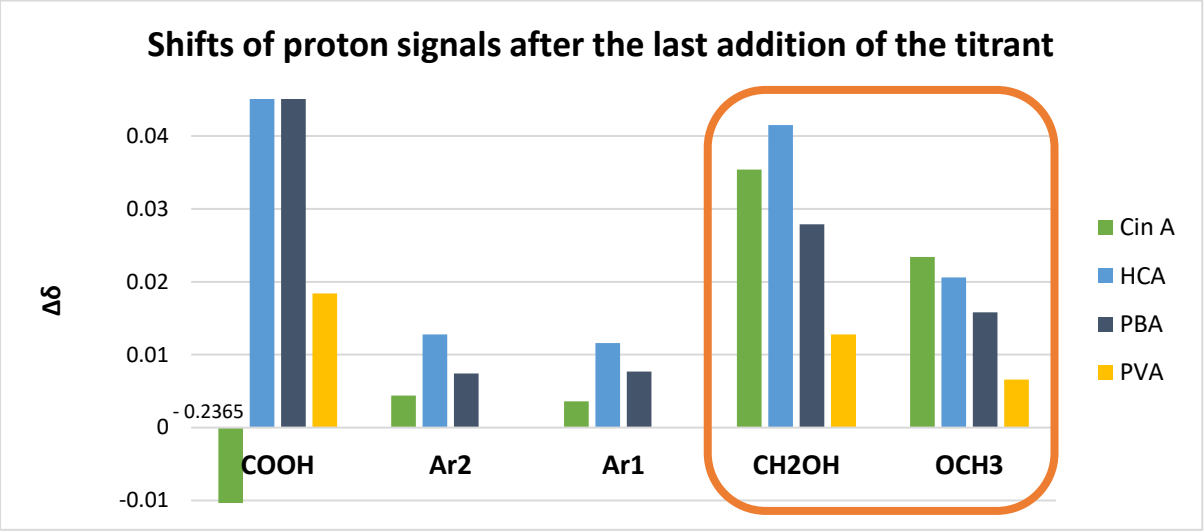

Figure 3.18: Shifts of relevant proton signals after addition of the last molar equivalent of the titrants.

When observing the presence of hydrogen bonds, we were mostly focusing on the changes in proton shifts of the signals for the -COOH group in the monomers and the -CH_2OH and -OCH_3 groups in the template molecule. Namely, all of them contain a hydrogen bond donor or a hydrogen bond acceptor. It is immediately noticeable, that hydrogen bonds play a much more imposing role in the sum of interactions between the two molecules, considering the differences in the shifts of the signals for the -COOH protons were in all titrations the biggest. Consequently, in the spectra of the template, the differences in the shifts of proton signals on the carbon next to the hydroxy group, are with all the titration attempts more noticeable when compared to the differences of the signal for the methoxy group.

Nevertheless, the π-methyl interaction is also present, confirmed by the changes in the original shifts of the aromatic protons of the monomers through titrations. They appeared in all cases but when the titrant was **9a**. One possible explanation for this phenomenon is in the length of the alkyl or alkenyl chain in the monomers. It is possible, that with a longer alkyl chain between the phenyl and carboxyl end groups in the system we established, the possibility of formation of a π-methyl interaction decreases, due to stronger hydrogen bonds displacing the π-methyl interactions.

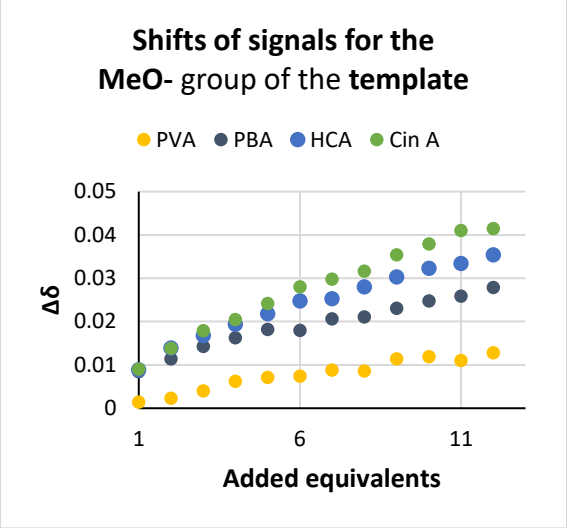

Figure 3.19: Shifts of signals for the MeO- group of the template after the final addition of titrants.

At the same time the phenyl group on the other side of the alkyl chain is now much further away, making it more challenging to maintain a good π-methyl interaction. The fact, that the difference in the signal of the methoxy group becomes smaller with the length of the alkyl chain in between the tested titrants, confirms this theory.

After the addition of all molar equivalents of the titrants, the biggest difference in the signal for the methoxy group of the template occurs when the titration is performed with **7a**. Soon to follow is the difference occuring in the titration with trans-cinnamic acid. This result lead us to believe, that should we use **10a** as a functional monomer, the π-methyl effect would remain even after the synthesis of the polymer, as the absence of double bond in **9a** only slightly decreases the difference in the signals of the methoxy group (**Figure 3.19**).

NMR Titrations of 5 with imidazoleacrylic acid

Different from the previous ones, this round of titrations was performed in DMSO-d_6 rather than in $CDCl_3$, due to poor solubility of imidazoleacrylic acid in the latter. Imidazoleacrylic acid is in structure very similar to trans-cinnamic acid, however with an imidazole ring substituting the phenyl ring of the trans-cinnamic acid.

Figure 3.20: Structures $CDCl_3$ (left) of and DMSO-d_6 (right).

Opposite to the non-polar $CDCl_3$, where hydrogen bonds and π-methyl interactions can be well monitored, DMSO-d_6 is a polar solvent (**Figure 3.20**). With the oxygen in its structure it might interfere when observing the hydrogen bonds between the monomer and the template. At the same time, due to the two methyl groups in its structure, it might also interfere with the formation of π-methyl interactions between the template and the monomer. For those reasons, another titration of **5** with **10a** was performed, this time in DMSO-d_6, to allow comparison of the results with the ones obtained for the two monomers (**Figure 3.21**).

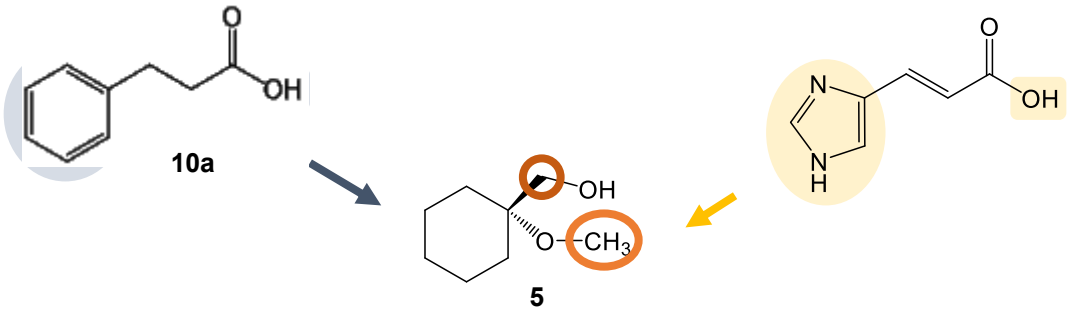

Figure 3.21: Trans-cinnamic acid (10a), (1-methoxycyclohexyl)methanol (5) and imidazoleacrylic acid (right).

Up to 12 molar equivalents of the monomer was added to the template in two experiments, to observe the interactions between the monomers and the template. Again, hydrogen bonds and π-methyl interactions were expected, although perhaps less intensive than in the experiments before, to the interference of the solvent (**Figure 3.22**).

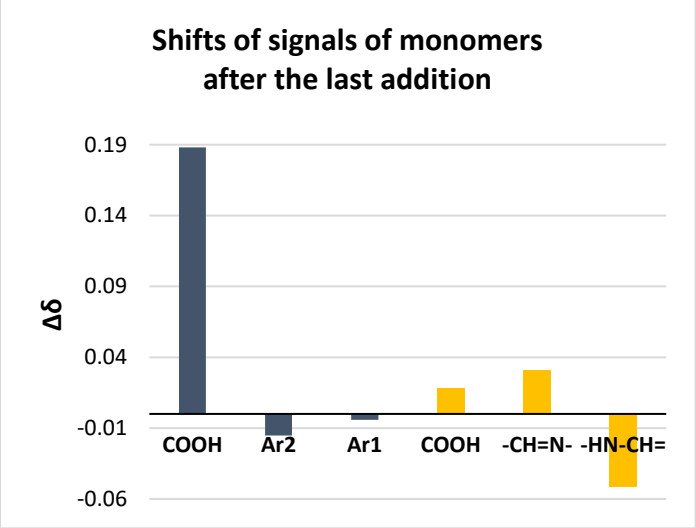

Figure 3.22: Shifts of signals of monomers after the addition of the last equivalent.

Functional groups of the two monomers, most probably involved in formation of hydrogen bonds, are -COOH in both, cinnamic acid and imidazoleacrylic acid, and the -NH- part of the imidazole ring in imidazoleacrylic acid. Shifts of signals, representing their protons, are noticeable, however substantially less when comapred to the shifts appearing during titrations in $CDCl_3$.

When observing proton signals of **5**, an additional signal in the spectrum can be found. Representing the -OH group, it is not visible during the titrations in $CDCl_3$, due to rapid exchange of the proton with traces of water in $CDCl_3$. The shifts of this signal during titration further confirm formation of hydrogen bonds between the monomers and the template, a bit more imposing when the titrant is trans-cinnamic acid.

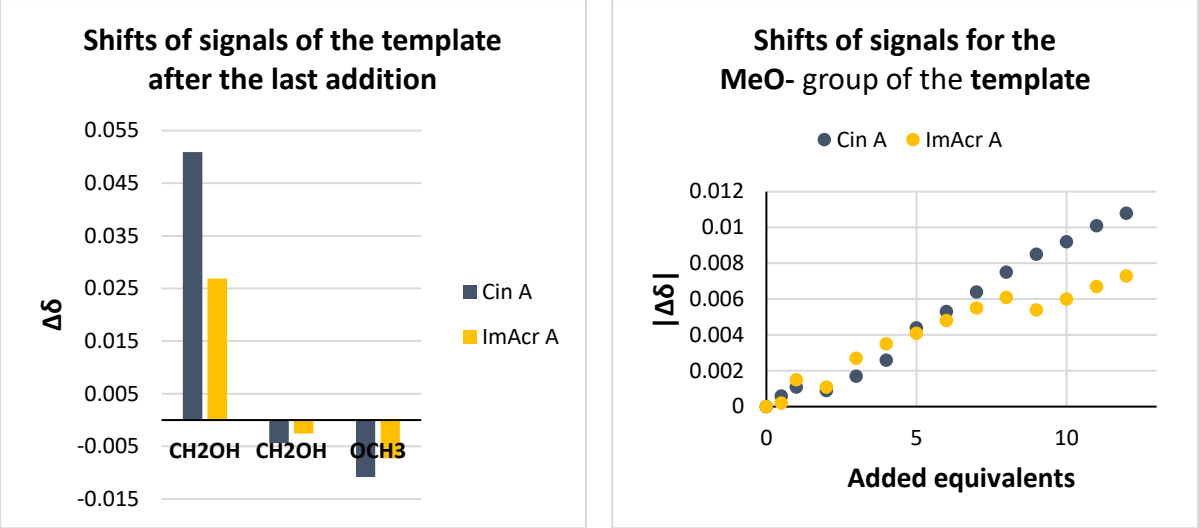

Figure 3.23: Graphs representing shifts of signals of the template after the last addition of the monomer (left) and shifts of signals for the MeO- group of the template throughout the titration (right).

Formation of the π-methyl interaction is also observable in both cases, and again more imposing when the template is titrated with trans-cinnamic acid (**Figure 3.23**). Additionally, the π-methyl effect after the addition of the 12th molar equivalent of trans-cinnamic acid seems to be less intensive in DMSO-d_6 than in $CDCl_3$. As due to interferences of the solvent such a result was expected, we hope the decreased occurrence of π-methyl interactions in presence of DMSO will not decrease the formation of a selective recognition site in the MIPs during the forthcoming polymerisations.

NMR titration of 5 with methyl trans-cinnamate (6)

As 10a was the most promising monomer during the titrations, we wanted to examine its capability of formation of π-methyl interactions more thoroughly. We were particularly interested in reducing the number of positions where a hydrogen interaction can be formed. For the purpose, we decided to convert the monomer into its methyl ester (**Figure 3.24**).

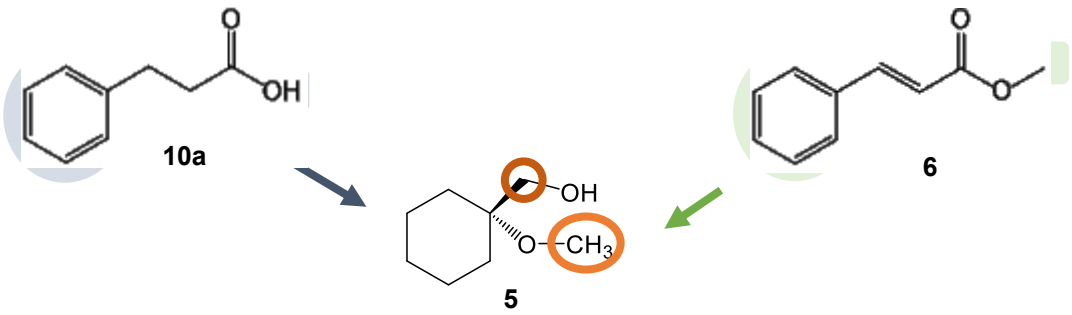

Figure 3.24: Trans-cinnamic acid (10a), (1-hydroxycyclohexyl)methanol (5) and methyl trans-cinnamate (6).

Synthesis of methyl trans-cinnamate (6)

The synthesis of **6** was performed via Fischer esterification, a reaction starting with a carboxylic acid in presence of an alcohol as a solvent and a Lewis or Brønstedt acid as a catalyst. During the reaction, the carbonyl group in the carboxylic substituent undergoes an addition of a proton and thusly formed carbocation a nucleophilic attack of the alcohol to give a tetrahedral intermediate. With two equivalent hydroxy groups. Upon a shift of a proton and subsequent elimination of one of the hydroxy groups, an ester is formed:

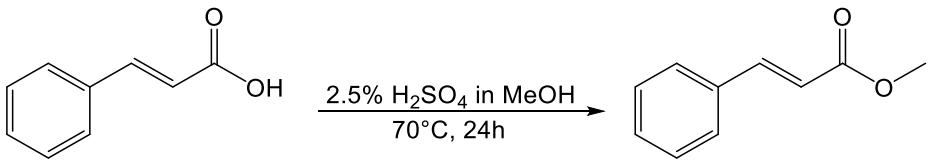

NMR titration

Up to 12 molar equivalents of methyl trans-cinnamate were added to 8 µmol of the template in two separate experiments to form a 10 mM solution in $CDCl_3$. To better observe π-methyl interactions, the shifts of signals upon every addition were plotted to the number of added equivalents of the titrant.

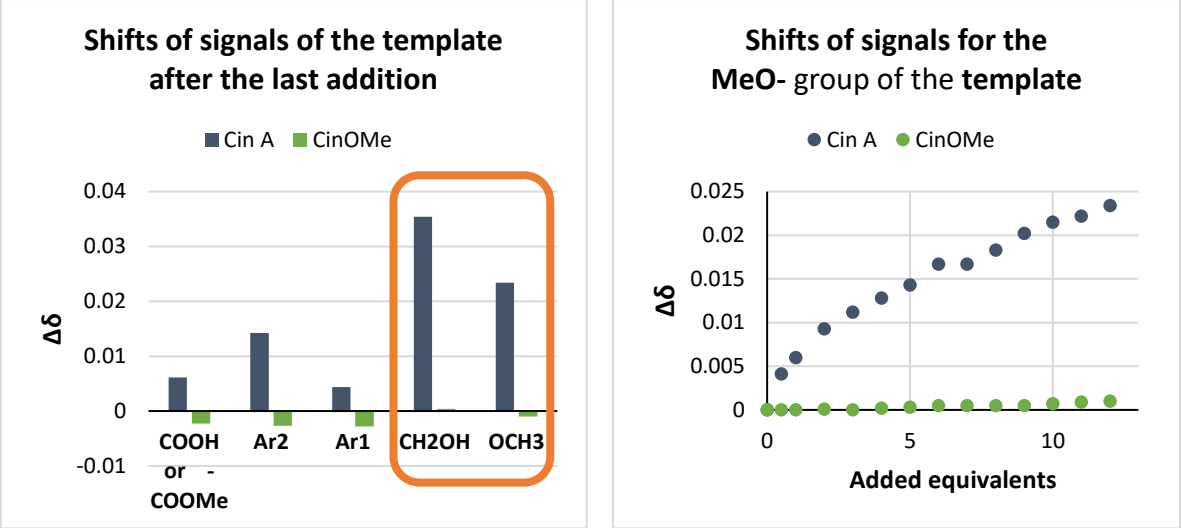

Figure 3.25: Graphs representing shifts of signals of the template after the last addition of the monomer (left) and shifts of signals for the MeO- group of the template throughout of the titration (right).

We can immediately see that both, shifts of signals due to hydrogen bonds and shifts of signals we previously connected to π-methyl interactions, decreased when the titrant was **6** (**Figure 3.25**). This behaviour was expected for hydrogen bonds and can be well explained for the signal of the methoxy group. Namely, the oxygen of the methoxy group is a hydrogen acceptor, also taking part in the formation of hydrogen bonds between the titrant and the template. As we removed the hydrogen on the electronegative oxygen of the carboxylic group in **10a** by forming its methyl ester, we also took away the possibility of formation of an intermolecular hydrogen bond between the oxygen of the methoxy group and a suitable substituent in the molecule of the titrant.

3.2.4 Determination of the proper length of the alkyl chain

To ensure that trans-cinnamic acid would cause a significant enough recognition effect in the MIP, we attempted to mimic the setting inside of a future MIP by synthesizing esters of **5** with **7a**, **8a** and **9a**. As none of the acids contain a double bond in the structure, and all of their carboxylic groups are connected with the hydroxy group of **5** into an ester bond, we were able to get a more precise insight into the formation of the π-methyl interaction.

The three acids contain an ethenyl, propenyl or butenyl chain as a linker between the phenyl ring and the carboxylic group, so the synthesis of the ester would give us an additional confirmation about the optimal number of carbon atoms between the two functionalities for the best presented π-methyl effect.

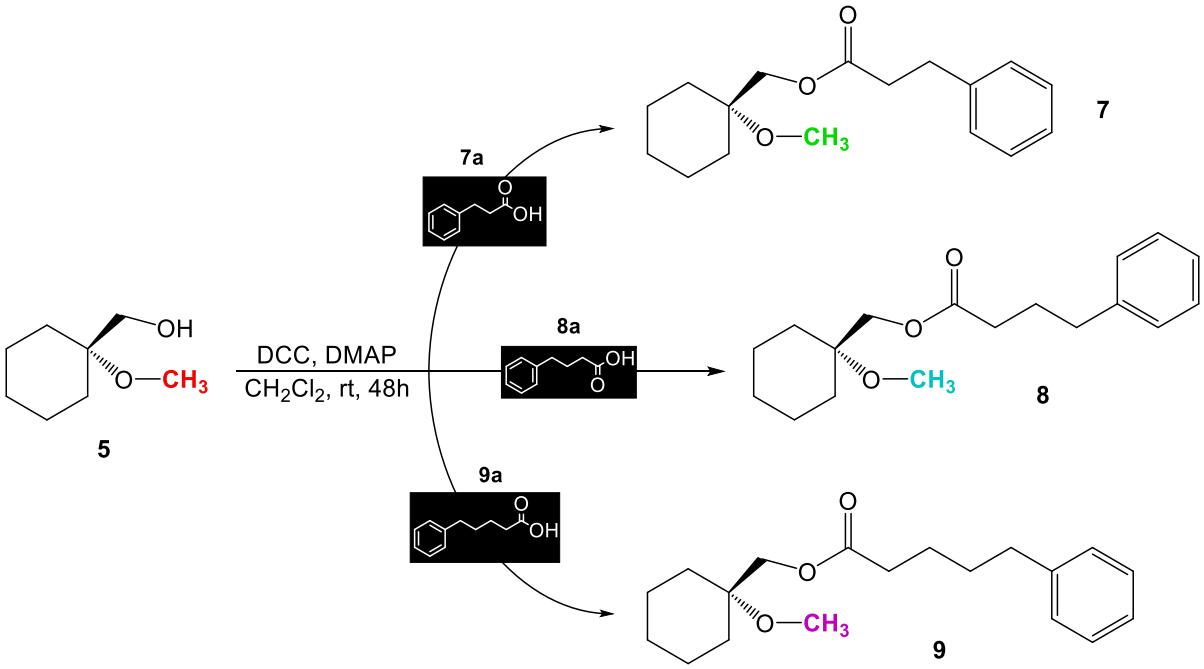

Figure 3.26: Esterifications of 5 with hydrocinnamic acid (7a), phenylbutyric acid (8a) and phenylvaleric acid (9a), yielding esters 7, 8 and 9.

The esters were synthesized via Steglich esterification[153] (**Figure 3.26**). The reaction proceeds via activation of the carboxylic group with dicyclohexylcarbodiimide in presence of 4-dimethylaminopyridine as an acyl group transfer agent. The by-product of the reaction is therefore in dichloromethane poorly soluble dicyclohexyl urea, easily removable with filtration prior to the work-up. The yields of the three esters were comparable.

^{1}H NMR spectra of purified esters were recorded in $CDCl_3$. The signals of the protons of their methoxy groups were compared with the signal of protons of the methoxy group of **5** (**Figure 3.27**). It was assumed, that bigger shifts of the signals are correlated with a greater π-methyl effect.

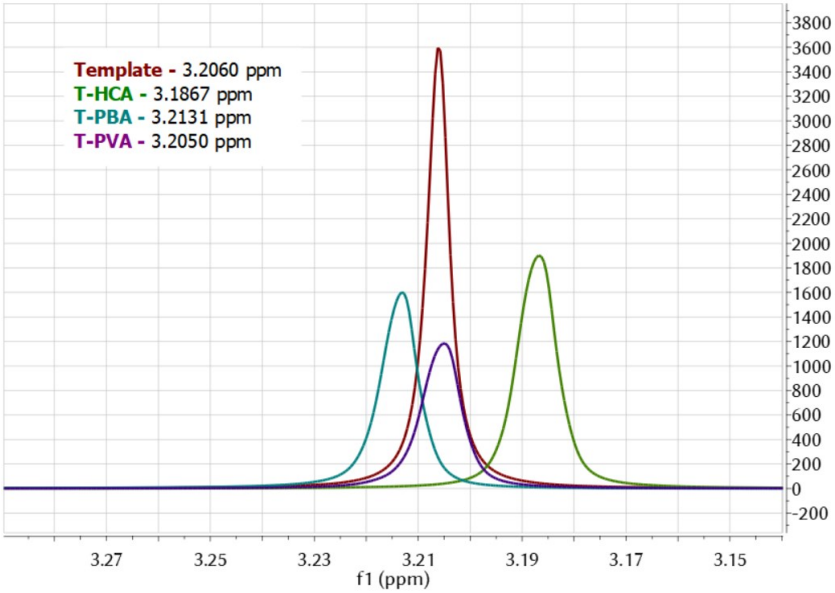

Figure 3.27: Overlapped ^{1}H NMR spectra of all three esters in $CDCl_3$.

The biggest deviation occurs in the spectra of the ester **7**, predicting the greatest π-methyl effect when the phenyl ring and the carboxylic group are connected with two carbon atoms. This result further confirms the choice of **7a** as the optimal functional monomer for 16-O-methylcafestol, eventhough the obtained shifts are substantially lower than the ones, reported in the literature.[152]

Titration of T-HCA with D_2O

Although we already connected the shift of the signal of the methoxy group in the ester with the formation of a π-methyl interaction, we have seen before, that the shift could partially also occur due to the presence of hydrogen bonds. To see which kind of interaction prevails, NMR titration of the ester with D_2O was performed. Addition of D_2O should have an influence on the shift of the signal of the methoxy group in the molecule, if the prevailing interactions would be hydrogen bonds.

40 µmol of **7** in a 50 mM solution in $CDCl_3$ were titrated with up to 12 molar equivalents of deuterated water, with each addition consisting of 2 molar equivalents. Each time a ^{1}H NMR spectrum was recorded and compared with the spectrum of the ester before additions (**Figure 3.28**).

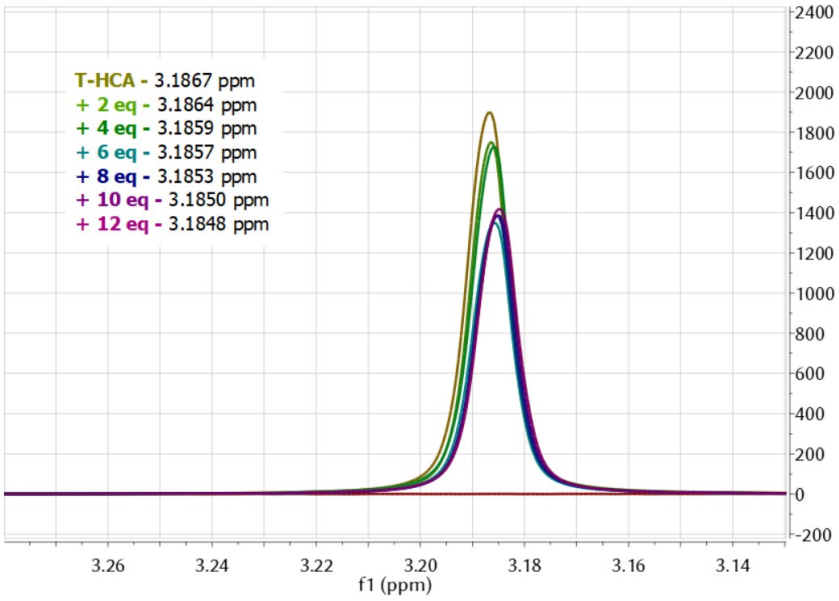

Figure 3.28: Overlapped ^{1}H NMR spectra of the original ester and after every round of addition of D_2O.

When comparing readings for the signal of the methoxy group, a gradual change in their fourth decimal is noticeable with an SD value of the measurements of 0.0007. This shift, however, is negligible when compared to the initial shift of the signal of the same methoxy group of **5**, thus confirming the prevalence of intramolecular π-methyl interactions.

3.2.5 Synthesis of the polymerizable derivative for 16-OMC

As the Steglich esterification worked well for all esters with **5**, it was also the method of choice in the synthesis of the polymerizable derivative of 16-O-methylcafestol (**10**). An issue with the synthesis was the removal of dicyclohexylurea from the product mixture, as it has a similar polarity as the product. It was primarily removed by filtration and subsequently by dissolving **10** in a small amount of acetonitrile, leaving behind a small amount of a precipitate after 10 min on an ice bath., which was then easily removed by filtration, leaving behind **10** with a yield of 46% and spectroscopically pure enough to use it as a template for imprinting:

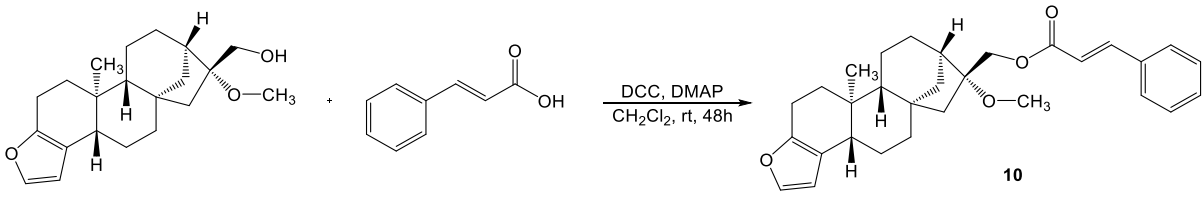

The identity and purity of the compound was confirmed with ^{1}H NMR, ^{13}C NMR, IR and MS, showing that the product was ready to use in the reaction of polymerization.

Bibliography

1. Gunning, Y. *et al.* 16-O-methylcafestol is present in ground roast Arabica coffees: Implications for authenticity testing. *Food Chem.* **248,** 52–60 (2018).

9. Speer, K. & Kölling-Speer, I. The lipid fraction of the coffee bean. *Braz. J. Plant Physiol* **18,** 201–216 (2006).

10. D'Amelio, N., De Angelis, E., Navarini, L., Schievano, E. & Mammi, S. Green coffee oil analysis by high-resolution nuclear magnetic resonance spectroscopy. *Talanta* **110,** 118–127 (2013).

42. Kamm, W. *et al.* Rapid and simultaneous analysis of 16-O-methylcafestol and sterols as markers for assessment of green coffee bean authenticity by on-line LC-GC. *J. Am. Oil Chem. Soc.* **79,** 1109–1113 (2002).

61. Wulff, G. & Poll, H.-G. Enzyme-analogue built polymers, 23. Influence of the structure of the binding sites on the selectivity for racemic resolution. *Die Makromol. Chemie* **188,** 741–748 (1987).

140. Frost-Meyer, N. J. & Logomarsino, J. V. Impact of coffee components on inflammatory markers: A review. *J. Funct. Foods* **4,** 819–830 (2012).

141. Amigos. *Qualità Rossa*.

142. Knothe, G. & Kenar, J. A. Determination of the fatty acid profile by 1H-NMR spectroscopy. *Eur. J. Lipid Sci. Technol.* **106,** 88–96 (2004).

143. Shen, F. & Ren, X. Covalent molecular imprinting made easy: a case study of mannose imprinted polymer. *RSC Adv.* **4,** 13123–13125 (2014).

144. Lacina, K., Skládal, P. & James, T. D. Boronic acids for sensing and other applications - a mini-review of papers published in 2013. *Chem. Cent. J.* **8,** 1–17 (2014).

145. Kobayashi, K., Asakawa, Y., Toi, H., Aoyama, Y. & Kikuchi, Y. CH-π Interaction as an Important Driving Force of Host-Guest Complexation in Apolar Organic Media. Binding of Monools and Acetylated Compounds to Resorcinol Cyclic Tetramer As Studied by 1H NMR and Circular Dichroism Spectroscopy. *J. Am. Chem. Soc.* **115,** 2648–2654 (1993).

146. Kolb, H. C., VanNieuwenhze, M. S. & Sharpless, K. B. Catalytic Asymmetric Dihydroxylation. *Chem. Rev.* **94,** 2483–2547 (1994).

147. Furikado, Y. *et al.* Universal Reaction Mechanism of Boronic Acids with Diols in Aqueous Solution: Kinetics and the Basic Concept of a Conditional Formation Constant. *Chem. - A Eur. J.* **20,** 13194–13202 (2014).

148. Roy, C. D. & Brown, H. C. Stability of boronic esters - Structural effects on the relative rates of transesterification of 2-(phenyl)-1,3,2-dioxaborolane. *J. Organomet. Chem.* **692,** 784–790 (2007).

149. Bermand, C. Trimethylsulfonium and trimethylsulfoxonium as versatile epoxidation reagents. A comparative study. *Arkivoc* **2000,** 128–132 (2000).

150. Li, A.-H., Dai, L.-X. & Aggarwal, V. K. Asymmetric Ylide Reactions: Epoxidation, Cyclopropanation, Aziridination, Olefination, and Rearrangement †. *Chem. Rev.* **97,** 2341–2372 (1997).

151. Chakrabarti, P. & Bhattacharyya, R. Geometry of nonbonded interactions involving planar groups in proteins. *Prog. Biophys. Mol. Biol.* **95,** 83–137 (2007).

152. Li, P. *et al.* The CH-π interactions of methyl ethers as a model for carbohydrate-N-heteroarene interactions. *Org. Lett.* **16,** 5064–5067 (2014).

153. Neises, B. & Steglich, W. Simple Method for the Esterification of Carboxylic Acids. *Angew. Chemie Int. Ed. English* **17,** 522–524 (1978).

154. Kriz, D., Ramström, O. & Mosbach, K. Molecular Imprinting: New Possibilities for Sensor Technology. *Anal. Chem.* **69,** 345A–349A (1997).

3.3 Synthesis of MIPs for cafestol and 16-OMC

Molecular imprinting is a technique of co-polymerization of functional and cross-linking monomers in presence of a template molecule. This way, molecular memory is introduced into the polymer. After the removal of the template molecule, ideally, a material with highly specific rebinding capability is formed. It is possible to form molecularly imprinted polymers by following either the covalent and the non-covalent approach to imprinting, both of which depend on the interactions formed between the functional monomer and the template[154]. Thus, covalent bonds are formed prior to covalent imprinting and non-covalent interactions during non-covalent imprinting.[155]

For the needs of our project, we opted for covalent formation of the polymerizable derivative, which should provide with a higher imprinting efficiency and improved selectivity of the polymers.[67] This choice is crucial, as our two target molecules are greatly similar in structure and differ only in functionalisation on the carbon 16.[9] Different approaches to form polymerizable derivatives allowed us to form molecular imprinted polymers with higher probability of being able to select between the two target molecules.

Synthesis of MIPs requires several building components. Monomers influence the physico-chemical properties of the polymers, cross-linkers form their 3D network and co-monomers introduce the template molecules into the polymer. In our case, acrylamide or N-isopropylacrylamide (NIPAM) were used as monomers, N,N'-methylenebisacrylamide (MBA) was always used as a cross-linker, azobisisobutyronitrile (AIBN) as the initiator and dimethyl sulfoxide as the solvent (**Figure 3.29**). The polymers were synthesized via high dilution radical polymerization[156].

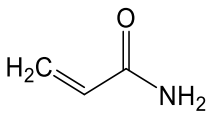

Acrylamide

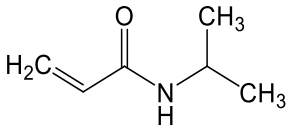

NIPAM

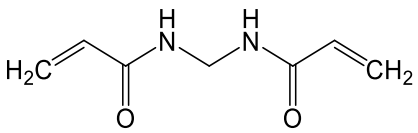

MBA

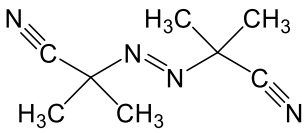

AIBN

Figure 3.29: Structures of the monomers acrylamide and NIPAM, cross-linker MBA and the initiator AIBN.

The co-monomers were the polymerizable derivatives when synthesizing the imprinted polymers, functional monomers when synthesizing the NIPs and absent when synthesizing the control polymers. The compositions of the polymers will be described with molar ratios of monomer to cross-linker to co-monomer. The used amounts of the initiator were 1%, 2% or 5% of the moles of all double bonds in the reaction. The amount of the solvent, always anhydrous DMSO, was calculated to comply with the critical monomer concentration (c_M)[157] of 1%. The polymerisations took 24 or 48 h to complete and were performed in an inert atmosphere of nitrogen or argon at 70°C. The flasks were always checked for undissolved particles and transparency before and after synthesis.

In most part, the polymers were dialysed and freeze-dried upon the end of the reaction. Some of them, however, were analysed as product mixtures, to calculate the percentage of incorporation of the polymerizable derivative in the MIP.

All imprinted and non-imprinted polymers were characterized with measurements of the size of particles and zeta potential. The imprinted polymers were also a subject of rebinding studies and ^{1}H NMR analyses, when removal of the template was needed. In some cases, UV-Vis studies were made, to calculate the percentage of incorporation of the template or functional monomer into the polymer.

Characterization of the polymers

Upon synthesis, dialysis and freeze-drying, yields of the polymers, size of the polymer particles and their zeta potential were determined. Additionally, the amount of the imprinted template was determined, as well as the rebinding capabilities of the polymers.

DLS measurements

We wanted to examine how different ratios of the monomer, cross-linker and co-polymer, different co-monomers and different amounts of the initiator used in the polymerization influence the size of the synthesized particles. For the purpose, dynamic light scattering measurements were performed.

Dynamic light scattering is a technique, which can be used for determination of the size distribution of the particles in suspensions or emulsions. The samples are illuminated by a laser beam or other monochromatic light source, led through a polariser. This causes Rayleigh scattering to occur. The scattered light is led trough another polariser, collected by a photomultiplier, and projected onto a screen. The projection shows a speckle pattern, as due to the particles scattering light in all directions, the light interferes constructively in light regions or destructively in dark regions. Due to the fact, that small particles in the solution undergo Brownian motion due to collision with fast moving particles in the liquid[158], the distance between the scaterers is changing with time. With that, the pattern in the speckle is changing over time as well.

The measurements are repeated in short time intervals and the resulting set of speckle patterns is analysed by an autocorrelator. Thus, the fluctuations of the scattered light are detected at a known scattering angle by a fast proton detector. The results are then analysed by the means of the auto-correlation function, with the correlation deteriorating over time due to particle movement (**Figure 3.30**).

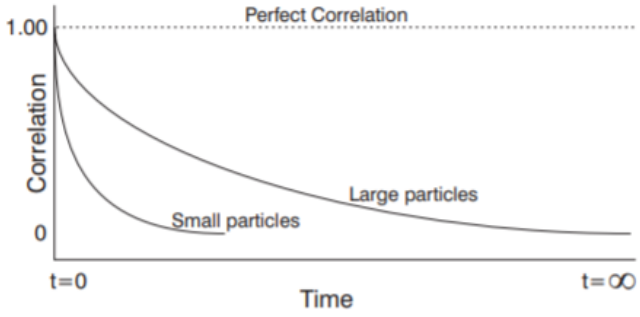

Figure 3.30: Deterioration of the auto-correlation function through time.[159]

The results of the size measurements are given as distributions of particles, either in regard to intensity or volume of the particles. Differences between the modality of particle size distribution by intensity and by volume can be found. As such, in several of our polymer samples, a bimodal distribution of size by intensity was observed, while simultaneously a unimodal distribution by volume was found. This happens, as the relationship between the intensity of the scattered light to the diameter of the particle, found in the Rayleigh scattering equation, is I to d^6: [160]

$$I = I_0 \frac{1+\cos^2\theta}{2R^2}\left(\frac{2\pi}{\lambda}\right)^4\left(\frac{n^2-1}{n^2+2}\right)^2\left(\frac{d}{2}\right)^6$$

Namely, as bigger particles scatter the light more, even a small percentage of them can give a bigger signal than a big population of substantially smaller particles. On the other hand, when their size is weighed to volume, the ratio lowers in favour of the diameter, causing the signal for the bigger particles to appear much less intensively. One of such cases is presented in **Figure 3.31**, where the bimodal size distribution by intensity gives a notion of prevalence of bigger sized particles, and the size distribution by volume shows, that the number of larger particles is, in reality, much smaller.

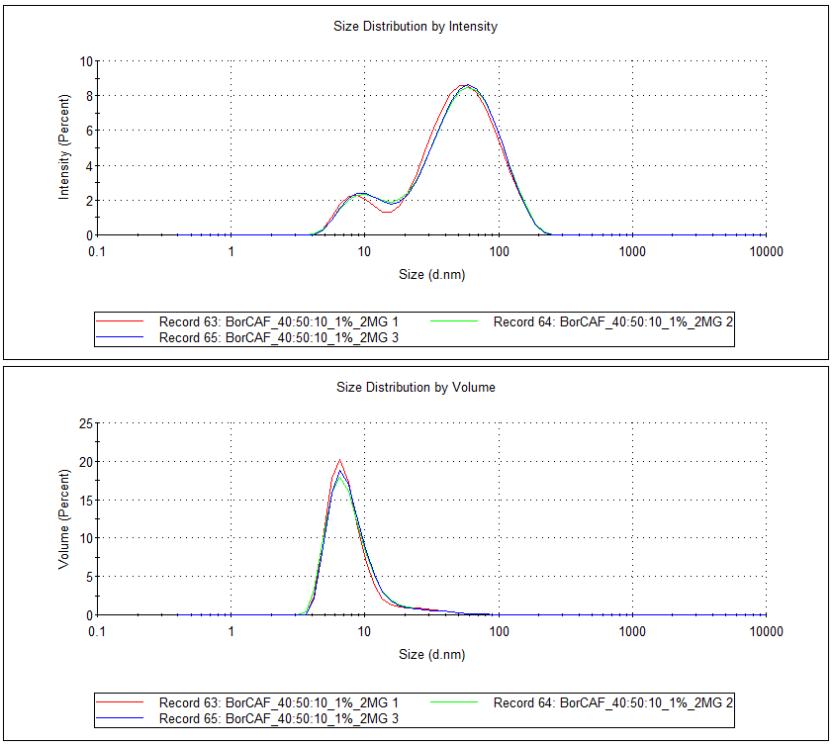

Figure 3.31: Size distribution by intensity (above) and size distribution by volume (below) for the imprinted polymer Cb1.

Zeta potential

Measurements of zeta potential gave us an information on the stability of the colloid dispersions, thus supplementing the data of size measurements.

Namely, when charged particles are suspended in a liquid, they attract ions of the opposite charge to their surface, with the attraction strength of the counterions greatly depending on their distance from the particle. Thus, the counterions close to the particle surface are strongly bound to the particles, forming the Stern layer. The layer of the more distant counterions is less firmly bound and forms the diffuse layer. Within the diffuse layer, we can find counterions forming another stable layer around the Stern layer, capable of travelling with the particle through the solvent. The remaining counterions in the diffuse layer are too weakly bound for that to occur and upon Brownian motion of the particles do not follow their dynamics. The boundary between the two types is called the slipping plane and the difference in the charge on both sides of the slipping plane forms a potential, called zeta potential (**Figure 3.32**).

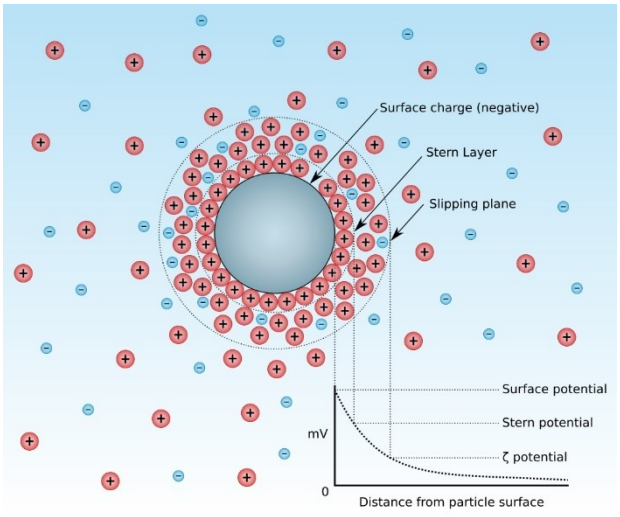

Figure 3.32: Presentation of a counterion layers around a particle.

The stability of the dispersion, therefore, depends on the dimension of the zeta potential. If the particles have a very positive or very negative zeta potential, they will repel each other enough to avoid flocculation. In the opposite case, the particles will be able to approach each other enough to be able to flocculate. The border values for stability of the dispersion +30 mV and -30 mV. Zeta potential is calculated via theoretical models, using data obtained from the measurements of electrophoretic mobility. The technique of laser Doppler velocimetry was in our case applied and zeta potential was calculated via the Henry equation:

$$U_E = \frac{2\,\varepsilon z\, f(K_a)}{3\,\eta}$$

where z is zeta potential, U_E electrophoretic mobility, ε dielectric constant, $f(K_a)$ Henry's function and η viscosity. The output of the measurement was a distribution of zeta potentials, an example of which is presented in **Figure 3.33**.

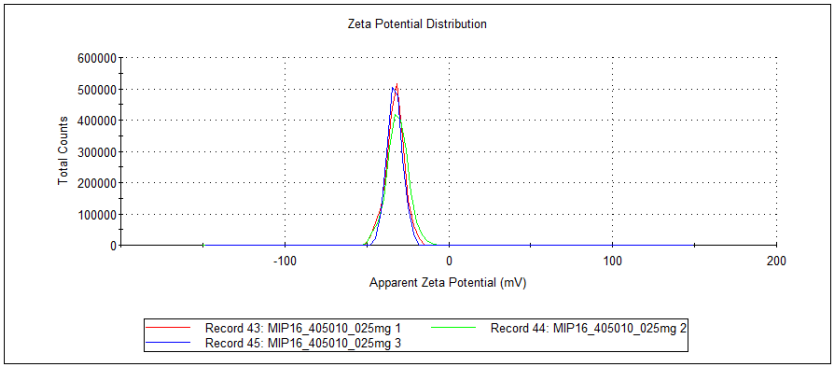

Figure 3.33: Zeta potential of the imprinted polymer 16b1.

NMR analysis

^{1}H NMR spectra were recorded, to either confirm the incorporation of the template into the MIP or to find if the template was successfully removed from it. For verification of template incorporation, ^{1}H NMR spectra of the MIPs were compared with the ^{1}H NMR spectra of suitable NIPs and observed for the characteristic signals of cafestol, isoamyl hydrocinnamate or 16-OMC. Upon removal of the template, ^{1}H NMR spectra of the MIPs with the removed template were compared to ^{1}H NMR spectra of the MIPs before the removal of the template (**Figure 3.34**).

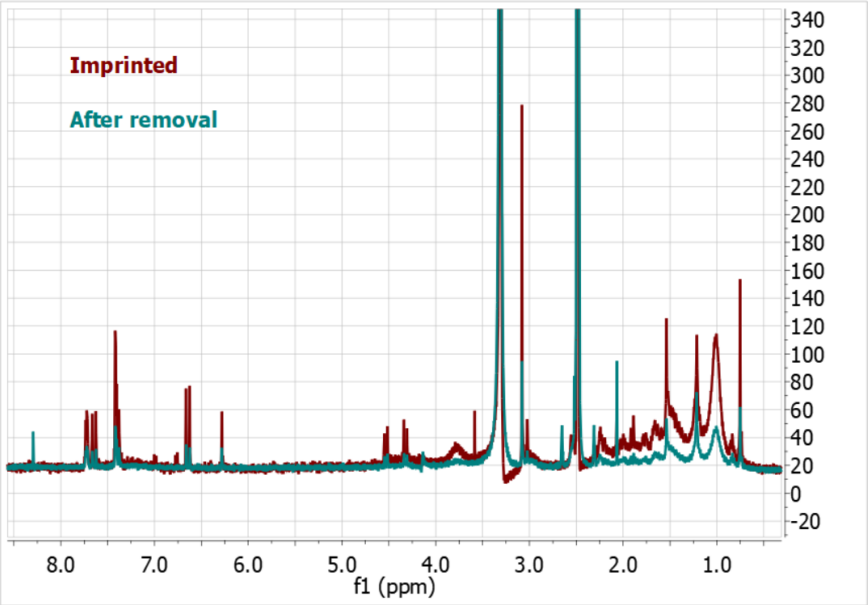

Figure 3.34: Example of a comparison between the imprinted polymer 16a1 and the same imprinted polymer after removal of the template.

3.3.1 Molecularly imprinted polymers for cafestol

MIPs for cafestol were synthesized by using its **3** as a co-monomer in the reaction of polymerization (**Figure 3.35**). NIPAM was chosen as a monomer instead of in initial experiments tested acrylamide, to help with the water solubility of the final product, and MBA as a cross-linker. The polymers were synthesized in two different ratios of monomer to cross-linker to co-monomer, 60:30:10 and 40:50:10. The synthesis of the imprinted polymer with the ratio of components 60:30:10 was performed in presence of 1% of the initiator (**Ca1**), while the polymers with the ratio of compounds 40:50:10 in presence of 1% (**Cb1**), 2% (**Cb2**) or 5% (**Cb5**) of the initiator. The synthesis went on under the same conditions for all polymers and lasted for 48 h.

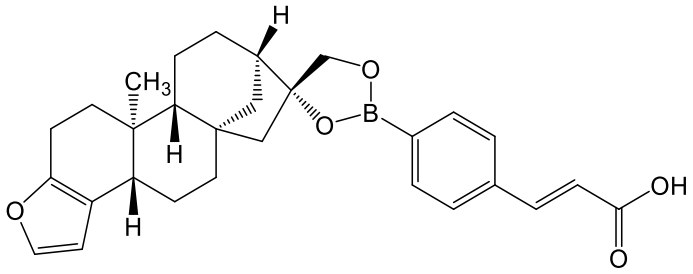

Figure 3.35: Polymerizable derivative for cafestol (3).

Simultaneously, non-imprinted polymers were synthetized, where as a co-monomer only the functional monomer for cafestol (**3b**, **Figure 3.36**) was used. This type of polymers was needed for the rebinding studies, whose main focus was to determine if imprinting in the polymers was successful.

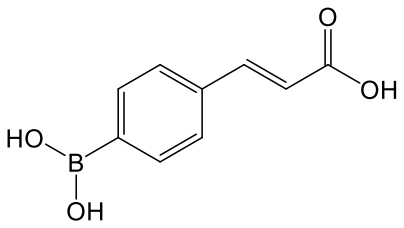

Figure 3.36: Structure of 4-(trans-2-carboxyvinyl)phenylboronic acid.

NIPs were synthesized from the same two ratios of monomer to cross-linker to co-monomer, 60:30:10 and 40:50:10. The synthesis of the polymer with the ratio of components 60:30:10 was performed in presence of 1% of the initiator (**Ca 1.1**), while the polymers with the ratio of compounds 40:50:10 in presence of 1% (**Cb 1.1**), 2% (**Cb 2.1**) or 5% (**Cb 5.1**) of the initiator.

With different percentages of the initiator, we wanted to see if an increase in the yield of the MIPs or in incorporation of the polymerizable derivative into the MIPs can be observed. All the polymers were synthesized in two parallels, the first one was dialysed and freeze-dried, while the product mixture of the second parallel was directly used for the study of determination of incorporation of the functional monomer in the MIP (**Figure 3.37**).

	MBA	AIBN	Time	Yield
Ca1	30 %	1 %	48 h	13 %
Ca 1.1	30 %	1 %	48 h	57 %
Cb1	50 %	1 %	48 h	26 %
Cb 1.1	50 %	1 %	48 h	82 %
Cb2	50 %	2 %	48 h	22 %
Cb 2.1	50 %	2 %	48 h	28 %
Cb5	50 %	5 %	48 h	23 %
Cb 5.1	50 %	5 %	48 h	50 %

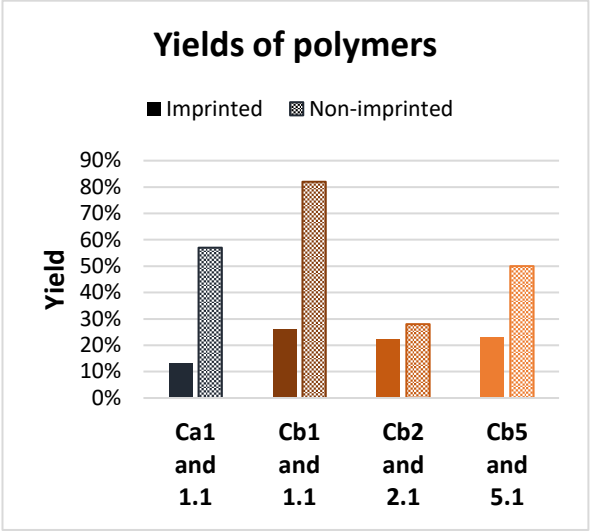

Figure 3.37: Yields of MIPs and NIPs for cafestol, presented in a table (left) and a graph (right).

We can immediately see, that the yield of the polymers depends greatly on the amount of the cross-linker in the polymer reaction mixture. Namely, the yield of the polymer **Cb1** with 50 % of the cross-linker in the reaction mixture is twice as high than the yield of the polymer **Ca1** with 30% of the cross-linker in the reaction mixture, while the same amount of the initiator is used. On the other hand, an increased amount of the initiator does not increase the yield of the polymers.

The yields of NIPs were much higher than the ones of MIPs, when a NIP was compared to a MIP, synthesized from the same ratio monomer to cross-linker to co-monomer, with the same percentage of AIBN added to the reaction mixture. The biggest difference between the imprinted polymers and their non-imprinted relatives was noticed in polymers with 1% of the initiator in the reaction mixture (**Ca1** and **Ca 1.1**, **Cb1** and **Cb 1.1**). With increasing amounts of the initiator in the reaction mixtures of non-imprinted polymers, the yields of polymerisations decreased. This might be due to the fact that with an increasing amount of the initiator the number of primary monomer radicals grows, resulting in an increased amount of polymer particles with a shorter chain in the product mixture. The loss could occur during dialysis, as the sizes of a bigger degree of the polmer particles fall under the cut-off of the pores in the dialysis tubes.

Upon characterization of the size of polymer particles (**Table 3.1**), it is immediately noticeable, that the size and volume distributions do not match. Namely, the size distribution of particles is, according to the intensity of scattered light, in most cases bimodal, while the size distribution of particles according to their volume remains unimodal. Due to the relationship between the intensity and the particle diameter, the distribution of particles according to their volume, therefore, serves as good orientation for the more realistic particle size.

Distribution by:	Intensity (d.nm)	Distrib.	Volume (d.nm)
Ca1	11.34	BM	5.157
Ca 1.1	14.06	UM	6.216
Cb1	9.597	BM	8.726
Cb 1.1	25.12	UM	9.701
Cb2	50.64	BM	6.749
Cb 2.1	28.97	BM	22.95
Cb5	32.85	BM	7.562
Cb 5.1	10.69	BM	9.491

Table 3.1: Sizes of particles of MIPs and NIPs for cafestol, according to the size distribution by intensity and size distribution by volume.

According to the measurements, NIPs have in most cases a bigger particle size than MIPs. All the particle size distribution by intensity were bimodally distributed in imprinted polymers, indicating possible formation of clusters. Simultaneously, sizes of the particles of non-imprinted polymers were in more cases unimodally distributed. The particles of the polymer series **Cb**, were generally bigger than the ones found in the polymer series **Ca**, which leads to believe the increase in size occurs due to a larger percentage of cross-linker (50%) used in the polymerisation mixture. The biggest particle size was observed in the imprinted polymer **Cb2**, where at the same time a much smaller size distribution of the particles by size volume was observed. This could be due to an uneven formation of the polymer particles during synthesis or their tendency to aggregate. This theory was put to a test by measuring the zeta potential of the particles (**Figure 3.38**).

	ζ (mV)
Ca1	-28.2
Ca 1.1	-24.3
Cb1	-23.3
Cb 1.1	-27.4
Cb2	-30.9
Cb 2.1	-33.9
Cb5	-30.9
Cb 5.1	-30.5

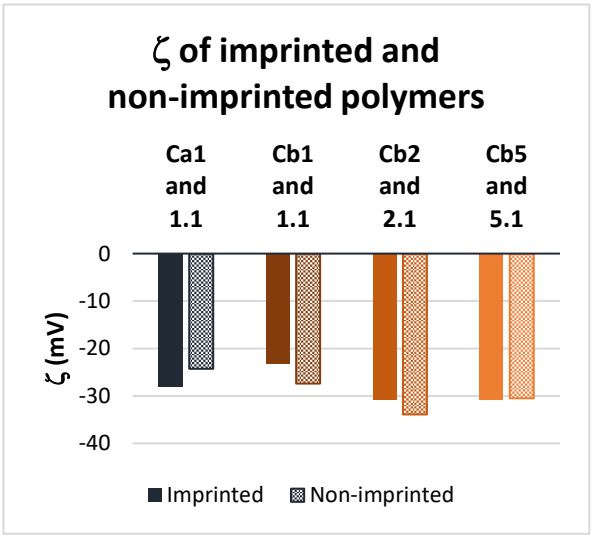

Figure 3.38: Zeta potential of imprinted and non-imprinted polymers for cafestol, presented in a table (left) and in a graph (right).

In polymers, prepared with 1% of the initiator in the mixture, **Ca1** and **Cb1** with their non-imprinted relatives, the zeta potential was inside of the interval -30 mV to 30 mV, meaning that the particles are more inclined to clustering in a dispersion. The zeta potential of the rest of the polymers was below 30 mV, thus their suspension should be more stable. The difference between the imprinted and non-imprinted polymers was not as pronounced as expected due to the presence of additional free boronic acid moieties in the non-imprinted polymer particles.

Incorporation of the polymerizable derivative in the MIP

To define the degree of incorporation of cafestol in the MIPs, non-dialysed polymer product mixtures were used. The polymer was removed from the solutions with centrifugal filters and the incorporation of its polymerizable derivative was determined by quantifying cafestol, released from the unreacted polymerizable derivatives. Their amounts were deducted from the initial amount of the polymerizable derivative, used in the reactions of polymerization. Agilent's version of DIN 10779[13] method was used for quantification of cafestol. The amount of the incorporated boronic ester was calculated based on the results obtained for the external standards with known concentrations of 50 µg/mL of cafestol and its polymerizable.

Incorporation of the polymerizable derivative

Polymerization product mixtures for all the MIPs for cafestol were filtered through centrifugal filters in two parallels. The filtrates were then treated with an 1M aqueous solution of NaOH, to release cafestol. The samples were appropriately diluted and analysed on HPLC. Upon calculation of the ratio between the cafestol in the samples and the theoretical amount of cafestol expected in the samples, the % of incorporated boronic ester of cafestol into the polymer was calculated (**Figure 3.39**).

	MBA	AIBN	Time	Incorp.
Ca1	30 %	1 %	48 h	55 %
Cb1	50 %	1 %	48 h	38 %
Cb2	50 %	2 %	24 h	45 %
Cb5	50 %	5 %	24 h	45 %

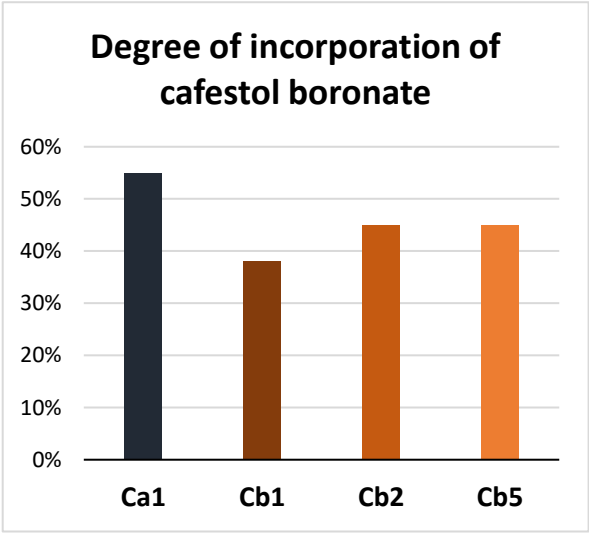

Figure 3.39: Degree of incorporation of the boronic ester of cafestol in MIPs, presented in a table (left) and in a graph (right).

The percentages of incorporation are rather high, considering that only up to 10% of an incorporation was expected. Given the relatively low yields of the polymer syntheses, this could be due to the fact, that substantially more of the polymerizable derivative reacted in comparison with the monomer and the cross-linker in the reaction. This consequently lead to the shift in the ratio of the components in the final product.

Removal of cafestol from the MIPs

In the literature, several sources describe that the stability of boronic esters in aqueous solutions depends greatly on the pH of the solvent and the pK_a values of the alcohol and the boronic acid. It has been shown in many cases, that pH below the pK_a value of the boronic acid and the alcohol or between them can have a stabilising effect on the boronic ester, while pH above the pK_a values of both can have a destructive effect.[161]

The experiment was attempted by treating the polymer with a 1M aqueous solution of NaOH for an hour, then the product mixture was put up for a dialysis and freeze-dried. The removal of the template was confirmed with ^{1}H NMR, as the peaks of cafestol ceased to be visible in the spectrum.

Rebinding studies

To see if the imprinting process was successful and if the polymers are capable to selectively rebind cafestol, rebinding studies were attempted. Each of the four imprinted polymers had their template removed prior to the study. They were then tested by preparing a 1 mg/mL solution of a polymer in a 200 µM solution of cafestol and in a 200 µM solution of 16-OMC.

The solutions were sampled after 30 min, 60 min, 120 min, 240 min and 360 min, then the quantity of the remaining diterpene was determined with a HPLC-UV measurement. From the difference between the moles of the chosen diterpene in the initial sample and the moles found in the aliquot at each time of the sampling, the amount of rebound diterpene was calculated and plotted to the time of sampling. First, the rebinding capabilities of all the MIPs with cafestol were investigated (**Figure 3.40**).

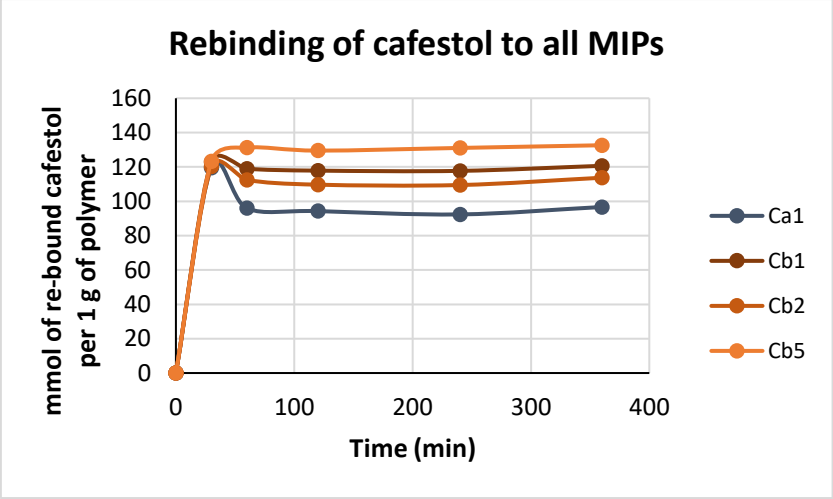

Figure 3.40: Rebinding capabilities of MIPs for cafestol.

According to obtained data, the most significant rebinding of cafestol is observed in polymer **Ca5**. Additionally, a substantial increase in the rebinding capability of the polymers, prepared with a higher percentage of the cross-linker, was observed in all three polymers of the series **Cb**. Similarly, an increased amount of AIBN in the polymers of the series **Cb**, appears to improve the amount of the rebound cafestol as well.

In all polymers a plateau of the rebound diterpene is reached by minute 120. The behaviour of the polymers before that time-point, however, varies a bit. With a decrease of the percentage of the cross-linker and the initiator in the polymers, the amount of rebound cafestol in all cases but in the case of the polymer **Cb5** peaks. The peaking very likely occurs due to adsorption of the molecules of cafestol on the surface of the MIPs prior to penetration into their pores. Upon penetration, increase of the concentration of cafestol in the polymer solution occurs, likely due to a certain degree of desorption of the diterpene.

Next, the degree, to which molecular imprinting actually occurred was explored. For the purpose, rebinding of cafestol to non-imprinted polymers was attempted. Namely, NIPs ideally structurally differ from their imprinted relatives. They should be capable of a significantly lower degree of rebinding, due to the lack of specifically tailored pores for recognition of cafestol. It was expected, however, that some rebinding would occur, due to the boronic moiety on the surface of polymer particles. The rebinding was performed in the same conditions as beforehand with MIPs, to allow comparison of the results (**Figure 3.41**).

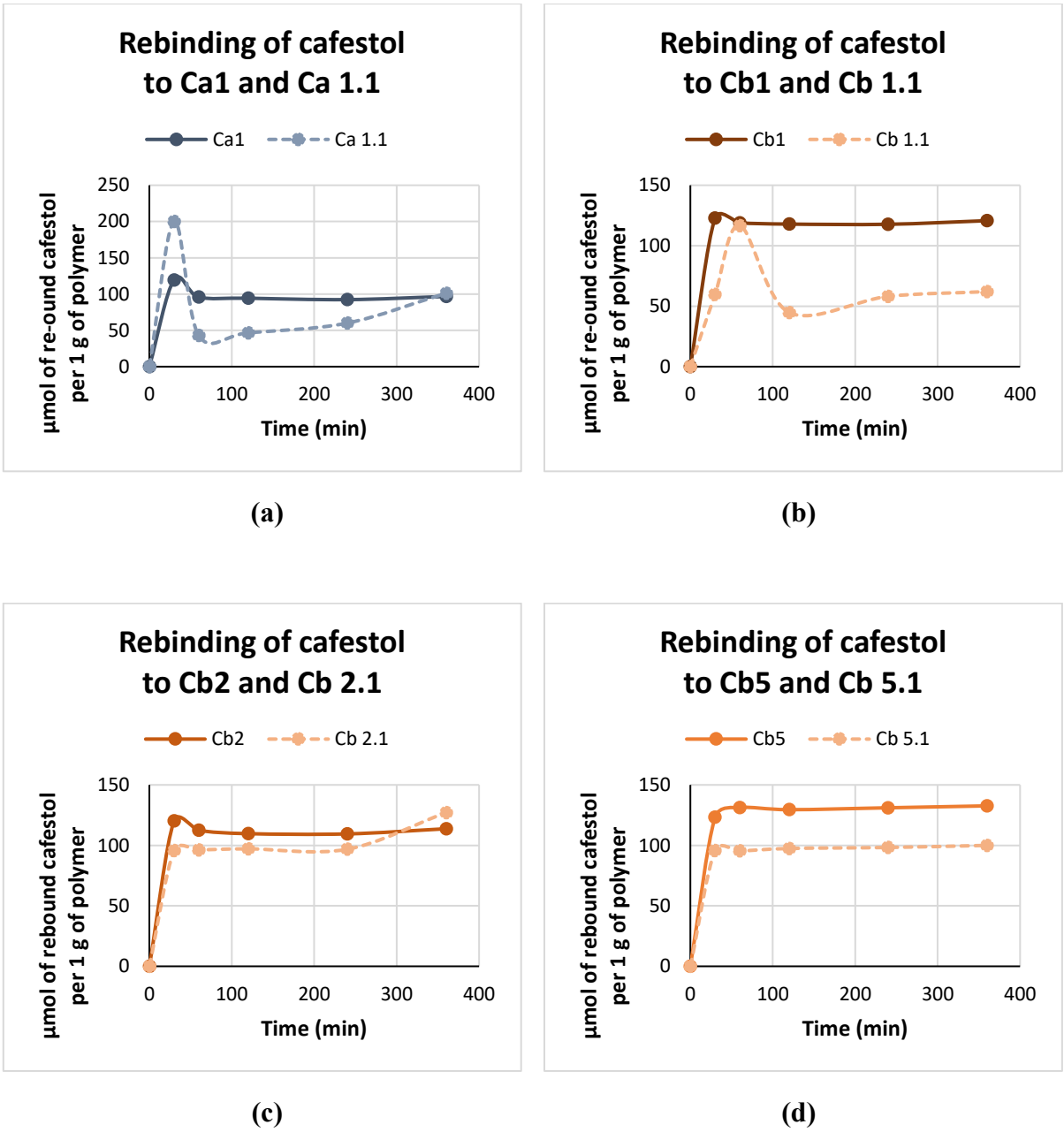

Figure 3.41: Comparison of rebinding capabilities of the MIPs and their corresponding NIPs for cafestol.

From the results, imprinting factors were calculated (**Table 3.2**), to determine, which of the polymers exhibits the most significant selective binding. The caluculations were made following the equation:

$$\mathrm{IF} = \frac{N_{MIP}}{N_{NIP}},$$

where N_{MIP} represents moles of cafestol, rebound to MIPs, and M_{NIP} moles of cafestol, ebound to MIPs. Data at the time-point of 120 min was taken into account, as at that point a plateau in all samples was reached.

	Co-monomer	MBA	AIBN	Incorp. of 3	IF
Ca1	10 %	30 %	1 %	55 %	2.02
Cb1	10 %	50 %	1 %	38 %	2.63
Cb2	10 %	50 %	2 %	45 %	1.13
Cb5	10 %	50 %	5 %	45 %	1.33

Table 3.2: Imprinting factors of imprinted polymers for cafestol.

Among the results, the biggest imprinting factor is observed in the imprinted polymer **Cb1**, with **Ca1** following relatively close by. Considering that the same amount of the polymerisable derivative for cafestol (**6**) has been added to the polymerisation mixture and that the same amount of AIBN was used, use of 50% of MBA insteade of 30% of it, aparently yields in a more selective polymer scaffold. It is well explicable by the fact, that with an increase of MBA, the polymers become more cross-linked, which can increase the stability of the pores.

Increasing the amount of the initiator to 2% or 5%, as seen in polymers **Cb2** and **Cb5**, decreased the imprinting factor furhter. as an increased amount of the initiatorleads to an increased amounts of initial monomer raicals in the mixture, the result of the polymerisation are numerous smaller particles. This increases the surface of the polymers and with that increases the possibility of non-specific binding. In the graphs, this can be seen as the curves for the imprinted and nonimprinted polymer reaching a plateau of similar height, as observed with the combintion of polymers **Cb2** and **Cb2.1**, and **Cb5** and **Cb5.1**.

Finally, selectivity of the imprinted polymers was examined. To gain insight into the topic, rebinding studies for the imprinted and non-imprinted polymers for cafestol with 16-OMC were attempted. It was expected, that a selective MIP would be capable to rebind cafestol in substantialy greater quantities than it would do so with 16-OMC (**Figure 3.42**).

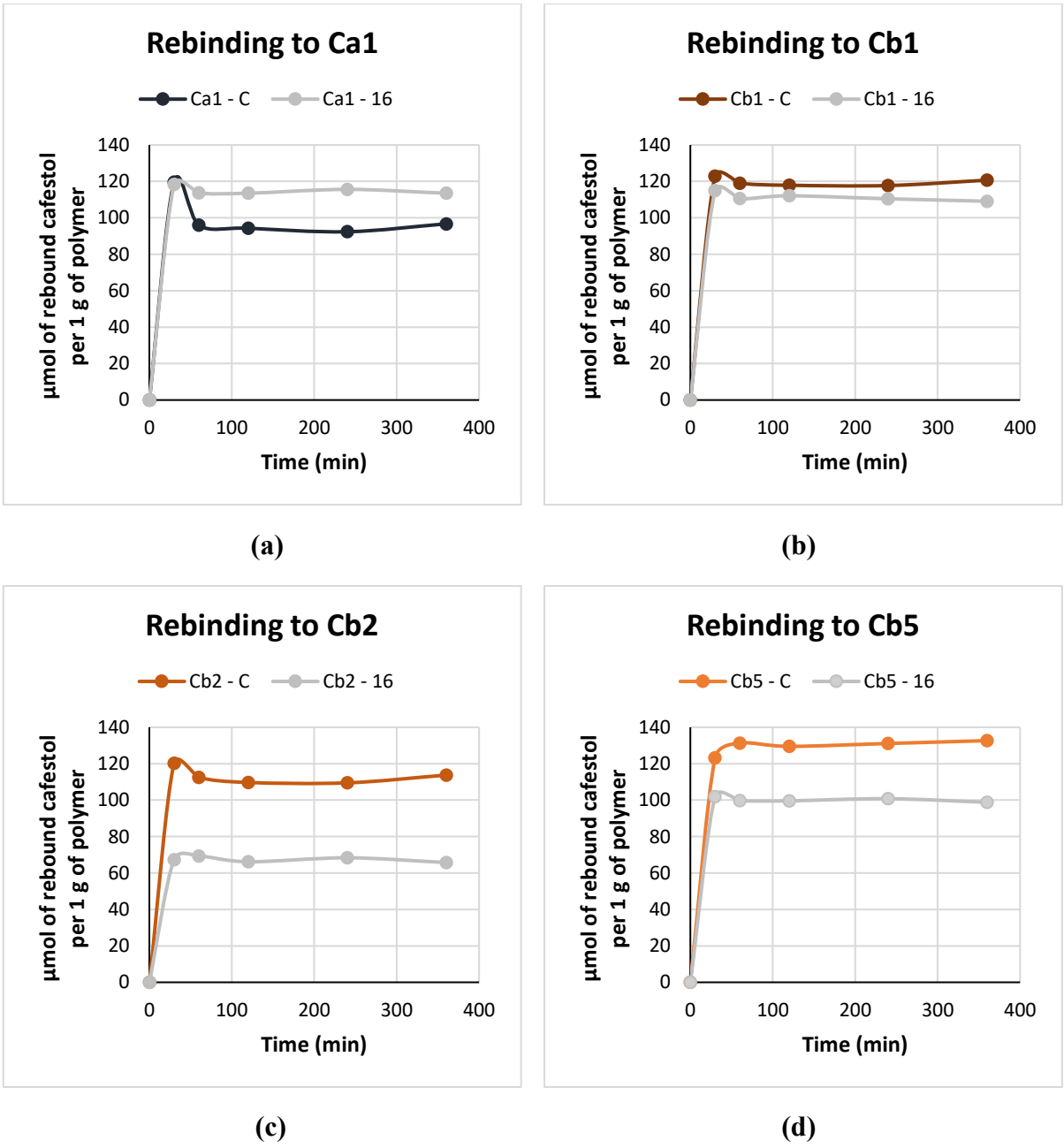

Figure 3.42: Selectivity of the MIPs for cafestol upon rebinding cafestol and 16-OMC under the same conditions.

The best selectivity was observed in the imprinted polymer **Cb2**, where nearly twice as much of cafestol was rebound in the course of 360 min than 16-OMC. In case of the polymers **Cb1** and **Cb5**, the trend of a higher amount of rebound cafestol is still observed, while the polymer **Ca1** is capable of rebinding more 16-OMC than cafestol.

This suggests, that selectivity of the polymers is greatly increased with more cross-linked polymers, and that a “sweet-spot” for the amount of the initiator that needs to be present in the polymerisation mixture is about 2%.

Competitive rebinding

As we were planning to use the MIPs in matrixes, where both diterpenes are present, we examined the rebinding dynamics of cafestol while an equal amount of 16-OMC is present in the solution. Each of the four imprinted polymers had their template removed prior to the study. They were then tested by preparing a 1 mg/mL solution of a polymer in a solution, simultaneously containing 200 µM of cafestol and 200 µM of 16-OMC. Aliquotes were sampled after 30 min, 60 min, 120 min, 240 min and 360 min, then the quantity of both diterpenes in the solution was determined.

The difference between the moles of cafestol and 16-OMC in the initial sample and the moles of the diterpenes found in aliquotes at each time-point was calculated and plotted to the time of sampling (**Figure 3.43**).

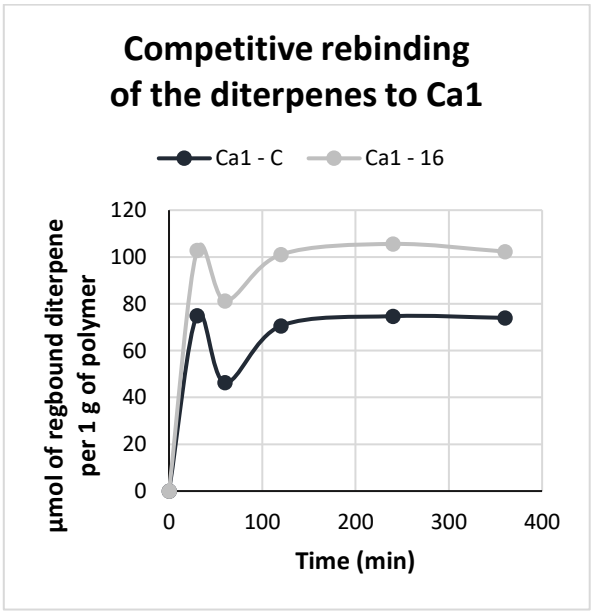

(a)

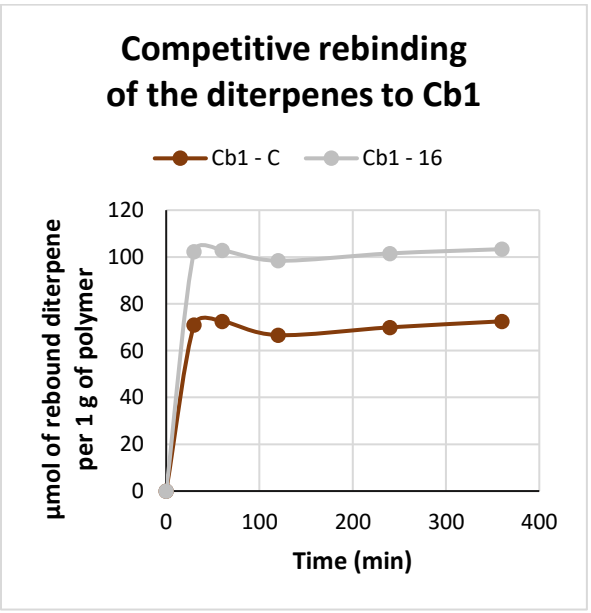

(b)

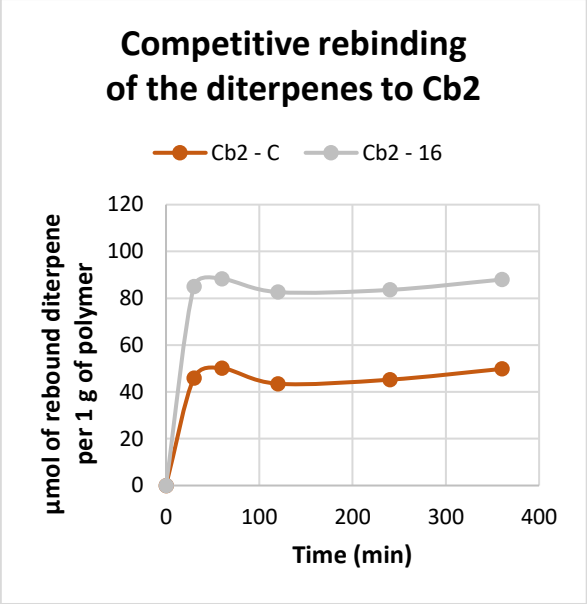

(c)

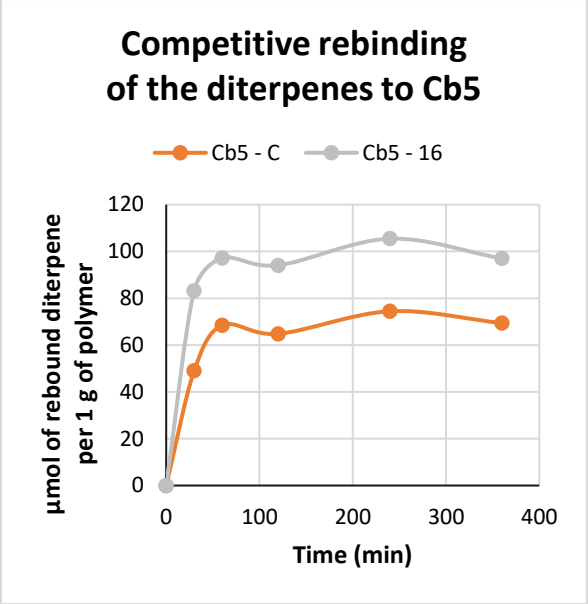

(d)

Figure 3.43: Results of the competitive rebinding of 16-OMC and cafestol to imprinted and non-imprinted polymers of the series Ca and Cb.

Uptake of cafestol was in all cases lower than the uptake of 16-OMC, when compared to the rebinding of the diterpenes being tested separately. An explanation for this could be given from a kinetic point of view. Namely, due to similarity of the structures of cafestol and 16-OMC and because of it both diterpenes can enter the pores of the polymers, it is possible, that the difference occurs due to a generally faster formation of non-covalent hydrogen and π-methyl interactions, compared to a longer time needed to form covalent boronic esters. Thus 16-OMC prevents cafestol from rebinding in such a proportion as it would, should it be interacting with cafestol alone. This can be well observed in the results of rebinding of the polymers **Cb2** and **Cb5**, where the slope of the curve, representing rebinding of 16-OMC is steeper than the slope of the curve, representing rebinding of cafestol. The results were similar for the competitive rebinding to the NIPs.

The results of rebinding of cafestol to the polymers either via normal or competitive rebinding experiments are in accordance with the literature.[162] Results of rebinding of 16-OMC, on the other hand, are in both cases higher than expected for the type of rebinding.[163]

3.3.2 Molecularly imprinted polymers for 16-OMC

High dilution polymerisations in DMSO were again attempted and 16-OMC cinnamate and isoamyl cinnamate were used as polymerizable derivatives in the reactions. Acrylamide and NIPAM were used as monomers, MBA as a cross-linker and AIBN as the initiator, added as 1 molar % of all double bonds in the reaction. The critical concentration of monomers during the polymerisation was always calculated to 1%, with the times of polymerization either 24 h or 48 h. Control polymers, imprinted polymers and non-imprinted polymers were synthesized.

Control polymers

Control polymers were synthesized without a co-monomer, with a main purpose of participation in UV-Vis studies for quantification of the amount of isoamyl cinnamate, incorporated in the MIPs. They consisted of either acrylamide or NIPAM as a monomer and MBA as a cross-linker. Two ratios monomer to cross-linker were used in both cases, 50:50 and 70:30, so the percentages of the cross-linker corresponded to the percentage of the cross-linker in later synthesized MIPs and NIPs. The reaction time of all polymerizations was 48 h (**Figure 3.44**).

	MBA	AIBN	Time	Yield
AA 50:50	50 %	1 %	24 h	69 %
AA 70:30	50 %	1 %	24 h	53 %
NIPAM 50:50	50 %	1 %	24 h	84 %
NIPAM 70:30	50 %	1 %	24 h	83 %

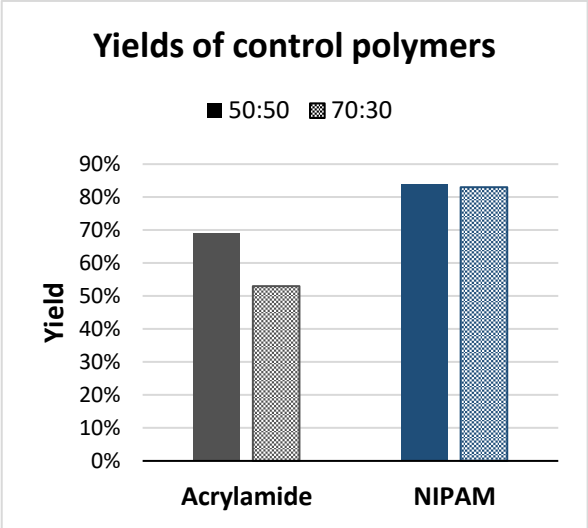

Figure 3.44: Yields of control polymers with acrylamide and NIPAM, presented in a table (left) and in a graph (right).

It is immediately noticeable, that NIPAM based polymers gave a much better yield than the polymers with acrylamide as a monomer. Polymers with NIPAM were much better water-soluble, as both of them gave a clear solution at 1 mg/mL. The acrylamide polymer with a lower percent of a cross-linker at 30 % was still well water-soluble at 1 mg/mL, while the polymer with 50 % of the cross-linker gave a cloudy solution. The sizes of polymers were again determined with DLS and are presented in the table below (**Table 3.3**)

Distribution by:	**Size** (d.nm)	**Distri b.**	**Volume** (d.nm)
AA 50:50	14.70	BM	12.40
AA 70:30	13.72	BM	10.25
NIPAM 50:50	76.97	UM	47.89
NIPAM 70:30	32.55	BM	14.78

Table 3.3: Sizes of particles of control polymers on the base of acrylamide and NIPAM, presented in a table (left) and in a graph (right).

The polymers on the basis of NIPAM have substantially bigger particles than both types of the acrylamide polymers. This difference could appear due to a slightly bigger size of the molecule of NIPAM, compared to acrylamide. Interestingly, the size distribution of the particles was unimodal in both cases of NIPAM polymers and bimodal in cases, where the monomer was acrylamide. A higher amount of the cross-linker in the reaction mixture seemed to have yielded bigger particles both kinds of polymers.

MIPs for isoamyl cinnamate

Due to having a limited amount of the polymerizable derivative for 16-OMC on disposal, we decided to test the reactivity of the double bond in the cinnamic part of the polymerizable derivative on a model ester, prior to the synthesis of MIPs for 16-OMC. For the purpose, isoamyl cinnamate was selected (**Figure 3.45**). The compound is a cinnamic acid ester with isoamyl alcohol and was a model molecule of choice due to its position of the double bond, presence of an ester bond and commercial availability.

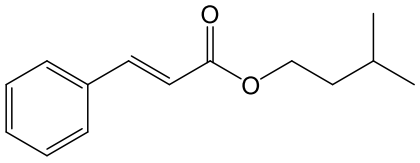

Figure 3.45: Structure of isoamyl cinnamate.

The MIPs were prepared with either acrylamide or NIPAM as a monomer, with percentages of MBA of 50% and 30%, to make the polymer skeleton comparable to the one in control polymers. The amount of isoamyl cinnamate used was either 10% or 20%, to see which would result in an optimal degree of incorporation. Polymerisations took part for 24h where the monomer was acrylamide and 24h or 48 h where the monomer was NIPAM. A prolonged polymerization of 48h was attempted to increase the yield of the reaction (**Figure 3.46**).

	AA 24 h	NIPAM 24 h	NIPAM 48 h
50:30:20	59%	29 %	45 %
30:50:20	31%	44 %	45 %
60:30:10	51%	44 %	53 %
40:50:10	55%	53 %	45 %

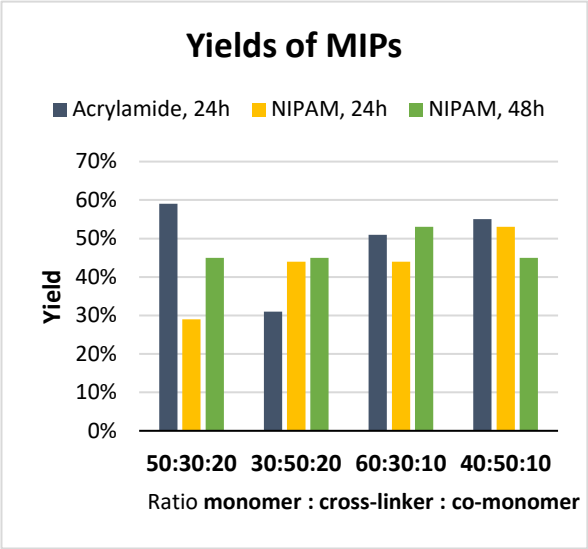

Figure 3.46: Yields of MIPs of the basis on acrylamide and NIPAM, presented in a table (left) and graphically (right).

Comparing the acrylamide and NIPAM polymers, the latter ones gave lower yields in nearly all combinations of monomer to cross-linker to polymerizable derivative. When comparing the yields of NIPAM polymers with a 24h and 48h reaction time, apart from the NIPAM polymer with the ratio of components 50:30:20, no significant increase of the yields is observed. The polymers were characterized by size and zeta potential measurements (**Table 3.4 and 3.5**).

When comparing the sizes of polymer particles with the same ratio monomer to cross-linker to co-monomer, the polymer particles on the base of NIPAM appeared to be of smaller sizes. A possible explanation for such results could be a vastly different degree of incorporation of the template in the polymers, which will be further discussed in the follow-up of this chapter. Additionally, an increase in the particle sizes was observed with a higher percentage of the cross-linker used in the polymer mixtures.

Distribution by:	**Intensity** (d.nm)	**Distrib.**	**Volume** (d.nm)
AA 50:30:20	14.37	UM	8.729
AA 30:50:20	35.38	UM	14.35
AA 60:30:10	1142	UM	1167
AA 40:50:10	47.40	UM	25.82

Table 3.4: Sizes of particles of the MIPs based on after 24h of polymerization.

Distribution by:	**Intensity** (d.nm)	**Distrib.**	**Volume** (d.nm)
N24 50:30:20	10.44	UM	7.867
N24 30:50:20	16.52	UM	10.95
N24 60:30:10	15.56	UM	9.267
N24 40:50:10	53.98	BM	13.94
N48 50:30:20	10.05	UM	5.521
N48 30:50:20	21.71	UM	10.21
N48 60:30:10	16.84	BM	8.545
N48 40:50:10	21.06	UM	13.73

Table 3.5: Sizes of particles of the MIPs based on NIPAM, after 24h and 48h of polymerization.

Distributions of the sizes of the polymer particles were generally unimodal, showing a great degree of uniformity of the particles. An obvious exception was the polymer N24 with the ratio of components 40:50:10. Comparing the size distributions of its particles by intensity and volume shows, that the particles are in reality in a greater degree much smaller than when represented with a distribution by intensity. A unimodal distribution of the particles is observed in this case, showing there is a rather small percentage of larger particles. To check, if the bimodal size distribution by intensity occur due to formation of clusters, the samples were diluted and additionally sonicated. As no changes were found, it was concluded that the distribution of the particles is an inherent characteristic of the material.

The stability of the dispersions was further examined with zeta potential measurements (**Figure 3.47**). The stability of all aqueous dispersions of polymers with NIPAM as a monomer was low, regardless of the amount of the cross-linker used in the synthesis. When acrylamide was used, however, the stabilities of polymer suspension with ratios of monomer to cross-linker to co-monomer 30:50:20 and 60:30:10 was improved.

	ζ (mV)
AA 50:30:20	-11.2
AA 30:50:20	-31.3
AA 60:30:10	-30.1
AA 40:50:10	-9.25
N24 50:30:20	-8.31
N24 30:50:20	-26
N24 60:30:10	-22.8
N24 40:50:10	-3.43

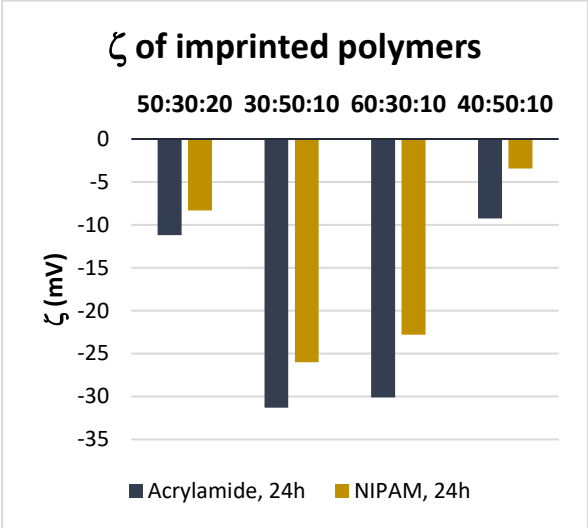

Figure 3.47: Zeta potential results of the MIPs for isoamyl alcohol on the basis of acrylamide and NIPAM, presented in a table (left) and a graph (right).

Incorporation of isoamyl cinnamate

To determine the amount of isoamyl hydrocinnamate incorporated in the MIPs, UV-Vis studies were performed. This type of a quantification was possible due to the presence of phenyl rings of the cinnamic acid moiety in the imprinted and non-imprinted polymers, detectable at 264 nm. Control polymers were used as background samples, as the polymer matrix usually absorbs a small degree of the UV light. The measurements were performed in DMSO, to allow solubilization of all polymers. Prior to quantification of the incorporated isoamyl cinnamate, a calibration curve for isoamyl hydrocinnmate was formed (**Figure 3.48**).

Calibration curve for isoamyl hydrocinnamate

A calibration curve was formed from readings of absorbance of samples with various concentrations of isoamyl hydrocinnamate in DMSO, at 264 nm. Rather than the original polymerizable derivative, isoamyl hydrocinnamate was used, to create comparable environment of the phenyl rings in the solution, to the one found in the polymers.

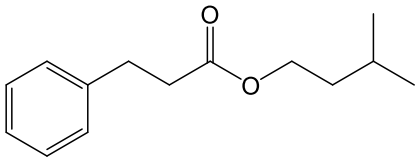

Figure 3.48: Structure of isoamyl hydrocinnamate.

For the purpose, isoamyl hydrocinnamate was synthesized from isoamyl cinnamate.[164] Catalytic hydrogenation of the double bond of the ester with Pd/C in a H_2 atmosphere was performed. Pd/C was a catalyst in the reaction and anhydrous ethanol was used due to presence of hydrogen in the round-bottom flask. Stirring for 6h at room temperature sufficed for the formation of a spectroscopically clean product in high yield, with no hydrogenation of the carbonyl group of the ester observed. Additional purification of the product was not required. The reaction was monitored with TLC:

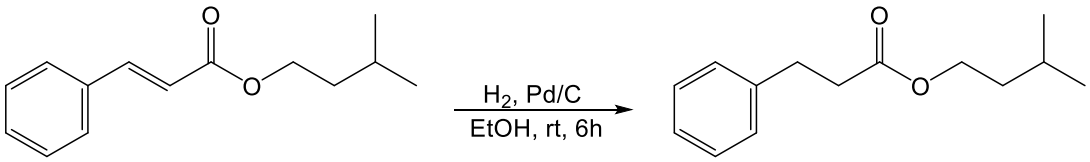

For the UV-Vis measurements, three stock solutions in DMSO were prepared, with concentrations 1 mg/mL, 2 mg/mL and 5 mg/mL. Each was then further diluted to 50 µg/mL, 100 µg/mL, 150 µg/mL, ... and 600 µg/mL with DMSO. Thus, three samples for each concentration point were measured. The results were averaged and plotted to concentration. A tendency line was determined via linear regression, showing a high R^2 factor (**Figure 3.49**).

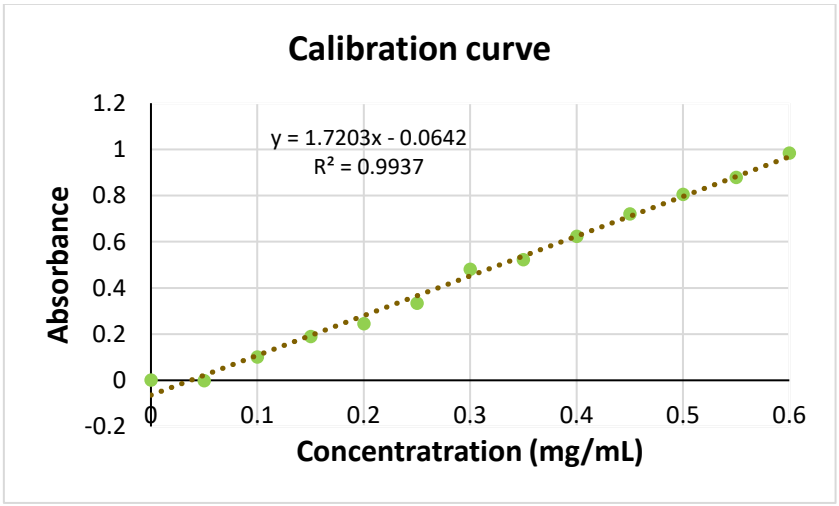

Figure 3.49: Calibration curve for isoamyl hydrocinnamate in DMSO.

Incorporation of isoamyl cinnamate in MIPs

UV-Vis measurements of acrylamide and NIPAM based polymers were performed, involving MIPs and control polymers. Spectra of control polymers were recorded as blank samples, to evaluate the absorbance of the polymer matrix at 264 nm. Samples of the polymers in DMSO were prepared and their absorbances at 264 nm were documented. Using the calibration curve, the measurements were assigned to concentrations. Dividing them with the initial concentration of the polymer, the percentage of incorporation of isoamyl cinnamate was calculated (**Figure 3.50**).

	AA 24 h	**NIPAM** 24 h	**NIPAM** 48 h
50:30:20	6.3%	3.0%	11.7%
30:50:20	9.3%	3.4%	5.5%
60:30:10	5.0%	2.3%	1.7%
40:50:10	2.3%	5.4%	5.5%

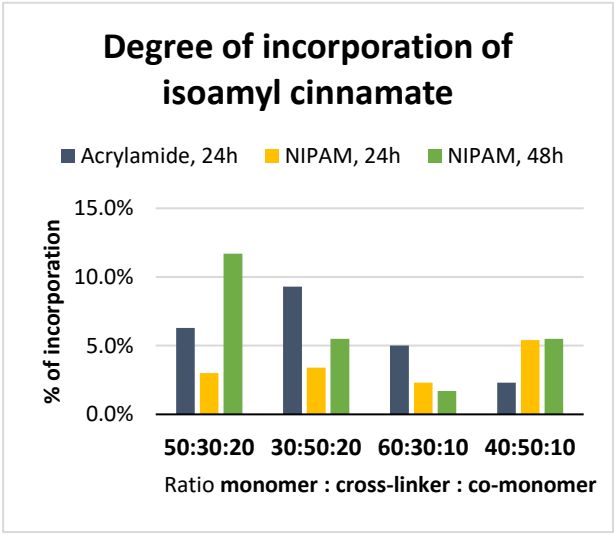

Figure 3.50: Degrees of incorporation of isoamyl cinnamate into the MIPs, based on acrylamide and NIPAM, presented in a table (left) and graphically (right).

Before the calculations, the absorbances of polymers were grouped according to the type of the monomer and the percentage of the cross-linker used during polymerization, and the reaction time. This way, correct absorbances of the polymer matrix were deducted from the absorbances of imprinted polymers, allowing for a more precise calculation of the incorporation of isoamyl cinnamate. With NIPAM polymers, the degree of incorporation in the most part increased with a prolonged polymerisation time, when compared to the same formulations after 24h of reacting.

The amount of the cross-linker and type of the monomer did not immensely influence the incorporation of isoamyl cinnamate. From a higher amount of the polymerizable derivative put into the polymerisaiton mixture, however, the incorporation in general increased. All incorporation values are much lower than expected, suggesting a slower rate of polymerization of the double bond in the cinnamide moiety, compared to the ones found in NIPAM and MBA.

Removal of the template

To remove the templates from the imprinted polymers, an ester bond needed to be broken. Its hydrolysis was successfully attempted by stirring the polymer with an 0.1 M aqueous solution of NaOH for 24h. Clearing up of initially cloudy solutions was observed after 2 h of stirring at room temperature. Upon dialysis against water and freeze-drying, the signal for the ester bond in the ^{1}H NMR spectra of the polymers was absent, indicating that the hydrolysis was successful.

Rebinding studies

To see if there are any rebinding indications for the synthesized imprinted polymers, rebinding studies of isoamyl alcohol were performed. NMR was the method of choice due to difficulties of detection of isoamyl alcohol in presence of DMSO with gas chromatography. Quantification of isoamyl alcohol was made possible by the use of toluene as an external standard, added before each measurement and chosen its peaks did not interfere with the peaks of isoamyl cinnamate or the residues of the polymer in the solution.

For the experiment an imprinted polymer on the basis of NIPAM was chosen, with the highest determined incorporation of isoamyl cinnamate, the ratio of components of 50:30:20, and the time of reaction 24h. The difference between the initial amount of the isoamyl alcohol and the amount of isoamyl alcohol was determined after 1h, 2h, 3h and 24h of rebinding were plotted to time and the behaviour of the concentration was observed (**Figure 3.51**).

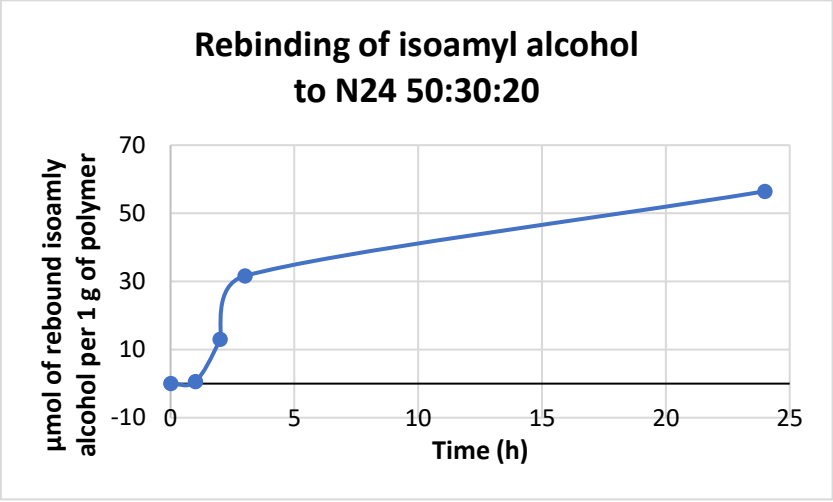

Figure 3.51: Rebinding behaviour of isoamyl alcohol to the imprinted polymer N24 50:30:20.

It can be observed, that rebinding of isoamyl alcohol does occur and starts reaching a plateau after about 3 hours of rebinding. This gives us a lead that the formation of a carboxylic ester of the alcohol ith a free methyl group with cinnamic acid could be successfully applied to the formation of imprinting polymers for 16-OMC.

Synthesis of the MIPs and NIPs for 16-O-methylcafestol

For the synthesis of the imprinted and non-imprinted polymers **11** was used as the polymerizable derivative. Two different ratios of monomer to the cross-linker to the polymerizable derivative were applied. For the ratio 60:30:10, **16a1** as an imprinted polymer and **16a 1.1** as a non-imprinted polymer were prepared. Similarly, for the ratio 40:50:10, **16b1** as an imprinted polymer and **16b 1.1** as a non-imprinted polymer were prepared. For all the polymers NIPAM was used as a monomer, while MBA was used as a cross-linker. The amount of AIBN was 1% for both ratios, calculated to moles of all the double bonds in the reaction. The critical concentration of monomers was 1% in anhydrous DMSO and the reaction time was common at 48h.

	MBA	AIBN	Time	Yield
16a1	30 %	1 %	48 h	57 %
16a 1.1	30 %	1 %	48 h	41 %
16b1	50 %	1 %	48 h	54 %
16b 1.1	50 %	1 %	48 h	40 %

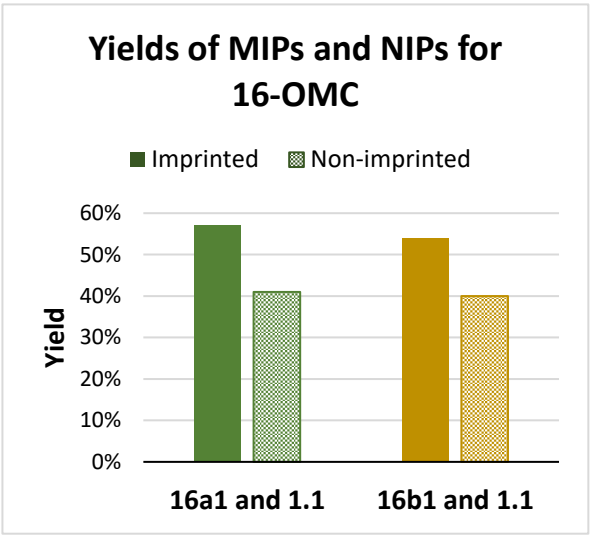

Figure 3.52: Yields of MIPs and NIPs for 16-OMC, presented in a table (left) and a graph (right).

The yields of both MIPs were higher compared to the yields of to them corresponding NIPs (**Figure 3.52**). This fact is encouraging and has led us to believe the incorporation of the polymerizable derivative for 16-OMC has occurred in a relatively high degree. Upon examining the ^{1}H NMR spectra of the polymers, peaks of 16-OMC and a clear signal of an ester bond were found, confirming our theory. Additionally, when inspecting the yields of all polymers, it appeared that an increase of the amount of cross-linker in the polymerization mixture slightly decreases the yields of the polymers.

When comparing the sizes of the synthesized polymer particles (**Table 3.6**), in both series of polymers, **16a** and **16b**, the particles of MIPs are smaller than the particles of their corresponding NIPs. At the same time, a decrease in size seems to occur with the increase of the percentage of the cross-linker in the polymerization mixtures, when among the MIPs 16a1 and 16b1 are compared. The same was observed for both NIPs.

The distribution of the sizes was in most cases unimodal. The only measurement, stepping out of the range of the polymer particle sizes, is the value of the size of polymer particles **16b 1.1**, determined from the size distribution by intensity, where two barely separable peaks were

reported. Upon examining the results of the particle size distribution by volume, we can see that the quantity of larger particles is minor and observed due to their bigger scattering.

Distribution by:	**Size** (d.nm)	**Distrib.**	**Volume** (d.nm)
16a1	19.54	UM	10.36
16a 1.1	18.46	UM	11.46
16b1	11.07	BM	7.023
16b 1.1	52.03	UM	18.08

Table 3.4: Sizes of particles of MIPs and NIPs for 16-OMC.

Finally, zeta potential was measured for all the polymers. It was found, that the measured value of all of them was below -30 mV, indicating that the dispersions of the polymers were not inclined to clustering. The lowest zeta potential was observed in the polymer **16a1**. This was rather surprising, as lower zeta potentials were generally expected for NIPs (**Figure 3.53**).

	ζ (mV)
16a1	-51.3
16a 1.1	-36.2
16b1	-31.5
16b 1.1	-32.7

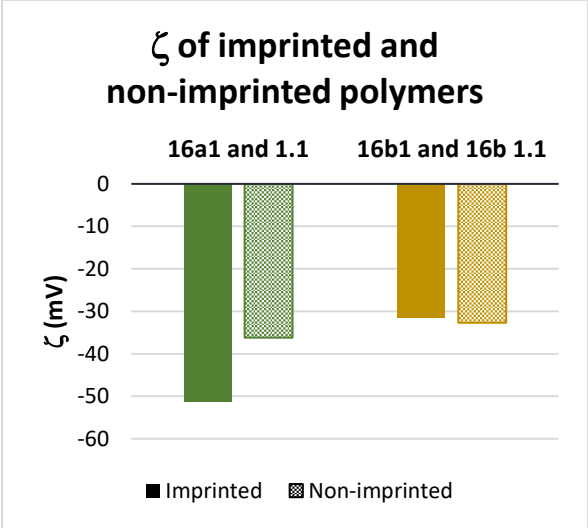

Figure 3.53: Zeta potential results of the MIPs and NIPs for 16-OMC, presented in a table (left) and a graph (right).

Removal of the template

As the template is connected to the MIP with an ester bond, similarly as in the MIPs for isoamyl cinnamate, hydrolysis was a method of choice for the removal of the template. It was successfully attempted by stirring the polymer with a 0.1 M aqueous solution of NaOH for 24h. Upon dialysis against water and freeze-drying, the signal for the ester bond and the rest of the template in the ^{1}H NMR spectra of the polymers was absent, indicating that the removal of 16-OMC was successful.

The incorporation of the incorporated polymerizable derivative (**11**) was determined by sampling the hydrolysis solution after 24 h and quantifying the amount of the released 16-OMC. Percentages of incorporation of the polymerizable derivative are presented in **Table 3.6**.

	MBA	AIBN	Incorp.
16a1	30 %	1 %	29 %
16b1	50 %	1 %	32 %

Table 3.5: Incorporation of 11 into the MIPs.

A slight increase in the incorporation of 16-OMC can be observed in the polymer **16b1**, correlated to the increase of the cross-linker used in the reaction of polymerisation.

Rebinding studies

To examine the rebinding capability of the polymers and their selectivity, rebind studies were made. For the study, a 1 mg/mL solution of a polymer in a 200 mM solution of cafestol and in a 200 mM solution of 16-OMC were prepared. The solutions were sampled after 30 min, 60 min, 120 min, 240 min and 360 min, and the quantity of the remaining diterpene or the combination of diterpenes was determined with HPLC-UV analysis. The difference between the moles of the chosen diterpene in the initial sample and the moles found in aliquots at each time-point was calculated and plotted to the time of sampling. First, the rebinding capabilities of both MIPs for 16-OMC were investigated (**Figure 3.54**).

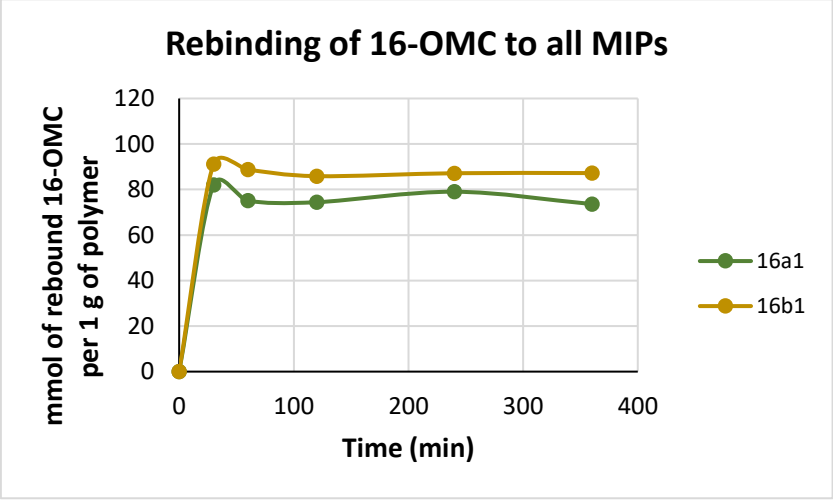

Figure 3.54: Comparison of rebinding capabilities of the MIPs for 16-OMC.

A more significant rebinding of 16-OMC was observed in the polymer **16b1**, compared to the one observed in the polymer **16a1**, indicating that a higher percentage of the cross-linker

during imprinting is beneficial. In both polymers a plateau of the rebound 16-OMC occurs at minute 120, in the polymer **16a1** appearing as noticeably less stable than in the polymer **16b1**. This as well could could be assigned to a beneficial effect of a higher degree of cross-linking. Before the time-point 120 min, peaking of the rebound amount of the diterpene occurs, leading us to believe adsorption of 16-OMC to the polymers is the primary interaction between the two. Upon penetration of the compound into the pores of the polymer, a slight increase of 16-OMC in the surrounding concentration follows.

To study the imprinting effect further, rebinding of 16-OMC to non-imprinted polymers **16a 1.1** and **16b 1.1** was attempted and their profile of rebinding was compared to the ones of imprinted polymers **16a1** and **16b1**. The rebinding studies were performed in the same conditions as the ones with the imprinted polymers for 16-OMC to allow comparison of the results (**Figure 3.55**).

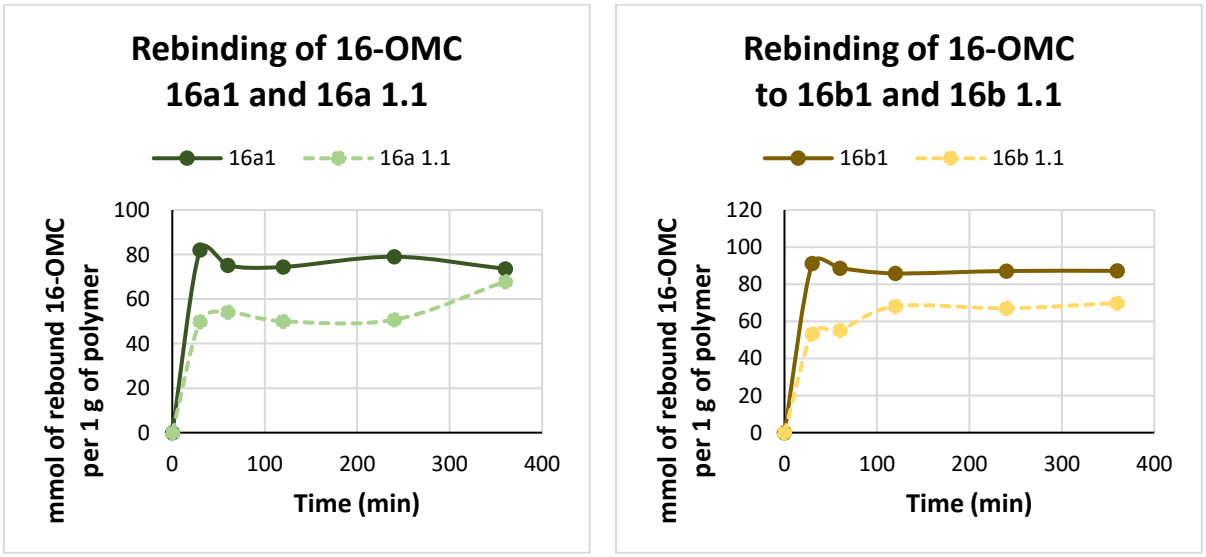

(a) **(b)**

Figure 3.55: Comparison of rebinding capabilities of the MIPs and their corresponding NIPs for 16-OMC.

From the results, imprinting factors were calculated, to determine, which of the polymers exhibits the most significant selective binding. The caluculations were made following the equation:

$$IF = \frac{N_{MIP}}{N_{NIP}},$$

where N_{MIP} represents moles of cafestol, rebound to MIPs, and M_{NIP} moles of cafestol, ebound to MIPs. Data at the time-point of 120 min was taken into account, as at that point a plateau in all samples was reached (**Table 3.7**).

	co-monomer	MBA	AIBN	Incorp. of 3	IF
16a1	10 %	30 %	1 %	29 %	1.48
16b1	10 %	50 %	1 %	32 %	1.26

Table 3.6: Imprinting factors for polymers 16a1 and 16b1

In both series of polymers, **16a** and **16b**, the effect of rebinding is well observed, as the amounts of the rebound 16-OMC are substantially higher in both imprinted polymers, **16a1** and **16b1**, than in their non-imprinted relatives. Imprinting factors suggest a beter expressed capability of selective binding of 16-OMC in the polymer **16a1**.

The rebound amount of 16-OMC in the non-imprinted polymer **16b 1.1** reaches a plateau at minute 120, while the amount of the rebound diterpene on the non-imprinted polymer **16b 1.1** changes through time and reaches its highest point at the last time-point of the measurement. Due to the rebinding depending on the formation of hydrogen bonds and π-methyl interactions, DMSO poses a significant interference in competing with 16-OMC for the formation of both types of interactions.

As we were also interested in the selectivity of the imprinted polymers, rebinding of cafestol to **16a1** and **16b1** was attempted (**Figure 3.56**). It was expected that a selective polymer would rebind cafestol to a much lesser degree than 16-OMC. Unfortunately, however, the result of experiments on both imprinted polymers was rather the opposite, resulting in a higher degree of rebinding of cafestol, compared to the one of 16-OMC. The result is well explicable when considering that the polymers contain several opportunities for the formation of hydrogen bonds with molecules of cafestol.

In the case of the imprinted polymer **16a1** and its non-imprinted relative **16b1**, the difference between their uptake of cafestol is relatively big, even when compared to the difference between their uptake of 16-OMC, suggesting that cafestol is capable of penetrating into the polymer, even more so as 16-OMC. This suggests, that a π-methyl interaction in the recognition spot of the imprinted polymers for 16-OMC did not suffice in the attempt to reach selectivity of the polymer, and the much stronger hydrogen interactions played a bigger role in the process.

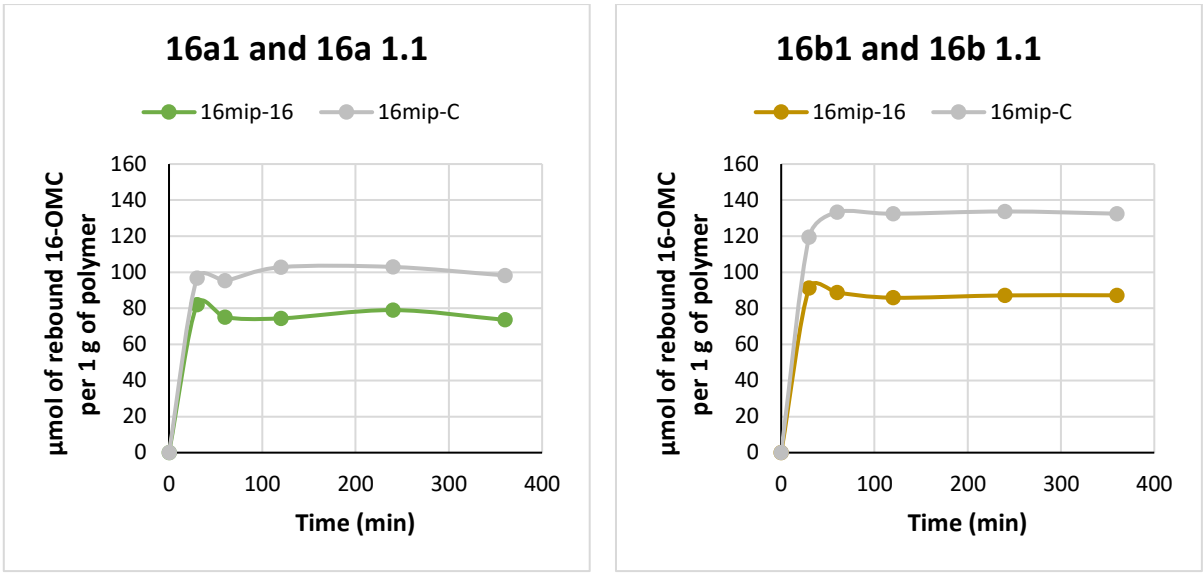

(a) **(b)**

Figure 3.56: Selectivity of the MIPs for 16-OMC upon rebinding of cafestol and 16-OMC under the same conditions.

Additionally, we need to consider, that not only are the hydrogen interactions stronger, there are many more opportunities for cafestol and 16-OMC to form them throughout the polymers. Namely, 16-OMC was initially connected to the polymer via an ester bond, which was broken upon removal of the template. This makes it reasonable to assume, that should a molecule of cafestol be able to enter the pores of imprinted polymers **16a1** and **16b1**, it would be capable to interact with the residual carboxylic group in the polymer better than 16-OMC, due to being capable of forming hydrogen bonds with both hydroxy groups of the vicinal diol. 16-OMC, on the other hand, is capable of forming hydrogen bonds only with one hydroxy group and the oxygen of the methoxy group in this part of the molecule, causing a less intensive interaction in the recognition spot of the polymer.

Competitive rebinding

In the next step we wanted to examine the rebinding kinetics of 16-OMC to the imprinted polymers, while an equal amount of cafestol is present in the solution (**Figure 3.57**). Each of the two imprinted polymers had their template removed prior to the study. They were then tested by preparing a 1 mg/mL solution of a polymer in a solution, simultaneously consisting of 200 mM of cafestol and 200 mM of 16-OMC. The solution was sampled after 30 min, 60 min, 120 min, 240 min and 360 min and the quantity of the diterpenes was determined with HPLC-UV. The difference between the moles of cafestol and 16-OMC in the initial sample and the moles found in aliquots at each time-point was calculated and plotted to the time of sampling.

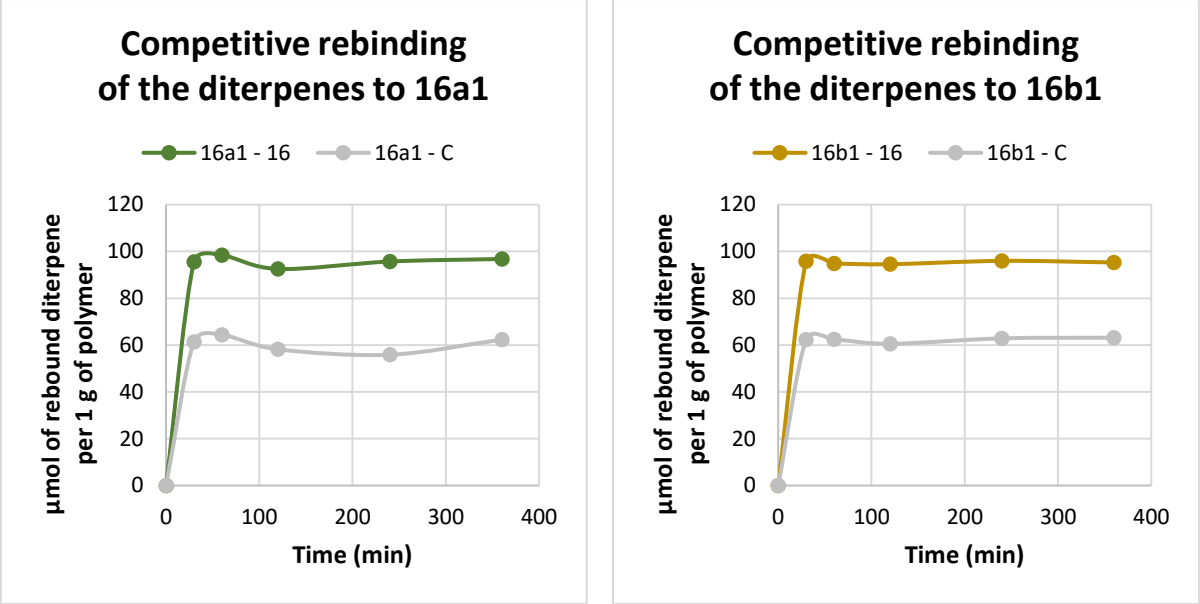

Figure 3.57: Results of competitive rebinding of 16-OMC and cafestol to the polymers imprinted and non-imprinted polymers of the series 16a and 16b.

When compared to the separate rebindings of 16-OMC and cafestol, where the uptake of cafestol in both polymers was bigger than the uptake of 16-OMC, the situation in this case is quite the opposite. While the same amounts of both diterpenes were present in the solution, in both imprinted polymers, **16a1** and 1**6b1**, the rebinding of 16-OMC occurred in a much bigger part than rebinding of cafestol. An explanation for this could be, that 16-OMC forms interactions with the polymer fast enough to occupy binding spots for cafestol. Thus, even though cafestol might interact with the polymer more intensively, it prevents it from rebinding in a similarly big proportion as when it is rebound with the polymer alone. This is a very good lead for the practical use of the imprinted polymers, as their main purpose would be exploration in determination of the presence of 16-OMC in extract mixtures of Arabica and Robusta, where both diterpenes are naturally present.

Interestingly, the amount of the rebound templates via normal and competitive rebinding is higher than expected for the non-covalently imprinted polymers, found in literature.[163]

Bibliography

9. Speer, K. & Kölling-Speer, I. The lipid fraction of the coffee bean. *Braz. J. Plant Physiol* **18,** 201–216 (2006).

13. Naegele, E. Determination of Methylcafestol in Roasted Coffee Products According to DIN 10779. *Agil. Technol.* (2016).

154. Kriz, D., Ramström, O. & Mosbach, K. Molecular Imprinting: New Possibilities for Sensor Technology. *Anal. Chem.* **69,** 345A–349A (1997).

155. Hashim, S. N. N. S., Boysen, R. I., Schwarz, L. J., Danylec, B. & Hearn, M. T. W. A comparison of covalent and non-covalent imprinting strategies for the synthesis of stigmasterol imprinted polymers. *J. Chromatogr. A* **1359,** 35–43 (2014).

160. Bhattacharjee, S. DLS and zeta potential - What they are and what they are not? *J. Control. Release* **235,** 337–351 (2016).

161. Yan, J., Springsteen, G., Deeter, S. & Wang, B. The relationship among pK a, pH, and binding constants in the interactions between boronic acids and diols - It is not as simple as it appears. *Tetrahedron* **60,** 11205–11209 (2004).

162. Miyamae, Y., Kurisu, M., Han, J., Isoda, H. & Shigemori, H. Structure-activity relationship of caffeoylquinic acids on the accelerating activity on ATP production. *Chem. Pharm. Bull. (Tokyo).* **59,** 502–507 (2011).

163. Pellizzoni, E. *et al.* Fluorescent molecularly imprinted nanogels for the detection of anticancer drugs in human plasma. *Biosens. Bioelectron.* **86,** 913–919 (2016).per filling of apolar pockets at enzyme active sites. *J. Org. Chem.* **73,** 4345–4361 (2008).

4. RESULTS AND DISCUSSION:

A colorimetric assay for quantification of Arabica and Robusta

4.1 Introduction

In literature[48], colour reactions of several molecules with antimony(III) chloride have been described, giving a possibility to differentiate between them based on their colour reactions. Interestingly, the differentiation appears to occur even when minor differences in the structure of treated compounds are present. Several oils, as well as sterols and diterpene molecules, were tested providing intriguing results.

Following those, we wanted to apply the same treatment to the two diterpenes in our focus, cafestol and 16-O-methylcafestol, to see if it would give us an opportunity to differ between them.

4.2 Preliminary tests on cafestol and 16-OMC

A 30% solution of antimony(III) chloride in chloroform was prepared in five parallels. One was left as it was, while a drop of acetic acid, a drop of acetic anhydride, a drop of HCl or a drop of H_2SO_4 were added to the others. Pairs of samples of cafestol and 16-O-methylcafestol were treated with each solution to form a concentration of 5 mg/mL for all the samples. Differences in colours were observed.

Coloration of samples appeared in a matter of seconds and the colour continued to develop for several minutes to follow. At minute 10, the samples of cafestol and 16-OMC treated with the same solution were placed side by side and compared. Apart from the ones treated with the antimony(III) chloride solution with a drop of H_2SO_4, all of the samples exhibited a red colouring of 16-O-methylcafestol and an orange one of cafestol. The antimony(III) chloride solution with a drop of H_2SO_4, on the other hand, coloured both samples bright orange.

The biggest difference in colour was observed in the samples treated with the solution of antimony(III) chloride with a drop of acetic acid (**Figure 4.1**), where the obtained colours were bright red for 16-O-methylcafestol and bright orange for cafestol. The results were similar when both samples were treated with the 30% solution of antimony(III) chloride in chloroform with no additions, however the colour appeared several minutes later.

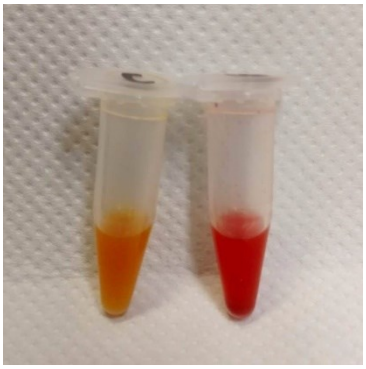

Figure 4.1: Samples of cafestol (left) and 16-O-methylcafestol (right) 10 min after the addition of the antimony(III) chloride solution with acetic acid.

Due to the encouraging result, UV-Vis spectra were recorded for the samples of Arabica and Robusta, 10 min after the treatment with the antimony(III) chloride solution with acetic acid. For the purpose, the samples were diluted 1:10 with chloroform and the UV-Vis spectrum was recorded from 300 nm to 750 nm. The obtained spectral lines differed enough to give us several opportunities for discrimination between the two diterpenes.

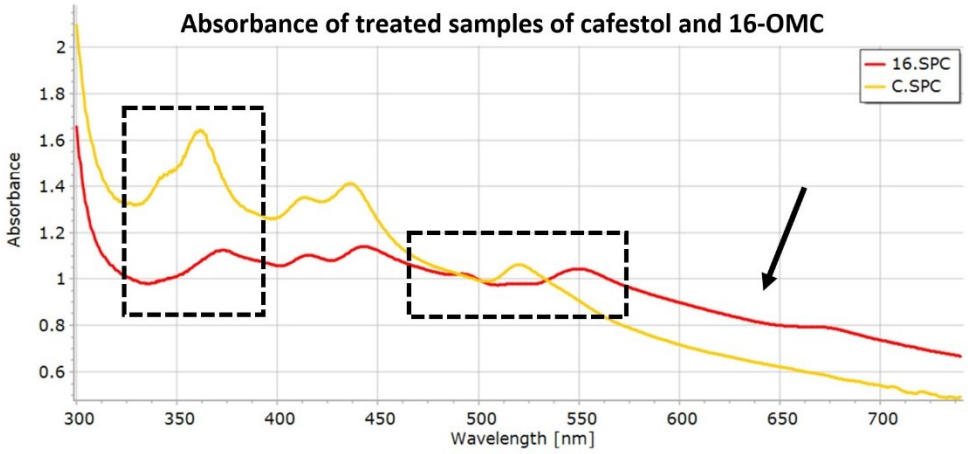

Figure 4.2: Overlapped spectra of cafestol and 16-O-methylcafestol 10 min after the treatment with the antimony(III) chloride solution with acetic acid and subsequent dilution.

In the spectra, areas of difference appear as higher readings of absorbance for cafestol in the range 325 nm to 395 nm, compared to the ones for 16-O-methylcafestol, several crossing points of the two spectral lines in the range 465 nm to 570 nm, and visibly different slopes of the spectral lines from 550 nm onwards (**Figure 4.2**).

The results are in compliance with the literature, reporting the formation of organo-metalic products with unsaturated compounds[52], yet the fact that such a minor difference in the structure of the two diterpenes can lead to their differentiation is rather surprising.

4.2.1 Coffee extracts in various solvents

Knowing that the lipid fraction of the coffee bean is rich with sterols and diterpenes[9], and that the profile of sterols and diterpenes in Arabica has only a minor resemblance to its profile in Robusta, the possibility to develop a colorimetric method had a great potential in our pursuit of finding a way to differentiate between the two coffee species.

Preparation of coffee extracts

Extracts of ground roasted beans of Arabica and Robusta were prepared. For the extractions, several solvents with different polarities were used, as we wanted to see which profile of the extracted compounds could give the most characteristic difference between the treated extracts of Arabica and Robusta, if any would be found. Extracts of Arabica and Robusta in the same solvent were always observed.

The solvents used, listed by increasing polarity, were diethyl ether, ethyl acetate, chloroform, dichloromethane, acetone, acetonitrile and methanol. The extracts were prepared in ratio 1 g of coffee to 5 mL of the chosen solvent. After 1 h of stirring and removal of the coffee particles with filtration, the transparent extracts of various shades of yellow were used for the treatment with the antimony(III) chloride solution.

Preparation of the antimony(III) chloride solution

A 30% antimony(III) chloride solution in chloroform was prepared again and a drop of acetic acid was replaced with 20 µL of acetic acid. To completely dissolve antimony(III) chloride sonication was necessary. When completely transparent, the solution was ready to be used.

Treatment of coffee extracts

The initial ratio between the volume of the antimony(III) chloride solution and the volume to coffee extract was 1 to 1, with 250 µL of the antimony(III) chloride solution being added to 250 µL of the extract. The vials were capped to prevent the evaporation of the solvents, gently shaken and observed at room temperature.

In a matter of seconds the colour started changing in the samples containing the dichloromethane and chloroform extracts, gradually turning the extract of Robusta first pale and with time darker blue, and the extract of Arabica first bright yellow and with time darker yellow with a reddish accent (**Figure 4.3**).

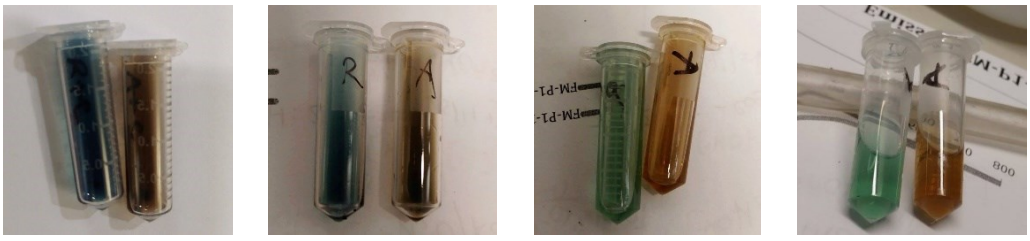

(a) **(b)** **(c)** **(d)**

Figure 4.3: Colour of the treated chloroform (a) and dichloromethane (b) extracts after 5 min, acetonitrile (c) extracts after 10 min and diethyl ether (d) extracts after 10 min.

About a minute into the experiment, a change of colours in the extracts of the samples of Arabica and Robusta in acetonitrile and diethyl ether started to be noticeable. In both solvents the extract of Robusta went from pale blue to bright blue, and the extract of Arabica from yellow to red. To develop the most characteristic colour difference between the Arabica and Robusta sample, the samples in acetonitrile needed 10 min and the samples in diethyl ether 15 min. The latter were also less stable, as their colour soon began displaying a gray undertone. The extracts prepared in methanol, acetone and ethyl acetate did not display comparably good results even after 15 min and were not further investigated (**Figure 4.4**).

(e) **(f)** **(g)**

Figure 4.4: Colour of treated methanol (e), acetone (f) and ethyl acetate (g) extracts after 10 min.

UV-VIS spectra

Due to the intensity of the obtained colour when dichloromethane, chloroform and acetonitrile extracts were tested, UV-Vis spectra were recorded for all of them. For the chloroform extract the spectrum was recorded from 300 nm to 700 nm in baseline correction mode with chloroform as a background sample, 5 min after the addition of the antimony(III) chloride solution to the coffee extract.

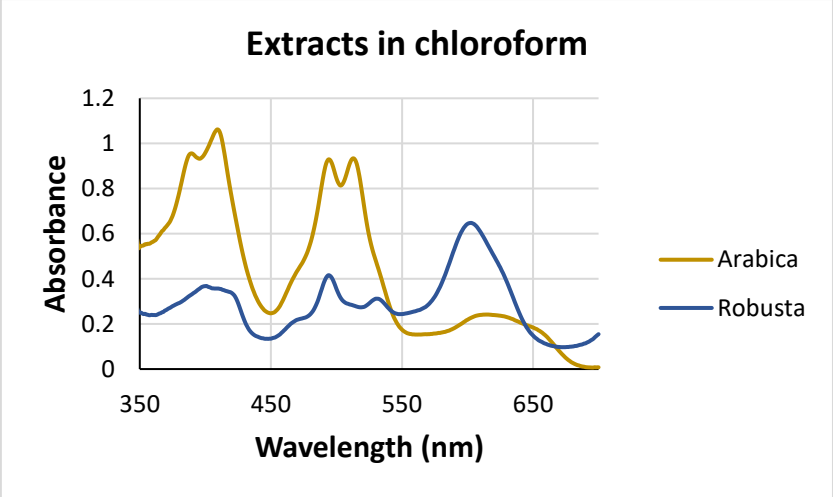

Figure 4.5: Spectra of treated extracts of Arabica and Robusta in chloroform.

As observed in **Figure 4.5**, the spectral lines of the Arabica and Robusta samples differ greatly. Moreover, the peak in the spectral line of the Robusta sample at 603 nm rises above the spectral line of the Arabica sample, giving the absorbance reading of 0.648 and differing from the absorbance reading for Arabica of 0.420 units. This also gives a possibility to try to explore the result in a quantitative way, to determine the ratio of Arabica and Robusta in the mixture.

Additionally, the spectral line of the Robusta sample appears to be rising towards the end of the measuring interval. For this reason, the spectra of treated acetonitrile and dichloromethane extracts of Arabica and Robusta were recorded in the range from 300 nm to 800 nm in otherwise identical conditions, 5 min after the addition of the antimony(III) chloride solution (**Figure 4.6**).

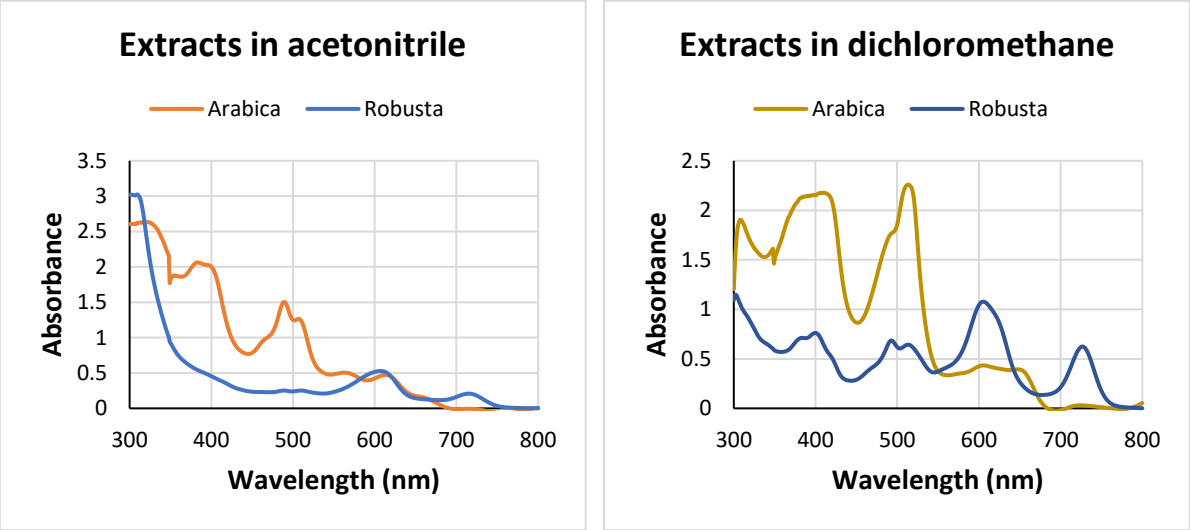

Figure 4.6: Overlapped spectra of treated extracts of Arabica and Robusta in acetonitrile (left) and dichloromethane (right).

It is immediately noticeable that the peaks in the spectra of the dichloromethane extracts of both coffee samples are more pronounced when compared to both spectra of the acetonitrile extracts, especially in the range from 500 nm to 800 nm. As a consequence of the enlargement of the recording range of the spectra, a peak at 726 nm was discovered, well visible in the spectral lines of the treated Robusta extracts in both solvents, but far more imposing in the treated dichloromethane extract of Robusta. As such, it gave a reading of absorbance of 0.624, much higher than the treated acetonitrile extract of Robusta at 0.174.

The peak appears to be characteristic for Robusta, as for the treated dichloromethane extract of Arabica only an absorbance value of 0.031 was measured.

Diagnostic capability of the peak

Due to good results obtained with the dichloromethane extracts of Arabica and Robusta, we wanted to further investigate the behaviour of the peak at 726 nm. To see if the peak is diagnostic for various degrees of contamination of Arabica with Robusta, several volumetric mixtures of the two extracts were prepared, in volumetric ratios 1:3 (**halfA** + **R**), 1:1 (**halfA** + **halfR**) and 3:1 (**A** + **halfR**) of Arabica to Robusta. Together with the extracts of Arabica and Robusta alone, each extract was again treated with the antimony(III) chloride solution with acetic acid (1:1, volumetrically). The vials were capped and gently shaken. After15 min their content was diluted 1:10 with dichloromethane. The time of reacting was prolonged to see if it would be possible to obtain an even greater difference between the readings of absorbance for Arabica and Robusta at 726 nm.

The spectra were recorded under the same conditions as before and still in the range of 300 nm to 800 nm (**Figure 4.7**). It was confirmed that the peak at 726 nm is diagnostic for the degree of contamination of Arabica with Robusta, as its height was changing expectedly with the changing ratio between the two coffees.

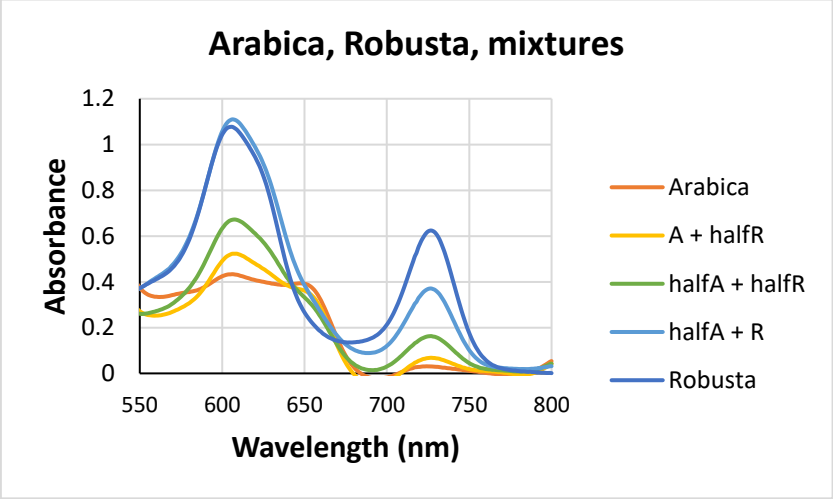

Figure 4.7: Treated samples of Arabica, Robusta and their mixtures.

Other commercially available coffees

As illy's blend for the sample of Arabica and Amigos as a representative of Robusta were always used, we wanted to see if our results are relevant when expanded to other commercially available brands of coffee. Tesco Arabica as pure Arabica, and Sainsbury's Italian Style, Lavazza Qualità Rossa and Co-op as mixtures of Arabica and Robusta were tested. Their extracts were prepared as before, from 1 g of ground roasted coffee samples in 5 mL of dichloromethane, with the extractions going on for 1 h and finishing with a titration.

Evaporation of the solvent with a stream of N_2 was introduced after the filtration step, and re-dissolution of the residues to form 100 mg/mL stock extract solutions. This was attempted as we noticed that less oil gets extracted from Robusta than from Arabica and wanted to further improve the difference between the readings of absorbance of the treated extracts of Robusta and Arabica.

The preparation of the 30% antimony(III) chloride solution in chloroform with acetic acid remained the same. On the other hand, preparation of the samples for the UV-Vis measurements was slightly changed. With the addition of 25 µL of antimony(III) chloride solution to 950 µL of dichloromethane first, and of 25 µL of a stock extract solution afterwards, we wanted to lower the concentration of reactants in order to lower the rate of the occurring reaction and gain better controlled conditions of the experiment.

The spectra were still recorded in baseline correction mode with dichloromethane as a blank sample. The range of recording was set from 650 nm to 900 nm 25 min from the addition of the stock extract solution to the mixture of dichloromethane and the antimony(III) chloride solution. The spectra were overlapped and the peak at 726 nm was observed (**Figure 4.8**).

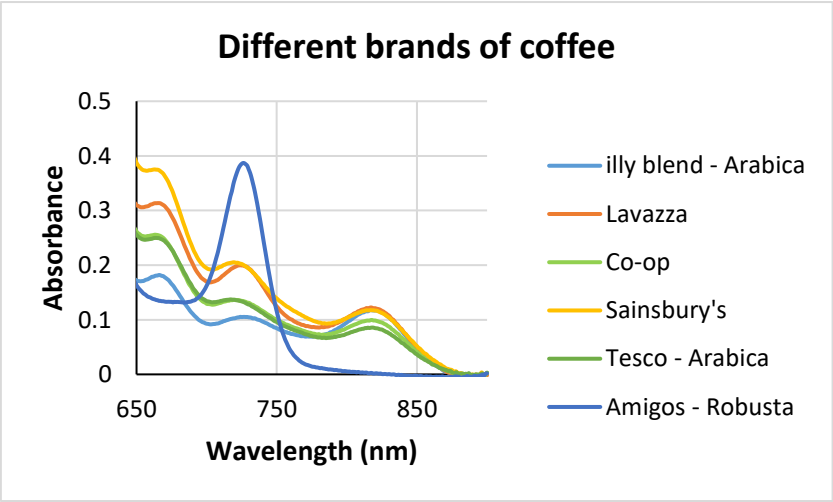

Figure 4.8: Overlapped spectra of treated samples of various brands of coffee at minute 25.

As expected, the highest absorbance was reached for Amigos Robusta at 0.387 and the lowest for illy's Arabica at 0.105. The spectral lines for the rest of the coffees were between the spectral lines of Arabica and Robusta, with the peak absorbance readings trending towards the absorbance of the Arabica sample, confirming our expectations. Interestingly, by increasing the upper limit of the recording range to 900 nm, another peak was discovered at 819 nm. Opposite to the one at 726 nm, this peak appeared to be characteristic for Arabica with the highest absorbance at 0.117, while the absorbance of Robusta was only 0.001. The spectral lines for the rest of the coffee samples were again between the two spectral lines, with the absorbances trending towards the absorbance reading of the sample of Arabica.

4.2.2 Development of the extraction procedure

Dichloromethane was used as the solvent for extraction due to its slightly lower health hazard, providing comparable results to the ones obtained with the chloroform extracts. The extractions were always executed using commercially available ground roasted coffee. The extracts were prepared in glass vials.

First attempts of extractions consisted of adding 5 mL of dichloromethane to 1 g of coffee. The vials were capped and wrapped in parafilm to prevent evaporation of the solvent, then placed on a shaker for 1 h. Coffee was then filtered off with the use of syringe filters and clear extracts were treated with the antimony(III) chloride solution immediately.

Soon after an evaporation step was introduced, with a stream of N_2 at room temperature, followed by re-dissolution of the residues in dichloromethane to form 100 mg/mL stock extract solutions. This was done to improve the precision of the readings of absorbance for Arabica and Robusta, and to lower the variability of the measurements due to changes in concentration of the extracts during the filtration step of the extraction. As nitrogen is an inert gas at room temperature, it was also a way to keep the extracts as intact as possible.

For the sake of obtaining a bigger difference in the readings of absorbance for the samples of Arabica and Robusta, the time of extraction was prolonged to 24 h in hope to extract a bigger amount of the substrates giving the colour reaction. Apart from that, the extraction procedure and the sample preparation for the measurements remained the same. The prolonged time of extraction showed an increase in the amount of the extract residue in the samples of Arabica and Robusta (**Table 4.1**).

	1 h	**24 h**
Arabica	100 mg	122 mg
Robusta	57 mg	62 mg

Table 4.1: Yields of extractions after 1 h and 24 h.

To further increase the yields of extractions, a larger volume of dichloromethane was used. 1 g of coffee was extracted with 25 mL of the solvent, instead of 5 mL, per extraction. At the same time, stirring was introduced rather than extraction on a shaker, as it assures a bigger contact area between the coffee particles and the solvent, thus additionally aiding with the extraction.

The final improvements were substitution of plastic pipette tips with Hammilton syringes, to improve precision of the method and eliminate the possibility of interference of melted plastic with the results, and filtration through 1 to 2 cm layer of Celite® instead of trough syringe filters, to again avoid the contact of dichloromethane with plastic and to improve the cost-efficiency ratio of the method. Substituting the filtration method was successful, as the resulting filtrates were clear, while the results of the colorimetric method remained unchanged.

The extracts are advised to be prepared fresh for each experiment, as it was reported in the literature that rancid oils could cause interferences with the method[4]. Storing the residues after removal of dichloromethane for several days in the freezer, however, did not alter the results of the measurements.

4.2.3 Development of the antimony(III) chloride solution

Preparation of the 30% antimony(III) chloride was attempted in chloroform and dichloromethane, giving similarly intensive colour reactions with coffee extracts in both solvents. Due to issues with precipitation in the antimony(III) chloride solution when prepared in chloroform, the solvent was eventually switched to dichloromethane, in which antimony(III) chloride was much better soluble. Preparation of the antimony(III) chloride solution in several non-chlorinated solvents was also attempted, however with no useful results.

To avoid the evaporation of dichloromethane and minimize the changes in its concentration, the antimony(III) chloride solution was kept on dry ice if a bigger number of samples needed to be tested. Storage on normal ice was attempted, however since antimony(III) chloride is very sensitive to moisture, if exposed, hydrolysis of the compound occurred almost instantly. The exposure of antimony(III) chloride to moisture leads to formation of antimony oxychloride.

$$\mathbf{SbCl_3 + H_2O \rightarrow SbOCl + 2HCl}$$

When exposed to larger amounts of water, $Sb_4O_5Cl_{12}$ is formed, a white precipitate with no colouring effect, following the equation[165]:

$$\mathbf{4SbCl_3 + 5H_2O \rightarrow Sb_4O_5Cl_{12} + 10HCl}$$

Addition of acids, acetic anhydride

In literature, additions of 1-3% of acids, alcohols or acetic anhydride to a 30% solution antimony(III) chloride in chlorurated solvents were described to give a moderately to significantly improved results of its colour reactions. For this reason, we decided to test the addition of several acids and acetic anhydride to the antimony(III) chloride solution to observe differences in the spectra of treated extracts of Arabica and Robusta, specifically the behaviour of the peak at 726 nm.

For the measurements, 100 mg/mL stock extract solutions of Arabica and Robusta in dichloromethane were used. First, 30% solutions of antimony(III) chloride in dichloromethane with the additions of 2% (V/V) of acetic acid, acetic anhydride, 10% solution of HCl or 5% solution of H_2SO_4 were tested. The samples for UV-Vis measurements were prepared by adding 25 µL of the antimony(III) chloride solution to 950 µL of dichloromethane, then adding 25 µL of the stock extract solution to the mixture. Its addition represents minute 0 of the measurement.

30 min after its addition a UV-Vis spectrum was recorded in the range from 650 nm to 950 nm. A sample of Arabica and a sample of Robusta were treated with each variation of the antimony(III) chloride solution. The spectra of both were always overlapped, their readings of absorbance at 726 nm and 819 nm were compared (**Figure 4.9**), and the differences of absorbance values for both peaks were reported (**Table 4.2**).

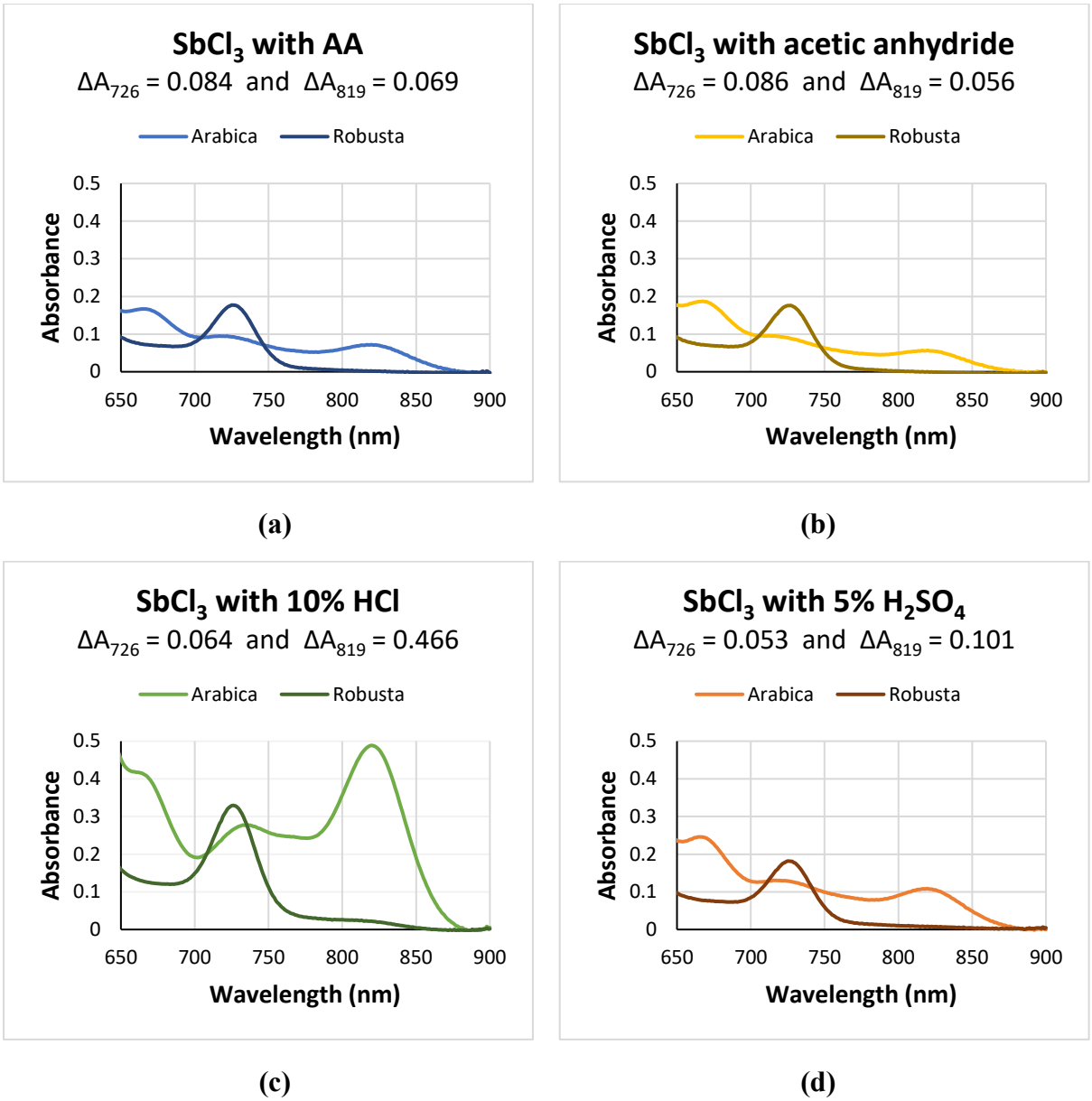

Figure 4.9: Comparisons of the spectral lines of Arabica and Robusta samples, treated with the antimony(III) chloride solution with 2% of acetic acid (a), acetic anhydride (b), 10% HCl (c) and 5% H_2SO_4 (d).

In all the spectra, a difference in the absorbances between the sample of Arabica and the sample of Robusta occurs; the biggest one was observed when the samples were treated with either the antimony(III) chloride solution with acetic acid or acetic anhydride (**Figure 4.10**).

The difference is a little bigger when acetic anhydride is used as a colour catalyst, however, as it simultaneously raises the absorbance of the sample of Arabica more than acetic acid, we decided to continue developing the method with the use of the latter.

	ΔA_{726}	ΔA_{819}
Acetic acid	0.084	0.069
Acetic anhydride	0.086	0.056
10% HCl	0.064	0.101
5% H_2SO_4	0.053	0.466

Table 4.2: Differences of absorbance between Arabica and Robusta at 726 nm and 819 nm for various additions to the antimony(III) chloride solution.

Another interesting observation is that the addition of 5% HCl to the antimony(III) chloride solution vastly increases the peak at 819 nm, which could be explored, should we decide to target it instead of the peak at 726 nm.

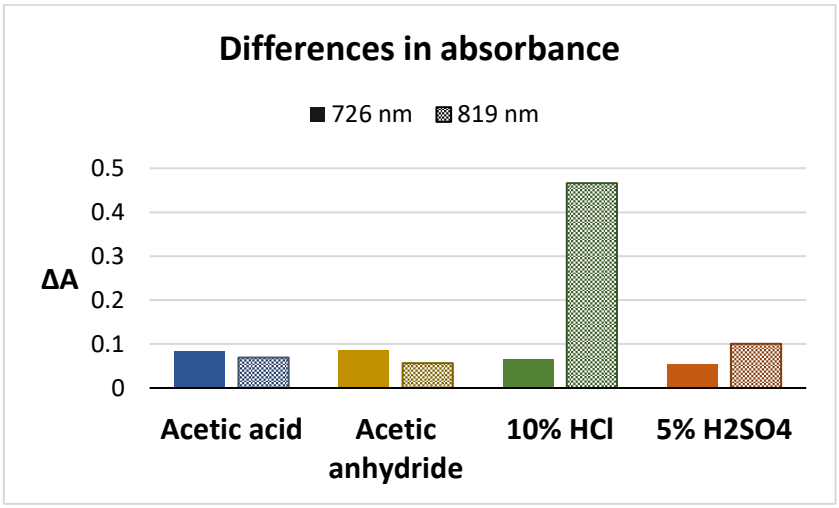

Figure 4.10: Differences in absorbance between the peaks of treated samples of Arabica and Robusta at wavelengths 726 nm and 819 nm, with the antimony(III) chloride solution with different acids.

To see what amount of acetic acid is necessary to achieve an optimal result, two new variations of the antimony(III) chloride solution were prepared. In the first one to a 30% solution of the antimony(III) chloride in dichloromethane instead of 2% of acetic acid 20% (V/V) were added, going from 10 µL to 100 µL of the acid to 410 µL of dichloromethane. The second solution was prepared by dissolving 150 mg of antimony(III) chloride directly in 510 µL of acetic acid.

The samples for the UV-Vis measurements were prepared as before and were again measured at minute 30 after the addition of the stock extract solution of Arabica or Robusta to the mixture of the chosen antimony(III) chloride solution and dichloromethane. The spectra of the samples of Arabica and Robusta were in both cases overlapped and their readings of absorbance at 726 nm and 819 nm were compared (**Figure 4.11**).

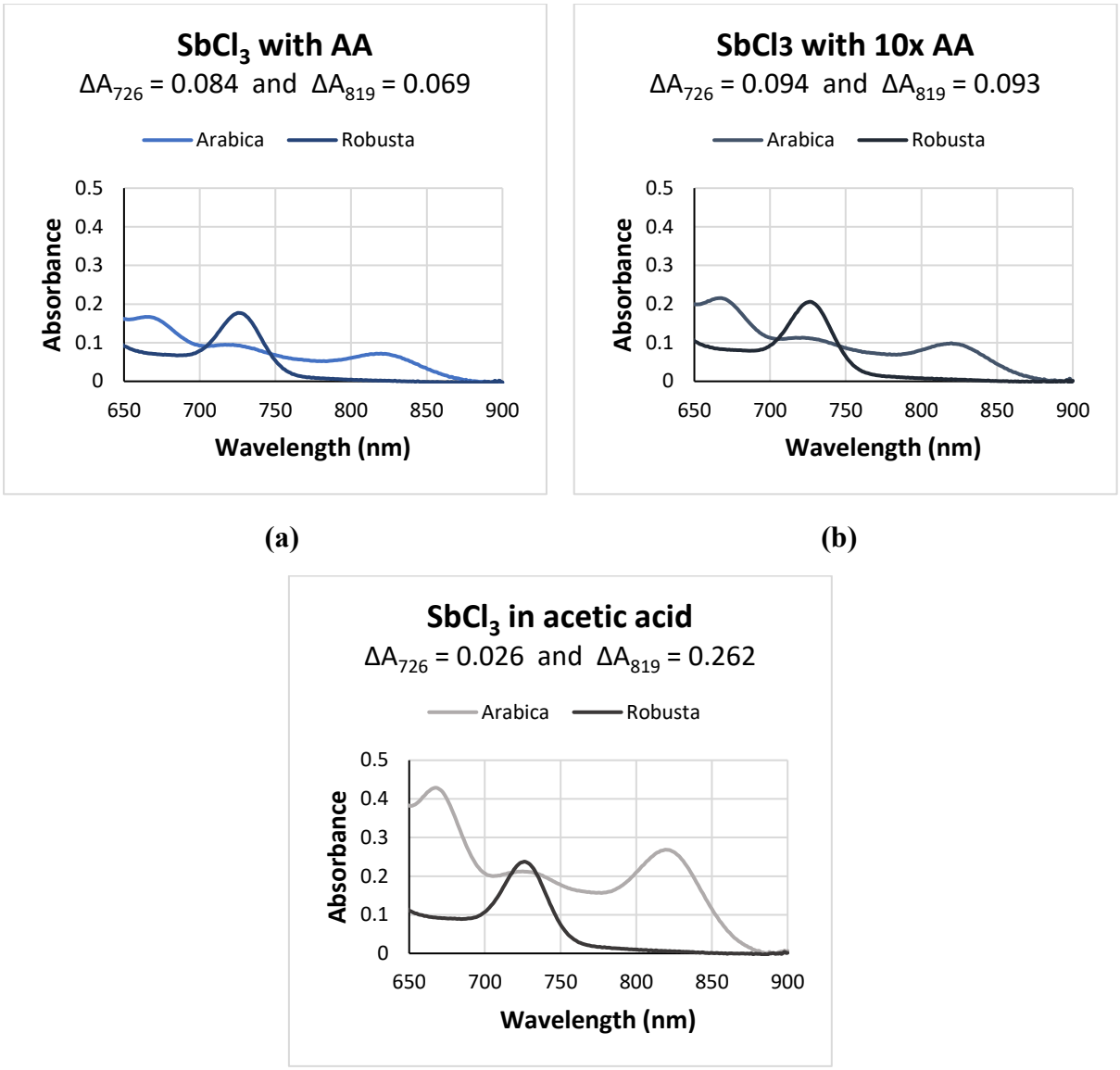

Figure 4.11: Comparisons of the spectral lines of Arabica and Robusta samples, treated with the antimony(III) chloride solution with 2% of acetic acid (a), 20% of acetic acid (b) and 100% of acetic acid (c).

Where the antimony(III) chloride solution with a 10-fold increase of the acetic acid addition was used, the difference between the absorbances between the samples of Arabica and Robusta at 726 nm slightly increases (**Table 4.3**, **Figure 4.12**), however with the price of simultaneously increasing the absorbance of Arabica. Where the antimony(III) chloride solution in acetic acid was used, the difference between the absorbances of the samples of Arabica and Robusta decreases with an accompanying increase of the absorbance of the Arabica sample, when compared to its absorbance after treatment with the solution of antimony(III) chloride with 2% of acetic acid.

	ΔA_{726}	ΔA_{819}
Acetic acid	0.084	0.069
10x acetic acid	0.086	0.056
In acetic acid	0.064	0.100

Table 4.3: Differences of absorbance between Arabica and Robusta at 726 nm and 819 nm for various degrees of added acetic acid.

The biggest difference between the absorbances at 819 nm occurs when the antimony(III) chloride solution in acetic acid is used, raising the absorbance of the sample of Arabica while keeping the absorbance of the sample of Robusta relatively close to 0.

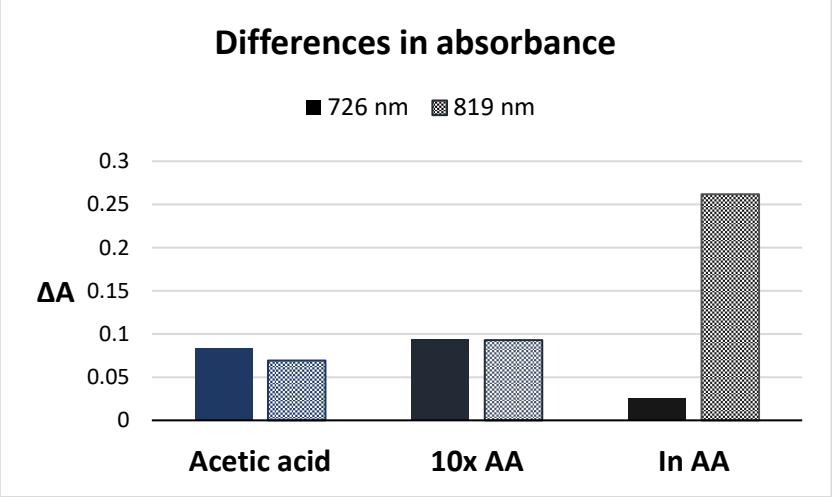

Figure 4.12: Differences in absorbance between the peaks of treated samples of Arabica and Robusta at wavelengths 726 nm and 819 nm, with the antimony(III) chloride solution with different degrees of acetic acid.

Different ratios of antimony(III) chloride reagent to the coffee extract

The next step in the development of our method was determination of the ratio between the volume of the antimony(III) chloride solution and the stock extract solution used in the preparation of the samples for UV-Vis measurements. The antimony(III) chloride solution was prepared as a 30% solution in dichloromethane with 2% of acetic acid.

For the measurements 100 mg/mL stock extract solutions of Arabica and Robusta in dichloromethane were used. The chosen V/V ratios between the stock extract solutions and the antimony(III) chloride solution were 35 to 15, 25 to 25, 35 to 15 and 40 to 10. The samples for UV-Vis measurements were prepared by adding the decided amount of the antimony(III) chloride solution to 950 µL of dichloromethane, then adding the stock extract solution, Addition of the latter represented time 0 of the measurements.

30 min after its addition UV-Vis spectra were recorded in the range from 650 nm to 950 nm. A sample of Arabica and a sample of Robusta were treated in each experiment and the spectra of both were always overlapped. Their readings of absorbance at 726 nm and 819 nm were compared (**Figure 4.13**).

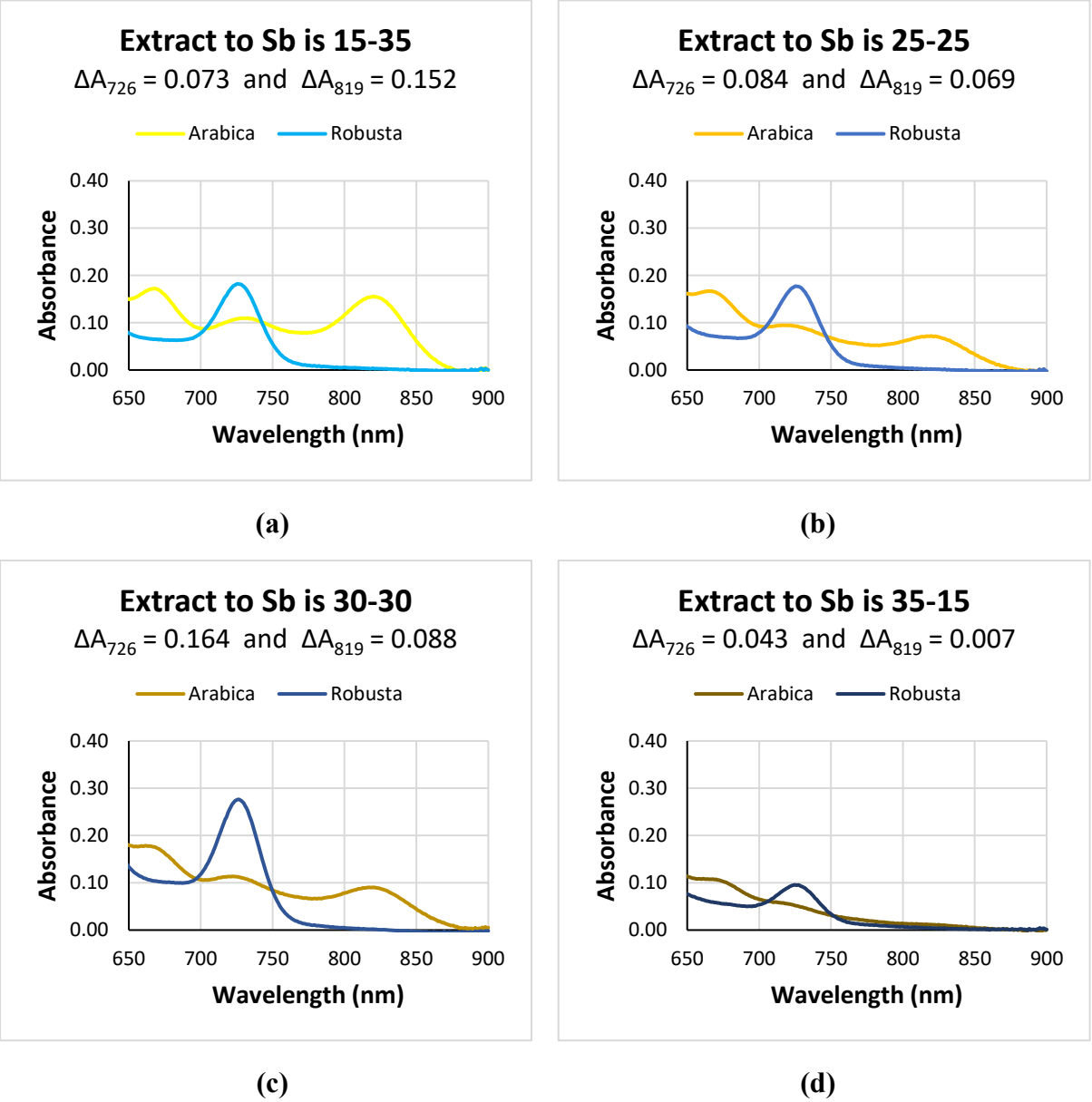

Figure 4.13: Comparisons of the spectral lines of the Arabica and Robusta samples, treated with the antimony(III) chloride solution in ratios 15-35 (a), 25-25 (b), 35-15 (c) and 40-10 (d).

The biggest difference between absorbances is of 0.084, measured at 726 nm occurs when the ratio between the antimony(III) chloride solution and the stock extract solutions of Arabica or Robusta is 25-25 (**Table 4.4**, **Figure 4.14**).

	ΔA_{726}	ΔA_{819}
15 to 35	0.074	0.152
25 to 25	0.084	0.070
35 to 15	0.044	0.007
40 to 10	0.002	0.001

Table 4.4: Differences of absorbance between Arabica and robusta at 726 nm and 819 nm for various ratios of the stock extract solution to antimony(III) chloride solution.[1]

Interestingly, the biggest difference in the absorbances at wavelength 819 nm occurs when the ratio between the stock extract solutions and antimony(III) chloride solution of Arabica and Robusta is 15 to 35, at 0.152. Nevertheless, as the peak at 726 nm was the one, characteristic for Robusta, we have decided to continue with the ratio 25 to 25.

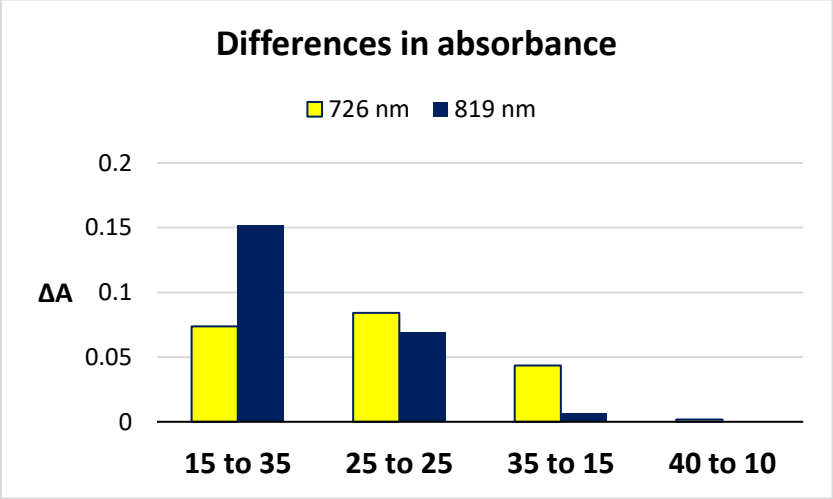

Figure 4.14: Differences in absorbance between the peaks of treated samples of Arabica and Robusta in different ratios of the stock extract solution to antimony(III) chloride solution at wavelengths 726 nm and 819 nm.

Since the values of the absorbance for both samples were relatively low in combination 25-25, we wanted to see if an increase in the volume of the antimony(III) chloride solution and the stock extract solution in the samples for the UV-Vis measurements would aid in broadening the difference between the absorbances. The tested ratio between the two was 30-30 and the results were compared to the results of the ratio 25-25 (**Figure 4.15**).

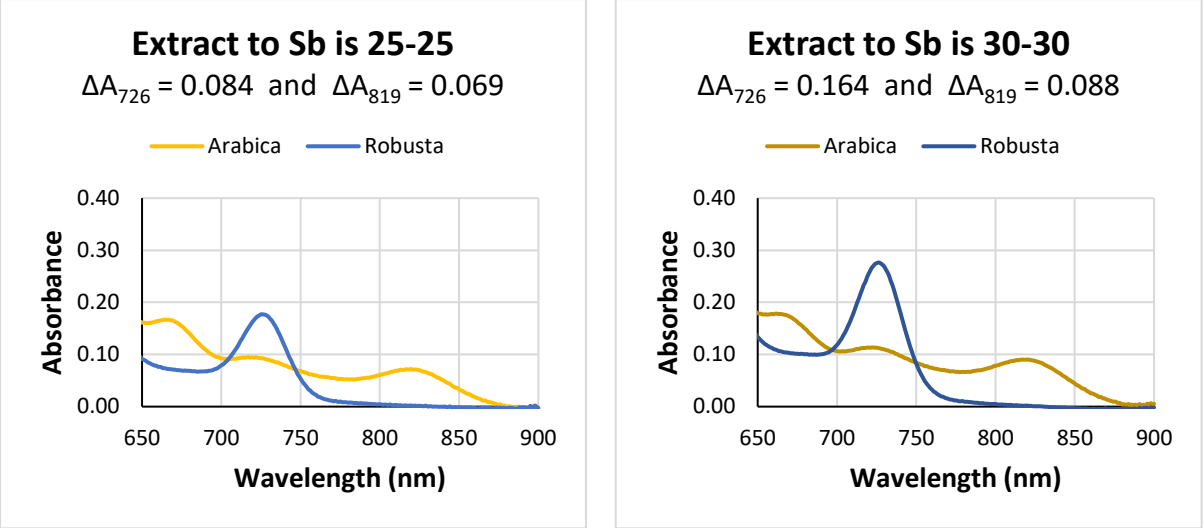

Figure 4.15: Overlapped spectra of the treatment ratios 25-25 (left) and 30-30 (right).

The samples were prepared by adding 30 µL of the antimony(III) solution to 940 µL of dichloromethane, then adding 30 µL of the stock extract solutions of Arabica or Robusta. The addition of the stock extract solution represented time 0.

At minute 30 the UV-Vis spectra were recorded. They were then overlapped and the differences in absorbance at 726 nm and 819 nm between Arabica and Robusta were observed (**Figure 4.16**, **Table 4.5**).

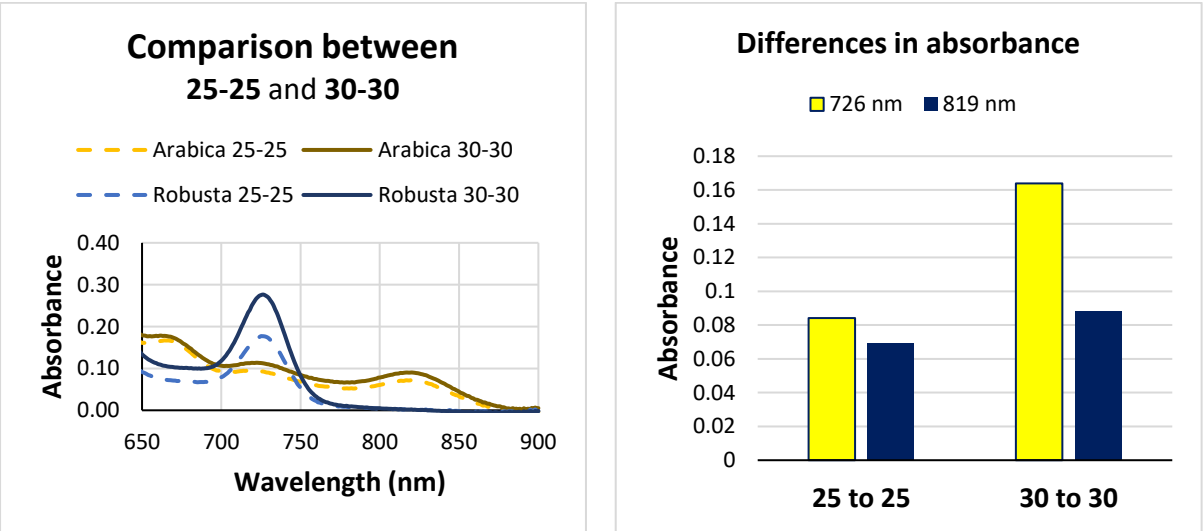

Figure 4.16: Comparison of the results of treatment ratios 25-25 and 30-30 (left) and a demonstration of differences in the absorbances at 726 nm and 819 nm (right).

At wavelength 726 nm, the difference in absorbance between the peaks of Arabica and Robusta increased, while barely rising the absorbance of Arabica. At 819 nm, the absorbance of Arabica was slightly raised while leaving the absorbance of the sample of Robusta unchanged and close to 0.

The sample preparation with a volumetric ratio of the antimony(III) chloride to the stock extract solution 30 to 30 was thus accepted as more beneficial when observing the peak at 726 nm.

	ΔA_{726}	ΔA_{819}
25 to 25	0.084	0.070
30 to 30	0.016	0.088

Table 4.5: Differences of absorbance between Arabica and Robusta at 726 nm and 819 nm for various ratios of the stock extract solution and antimony(III) chloride solution.

4.2.4 Kinetic studies

Due to instability of trivalent antimony and consecutively bad repeatability of the method, we pursued a search for a more stable antimony(III) chloride solution. In literature several possible improvements were offered as introduction of elementary antimony, zinc or tin in the solution for redox stabilization.[50] Due to availability in our laboratory, we have chosen to introduce zinc dust into the existing antimony(III) chloride solution.

Extracts of pure Arabica and Robusta were used for the study. Extractions were performed by stirring 1 g of each coffee with 5 mL of dichloromethane overnight and filtration. Removal of the solvent with a stream of N_2 followed, then re-dissolution in dichloromethane to form 100 mg mL^{-1} stock extract solutions.

Two antimony(III) chloride solutions were prepared. **Solution I** was a 30% solution of antimony(III) chloride in dichloromethane with 2% of acetic acid. **Solution II** was essentially solution I with the addition of 5% of zinc dust. Both solutions were sonicated until all the antimony(III) chloride was dissolved and solution II was additionally left standing until all zinc dust settled. 6 samples for UV-VIS measurements were prepared, among those 3 samples for Arabica and 3 samples for Robusta.

First, behaviour of the peak at 726 nm was observed in the samples of Arabica and Robusta, treated with the **solution I**. The samples for measurements were prepared in two parallels by adding 50 µL of the **solution I** to 900 µL of dichloromethane. To one parallel 50 µL of the Arabica stock extract solution were added and to the other 50 µL of the Robusta stock extract solution. Immediately after, the measurement was initiated (**Figure 4.17**).

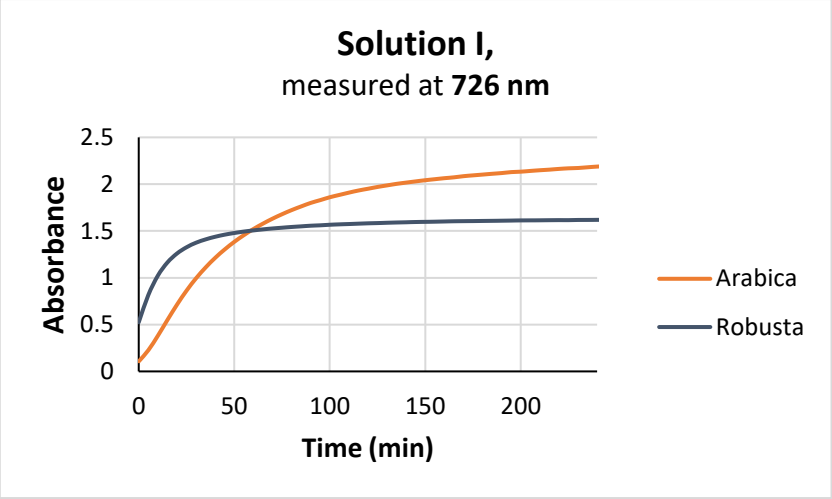

Figure 4.17: Result of the kinetic experiment at 726 nm with solution I.

With the experiment we wanted to see at which time-point the rising of absorbance at 726 nm stabilizes enough to improve the precision and repeatability of our measurements. A troubling observation we encountered was, that 60 min after the initiation of the experiment, the absorbance value of the sample of Arabica not only surpasses the absorbance value of the sample of Robusta but continues to rise for the whole time of the experiment. From the perspective of the sample of Robusta, on the other hand, minute 60 would already give good measurements as its absorbance value ceases to vastly change.

To get a good enough difference between the absorbance readings of Arabica and Robusta in this way, we would need to perform measurements inside of the time interval 10 to 30 min with a high time-wise precision to avoid increasing the variability of the measurements.

Next, the behaviour of the peak at 726 nm was observed in the samples of Arabica and Robusta, treated with the **solution II**. The samples for measurements were prepared in two parallels by adding 50 µL of the **solution II** to 900 µL of dichloromethane. Then to one parallel 50 µL of the Arabica stock extract solution were added and to the other 50 µL of the Robusta stock extract solution, and the measurement was initiated immediately (**Figure 4.18**).

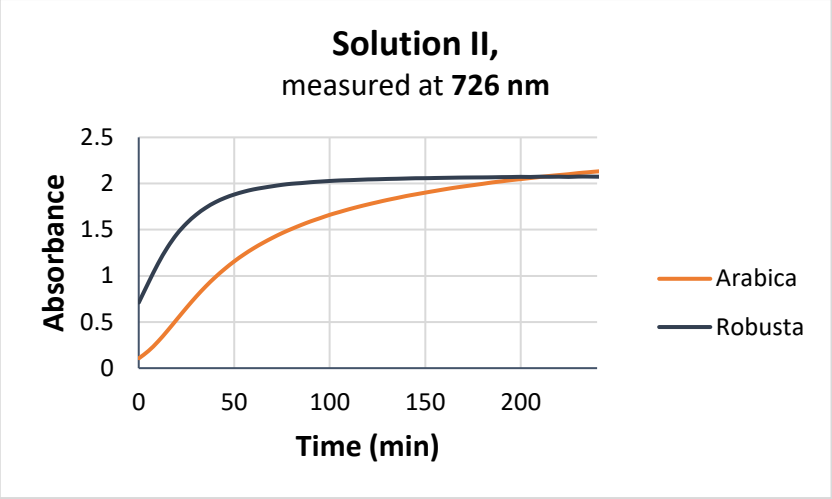

Figure 4.18: Results of the kinetic experiment at 726 nm with solution II.

Compared to the treatment with solution I, for the samples treated with the solution II the intersection of the spectral lines of the samples of Robusta and Arabica appears much later in time, at minute 200 (**Figure 4.19**).

Additionally, the solution II allows the spectral line of the Robusta sample to rise to a higher absorbance and stabilize later in time. The rising of absorbance immensely slows down at minute 60 and stops at minute 100. Since at minute 60 even the absorbance of Arabica is rising with a slower pace as in the previous experiment, we believe thad addition of zinc dust to the antimony(III) chloride solution is very suitable for the purpose of our experiment.

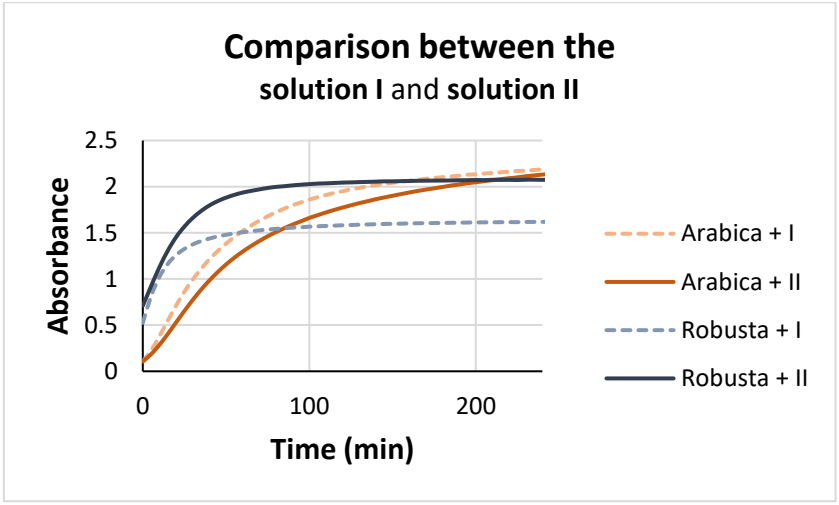

Figure 4.19: Compared results of the kinetic experiment at 726 nm for solutions I and II.

Lastly, the behaviour of the peak at 819 nm was observed in the samples of Arabica and Robusta, treated with the solution II. The samples for measurements were prepared in two parallels by adding 50 µL of the solution II to 900 µL of dichloromethane. Then, to one parallel 50 µL of the Arabica stock extract solution were added and to the other 50 µL of the Robusta stock extract solution (**Figure 4.20**).

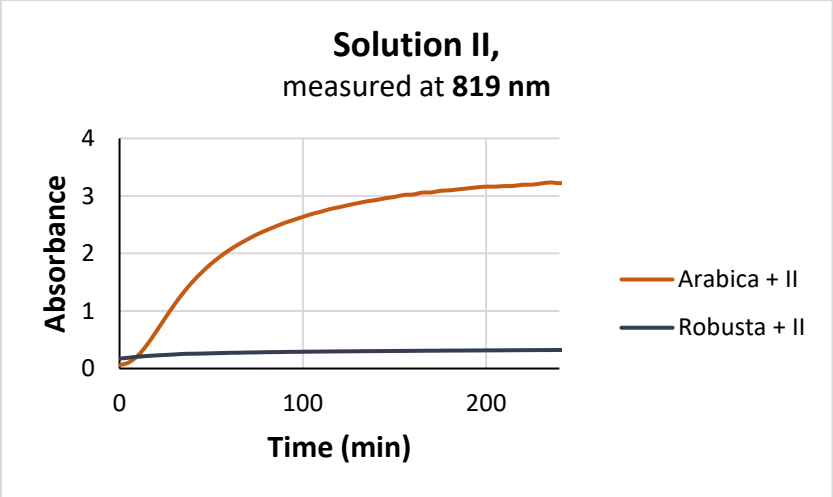

Figure 4.20: Results of the kinetic experiment at 819 nm.

In this case the absorbance value of the Robusta sample slightly rises until minute 50 and remains unchanged from that point on, never surpassing the value 0.350. The absorbance of the sample of Arabica initially rises very quickly and starts to slow down at minute 60.

An intersection between the two spectral lines still occurs, however already at minute 10. At the same time, the difference between the absorbances is much bigger than in both experiments of observing the behaviour of the peak at 726 nm. Eventhough the peak at 819 nm represents a characteristic feature for the sample of Arabica, it gives a difference of absorbances of 1.789 at minute 60 of the measurement, and thus offers a possibility of a more precise quantification of the amount of Robusta in its mixture with Arabica.

4.3 Experiments on Arabica, Robusta and mixtures

Once the improved antimony(III) chloride solution was defined, we decided to test it on different samples of Arabica, Robusta and mixtures of Arabica and Robusta (m/m) to see if the absorbances at wavelengths 726 nm and 819 nm give a linear response when plotted to concentration.

5%, 20%, 50% and 80% mixtures of Robusta with Arabica and were prepared by mixing roasted ground Arabica and Robusta coffee beans to corresponding ratios and then performing an extraction of 1 g of the mixtures with 25 mL of dichloromethane for 24 h. Extracts of pure Arabica and pure Robusta were prepared as well and in the same way. After removal of the coffee and evaporation of the solvent, 100 mg/mL stock extract solutions in dichloromethane were prepared.

The samples for measurements were prepared by adding 50 µL of the antimony(III) chloride solution II to 900 µL of dichloromethane through, then 50 µL of a stock extract solution. The samples were incubated at 25°C and at minute 60, then UV-Vis spectra were recorded. The spectra of the samples were overlapped to observe if their absorbances at wavelengths 726 nm and 819 nm for various ratios of Arabica and Robusta fall in a logical order (**Figure 4.21**).

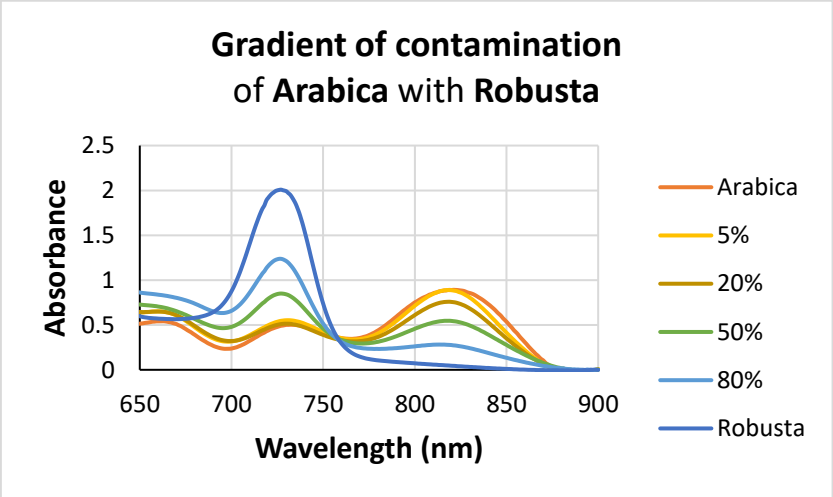

Figure 4.21: Treated samples of mixtures of Arabica and Robusta.

It is clearly noticeable that the peaks at 726 nm and 819 nm are both diagnostic, as the readings of absorbance ascend with a rising part of Robusta in the mixture at 726 nm and with a rising part of Arabica in the mixture at 819 nm. An isoasbestic point is observed at 760 nm, showing that just two molecular species are involved in the system, one in Arabica and one in Robusta. Readings of absorbance at both wavelengths were then plotted to % of Robusta in the mixture with Arabica. A calibration curve was assigned and the R^2 factor was determined (**Figure 4.22**).

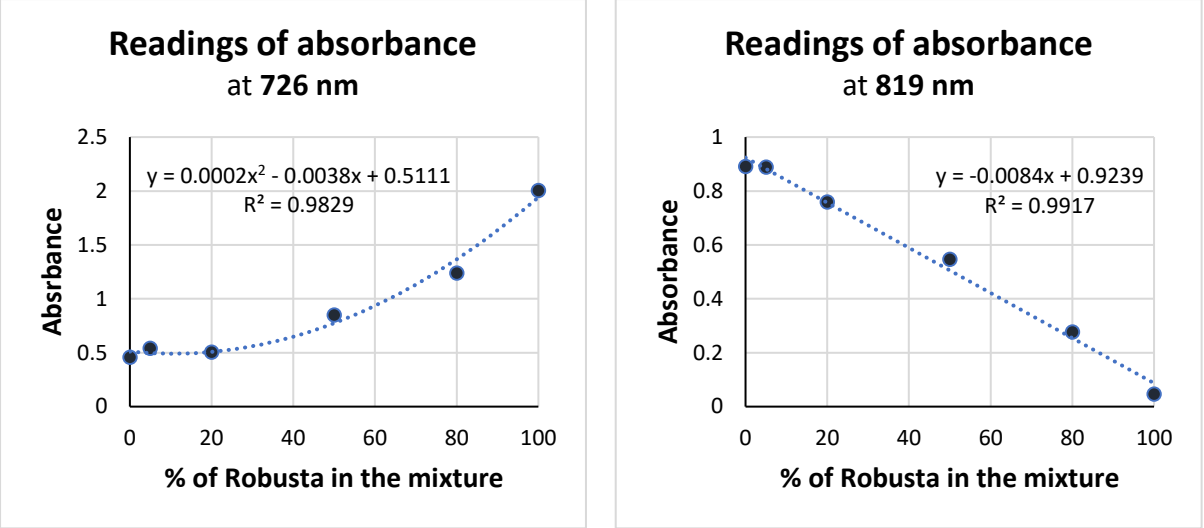

Figure 4.22: Plotted readings of absorbance at 726 nm (left) and 819 nm (right).

When comparing the two calibration curves, however, the peak at 819 nm gives a much better linearity with the R^2 value of over 0.99. Meanwhile, the correlation between the absorbances at 726 nm and degree of Robusta in the samples fits far more to a polynomial than to a linear calibration curve. The limit of detection (LOD) for the peak is 72.6 % of Robusta in the mixture, following the method of linear regression.

The limit of detection when observing the peak at 819 nm is 18.3 % of Robusta in the mixture, far more agreeable as the one found at 726 nm. The value is acceptable according to the 2SD criterion and preliminary repetitions of the calibration experiment, which showed an SD value of 8 to 9 % per chosen data point. The SD value reduced to 3 to 4 % when a ratio of absorbances A_{819} to A_{726} was calculated, which points to a possible further reduction of the LOD value of the method. More experiments will have to be performed for confirmation.[181]

4.4 Experiments on Arabicas and Robustas

With the experiment we wanted to confirm that the method is not specific just for brands of Arabica and Robusta we were using. The extracts of three Arabicas and three Robustas were prepared as above by using Marcafe Oro, Amigos and Lavazza Suerte as Robusta coffees, and illy Guatemala, illy Ethiopia and illy Brazil as Arabica coffees.

Their 100 mg/mL stock extract solutions were treated with the antimony(III) chloride solution II. The samples for UV-Vis measurements were prepared by adding 50 µL of the antimony(III) chloride solution to 900 µL of dichloromethane, then 50 µL of the chosen coffee extract solution. Incubation at 25 °C followed.

At minute 60 UV-Vis spectra were recorded from 650 nm to 900 nm. Spectra of different samples were overlapped to better observe the differences in absorbance at 726 nm and 819 nm (**Figure 4.23**).

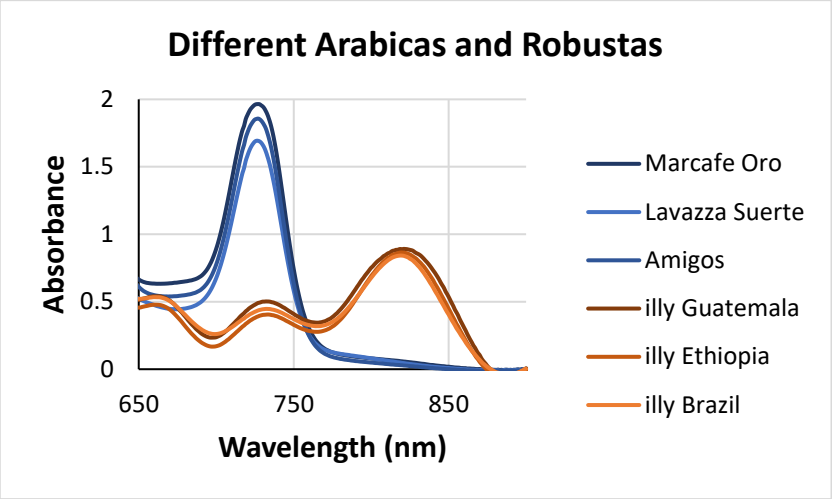

Figure 4.23: Overlapped spectra of treated samples of different Arabicas and Robustas.

From the spectra we can see a relatively good matching of the spectral lines between the three samples of Robusta and the three samples of Arabica, especially around the wavelengths 726 nm and 819 nm. The absorbance values for Arabicas and Robustas were gathered for both wavelengths and for each wavelength an average of absorbances and standard deviations for Arabicas and Robustas were calculated (**Table 4.6**).

	A_{726}	A_{819}
Marcafe Oro	1.964	0.059
Amigos	1.693	0.049
Lavazza Suerte	1.855	0.030
Average	**1.837**	**0.046**
SD	**0.136**	**0.015**
illy Guatemala	0.485	0.891
illy Ethiopia	0.387	0.865
illy Brazil	0.430	0.843
Average	**0.434**	**0.866**
SD	**0.049**	**0.024**

Table 4.6: Readings of absorbance for treated samples of various Arabica and Robusta coffees at 726 nm and 819 nm.

All the values led us to confirm that the peak at 819 nm is a better choice for the analysis, as it gives a lower SD value for Robusta samples than the peak at 726 nm, and still a good SD value for Arabica coffees. Moreover, at both wavelengths even at the value of 2x SD, the absorbances of Arabica do not overlap with those of Robusta, which gives the method a great potential. As those are only the initial results, validation on real samples still needs to be performed.

4.5 Final protocol

Following the experiments, a method protocol has been established:

Preparation of coffee extracts

To 1 g of ground roasted coffee beans 25 mL of dichloromethane is added. The round bottom flask is capped, wrapped in parafilm and left stirring overnight. Next day, the mixture is filtered through a 1 to 2 cm layer of Celite® on a vacuum filter. Clear filtrate is collected, and the solvent is removed under vacuum.

Preparation of stock extract solutions for UV-VIS measurements - per sample

To 5 mg of the extract residue in a glass vial 50 µL of dichloromethane is added to form a 100 mg/mL solution.

Preparation of the antimony(III) chloride solution

150 mg of antimony(III) chloride and 7.5 mg of zinc dust are weighed into a glass vial and 500 µL of dichloromethane is added, then 10 µL of acetic acid. The mixture is sonicated until all antimony(III) chloride dissolves and left standing in a capped vial on dry ice until the zinc dust settles.

Preparation of samples for UV-Vis measurements - per sample

To 900 µL of dichloromethane in a closed glass vial 50 µL of the antimony(III) chloride solution is added through the cap, then 50 µL of stock extract solution. The vial is gently shaken and incubated at 25°C for 60 min. At minute 60 a UV-VIS spectra is recorded at the temperature of 25°C in baseline correction mode from 650 nm to 900 nm with a background sample of dichloromethane. Peak at 819 nm is observed, where the samples containing pure Arabica give the highest absorbance, spectra of the samples of pure Robusta lay close to 0 and samples of mixtures give a height of the peak linearly correlating to the ratio of the components.

4.6 Advantages with running methods

From a practical aspect, having a simple method to determine the ratio of Arabica and Robusta in a mixture could aid with labelling and quality control of coffee. Several chromatographic and infrared methods for authentication of Arabica exist nowadays, yet they mostly depend on costly equipment and are not always available for routine analysis[5,6,7]. Our method is affordable and capable of accurate detection of the amounts of components in a mixture of Robusta and Arabica, as well as determination of the species of coffee. It also requires a simple sample preparation with UV-VIS detection, which also gives us an opportunity to create a portable cost-effective detection device.

When searching for a correlation between coffee and antimony or antimony(III) chloride through literature, only studies of detecting elementary antimony in coffee samples exist with the main goal to determine the quantity of toxic elements in coffee or to describe its geographical origin.

Antimony(III) chloride is already well recognized as a TLC staining agent as many versions of TLC staining solutions derived from it are known. Its advantage is development of a significant colour with various groups of compounds. It has been previously used in a TLC method for differentiation between true cardamoms *Elettoria cardamomum Maton* and large cardamoms *Amomum subulatum Roxb.*.[8]

Probably the most known use of antimony(III) chloride is in quantification of vitamin A in cod-liver oil, a method developed and reported by Carr and Price in 1926.[9]

A simple portable device was created for quantification of vitamin A in palm oil with a saturated solution of antimony(III) chloride in chloroform and spectroscopic detection. The concept for our device would be similar but used for quantification of the ratio between two coffee species. The method, as well as the possible device, would be novel also by using a different wavelength and a differently prepared antimony(III) chloride reagent.

4.7 Fluorescence of coffee extracts

Coffee is known to be fluorescent, the characteristic very much in use in fluorescent microscopy. Additionally, coffee extracts treated with the antimony(III) chloride solution with or without the added zinc dust start exhibiting a very noticeable red shine an hour after the addition of the antimony(III) chloride solution, well observable when a sample is positioned near a light source.

Due to the fact, that samples of pure Arabica and mixtures of Arabica and Robusta give a much brighter red colour compared to the samples of 100% Robusta, we decided to investigate the possibility to use fluorometry to find a new way of differentiation of Arabica from Robusta and possibly quantify their ratio in a mixture.

4.7.1 Fluorescence of treated coffee extracts

The samples for the measurements were stock extract solutions of Arabica, Robusta and Lavazza Qualità Rossa, the latter one representing a mixture of 60 to 40 of Arabica to Robusta. They were prepared and treated with the antimony(III) chloride solution II in the same way as for the UV-Vis analysis, but instead of letting them react for 1 h, they were left standing at room temperature for 24 h, so the red shine would fully develop.

After 24 h the samples were diluted to 3 mL with dichloromethane and fluorescent spectra were recorded at several excitation wavelengths. The excitation wavelengths were chosen based on the peaks in a pre-recorded UV-VIS spectra, then fine-tuned while recording the fluorescent spectra to get the best response (**Figure 4.24**).

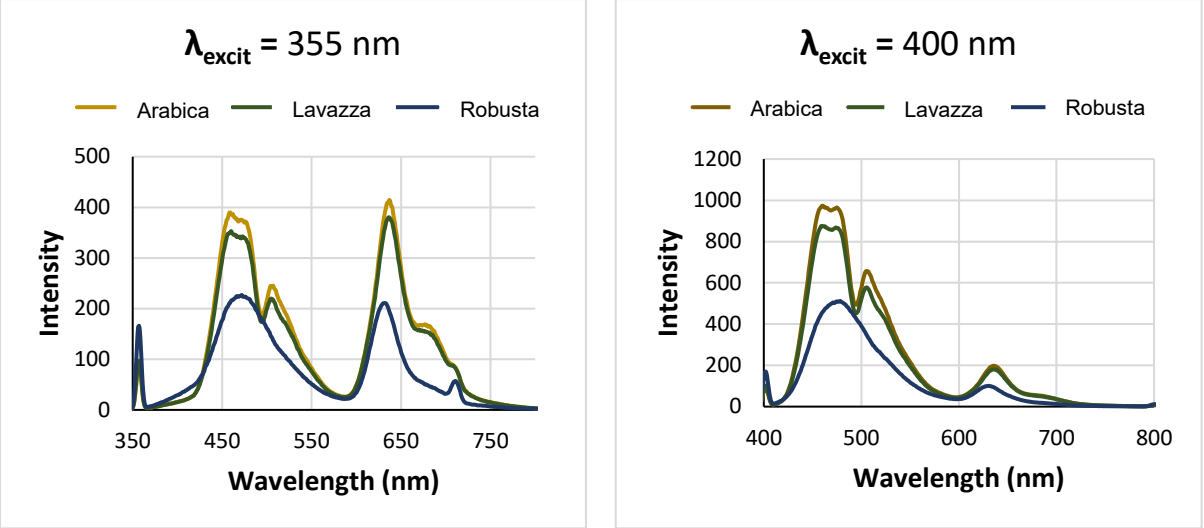

Figure 4.24: Overlapped fluorescent spectra with excitation wavelengths of 355 nm (left) and 400 nm (right).

Two obvious belts were found in the fluorescent spectra of Arabica, Lavazza and Robusta, with different intensities. The belts were peaking at about 460 nm and at about 650 nm after excitation with wavelengths of 355 nm and 400 nm. An interesting deviation, found when comparing the spectra of Arabica, Lavazza and Robusta, was an additional peak at about 505 nm, present in samples of Arabica and mixtures of Arabica and Robusta, but not Robusta alone.

4.7.2 Fluorescence of coffee extracts

As it is known that coffee exhibits fluorescence when slices of a coffee bean are observed under a fluorescent microscope and due to positive fluorometric results of treated dichloromethane extracts of Arabica, Robusta and Lavazza, when excited with wavelengths 355 nm and 400 nm, fluorometric spectra of dichloromethane extracts of the three coffees alone without treatment were also recorded.

Additional coffee extracts were prepared from mixtures of Arabica and Robusta in ratios 1 to 9, 1 to 1 and 9 to 1, by stirring 2 g of coffee with 50 mL of dichloromethane for 24 h. After filtration, the solvent from the extract was removed with a stream of N_2. The residues were re-dissolved in dichloromethane to form a solution with a concentration of 33 mg/mL.

Interesting results were observed, following the excitation at 410 nm, where a peak at 671 nm was found in the sample of Robusta alone and the samples of mixtures of Arabica and Robusta in all ratios. At the same time is was barely present in the sample of solely Arabica and could as such serve as another option for determination of the level of contamination of Arabica with Robusta. For the purpose, a calibration curve was formed with a relatively high R^2 factor (**Figure 4.25**).

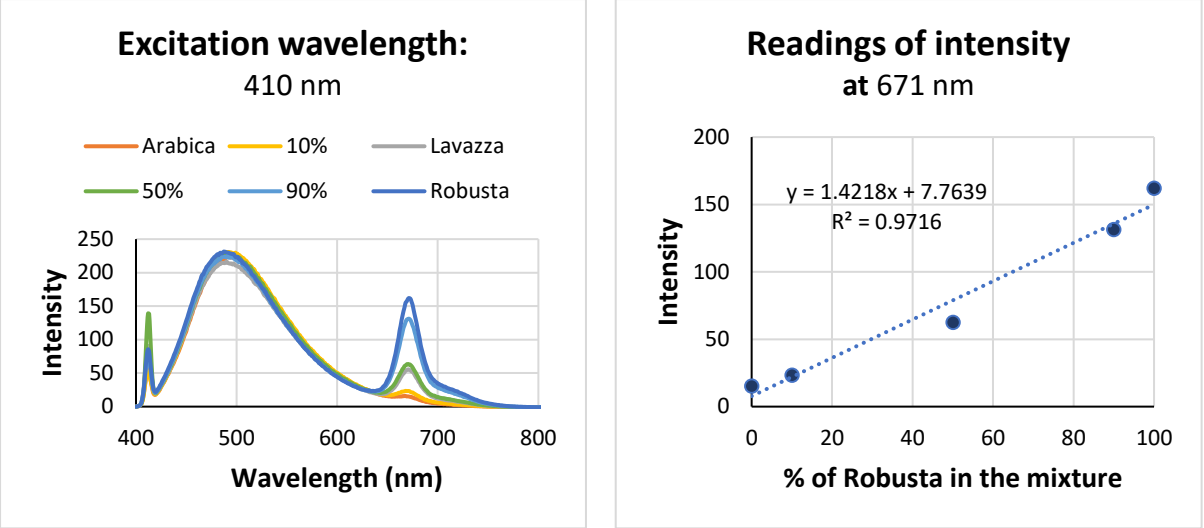

Figure 4.25: Overlapped fluorescence spectra of the samples (left) and a calibration curve of the plotted results at 671 nm (right).

4.8 Microscopy of coffee

After the initial success with the antimony(III) chloride method on dichloromethane coffee extracts, we were wanted to see if it would be possible to use it on microscopical preparations of Arabica and Robusta and thus differentiate the two species under a microscope. For the purpose, microscopical slides were prepared either with slices of green coffee beans of Arabica or Robusta. The antimony(III) chloride solution II was prepared from 3 g of antimony(III) chloride and 15 mg of zinc dust, 10 mL of dichloromethane and 200 µL of acetic acid. The mixture was sonicated until all the antimony(III) chloride dissolved, let sitting still until the zinc dust settled and was used as such for application on the microscopical slides.

Several fixing agents were tested as some were compromised in presence of dichloromethane and ceased to be transparent. Another issue with the original antimony(III) chloride solution was precipitation of antimony(III) chloride on the slide, causing poor visibility under the microscope. To avoid it, a solution of antimony(III) chloride was diluted 1:10 with dichloromethane and tested on the slides again.

Upon examination of the slides, we observed a red colour released from the slices of Arabica and a light blue colour released from the slices of Robusta, several minutes after addition of the 1:10 dilluted antimony(III) chloride solution. The colouring effect disappeared when the slides were examined under the microscope. The samples were first observed with a source of visible light (**Figure 4.26**).

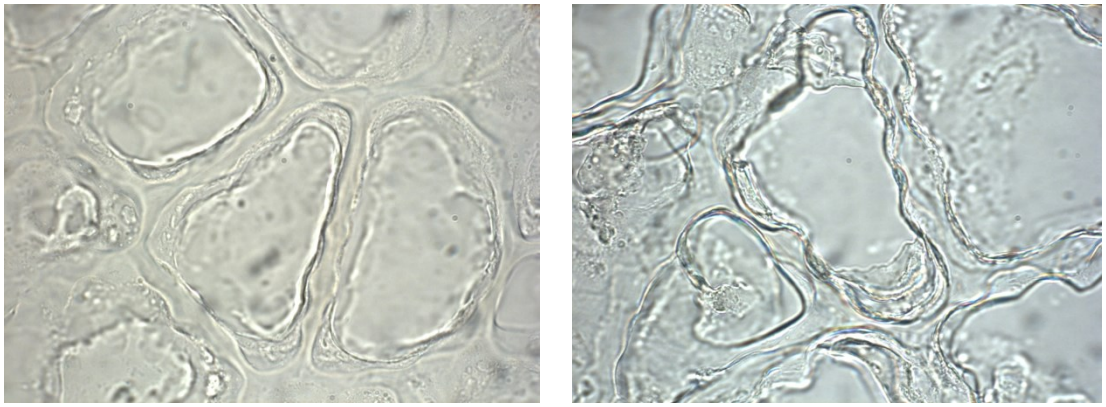

Figure 4.26: A non-treated sample of Arabica (left) and a sample of Arabica, treated with the 1:10 diluted antimony(III) chloride solution (right) with a 1000x magnification.

Two colours were still visible in both coffees, however. An elongated belt of blue and an elongated belt of red positioned next to it, observed close to the cell membrane. The only difference between the slices of the beans of Arabica and Robusta were wider coloured belts observed in the slices of Arabica (**Figure 4.27**).

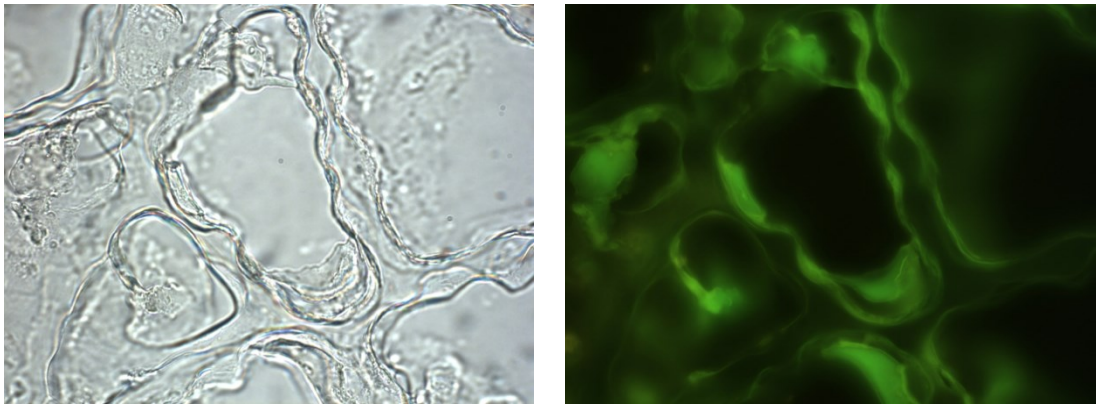

Figure 4.27: Sample of Arabica observed with light microscopy (left) and fluorescent microscopy (right) with a 1000x magnification.

With fluorescent microscopy, using the filter H3, it was concluded that antimony(III) chloride colours the lipids close to the membranes of cells of the coffee bean, exhibiting a slightly stronger green fluorescence as it is usually observed in non-treated coffee samples (**Figure 4.28**).

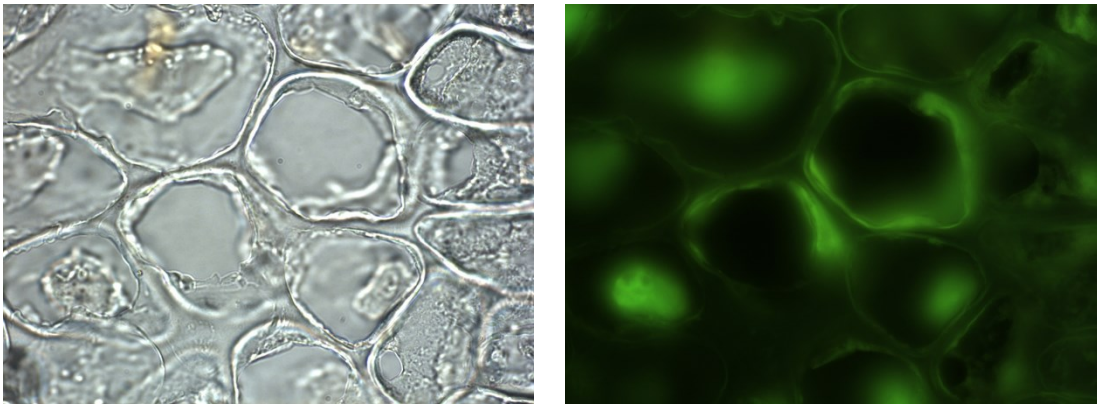

Figure 4.28: Sample of Robusta observed with light microscopy (left) and fluorescent microscopy (right), with a 1000x magnification.

Observing was also pursued with filters A and D, filtering light of different wavelengths, however the result remained only in the scope of improved visibility of cell membranes when both kinds of coffee beans were observed (**Figure 4.29**).

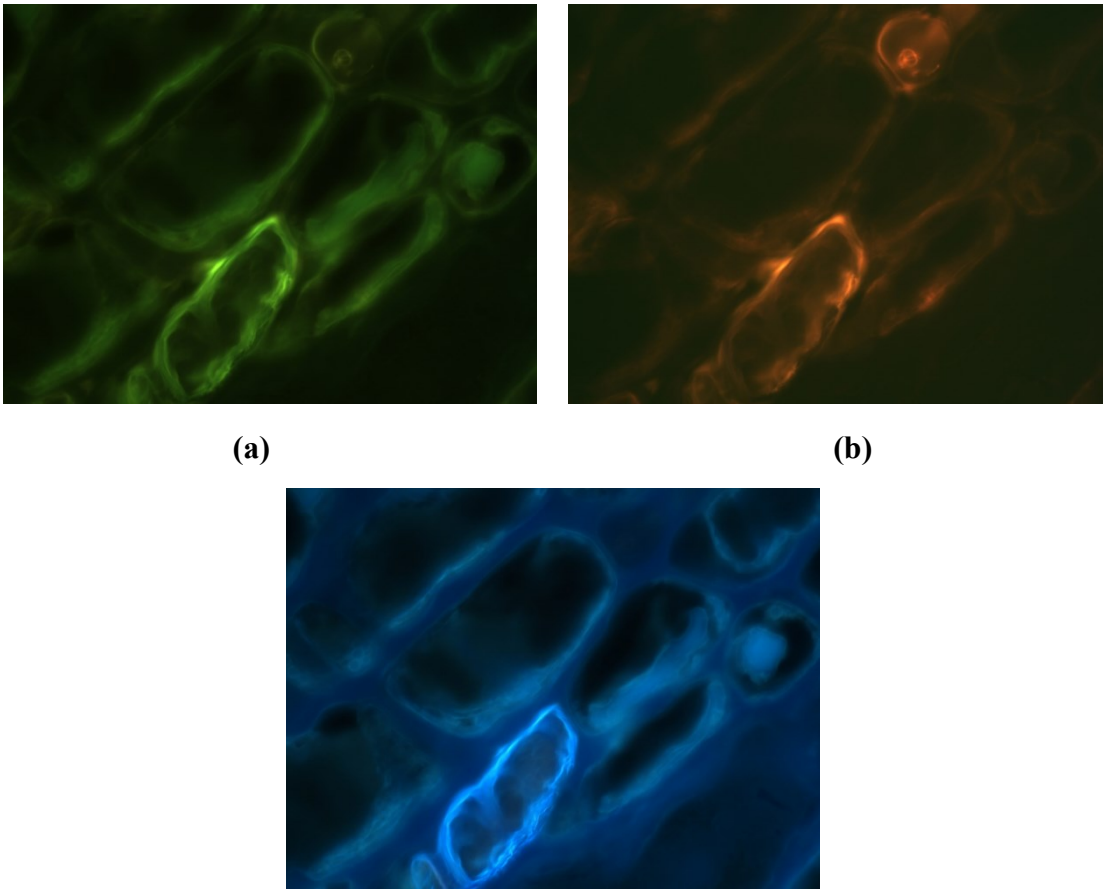

(a) **(b)**

(c)

Figure 4.29: A sample of Arabica observed with fluorescent microscopy, using filters H3 (a), A (b) and D (c), with a 1000x magnification.

Soaking the bean in 1 to 10 dilluted antimony(III) chloride solution, slicing it with a razor afterwards and observing it under the microscope did not improve the final result. On the other hand, applying several drops of the 1 to 10 diluted solution of antimony(III) chloride in dichloromethane on a thicker slice of a coffee bean resulted in red rings around the slices of Arabica and light grey-blue circles around the slices of Robusta, observed with light microscopy with the smallest magnification (**Figure 4.30**).

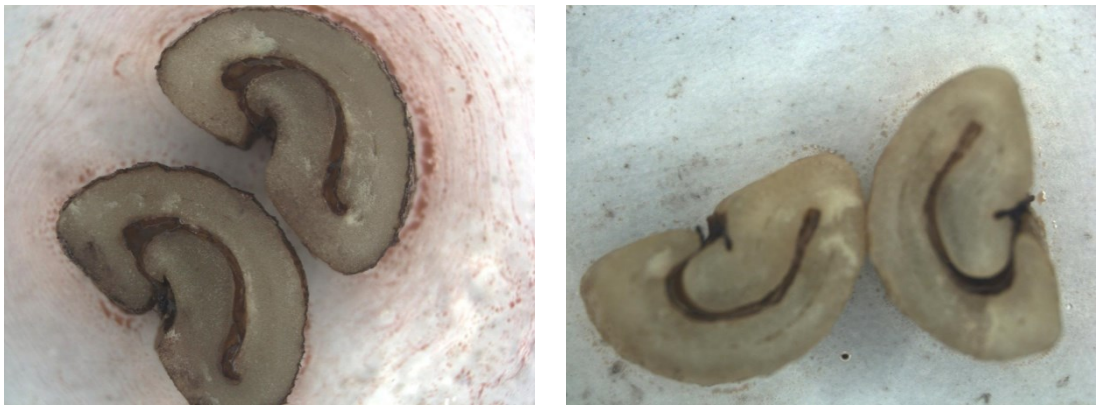

Figure 4.30: Treated coffee slices of Arabica (left) and Robusta (right) under a stereomicroscope with a 12.5x magnification.

Bibliography

9. Speer, K. & Kölling-Speer, I. The lipid fraction of the coffee bean. *Braz. J. Plant Physiol* **18,** 201–216 (2006).

48. Corbet, E. & Geisinger, H. TEST FOR VITAMIN Antimony Trichloride Color Test. (1933).

50. Nikolić, J. A. Letters to the Editors Letters to the Editors. *Br. J. Nutr.* **63,** 669–671 (1990).

52. Blatz, P. E., Estrada, A. & Estrada, A. Investigation of the Molecular Behavior of the Carr-Price Reaction. *Anal. Chem.* **44,** 570–573 (1972).

181. Wenzl T, et al. Guidance Document on the Estimation of LOD and LOQ for Measurements in the Field of Contaminants in Feed and Food. EURL (2016).

5. RESULTS AND DISCUSSION:

Quantification of acrylamide in coffee

5.1 Requirements for the method

DemusLab is an analytical laboratory for coffee samples, a spin-off of the coffee roasting company Demus S.p.A. Their main responsibilities are quantification of the caffeine content in roasted coffee blends, as well as caffeine content in decaffeinated coffee, the content of Ochratoxin A, dichloromethane residue in decaffeinated coffee and moisture content in green coffee.[166] Their main instrumentation in the laboratory is represented by a HPLC-UV and a GC-mass coupled spectrometer. Their main task is quality control of coffee for their parent company Demus S.p.A. and several other coffee roasters in their region by running routine analysis of the samples they receive.

Recently, Regulation 2017/2158 was issued for the member states of European Union, demanding from all coffee producers to control the amount of acrylamide (**Figure 5.1**) in their roasted coffee products and adhere to the benchmark levels of 400 µg of acrylamide per 1 kg of roasted coffee beans and 850 µg of acrylamide per 1 kg of soluble coffee.[167] Therefore, DemusLab decided to expand their offer of analytical services to quantification of acrylamide. Although they already developed a GC-MS method for the purpose, they now opted to develop an HPLC-UV method. This was due to the fact, that the existing GC-MS method included a tedious sample preparation with a health concerning bromination step prior to analysis. Additionally, the GC-MS analysis was relatively time-consuming and not particularly cost-effective. They hoped to develop an HPLC-UV method, which would be more health-friendly, less costly and shorter in time, to allow for more analyses to be performed in a day.

Upon development of the method, physico-chemical properties of coffee and physico-chemical properties of acrylamide need to be considered. Coffee is known to be a very complex matrix, due to containing several classes of compounds, mainly lipids, proteins and a wide variety of polar compounds.[9,38] This leaves several obstacles to be resolved in development of our method.

Acrylamide, on the other hand, is an unsaturated amide, very soluble in water and well soluble in polar organic solvents. It is poorly soluble in heptane and hexane. In it is slowly converting to acrylic acid with time. An aqueous solution with 50 wt.%, of acrylamide has a pH of 5 to 6.[96] The C=C double bond and the double bond in the carbonyl group of acrylamide form a conjugated system and a Michael acceptor, capable of participating in 1,4-additions. The melting point of the compound is at 84.5°C. It polymerizes at its melting point, in solution or under a UV light.[106]

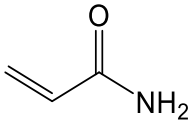

Figure 5.1: Structure of acrylamide.

In literature, several attempts of development of an HPLC-UV method for quantification of acrylamide have been reported[111,126,127]. In all of them, there are three common phases of sample preparation, finishing with an HPLC-UV analysis. The sample preparation usually consists of extraction of coffee into water or a polar organic solvent, removal of lipids and proteins, SPE purification to remove the majority of other possible interferences, and finally HPLC analysis. In analytical phase, UV detection at wavelengths 202 nm and 210 nm are most often reported, and MS detection is often mentioned.[107] An overview of possible approaches for sample preparation in the analysis of acrylamide is presented in **Table 5.1**. The concepts found in literature are referenced to their sources.

Lipids:	Defatting with hexane[168]
Proteins:	Sorbents, Carrez solutions*[125]
Polar interferences:	Varying time of extraction[125,168] Use of sorbents – MgO, C, C18[169] Salting out extractions[170] Liquid-liquid extractions[136] Varying temperatures of extraction Extraction into organic solvents[126] Extractions at low/high pH Extraction in presence of NaCl SPE columns[115,120,121] Costumized (MIP) SPE columns[64]
HPLC separation:	Proper sample preparation Column dimensions Column stationary phase Mobile phase
Detection:	UV FLD with derivatization MS

- A combination of potassium hexacyanoferrate(II) trihydrate $K_4[Fe(CN)_6]$ x $3H_2O$ solution and zinc sulfate heptahydrate $ZnSO_4$ x $7H_2O$. They are added to an aqueous sample to form a precipitate, consisting of $Zn_2Fe(CN)_6$, to which molecules with a higher molecular weight are bound by absorption and are consequently precipitated.

Table 5.1: Obstacles and possible solutions in the development of the HPLC-UV method for analysis of acrylamide.

5.1.1 Selection of chromatographic parameters

To successfully compose the HPLC-UV method, first the initial chromatographic conditions needed to be established. This phase consisted of choosing a proper column, the most suitable mobile phase, the optimal flow of the mobile phase through the column and a wavelength, at which the peak of acrylamide would be the most visible.

Selection of the mobile phase

As acrylamide is a very polar molecule, the selection of a suitable mobile phase was of vast importance. The expected characteristic of the chosen one was allowing a good separation of the peaks in coffee samples and leading to an optimal retention time of acrylamide during an isocratic elution. For the purpose, three mobile phases were tested. **MP1** consisted of water and acetonitrile in ratio 50 to 50 with 0.1 % of trifluoroacetic acid, **MP2** consisted of water and acetonitrile in ratio 80 to 20 with 0.1 % of trifluoroacetic acid and **MP3** consisted of water with 0.05 % of trifluoroacetic acid. A 500 µg/mL aqueous solution of acrylamide was chosen as a sample be tested with each mobile phase, always using the column Phenomenex Gemini 150x 2 mm, with the size of particles 4 µm (**Figure 5.2**).

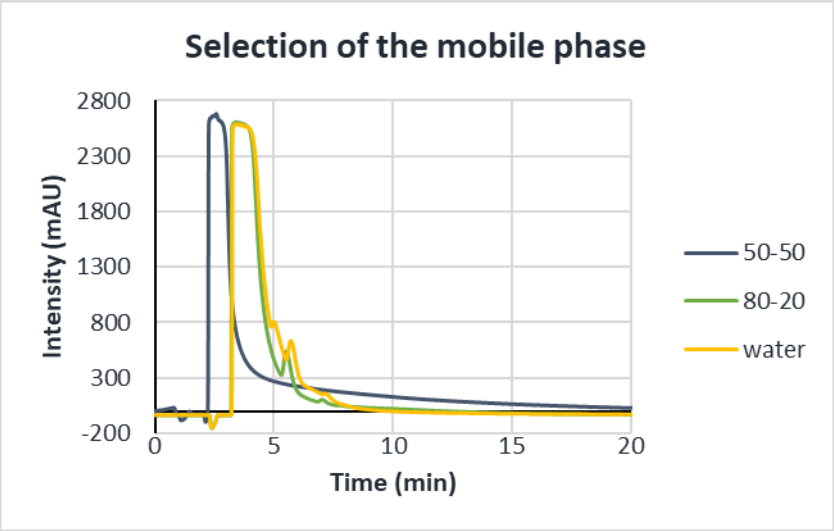

Figure 5.2: Overlapped chromatograms of acrylamide after elution with MP1 (50-50), MP2 (80-20) and MP3 (water).

The mobile phase **MP1** gave a relatively narrow peak, however a too short of a retention time of 2.18 min. This increases the possibility of interferences of the peaks of solvent with the peak of acrylamide. The mobile phase **MP2** gave a broader peak with an improved retention time of 3.21 min. Finally, the mobile phase **MP3** gave a slightly broader peak of acrylamide than the mobile phase **MP2** with approximately the same retention time. Due to a very complex matrix of the coffee samples and a polar analyte, **MP3** was chosen as the most promising mobile phase to begin with and to possibly modify it later on in the development of the method.

Selection of the column

As we wanted to further increase the retention time of acrylamide and improve the resolution of peaks in the chromatogram of coffee samples, two columns were tested. Their characteristics are presented in **Table 5.2**.

	Dimensions	Filling	Particle size	Chosen flow
Phenomenex Gemini	150 x 2 mm	C18	4 µm	0.2 mL/min
Agilent Poroshell 120	150 x 4.6 mm	C18	2.7 µm	0.5 mL/min

Table 5.2: Characteristics of the tested columns.

The criteria for the selection of the most appropriate column were: the shape of the peak of acrylamide, its retention time and resolution of peaks in a coffee sample. The comparison is given for the standard sample of acrylamide with both columns, at a flow found to be optimal for each of them. The rest of the chromatographic conditions in both experiments were the same to allow comparison of the results (**Figure 5.3**).

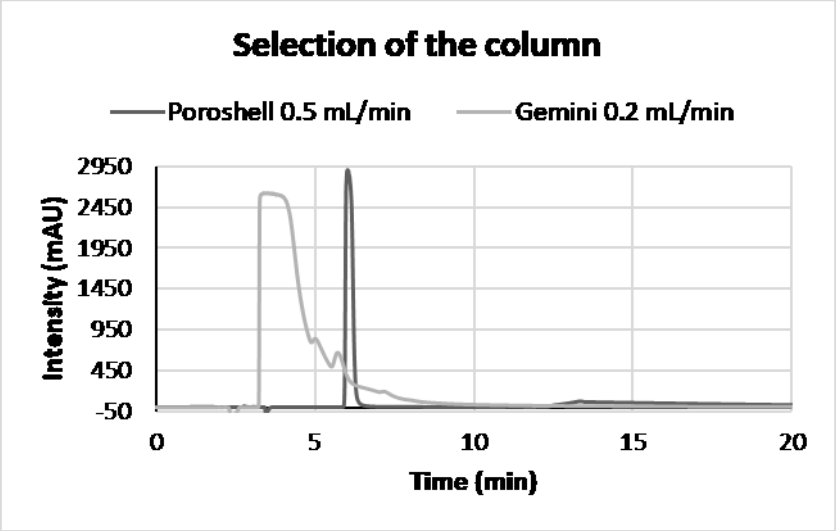

Figure 5.3: Chromatogram, representing the selection of the column.

The columns differ in the size of the particles and in their diameter, while their length is the same. At the same time, the flow through the two columns is different as well. 0.2 mL/min was stated to be the optimal flow for the Gemini column, while the column Poroshell functions better when the flows 0.5 to 1 mL/min are used. We can immediately see, that even at such high load of acrylamide in the system, the column Poroshell 120 increases the retention time of acrylamide to 6 min and greatly narrows the peak. Based on all that, we found the column Poroshell 120 to be more beneficial for our purpose and decided to use it in the further studies.

Selection of the flow

Upon selecting the column, we decided to look into the possible flows of the mobile phase, that would still be consistent with the optimal functioning of the column and would at the same time allow us to achieve the best separation of peaks of interest.

Namely, the flow greatly influences the retention time of analytes and their separation. An increased flow of the mobile phase usually results in an increased pressure in the column, leading to a faster movement of the analytes through the column. This way they are in contact with the stationary phase for a lesser time, which lowers their retention time and narrows their peaks in the chromatogram. Due to narrower peaks, an improvement in the peak separation is possible. If, however, we increase the flow too much, the resolution of the peaks can get worse. This is due to minimizing the contact of the analytes with the stationary phase, which does not allow them to separate in an optimal way anymore.

Lowering the flow, on the other hand, lowers the pressure in the column, moving the analytes through the column more slowly. This allows for a longer contact between the analytes and the stationary phase, thus improving their separation. If the flow gets lowered too much, widening and simultaneously lowering of the peaks in the chromatogram occurs. This can cause lowering of the limit of quantification of the analysed compounds.

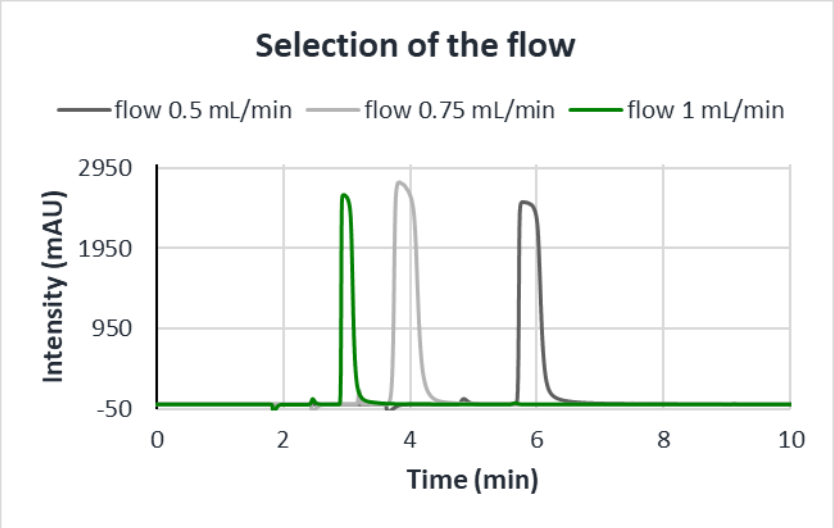

Figure 5.4: Chromatogram, representing the selection of the flow.

Three flow speeds, 0.5 mL/min, 0.75 mL/min and 1 mL/min, were tested with the same column in the same chromatographical conditions (**Figure 5.4**). The most optimal flow for our purpose was found to be 0.5 mL/min, as even though it increases the retention time for acrylamide, it does not drastically widen or lower its peak.

Selection of the detection wavelength

In literature, two wavelengths for detection of acrylamide mostly reported, 202 nm[168] and 210 nm[111]. Both were tested with a standard sample of acrylamide with a concentration of 500 ng/mL, in the same chromatographic conditions. Even though the wavelengths are not much different, we were hoping for an increased sensitivity of the method by moving from 210 nm to 202 nm. The wavelength of 202 nm did in fact increase the intensity of the peak and was therefore chosen as a more appropriate one for our experiments (**Figure 5.5**). Initial studies, however, were still performed at the wavelength of 202 nm.

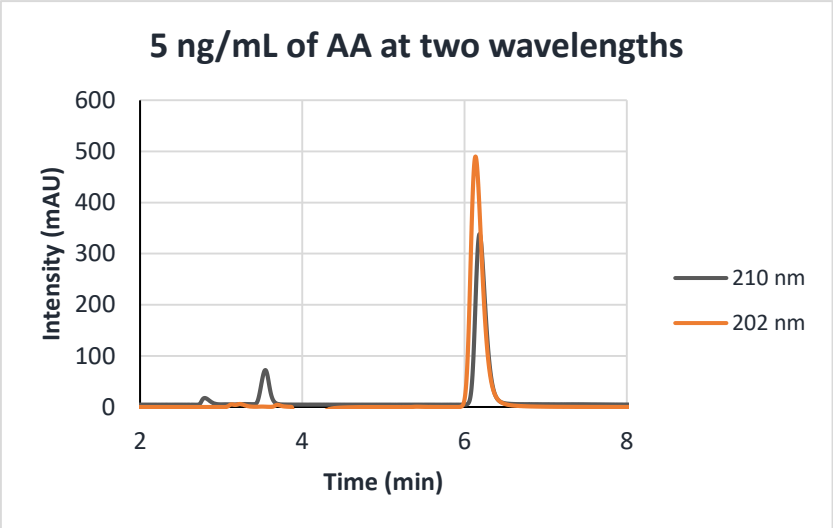

Figure 5.5: Chromatogram, representing selection of the wavelength.

5.2 Sample preparation

Due to the fact that coffee is a very complicated matrix, we tried out several possible sample preparations in order to improve the resolution of the peak of acrylamide, avoid interferences and minimize the matrix effect of the sample. Our first step was trying to prepare the sample according to the existing GC-MS method in the Demus Lab, but with skipping the bromination step and continuing with the HPLC-UV analysis.

Preparation of a sample according to the DemusLab GC-MS method

This sample preparation was pursued as the first orientation step in the method development. It consisted of extraction of coffee into water, in presence of the sorbent C18. C18 is a known bulk sorbent, usually used in solid phase extraction columns and columns for column chromatography. It is capable of non-selective retention of a great degree of organic compounds. Acrylamide, specifically, is known to be poorly retained on the sorbent.

Additionally, upon mixing the sorbent with coffee and water for several minutes, then centrifuging the sample, C18 entraps the coffee particles well enough, that decantation of the supernatant suffices afterwards, with no additional filtration needed to remove residual particles.

Extraction lasted for 30 min at room temperature. After centrifugation and decantation, the obtained extract was brown in colour and needed further purification. The following step was filtration of 5 mL of the sample through a pre-conditioned Agilent Bond Elute AccuCAT SPE column. The column contains a mixture of a strong cation and a strong anion exchange sorbent and is according to the producer effective for extraction of acidic, basic and neutral analytes.[171]

After this step, bromination of acrylamide generally follows, to form 2-bromopropenamide. It is done by treating the filtrate with potassium iodide while adjusting the pH to 1 to 3 with hydrobromic acid. A saturated solution of bromine in water is then added and stirring of the solution in the dark on an ice bath for 2h follows. Upon addition of triethylamine, 2,3-bromopropionamide is transformed into 2-bromopropenamide. Extraction with a mixture of ethyl acetate and hexane in ratio 1 to 4 is the last step before the GC-MS analysis:

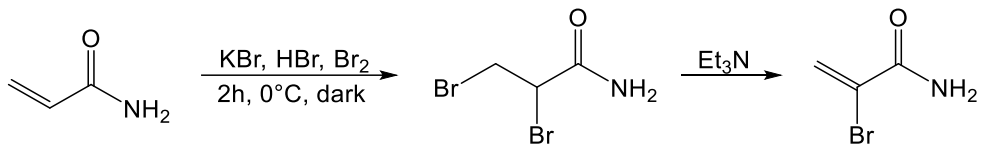

Although this method allows for a precise detection of acrylamide, it needs to be considered that it involves a tedious sample preparation and involvement of compounds, which upon continuous use impose a great health hazard. This step was therefore skipped in our sample preparation and the sample was analysed immediately after the SPE filtration (**Figure 5.6**).

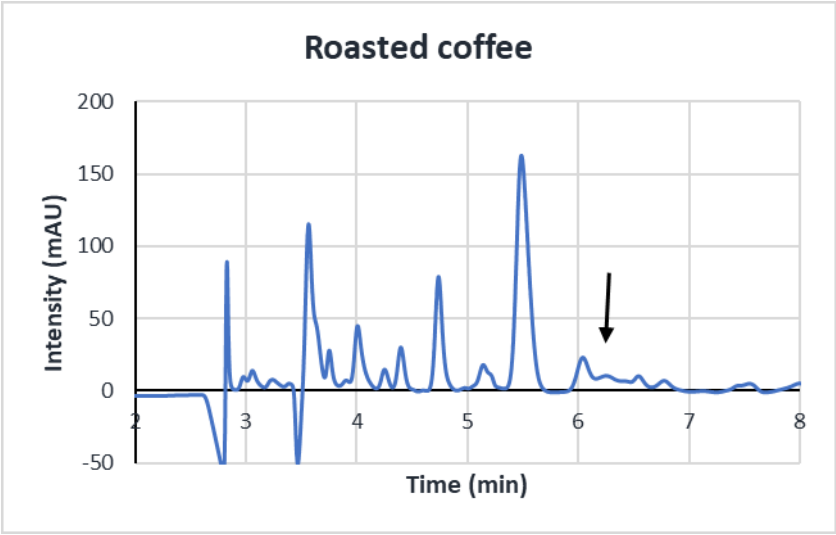

Figure 5.6: Chromatogram of a roasted coffee sample, prepared according to the Demus Lab method.

When examining the chromatogram of the sample, we found several downsides of this approach. The time of analysis, first of all, was relatively long at 60 min. The signal for acrylamide was relatively low and a noticeable matrix effect was observed. Based on all that, it was clear that an improved way of sample preparation needed to be found, mainly focused on reducing the amount of polar interferences in the sample.

Hindered extraction of polar compounds

Due to the fact that, along with acrylamide, several polar compounds are present in an aqueous coffee extract, ways to prevent their extraction were trying to be discovered, starting with changes in pH of the extraction solvent and increasing the ionic power of the solvent. Namely, extraction of coffee into water leads to extraction of a certain set of compounds. Should the extraction medium be altered for the purpose of the extraction, the set of extracted compounds would change as well.

Extraction in presence of NaCl

Adding NaCl into the extraction mixture was attempted, to allow better soluble compounds to dissolve in the NaCl solution sooner as the compounds that are not as well soluble or take a longer time to dissolve. With that, the set of extracted compounds should include acrylamide, surrounded by a slightly changed type of interferences. As a control to this preparation, a parallel extraction was performed into water and in presence of the sorbent C18, to monitor the difference between the chromatograms of the samples (**Figure 5.7**).

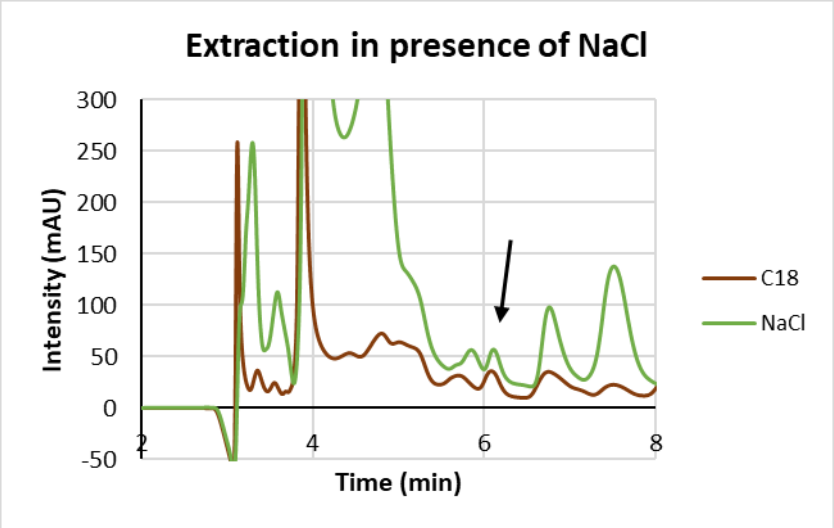

Figure 5.7: Extraction of coffee in presence of NaCl.

By looking at the chromatogram, it is clear that the addition of NaCl does not vastly improve the signal of acrylamide and even increases the matrix effect of the sample. The time of analysis of the sample did not improve as well and remained at 60 min.

Extraction into acidic or basic medium

Extraction of coffee into a 1% aqueous solution of acetic acid and 1% aqueous solution of ammonia was attempted, to see if modification of the pH would influence the set of extracted compounds in a way, that would allow the peak of acrylamide in the chromatogram to become better visible. Apart from the addition of the acetic acid or ammonia to the extraction mixture, a control parallel of extraction of coffee was performed, using water as a medium in presence of C18, to monitor the differences between the types of extractions (**Figure 5.8**).

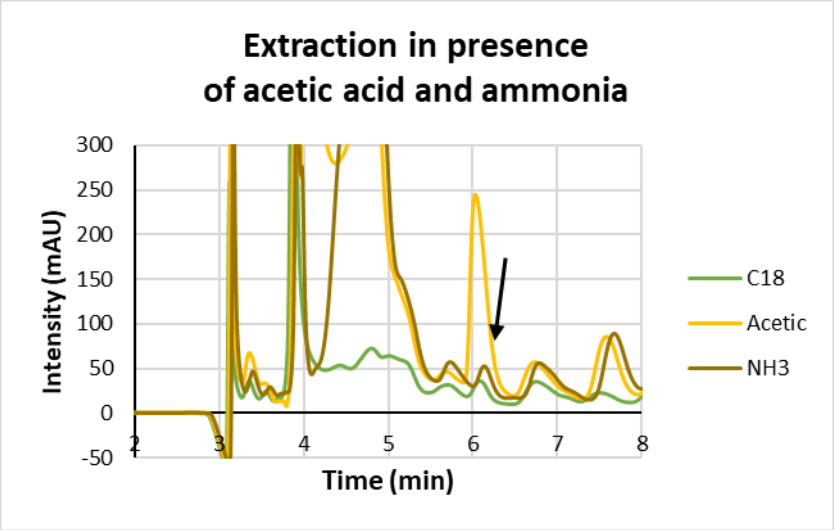

Figure 5.8: Extraction of coffee in presence of acetic acid and ammonia.

The peak of acrylamide is a little narrower in the basic extract, than the one found in the aqueous extract. Where the 1% acetic acid solution was used as a medium, it appears that the peak of acetic acid is overlapping with the peak of acrylamide, making the solution of acetic acid not suitable for the extraction of acrylamide. Additionally, an increased matrix effect is noticeable in the samples, where either acetic acid or ammonia solutions were used for the extraction.

5.3 Different treatments of acrylamide

To see how addition of sorbents influences the concentration of acrylamide in the sample, a 500 ng/mL solution of acrylamide was treated with various amounts of MgO and active charcoal. Namely, active charcoal is a non-water-soluble sorbent with a wide environmental and pharmaceutical use. Due to its porosity, it is capable of adsorbing a great variety of compounds. It has been discussed, that for the most part it is capable of adsorbing non-water-soluble compounds in aqueous solutions.[172] Magnesium oxide, on the other hand, is an alkali oxide, forming magnesium hydroxide in presence of water. Magnesium hydroxide is poorly soluble in water and makes water solutions slightly basic, usually with pH from 8 to 10. It has been proposed as an adsorptive mean in purification of pharmaceutical waste waters.[169]

When added, active carbon should therefore only act as an adsorbent, while MgO should lift the pH of usually slightly acidic aqueous extract of coffee and have an adsorptive effect as well. Both of them should be to some degree effective in removal of interferences from the coffee sample. The standard solution of acrylamide was treated with the two sorbents for 30 min, which is the time the extraction of coffee previously went on. The sorbents were then removed by centrifugation and decantation. The remaining supernatant was then analysed via HPLC-UV (**Figure 5.9**).

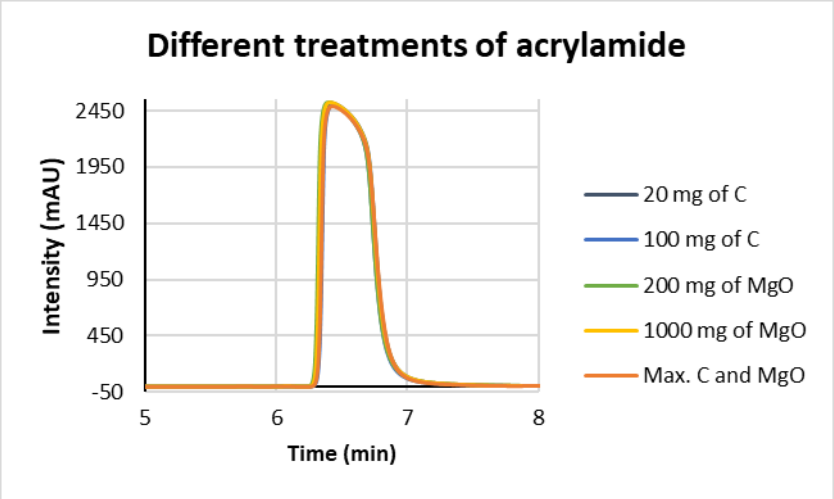

Figure 5.9: Different treatments of the acrylamide solution.

From the results we can find, that none of the used sorbents or sorbent amounts influence the concentration of acrylamide to a concerning degree. Clearly, the coffee extracts we are working with contain about 10 to 20x lesser concentrations of acrylamide in the solution. Yet, due to relatively big amounts of MgO and active carbon added to the sample, it may be concluded, that all the amounts of the two sorbents should not significantly minimize the contents of acrylamide in analysed coffee samples.

Removal of interferences with salting out extractions

Another option in improving the sample preparation for the analysis of acrylamide was removal of the interfering compounds from the coffee extract to a solvent of different polarity. Or, removing acrylamide itself while leaving the other impurities behind. This was attempted with several variations of salting out extractions, extractions in which compounds are pushed from the aqueous to the organic phase with the addition of salt.[170]

For the purpose, extractions of coffee were attempted either in water with the following addition of NaCl and a polar organic solvent, or in a polar organic solvent, with following addition of NaCl and water. The polar organic solvents were acetone, methanol, acetonitrile and isopropanol, as acrylamide is well soluble in all of them. It was expected, that:

- The polar solvents would hinder extraction of interfering compounds.
- Salting acrylamide out of the water phase or into it from another solvent would reduce the amount of interferences in the chromatogram.

Upon the addition of NaCl and a solvent of a different polarity, all samples, but the ones containing methanol, separated into two layers. Each of the two layers was sampled for every sample. HPLC-UV analysis showed larger amounts of organic solvents were still present in the aqueous phases of the samples, and vice versa.

Purification of samples with SPE columns

For the purification of coffee samples, SPE columns were proved to be beneficial. The Agilent Bond Elut AccuCAT SPE columns were initially used, containing a mixture of a strong cation adsorbent and a strong anion adsorbent in 600 mg of bed. They were usually preconditioned with acetone or methanol and water, dried completely, then the chosen amount of sample was applied. The columns were dried completely again, and acrylamide was washed out with water.

To see if any other SPE column would be capable of better purification of the samples, other SPE columns were tested as well. Among those, Discovery DSC MCAX, Biotage Isolute C18 and Biotage Isolute SAX/PSA were used. They differed from the originally used columns in the type and amount of sorbent (**Table 5.3**).

	Bond Elut AccuCAT[171]	**Isolute C18**[173]	**Discovery DSC MCAX**[174]	**Isolute SAX/PSA**[175]
Sorbent	Benzene sulfonic acid Quaternaty amine	C18	Octyl C8 Benzene sulfonic acid	Ethylenediamine -n-propyl
Load	600 mg	1000 mg	300 mg	500 mg
Target	Acidic, basic, neutral	Broad spectrum	Basic compounds	Strong acids Polyacidic compounds

Table 5.3: Characteristics of the SPE columns.

Next to examining if there is a better way of removal of the interferences from the coffee samples with any of those columns, the experiment was also a search for a column, capable of concentrating a sample of acrylamide and thus increasing the area of the peak of its signal in the chromatogram. For the purpose, a standard solution of acrylamide with a concentration of 500 ng/mL was prepared. The concentration of acrylamide was intentionally higher, to allow us to see the amount of eluted acrylamide even in fractions. Upon application of the standard solution of acrylamide, the column was dried completely, and the remaining eluate represented the first sample for each column, showing us how successfully the columns are capable of retaining acrylamide.

A wash with 1 mL of water followed, drying the column through again, to examine how much water is needed to elute acrylamide from the column. The last millilitre of water was added to remove the acrylamide from the column completely. For each eluate a chromatogram was recorded, and the amounts of eluted acrylamide were compared with the amount, initially found in the chromatogram of the standard solution of acrylamide. As acrylamide is at a neutral pH a non-ionizable molecule and due to its most abundant stationary phase, only the SPE column Isolute C18 was expected to retain it for a longer time.

The column Discovery DSC-MCAX (**Figure 5.9**) is purposed for extraction of basic compounds. At the same time, it contains the lowest amount of the sorbent among the tested columns, at 300 mg. Due to the fact, that acrylamide does not ionize at neutral conditions, it was expected to not retain acrylamide very successfully.

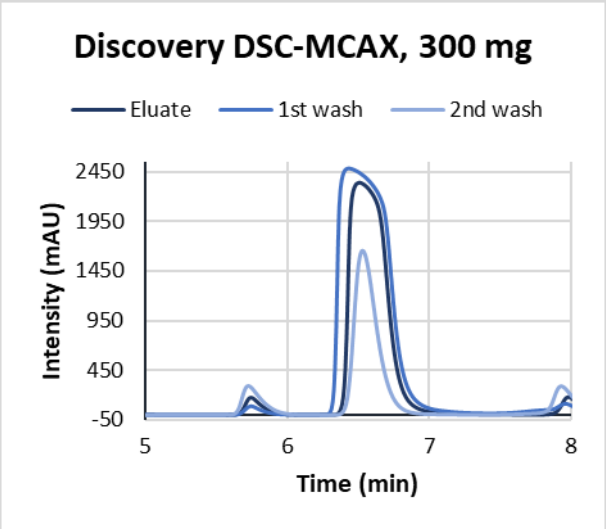

Figure 5.9: Results of the SPE column Discovery DSC-MCAX.

The applied sample indeed exceeded the load of the column. The most of acrylamide was eluted immediately after the application of the standard solution and with the first wash of the column, leaving behind about 15.5 % of acrylamide to be eluted in the second wash. This suggests, that this column would be of a good choice for removal of basic interferences from the coffee, while not very good in concentrating the sample.

The column Isolute SAX/PSA contains 500 mg of the sorbent and is according to the producer capable to retain strong acids and polyacidic compounds. The retention of acrylamide was expected to be improved in comparison to the column Discovery DSC-MCAX by a small degree due to a bigger amount of the sorbent in the column (**Figure 5.10**).

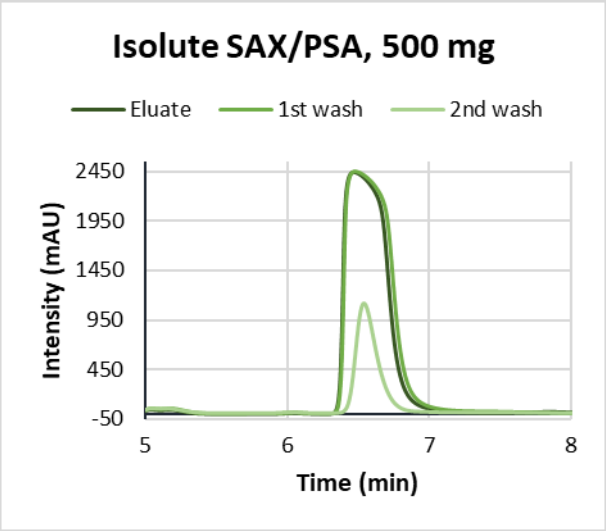

Figure 5.10: Results of the SPE column Biotage Isolute SAX/PSA.

The speculations of a greater load did not appear to be true, as most of the acrylamide again got eluted immediately after the application of the standard solution to the column and after the first wash. Thus, 9.7 % of acrylamide was removed in the last wash. This again suggests, that the column could not be purposed for concentration of the sample but could well remove the strongly acidic and polyacidic compounds from the aqueous coffee extract.

In the final case, the Isolute C18 column (**Figure 5.11**) was tested. With the stationary phase of C18, it was the most non-specific column among the three. With 1 g of the sorbent, it was expected to be able to bear the highest load of acrylamide. Our expectations were confirmed, as in the eluate immediately after application of the sample barely any acrylamide was eluted at 9.4 %. The majority of acrylamide was eluted in the first and in the second wash.

To optimally purify the coffee extracts, an good choice appeared to be the combination of the column Discovery DSC MCAX with the column Isolute C18. This way a great degree of basic impurities could be removed from the samples with the DSC MCAX column, while the Isolute C18 column on the bottom would prevent them from becoming too diluted.

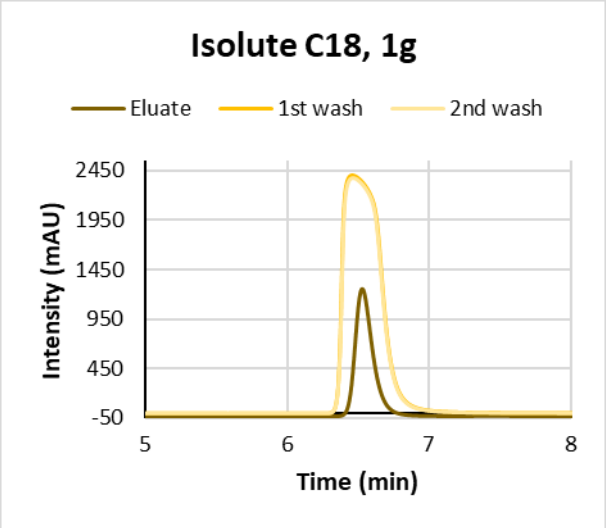

Figure 5.11: Results of the SPE column Biotage Isolute C18.

By in reality using lower volumes of applied coffee samples with a lower content of acrylamide, it was expected, that elution from the Discovery DSC MCAX columns would be completed within the application of the sample and washing with the first millilitre of water. Both eluates would fall onto the Isolute C18 column, where acrylamide should be able to concentrate the sample by retaining acrylamide and thus removing a big part of the excess solvent.

Calibration curve

A calibration curve was established for the purpose of quantification of acrylamide in the samples. Concentrations of the acrylamide from 2 ng/mL to 200 ng/mL were used for the purpose, representing the realistic range of concentrations of acrylamide in the coffee samples for HPLC analysis. The measurements were done at the wavelength of 202 nm (**Figure 5.12**).

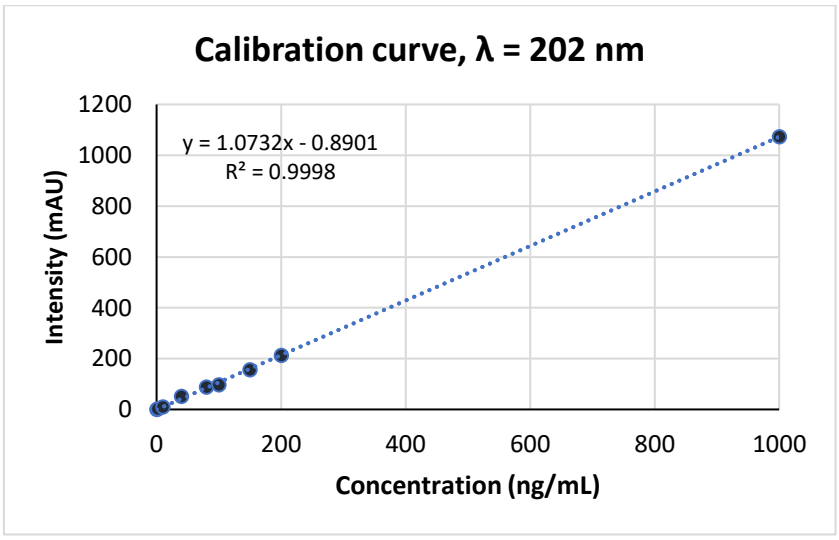

Figure 5.12: Calibration curve for acrylamide at the detection wavelength 202 nm.

5.4 Improvements of the Demus Lab method

Several points in the Demus Lab sample preparation were changed. Initially, the C18 sorbent during extraction was replaced with a combination of MgO and active charcoal in quantities of 1000 mg and 100 mg, respectively, as it was proved that their presence does not lower the content of acrylamide, yet effectively removes interferences from solutions.

Thus, the extraction took place in a basic medium with a pH around 8, opposed to previously used neutral medium, due to the use of MgO. Visually, the extracts of coffee prepared with MgO and active charcoal were of a much brighter brown colour than the extracts, prepared according to the Demus Lab method. As MgO entraps the coffee particles and active charcoal particles on the bottom of the test tube during centrifugation, no additional step of filtration needed to be introduced.

SPE purification with Agilent Bond Elut AccuCAT columns was substituted with a combination of the Discovery DSC MCAX column and Isolute C18 column, connected to each other. Several elution combinations were attempted to allow for the best signal of acrylamide in the chromatogram. Chromatograms of the coffee sample, representing the control sample, and the coffee sample with added MgO and active carbon were compared, to observe if addition of the two sorbents has a beneficial effect on the sample preparation (**Figure 5.13**).

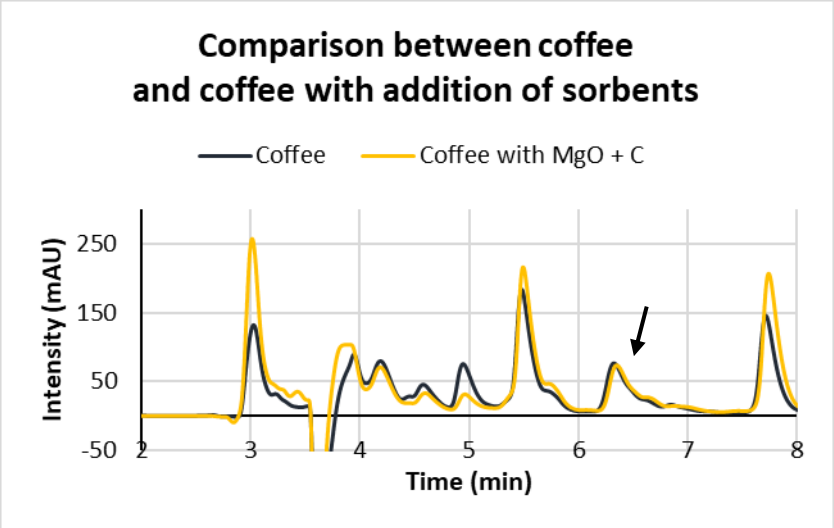

Figure 5.13: Comparison between the sample of coffee and the sample of coffee with added sorbents.

In the area where usually the peak of acrylamide can be found, we can see a broadened peak. The peak itself integrates 10x higher, compared to the range of values we would expect to find for acrylamide, when all dilutions are taken into account. Spiking the sample with a drop of 40 ng/mL solution of acrylamide led us to believe, that the peak of acrylamide is in fact hiding in this area of the chromatogram. When comparing the non-spiked samples of coffee and coffee with added sorbents, we can see, that the sorbents do not improve the resolution of the peaks in this area of the chromatogram.

Removal of lipids with hexane

To further reduce the matrix effect in the chromatograms of the samples, defatting of coffee was attempted prior to sample preparation. For the purpose, coffee was stirred with hexane at room temperature for 60 min. Upon filtration and additional washing of the coffee with hexane, the coffee was dried and used in the same sample preparation as normal coffee beforehand. To better observe the effect of defatting, initially no MgO or active carbon were used in the sample preparation. The chromatogram of defatted coffee was compared to the result, obtained with the normal coffee sample without added sorbents (**Figure 5.14**).

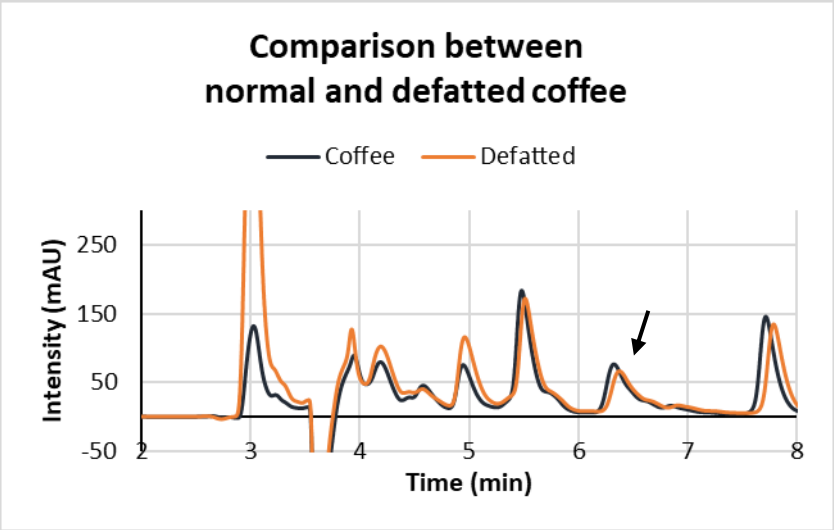

Figure 5.14: Comparison between normal and defatted coffee.

Where usually the peak of acrylamide can be found, again a broadened peak was observed, similar to the one observed in sample of normal coffee. The integration is similar as well. This suggests, that defatting of coffee is not as beneficial as initially thought. To try to further improve the result of the study, a sample of defatted coffee was prepared in presence of MgO and active carbon. Its chromatogram was then compared to the chromatogram of the sample of normal coffee (**Figure 5.15**).

As before, when samples of normal and defatted coffee were analysed, a broadened peak was found in the area that was usually assigned to acrylamide. The peak is essentially very similar to the peak found in the sample of normal coffee, prepared without added sorbents and still integrates 10-fold more as integration for acrylamide would be expected.

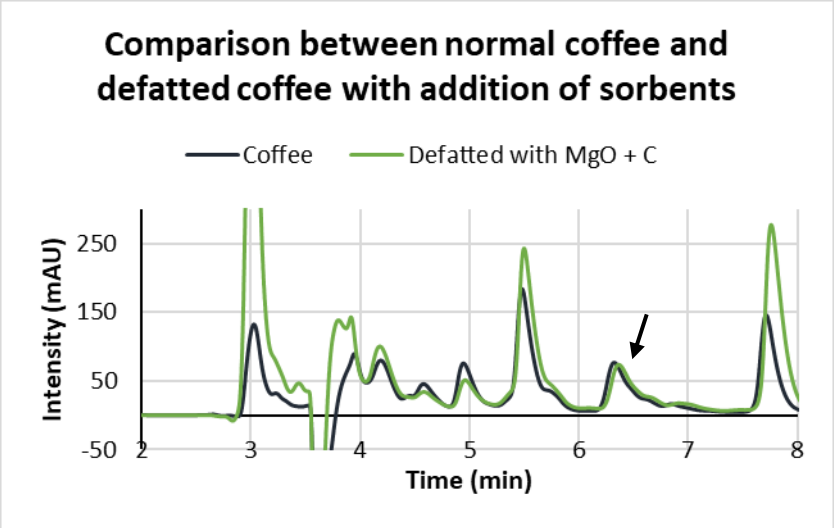

Figure 5.15: Comparison between normal coffee and defatted coffee with addition of sorbents.

Shorter time of extraction

Based on the discoveries in the first attempt to improve the Demus Lab method of sample preparation, the approach was found to be beneficial in reducing the matrix effect of the sample and shortening the sample analysis time. Further improvements needed to be accomplished, however, to improve the resolution of the peaks around acrylamide. A more optimised SPE purification protocol was considered, to potentially omit the interferences in the chromatogram.

As a way of controlling the extraction of acrylamide and its interferences, a shorter time of extraction was examined. For the purpose, it was shortened to 30 s and 5 min, to observe if the amount of extracted acrylamide is still comparable to the one, found after the 30 min long extraction, and if the amount of impurities in the sample really reduces with a shorter exposure to water. For the experiment defatted coffee was used, to allow a faster contact of water with acrylamide.

Another change was abandoning of the SPE system with two columns by the use of solely the Isolute C18 column. To further improve the result, addition of MgO and active charcoal to the extraction mixture of one sample for 30 s of extraction was attempted. The chromatograms after 30 s and 5 min of extraction were compared to each other and to the chromatogram of the sample after 30 s of extraction in presence of MgO and active carbon (**Figure 5.16**).

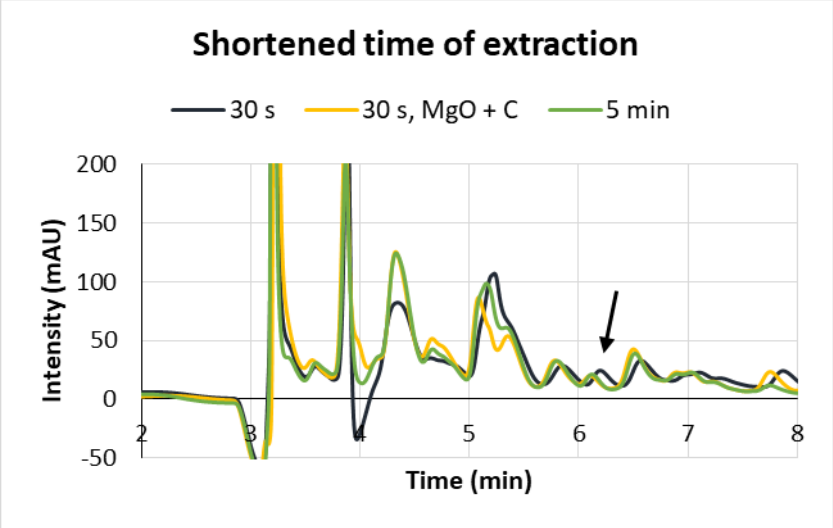

Figure 5.16: Chromatograms, following a shortened time of extraction.

A peak of acrylamide was in this case much better separated from its surrounding. This confirms, that the time of extraction of the sample influences greatly on the amount of the interferences co-extracted with acrylamide. Considering the dilution, the integration of the peak fits well. Due to the fact, that the peak is relatively small, it might be beneficial to try to find a way to increase the concentration of acrylamide in the final HPLC sample. Additionally, prolonging the extraction to 5 min did not increase the amount of acrylamide in the sample, nor did the addition of the MgO and active carbon improve the resolution of the chromatogram.

Combination of sorbents and acetone

It has been reported in literature, that extraction of acrylamide with a mixture of water and organic solvents can greatly improve the results of the HPLC-UV analysis of acrylamide.[126] Additionally, as acetone is a volatile organic solvent, its evaporation after the extraction of coffee could vastly increase its concentration in the sample and thus potentially give a better signal in the chromatogram. Presence of water in the extraction media improves the extraction of acrylamide from coffee due to further improving its solubility. Acetone, on the other hand, could give the possibility to extract acrylamide more selectively, as not all of the polar compounds in coffee are necessarily soluble in it.

In this experiment ground green and to a light, medium and dark degree roasted coffee beans were used (**Figure 5.17**). The extraction mixtures were prepared with the addition of MgO to the coffee sample, homogenisation with a spatula, addition of water and then another round of polymerisation to prevent MgO from attaching to the walls of the vessel. Finally, acetone was added and the mixture needed to be again stirred vigorously. The role of MgO in the sample was the one of a sorbent and simultaneously raising the pH of the extracting medium. Additionally, an improved protocol of SPE purification was introduced, including the application of a concentrated extract to Bond Elut AccuCAT SPE columns. This way the final concentration of acrylamide in the sample should be higher, while retaining a great deal of impurities in the column.

Figure 5.17: Green and to different degrees roasted coffee beans, and their extracts.

Evaporation of acetone followed after the extraction. It was done with a stream of compressed air at room temperature, until only water remained. Thus, acrylamide was left as intact as possible. At the same time, by removing acetone before the analysis, the unwanted additional peaks of acetone in the chromatograms are avoided as well (**Figure 5.18**).

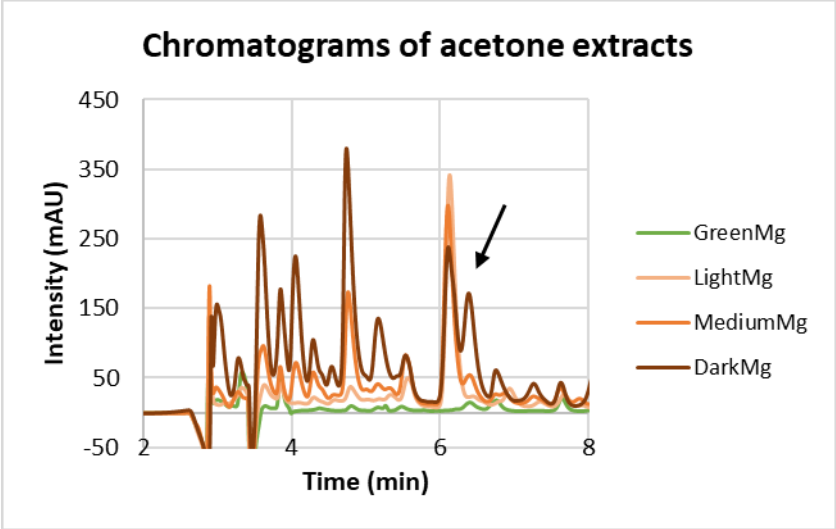

Figure 5.18: Chromatograms of acetone extracts of green and to different degrees roasted coffee.

A relatively big peak was found a little after the minute 6 in all chromatograms but the one of green coffee. This is generally a good sign, as green coffee should not contain noticeable amounts of acrylamide. Nevertheless, as the areas of the peaks represents about 10-fold too large concentrations, the explanation, that the peaks are interferences and the actual peak of acrylamide is hidden underneath them, is far more probable.

5.5 Follow-up

The essential concept of preparation of coffee samples for HPLC-UV analysis of acrylamide remained extraction of coffee into water or another polar solvent, followed by SPE purification and HPLC-UV analysis. During our work, however, it was found that there are many opportunities for improvement of the HPLC-UV analytical methods. Addition of sorbents, defatting of coffee, sonicating and variability of the time of extraction are just a few possibilities that can largely improve the coffee extraction process.

SPE purification is the next step, where improvements can be made. By tactically selecting the correct SPE column, capable of extracting and concentrating acrylamide from the coffee sample sufficiently enough, to assure a good result during the HPLC-UV analysis, addition of adsorbents, defatting of coffee and removal of proteins prior to extraction can be avoided. Recently, synthesis of MIPs for acrylamide, based on a dummy template, was reported to yield very good results.[64]

Finally, suitable chromatographical conditions are vital to conduct a successful analysis. Our results often showed overlapping of the peak of acrylamide with peaks of interferences. This issue could be solved by using an HPLC column of longer dimensions or with a more suitable Stationary phase. Columns with a hydrophilic stationary phase are often mentioned in literature as a good solution.

Another interesting option would be to take advantage of the fact, that acrylamide is chemically a Michael acceptor, capable of participating in 1,4-additions. Additions of thiosalicylic acid to acrylamide have already been described.[107] This mechanism could be further explored to form fluorescent or coloured adducts of acrylamide. This way its wavelength of detection or even mechanism of detection could change enough to solve the resolution issues.

5.6 Final method

Upon summing up all of our findings, we decided to try out the Agilent Bond Elut QuEChERS Acrylamide Kit.[176] Preparation of a sample for HPLC-UV analysis in this case consists of extraction and dispersive SPE cleanup. The extraction step is performed in water and lasts for 1 min during vigorous shaking. This corresponds nicely to the findings of our experiments, where a shorter time of extraction has been applied.

By subsequently adding acetonitrile, the Agilent Bond Elut QuEChERS extraction salt mixture for acrylamides and hexane, shaking the vial vigorously, then centrifuging it to separate the content of the vial, three phases appeared. The upper phase represented hexane and served to de-fat the sample. The middle phase represented the acetonitrile phase and the lower phase the aqueous phase. Namely, the addition of the Agilent Bond Elut QuEChERS extraction salt mixture, containing anhydrous $MgSO_4$ and NaCl, to the mixture of acetonitrile and water extract of coffee induced separation of the two otherwise miscible solvents. With that a salting-out extraction of acrylamide from the aqueous to the acetonitrile phase occurred.

The salting out extraction in this case worked better than a similar salting out reaction we attempted beforehand. Adding a combination of anhydrous $MgSO_4$ and NaCl resulted in a much better separation of the phases than adding solely 1 g of NaCl to a similar mixture of solvents.

To additionally purify the extracted acrylamide in the acetonitrile phase, SPE clean up with Bond Elut QuEChERS EN Dispersive SPE column, containing a mixture of 3 sorbents: PSA, C18EC and $MgSO_4$, was successfully attempted. After filtration of the acetonitrile sample through the column by centrifugation, the filtrate was collected into an HPLC vial and was immediately used in the HPLC-UV analysis.

For the analysis an Agilent ZORBAX HILIC Plus column was used, containing a polar stationary phase and thus improving the retention of acrylamide. As a mobile phase a mixture of acetonitrile with 3% of acetic acid was used. The peak of acetonitrile in this case was surpressd and did not interfere with the peak of acrylamide, as it was found during our previous attempts of salting out reactions and analysis in aqueous conditions. The time for the analysis of a single sample was well shortened, from the initial 60 min at the beginning of ourmethod development to 10 min with the current method (**Figure 5.19**).

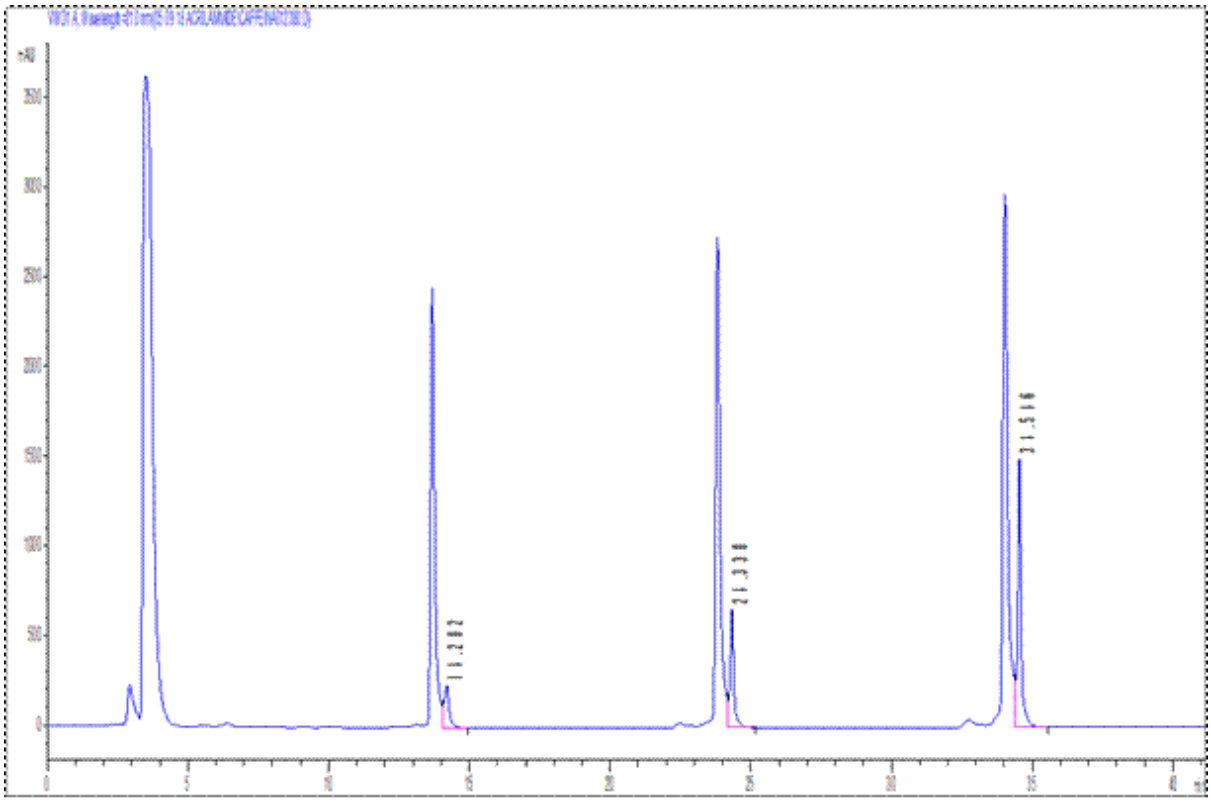

Figure 5.19: Chromatogram of a standard sample of acrylamide, a coffee sample after treatment with Agilent Bond Elut QuEChERS Acrylamide Kit and another two coffee samples following the same treatment, spiked with increasing amounts of acrylamide standard solution.

From the chromatogram we can see, that even though the sample preparation method this time worked much better, the separation of the peaks could still be further improved by adjusting the chromatographic conditions. The second and third cluster of peaks are dilutions of the sample, producing the fourth cluster of peaks. The fourth cluster of peaks represents the sample, obtained following the QuEChERS method. The outcome of the integration of the peak of acrylamide fits well in range within the expected range. As those are only initial results, validation of the method on real samples still needs to be performed.

Bibliography

9. Speer, K. & Kölling-Speer, I. The lipid fraction of the coffee bean. *Braz. J. Plant Physiol* **18,** 201–216 (2006).

38. Ky, C. L. *et al.* Caffeine, trigonelline, chlorogenic acids and sucrose diversity in wild Coffea arabica L. and C. canephora P. accessions. *Food Chem.* **75,** 223–230 (2001).

64. Arabi, M., Ghaedi, M. & Ostovan, A. Development of dummy molecularly imprinted based on functionalized silica nanoparticles for determination of acrylamide in processed food by matrix solid phase dispersion. *Food Chem.* **210,** 78–84 (2016).

96. IARC. Acrylamide. *IARC Monogr.* **60,** 389–433 (1994).

106. Sigma Aldrich. *Acrylamide, Specification sheet*.

115. Soares, C., Cunha, S. & Fernandes, J. Determination of acrylamide in coffee and coffee products by GC-MS using an improved SPE clean-up. *Food Addit. Contam.* **23,** 1276–1282 (2006).

116. Fernandes, J. O. & Soares, C. Application of matrix solid-phase dispersion in the determination of acrylamide in potato chips. *J. Chromatogr. A* **1175,** 1–6 (2007).

120. Xu, L., Zhang, L., Qiao, X., Xu, Z. & Song, J. Determination of trace acrylamide in potato chip and bread crust based on SPE and HPLC. *Chromatographia* **75,** 269–274 (2012).

121. Bortolomeazzi, R., Munari, M., Anese, M. & Verardo, G. Rapid mixed mode solid phase extraction method for the determination of acrylamide in roasted coffee by HPLC-MS/MS. *Food Chem.* **135,** 2687–2693 (2012).

125. Şenyuva, H. Z. & Gökmen, V. Study of acrylamide in coffee using an improved liquid chromatography mass spectrometry method: Investigation of colour changes and acrylamide formation in coffee during roasting. *Food Addit. Contam.* **22,** 214–220 (2005).

126. Khoshnam, F., Zargar, B., Pourreza, N. & Parham, H. Acetone Extraction and HPLC Determination of Acrylamide in Potato Chips. *J. Iran. Chem. Soc.* **7,** 853–858 (2010).

127. Paleologos, E. K. & Kontominas, M. G. Determination of acrylamide and methacrylamide by normal phase high performance liquid chromatography and UV detection. *J. Chromatogr. A* **1077,** 128–135 (2005).

136. Delatour, T., Périsset, A., Goldmann, T., Riediker, S. & Stadler, R. H. Improved Sample Preparation to Determine Acrylamide in Difficult Matrixes Such as Chocolate Powder, Cocoa, and Coffee by Liquid Chromatography Tandem Mass Spectroscopy. *J. Agric. Food Chem.* **52,** 4625–4631 (2004).

166. ALLE AZIENDE - Associate AIIPA – Settore " Comitato Italiano del Caffè " - componenti la " Commissione Tecnica Caffè " OGGETTO : ATTENZIONE : Acrilammide - Pubblicato il regolamento 2017 / 2158 che istituisce misure di attenuazione e livelli di riferiment. (2018).

167. Bagdonaite, K. Formation of Acrylamide during Roasting of Coffee by. 1–111 (2007).

168. Oxide, M., Adsorbent, A. N., Treatment, F. O. R. & Water, P. W. MAGNESIUM OXIDE AN ADSORBENT FOR TREATMENT OF. **5,** 103–107 (2012).

169. Hyde, A. M., Zultanski, S. L., Waldman, J. H., Zhong, Y. & Shevlin, M. General Principles and Strategies for Salting-Out Informed by the Hofmeister Series. (2017). doi:10.1021/acs.oprd.7b00197

170. Agilent. No Title.

171. Snoeyink, V. L. & Weber, W. J. The Surf ace Chemistry of Active Carbon. (1966).

172. Biotage Isolute C18. Available at: http://www.biotage.com/product-page/isolute-c18.

173. Discovery DSC-MCAX.

174. Biotage Isolute PSA.

175. Pule, B. O. & Torto, N. Determination of Acrylamide in Cooking Oil by Agilent Bond Elut QuEChERS Acrylamide Kit and HPLC-DAD. *Food Safety. Agil. Technol. Icnc.* (2012).

176. WANG Xiao-li, Z. S. Synthesis of Ethylene Glycol Ether by Montmorillonite Solid Acid Catalysis. *J. Liaoning Univ. Pet. Chem. Technol.*

6. EXPERIMENTAL SECTION

6.1 Instrumentation

Thin layer chromatography (TLC) analyses were performed on Merck 60 F254 silica gel plates; the plates were stained with an aqueous permanganate solution, with an ethanolic vanillin solution or with iodine vapours, or examined under ultraviolet light.

Column-chromatography purifications were carried out with Merck silica gel 60 (0.040-0.063 mm, 230-400 mesh ASTM), via flash chromatography.

Melting points (M. p.) were determined with a Sanyo Gallenkamp apparatus.

Nuclear Magnetic Resonance (NMR): ^{1}H NMR, ^{13}C NMR and 2D NMR (H-H COSY, H-C HSQC) spectra for characterizations of compounds were obtained on a Varian 400 spectrometer. All the ^{1}H NMR titrations were performed on a Varian 500 spectrometer.

Electrospray Ionization mass spectrometry measurements (ESI+/–MS) were performed on an Esquire 4000 (Bruker-Daltonics) spectrometer.

Infrared spectra (IR) were obtained on an Avatar 320-IR (Thermo-Nicolet) spectrometer, equipped with NaCl crystal windows.

Fluorescence spectra were recorded on an Agilent Cary Eclipse spectrometer, using a 1 cm quartz cuvette with a 3 mL volume.

Reverse phase high performance liquid chromatography (RP-HPLC) analyses of acrylamide were done on an Agilent 1100 series equipped with a UV Shimadzu detector, using an Agilent Poroshell 150 x 4.6 mm, 2.7 µm particle sized analytical column. Rebinding analyses were done on an Agilent 1260 series equipped with a UV Agilent detector, using a Phenomenex Kinetex 250 x 4.6 mm, 5 µm particle sized analytical column.

UV-visible spectra were recorded on an Agilent Cary 100 spectrometer, using a 1 cm quartz cuvette with a volume of 1 mL.

Crimp cap Weaton vials for the polymer synthesis were purchased from Sigma Aldrich.

Spectra/Por3 dialysis membrane MWCO 3500 Da was purchased from Spectrumlabs.

Zetasizer nano-S (Malvern) was used for particle size and zeta potential measurements.

Microscopy of coffee samples was done on a Leica DFC 7000T microscope.

6.2 Materials and general methods

Chemicals were purchased from Sigma-Aldrich Co. Europe , and used as received.

Solvents and deuterated solvents were purchased from Aldrich and Cambridge Isotope Laboratories.

TLC plates were plastic-backed, coated with 0.25 mm of silica gel 60F-254 and purchased from Merck KGaA (Darmstadt, Germany). They were observed under UV light, stained with aqueous permanganate solution, ethanolic vanillin solution or iodine vapours.

Silica gel 60 was used for "flash" column chromatography and as well from Merck KGaA (Darmstadt, Germany).

Low temperature baths were prepared using liquid N_2 before lyophilisation, H_2O/ice when temperature of 0°C was required, and dry ice in studies with antimony(III) chloride.

Anhydrous conditions were obtained by flame drying reaction flasks while alternatively placing them under vacuum (approx. 1 mmHg) via the Schlenk line and purging them with Ar or N_2 through silicon stoppers. A flow of of Ar or N_2 was used to keep the inert atmosphere.

6.3 Isolation of cafestol and 16-OMC

For the isolation of the two diterpenes, a commercially available blend of *C. canephora* was used, sold under the brand Amigos Qualitá Rossa. The coffee was roasted to a medium degree and finely ground, with the appropriate grind for preparation of Turkish coffee. For the isolation of both diterpenes a slightly adapted DIN 10779[13] method was used.

6.3.1 Extraction of coffee oil

About 60 g of coffee were precisely weighed into a cellulose extraction thimble and the thimble was inserted into a 500 mL Soxhlet extractor. 650 mL of methyl t-butyl ether were poured into a round bottom flask. The Soxhlet apparatus was assembled and the extraction went on for 6 h at 80°C. The solvent was then evaporated under vacuum and the weight of the residue was documented, ranging from 6 to 7 g (10 - 11%).

6.3.2 Saponification of coffee oil

To the coffee oil from **6.3.1** in a round-bottom flask, equipped with a stirring bar, 200 mL of a 10% ethanolic solution of KOH were added. The mixture was heated to 90°C in an oil bath or in a water bath, and the saponification went on for 4 h.

Afterwards, the mixture was diluted with 200 mL of water, heated to 70°C, transferred to a separating funnel and left to cool to room temperature. 240 mL of diethyl ether were added, the separating funnel was shaken moderately and upon the separation of the phases, the organic layer was collected. The organic phase was then washed 3x with 50 mL of water and dried by falling drop-wise through a layer of Na_2SO_4. The solvent was removed under vacuum, leaving behind on average 0.893 g of the unsaponifiable fraction (1.48 %).

6.3.3 Isolation of cafestol and 16-O-methylcafestol

The diterpenes were isolated via “flash” chromatography from the unsaponifiable fraction, obtained in **6.3.2**. Gradient elution was applied, with the mobile phase consisting of petroleum ether and ethyl acetate in ratios from 4:1 to 1:1 (V/V). The elution was monitored with TLC, with the chromatogram stained with aqueous permanganate solution. Fractions with a similar retention factor, corresponding to the one found in literature, were grouped for both diterpenes. The solvent was removed under vacuum and on average 62 mg of cafestol and 28 mg of 16-OMC were obtained.

6.3.4 Additional purification

If impurities were found in batches of cafestol and 16-OMC, another round of flash chromatography was carried out. For both diterpenes, an isocratic elution with a mixture of dichloromethane and acetonitrile in ratio 95:5 sufficed. The elution was again monitored with

TLC, with the chromatogram stained with an aqueous permanganate solution, and the fractions with a similar retention factor were combined for both diterpenes.

Cafestol

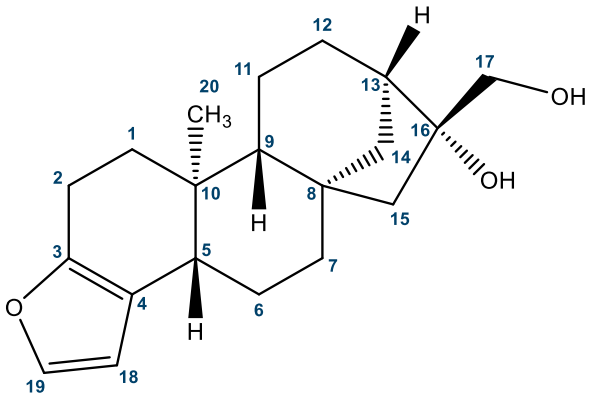

M.p. = 136-141°C.

R_f (petroleum ether to ethyl acetate 1:1**)** = 0.32, stained with aqueous $KMnO_4$ solution.

^{1}H NMR (400MHz, $CDCl_3$, ppm) δ = 7.24 (d, 1H, J=1.8 Hz, H_{19}), 6.21 (d, 1H, J=1.8 Hz, H_{18}), 3.84-3.68 (AB system, 2H, J=11.00 Hz, H_{17}), 2.65-2.59 (dd, 2H, J=5.8, 2.8 Hz, H_2), 2.30-2.23 (dq, 1H, J=12.7, 2.4 Hz, H_5), 2.09-2.02 (m, 3H, H_{13}, H_1, H_{14}), 1.84-1.79 (ddd, 1H, J=13.00, 6.4, 3.2 Hz, H_6), 1.74-1.47 (m, 10H, H_6, H_7, H_{11}, H_{12}, H_{14}, H_{15}), 1.27-1.21 (dt, 1H, J=12.4, 9.4 Hz, H_1), 1.18 (d, 1H, J=7.6 Hz, H_9), 0.84 (s, 3H, H_{20}).

^{13}C NMR (400MHz, $CDCl_3$, ppm) δ = 148.71 (s, C_3), 140.55 (d, C_{19}), 120.10 (s, C_4), 108.28 (d, C_{18}), 81.88 (s, C_{16}), 66.39 (t, C_{17}), 53.42 (t, C_{15}), 52.08 (d, C_9), 45.42 (d, C_{13}), 44.66 (s, C_8), 44.23 (d, C_5), 40.86 (t, C_7), 38.62 (s, C_{10}), 38.17 (t, C_{14}), 35.72 (t, C_1), 26.04 (t, C_{12}), 23.08 (t, C_6), 20.62 (t, C_2), 19.01 (t, C_{11}), 13.32 (q, C_{20}).

^{1}H NMR (400MHz, DMSO-d_6, ppm) δ = 7.37 (d, 1H, J=1.8 Hz, H_{19}), 6.27 (d, 1H, J=1.8 Hz, H_{18}), 4.33 (t, 1H J=5.6 Hz, OH), 3.88 (s, 1H, OH), 3.56-3.39 (AB part of an ABX system, 2H, J= 5.2 Hz, H_{17}), 2.55 (dd, 2H, J=8.0 Hz, H_2), 2.2-2.14 (dd, 1H, J=12.8, 2.4 Hz, H_5), 2.04-1.95 (m, 1H, H_1), 1.91 (d, 1H, J=3.6 Hz, H_{13}), 1.85 (d, 1H, J=11.4 Hz, H_{14}), 1.79-1.71 (ddd, 1H, J=12.8, 6.0, 3.0 Hz, H_6), 1.65-1.54 (m, 6H, H_7, H_{11}, H_{12}, H_{14}), 1.51-1.48 (dd, 1H, J=14.1, 1.1 Hz, H_{15}), 1.42- 1.39 (dd, 1H, J=12.8, 3.5 Hz, H_6), 1.37 (br, 1H, H_{12}), 1.35-1.32 (d, 1H, J=14.1 Hz, H_{15}), 1.21- 1.13 (dd, 1H, J=21.9, 9.6 Hz, H_1), 1.12 (d, 1H, J=5.6 Hz, H9), 0.73 (s, 3H, H_{20}).

^{13}C NMR (400MHz, $CDCl_3$, ppm) δ = 148.48 (s, C_3), 141.33 (d, C_{19}), 120.36 (s, C_4), 108.96 (d, C_{18}), 81.02 (s, C_{16}), 65.76 (t, C_{17}), 53.54 (t, C_{15}), 52.09 (d, C_9), 45.13 (d, C_{13}), 44.43 (s, C8), 44.11 (d, C_5), 41.15 (t, C_7), 38.56 (s, C_{10}), 38.25 (t, C_{14}), 35.56 (t, C_1), 26.14 (t, C_{12}), 23.19 (t, C_6), 20.61 (t, C_2), 19.08 (t, C_{11}), 13.65 (q, C_{20}).

IR (cm^{-1}) = 3582, 3381, 2924, 2850, 1736, 1627, 1456, 1129, 1042, 1015.

ESI$^+$-MS: $[M+Na]^+$ = 339 m/z; **$[M+H]^+$ =** 317 m/z.

16-O-methylcafestol

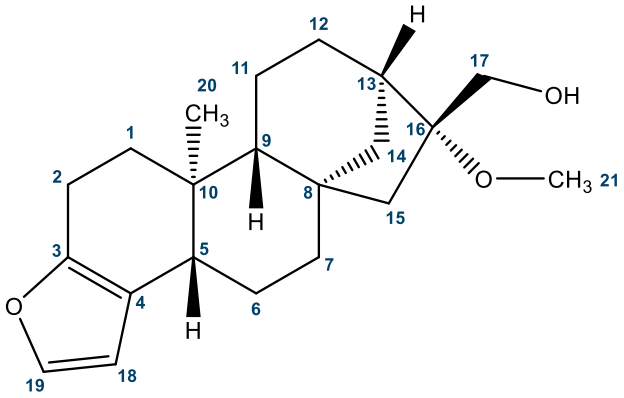

M.p. = 171-175°C

R_f (petroleum ether to ethyl acetate 1:1**)** = 0.38, stained with aqueous $KMnO_4$ solution.

^{1}H NMR (400MHz, $CDCl_3$, ppm) δ = 7.24 (br, 1H, H_{19}), 6.20 (d, 1H, J=1.8 Hz, H18), 3.77 (s, 2H, H_{17}), 3.17 (s, 3H, H_{21}), 2.62 (dt, 2H, J=5.6, 2.7 Hz, H_2), 2.27 (dd, 1H, J=12.6, 2.5 Hz, H_5), 2.22 (d, 1H, J=3.0, H_{13}), 2.05 (dt, 1H, J=8.9, 4.0 Hz, H_1), 1.99 (d, 1H, J=11.5 Hz, H_{14}), 1.83-1.78 (ddd, 1H, J=13.0, 6.3, 3.2, H_6), 1.71 (d, 1H, J=7.6 Hz, H_{11}), 1.67-1.48 (m, 8H, H_6, H_7, H_{11}, H_{12}, H_{14}, H_{15}) 1.43 (dd, 1H, J=14.7, 2.0 Hz, H_{15}), 1.30-1.22 (m, 1H, H_1), 1.19 (d, 1H, J=7.9 Hz, H_9), 0.83 (s, 3H, H_{20}).

^{13}C NMR (400MHz, $CDCl_3$, ppm) δ = 148.73 (s, C_3), 140.54 (d, C_{19}), 120.11 (s, C_4), 108.27 (d, C_{18}), 87.07 (s, C_{16}), 60.44 (t, C_{17}), 52.09 (d, C_9), 49.07 (t, C_{15}), 48.92 (q, C_{21}), 44.38 (s, C_8), 44.22 (d, C_5), 41.45 (d, C_{13}), 40.98 (t, C_7), 38.66 (s, C_{10}), 37.78 (t, C_{14}), 35.75 (t, C_1), 25.70 (t, C_{12}), 23.10 (t, C_6), 20.62 (t, C_2), 19.13 (t, C_{11}), 13.29 (q, C_{20}).

^{1}H NMR (400MHz, DMSO-d_6, ppm) δ = 7.39 (d, 1H,J=1.7 Hz , H_{19}), 6.29 (d, 1H, J=1.7 Hz, H_{18}), 4.29- 4.27 (t, 1H, J=5.2 Hz, OH), 3.65-3.53 (AB part of an ABX system, 2H, J= 5.2, H_{17}), 3.05 (s, 3H, H_{21}), 2.54 (d, 2H, J=8.4 Hz, H_2), 2.22-2.17 (dd, 1H, J=12.7, 1.7, H_5), 2.11 (d, 1H, J=3.4, H_{13}), 2.00 (m, 1H, H_1), 1.85 (d, 1H, J=11.3 Hz, H_{14}), 1.75 (dd, 1H, J=1.8 Hz, H_6), 1.65-1.55 (m, 4H, H7, H11, H_{12}), 1.51-1.34 (m, 6H, H_6, H_7, H_{12}, H_{14}, H_{15}), 0.74 (s, 3H, H_{20}).

^{13}C NMR (400MHz, DMSO-d_6, ppm) δ = 148.48 (s, C_3), 141.35 (d, C_{19}), 120.33 (s, C_4), 108.94 (d, C_{18}), 86.69 (s, C_{16}), 60.08 (t, C_{17}), 52.05 (d, C_9), 49.64 (t, C_{15}), 49.18 (q, C_{21}), 44.21 (d, C5), 44.07 (s, C8), 41.58 (d, C_{13}), 41.27 (t, C_7), 38.59 (t, C_{14}), 38.41 (s, C_{10}), 35.56 (t, C_1), 26.04 (t, C_{12}), 23.19 (t, C_6), 20.61 (t, C_2), 19.14 (t, C_{11}), 13.60 (q, C_{20}).

IR (cm^{-1}) = 3583, 3394, 2916, 2850, 1730, 1456, 1105, 1071, 1010.

ESI$^+$-MS: $[M+Na]^+$ = 353 m/z; **$[M+H]^+$ =** 331 m/z.

6.4 MIPs for cafestol and 16-OMC

6.4.1 Synthesis of the polymerizable derivative for cafestol

(1-hydroxymethyl)cyclohexan-1-ol

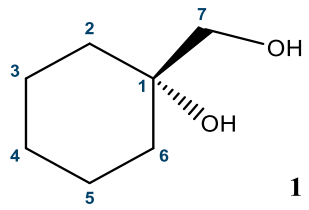

1

N-methyl morpholine (1.78 g, 15.2 mmol) was weighed into a round-bottom flask and dissolved in 1.25 mL of acetone and 3.1 mL of water. Methylenecyclohexane (1.25 mL, 10.4 mmol) was added, then 2.5% solution of osmium(VIII) oxide in n-butanol (1.04 mL, 0.10 mmol) in a light stream while the mixture was stirring. The reaction went on for 24 h and was stopped by the addition of sodium bisulfite (2.64 g, 25.4 mmol). The solution was stirred for additional 20 min until switching from brown to orange, then it was transferred into a separating funnel by using 280 mL of diethyl ether and 50 mL of water.

The organic phase was collected, and the water phase was washed twice more with 100 mL of diethyl ether. The organic phase was combined with the previous and both were dried over $CaSO_4$. After filtration, the solvent was removed under vacuum to give **1** as lightly gray crystals with a yield of 96 %.

M.p. = 79.5-83.1 °C.

R_f (petroleum ether to ethyl acetate 1:1**)** = 0.51, stained with aqueous $KMnO_4$ solution.

^{1}H NMR (400 MHz, D_2O, ppm) δ = 3.30 (s, 2H, H_7), 1.25-1.11 (m, 1H, H_4), 1.50-1.26 (m, 9H, H_2, H_6, H_3, H_5, H_4).

^{13}C NMR (400 MHz, D_2O, ppm) δ = 72.32 (s, C_1), 68.67 (s, C_7), 32.90 (s, C_2, C_6), 25.10 (s, C_4), 21.30.05 (s, C_3, C_5).

IR (cm^{-1}): 3264, 2928, 2852, 1711, 1208, 1043, 994, 894.

ESI$^+$-MS: [M+Na]$^+$=153 m/z.

Model polymerizable derivative for cafestol

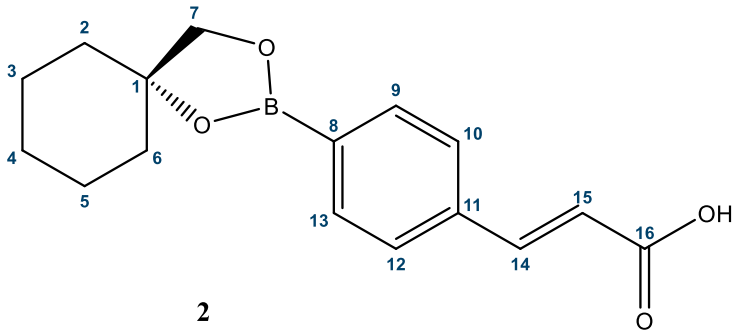

2

1 (19.2 mg, 0.1 mmol) and 4-(trans-2-carboxyvinyl)phenylboronic acid (**3b**, 13.0 mg, 0.1 mmol) were dissolved in 5 mL of THF. The mixture was left stirring for 5 h at room temperature. The solvent was then evaporated to give white crystals with a yield of 53%.[148]

M.p. = 115.5-118.2 °C.

R_f (petroleum ether to ethyl acetate 1:1**)** = 0.73, stained with aqueous $KMnO_4$ solution.

1H NMR (400 MHz, $CDCl_3$, ppm) δ = 7.84 (d, J=8.11 Hz, 2H, H_{10}, H_{12}), 7.78 (d, J=16.00 Hz, 1H, H_{14}), 7.55 (d, J=8.06 Hz, 2H, H_9, H_{13}), 6.50 (d, J=15.99 Hz, 1H, H_{15}), 4.06 (s, 1H, H_7), 1.88-1.74 (m, 4H, H_2, H_6), 1.70-1.60 (m, 4H, H_3, H_5), 1.55-1.48 (m, 2H, H_4).

13 NMR (400 MHz, $CDCl_3$, ppm) δ = 171.12 (s, C_{16}), 146.62 (s, C_{14}), 136.49 (s, C_8), 135.27 (s, C_9, C_{13}), 127.50 (s, C_{10}, C_{12})

IR (cm^{-1}) = 2932, 2858, 1687, 1628, 1422, 1364, 1308, 1217, 1039.

Polymerizable derivative for cafestol

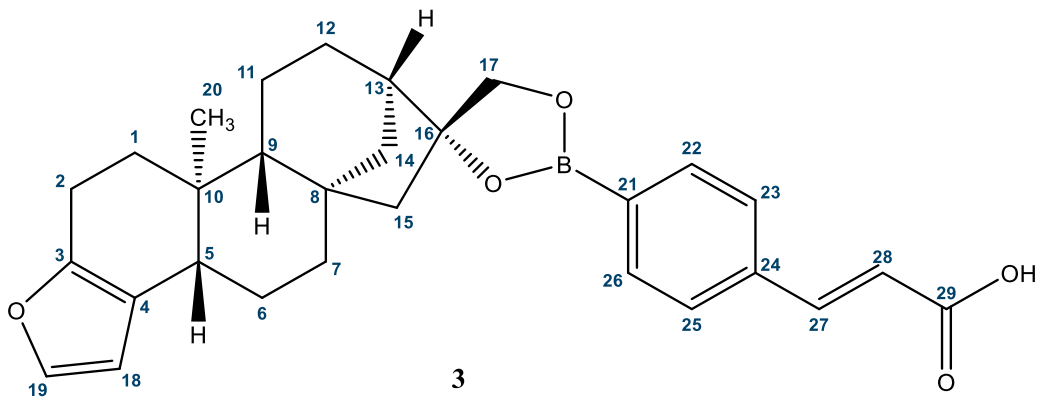

3

Cafestol (100 mg, 0.32 mmol) and 4-(trans-2-carboxyvinyl)phenylboronic acid (**3b**, 60.67 mg, 0.32 mmol) were suspended in 5 mL of THF and the reaction was left going for 5 h at room temperature. After, the solvent was evaporated giving white crystals (49%).

M.p. = 219-223 °C.

R_f (petroleum ether to ethyl acetate 1:1**)** = 0.65, stained with aqueous $KMnO_4$ solution.

^{1}H NMR (400 MHz, $CDCl_3$, ppm) δ = 7.84 (d, J=8.11 Hz, 2H, H_{10}, H_{12}), 7.78 (d, J=16.00 Hz, 1H, H_{14}), 7.55 (d, J=8.06 Hz, 2H, H_9, H_{13}), 7.24 (d, 1H, J=1.8 Hz, H_{19}), 6.21 (d, 1H, J=1.8 Hz, H_{18}), 6.50 (d, J=15.99 Hz, 1H, H_{15}), 4.06 (s, 1H, H_7), 3.84-3.68 (AB system, 2H, J=11.00 Hz, H_{17}), 2.65-2.59 (dd, 2H, J=5.8, 2.8 Hz, H_2), 2.30-2.23 (dq, 1H, J=12.7, 2.4 Hz, H_5), 2.09-2.02 (m, 3H, H_{13}, H_1, H_{14}), 1.84-1.79 (ddd, 1H, J=13.00, 6.4, 3.2 Hz, H_6), 1.74-1.47 (m, 10H, H_6, H_7, H_{11}, H_{12}, H_{14}, H_{15}), 1.27-1.21 (dt, 1H, J=12.4, 9.4 Hz, H_1), 1.18 (d, 1H, J=7.6 Hz, H_9), 0.84 (s, 3H, H_{20}).

^{13}C NMR (400 MHz, $CDCl_3$, ppm) δ = 170.70 (s, C_{29}), 148.66 (s, C_3), 146.22 (s, C_{27}), 140.33 (d, C_{19}), 136.43 (s, C_{21}), 135.26 (s, C_{22}, C_{26}), 127.51 (s, C_{23}, C_{25}), 120.03 (s, C_4), 117.91 (s, C_{14}), 108.31 (d, C_{18}), 81.02 (s, C_{16}), 65.76 (t, C_{17}), 53.54 (t, C_{15}), 52.09 (d, C_9), 45.13 (d, C_{13}), 44.43 (s, C8), 44.11 (d, C_5), 41.15 (t, C_7), 38.56 (s, C_{10}), 38.25 (t, C_{14}), 35.56 (t, C_1), 26.14 (t, C_{12}), 23.19 (t, C_6), 20.61 (t, C_2), 19.08 (t, C_{11}), 13.65 (q, C_{20}).

IR (cm^{-1}) = 2921, 2849, 1685, 1632, 1359, 1085, 1018, 987, 831.

ESI$^+$-MS: $[M+Na]^+$ = 495; **$[M+H]^+$** = 473 m/z.

6.4.2 Synthesis of the polymerizable derivative for 16-OMC

1-oxaspiro[2.5]octane

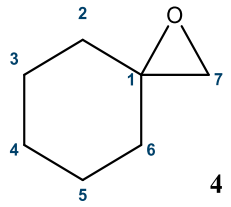

4

Tetrabutylammonium iodide (0.04 g, 0.16 mmol) and trimethylsulfonium bromide (2.04 g, 13 mmol) were weighed into a three-neck round-bottom flask. 120 mL of dichloromethane and 125 mL of 50 % aqueous solution of NaOH were added. A mechanical stirrer was used for stirring, one neck was attached to a condenser, the other one was capped after the addition of cyclohexanone (1036 µL, 13 mmol). After 48 h of stirring at 50 °C the solution was cooled to room temperature and the phases were separated. The organic phase was dried over Na_2SO_4 and the solvent was removed under vacuum giving a colourless oil. The identity of the oil was confirmed by ^{1}H NMR spectra of the oil.[149]

R_f (ethyl acetate**)** = 0.79, stained with ethanolic vanilin solution.

^{1}H NMR (400 MHz, $CDCl_3$, ppm) δ = 1.40-1.15 (m, 9H), 0.91-0.79 (m, 3H)

(1-methoxycyclohexyl)methanol

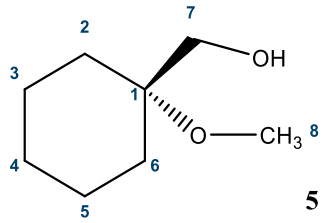

5

Aluminium(III) chloride (13.3 mg, 0.1 mmol) was dissolved in 50 mL of methanol, then the mixture was added to the residue of **4**. The solution was stirred for 40 min, then the solvent was removed under vacuum. The product was purified via "flash" column chromatography with an isocratic elution. Petroleum ether and ethyl acetate in ratio 1:1 were used as a mobile phase, and the elution was monitored with TLC. The solvent was removed under vacuum and the product was obtained as colourless oil (**4**, 42%).[177]

R_f (ethyl acetate**)** = 0.56, stained with ethanolic vanillin solution.

^{1}H NMR (400 MHz, $CDCl_3$, ppm) δ = 3.49 (s, 2H, H_7), 3.21 (s, 2H, H_8), 1.76-1.69 (m, 2H, H_2, H_6), 1.68-1.50 (m, 3H, H_2, H_6, H_4), 1.49-1.40 (m, 2H, H_3, H_5) 1.38-1.30 (m, 3H, H_3, H_5, H_4).

^{13}C NMR (400MHz, $CDCl_3$, ppm) δ = 72.32 (s, C_1), 68.67 (s, C_7), 32.90 (s, C_2, C_6), 25.10 (s, C_4), 21.30 (s, C_3, C_5).

IR (cm^{-1}) = 3416, 2932, 2857, 1738, 1446, 1148, 1081, 1043, 953.

ESI$^+$-MS: $[M+Na]^+$ = 167 m/z.

NMR titrations

A 10 or 20 mM solution of a template in DMSO-d_6 or $CDCl_3$ with a final volume of 800 μL was prepared, depending on the solubility of the monomer and its molecular weight. Two additions of 0.5 molar equivalents, then 11 additions of 1 molar equivalent of the chosen monomer were done, up to 12 molar equivalents altogether. ^{1}H NMR spectra were recorded first for the template and monomer alone, then after every addition of the monomer to the template.

^{1}H NMR Titration of methyl t-butyl ether with toluene

1.9 µL of methyl t-butyl ether were dissolved in 800 µL of $CDCl_3$, representing 8 µmol of the template and thus forming a 20 mM solution. After each addition of toluene, a ^{1}H NMR spectrum was recorded. The chemical shifts of the protons of the methoxy group of methyl t-butyl ether was observed after each addition and compared to their shift in the ^{1}H NMR spectrum before the titration.

	0.5 eq	**1 eq**	**12 eq**
	4 µmol	**8 µmol**	**96 µmol**
Toluene	0.85 µL	1.7 µL	20.4 µL

^{1}H NMR Titrations of 5 with toluene and imidazole

2.4 mg of **5** were dissolved in 800 µL of $CDCl_3$, representing 16 µmol of the template and thus forming a 20 mM solution. After each addition of the monomer, a ^{1}H NMR spectrum was recorded. The chemical shifts of the protons of the methoxy group of the template molecule were observed after each addition and compared to their shift in the ^{1}H NMR spectrum of the template before the titration.

	0.5 eq	**1 eq**	**12 eq**
	8 µmol	**16 µmol**	**192 µmol**
Toluene	1.7 µL	3.4 µL	40.8 µL
Imidazole	0.5 g	1.0 g	12.0 g

^{1}H NMR Titrations of 5 with monomers in $CDCl_3$

1.2 mg of **5** were dissolved in 800 µL of $CDCl_3$, representing 8 µmol of the template and thus forming a 10 mM solution. After each addition of a monomer, a ^{1}H NMR spectrum was recorded. The chemical shifts of the protons of the methoxy group of the template molecule were observed after each addition and compared to their shift in the ^{1}H NMR spectrum of the template before the titration.

	0.5 eq	**1 eq**	**12 eq**
	4 µmol	**8 µmol**	**96 µmol**
Trans-cinnamic acid	0.6 mg	1.2 mg	14.4 mg
Hydrocinnamic acid	0.6 mg	1.2 mg	14.4 mg
4-phenylbutyric acid	0.7 mg	1.3 mg	15.6 mg
5-phenylvaleric acid	0.7 mg	1.4 mg	16.8 mg

^{1}H NMR Titrations of 5 with monomers in DMSO-d_6

1.2 mg of **5** were dissolved in 800 µL of DMSO-D_6, representing 8 µmol of the template and thus forming a 10 mM solution. After each addition of a monomer, a ^{1}H NMR spectrum was recorded. The chemical shifts of the protons of the methoxy group of the template molecule were observed after each addition and compared to their shift in the ^{1}H NMR spectrum of the template before the titration.

	0.5 eq	1 eq	12 eq
	4 µmol	8 µmol	96 µmol
Trans-cinnamic acid	0.6 mg	1.2 mg	14.4 mg
Imidazoleacrylic acid	0.6 mg	1.1 mg	13.2 mg

^{1}H NMR Titrations of DMSO-d_6 with imidazoleacrylic acid

To 800 µL of DMSO-D_6, imidazoleacrylic acid was added in molar equivalents. After each addition, a ^{1}H NMR spectrum was recorded. Interactions between the solvent and the increasing amount of imidazoleacrylic acid were observed.

	0.5 eq	1 eq	12 eq
	4 µmol	8 µmol	96 µmol
Imidazoleacrylic acid	0.6 mg	1.1 mg	13.2 mg

Methyl trans-cinnamate

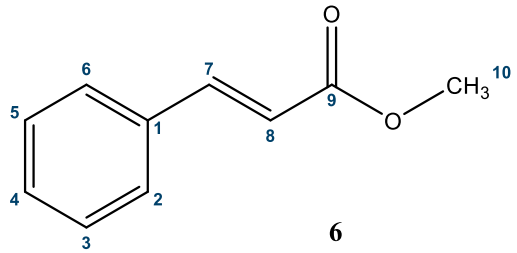

6

Trans-cinnamic acid (**10a**, 0.741 g, 5 mmol) was dissolved in 20 mL of methanol. 0.5 mL of H_2SO_4 was added and the reaction was going overnight at 70 °C. The solvent was evaporated, the residue was re-dissolved in 50 mL of ethyl acetate and the solution was washed with 50 mL of 5 % aqueous $NaHCO_3$ solution, 50 mL of water and 50 mL of brine, respectively. The organic phase was dried over Na_2SO_4 and the solvent was removed under vacuum. Purification via "flash" column chromatography with an isocratic elution with ethyl acetate followed, giving lightly yellow crystals of **6** (76%).[178]

M.p. = 37.1-39.3 °C

R_f (petroleum ether to ethyl acetate 5:1**)** = 0.64, stained with aqueous permanganate solution.

^{1}H NMR (400 MHz, $CDCl_3$, ppm) δ =7.71 (d, 1H, J=16.02 Hz, H_7), 7.53 (m, 2H, H_2, H_6), 7.39 (m, 3H, H_3, H_4, H_5), 6.45 (d, 1H, J=16.04 Hz, H_8), 3.82 (s, 3H, H_{10}).

^{13}C NMR (400 MHz, $CDCl_3$, ppm) δ = 167.39 (s, C_9), 144.85 (s, C_7), 134.38 (s, C_1), 130.29 (s, C_4), 128.88 (s, C_2, C_6), 128.06 (d, C_3, C_5), 117.81 (s, C_8), 51.67 (s, C_{10}).

IR (cm^{-1}) = 3491, 2926, 2853, 1719, 1637, 1450, 1276, 1170, 980.

ESI$^+$-MS: $[M+Na]^+$ = 185 m/z; **$[M+H]^+$** = 163 m/z.

^{1}H NMR Titrations of (1-methoxycyclohexyl)methanol with methyl cinnamate

1.2 mg of **5** were dissolved in 800 µL of $CDCl_3$, representing 8 µmol of the template and thus forming a 10 mM solution. After each addition of **6**, a ^{1}H NMR spectrum was recorded. The shifts of the proton signals of the methoxy group of the template molecule were observed after each addition and compared to their shift in the ^{1}H NMR spectrum of the template before the titration.

	0.5 eq	**1 eq**	**12 eq**
	4 µmol	**8 µmol**	**96 µmol**
Methyl cinnamate	0.7 mg	1.2 mg	14.4 mg

Determination of the proper length of alkyl chain

The most appropriate length of the alkyl chain between the carboxylic group and the phenyl ring allowing for the most significant π-methyl effect was determined. Esters of **5** with hydrocinnamic acid, 4-phenylbutyric acid and 5-phenylvaleric acid were synthesized.

Their ^{1}H NMR spectra in $CDCl_3$ were recorded, as well as the ^{1}H NMR spectra of **5** in the same solvent. The shifts of the proton signals of the methoxy group in the (1-methoxycyclohexyl)methyl part of the esters were observed. Assuming that the biggest shift is a consequence of the strongest π-methyl interaction, upon their comparison with the peak for the same functional group in (1-methoxycyclohexyl)methyl moiety, the ester with the most significant π-methyl effect was chosen. Consequently, the optimal length of the alkyl chain between the carboxylic group and the phenyl ring was determined.

Hydrocinnamic acid

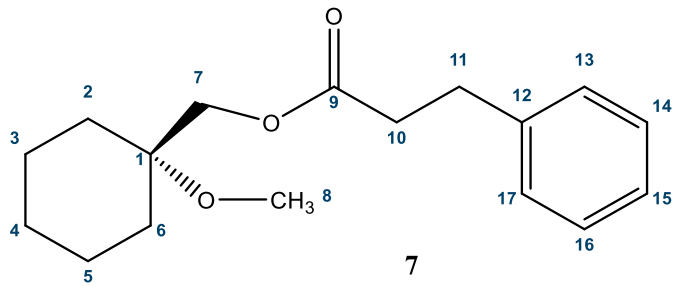

7

Hydrocinnamic acid (**7a**, 109 mg, 0.73 mmol), DCC (165 mg, 0.80 mmol) and DMAP (8.9 mg, 0.07 mmol) were dissolved in 10 mL of dichloromethane and the mixture was stirred on ice for 30 min. **5** (105 mg, 0.73 mmol) was added and the reaction was left going for 48h at room temperature. The solvent was removed under vacuum and the mixture was re-dissolved in 50 mL of ethyl acetate. The organic phase was washed with 50 mL of 5% aqueous solution of $NaHCO_3$, 50 mL of water, 50 mL of 10% aqueous solution of citric acid, 50 mL of water and 50 mL of brine, respectively. The organic phase was dried over Na_2SO_4 and the solvent was removed under vacuum. The residue was purified via flash chromatography using isocratic elution with a mobile phase of ethyl acetate and petroleum ether in ratio 1:1, giving **7** as a transparent oil (57%).[179]

R_f (petroleum ether to ethyl acetate 5:1**)** = 0.66, stained with aqueous permanganate solution.

^{1}H NMR (400 MHz, $CDCl_3$, ppm) δ = 7.32-7.25 (m, 2H, H_{13}, H_{17}), 7.23-7.17 (m, 3H, H_{14}, H_{16}, H_{15}), 4.03 (s, 2H, H_7), 3.19 (s, 3H, H_8), 2.97 (t, 2H, J=7.8 Hz, H_{11}), 2.69 (t, 2H, J=7.6 Hz, H_{10}), 1.73-1.65 (m, 2H, H_2, H_6), 1.60-1.48 (m, 2H, H_2, H_6), 1.48-1.39 (m, 2H, H_3, H_5), 1.31-1.20 (m, 2H, H_4, H_3, H_5).

^{13}C NMR (400 MHz, $CDCl_3$, ppm) δ = 172.84 (s, C_9), 140.39 (d, C_{12}), 128.46 (s, C_{13}, C_{17}), 128.26 (s, C_{14}, C_{16}), 126.23 (s, C_{15}), 73.99 (s, C_1), 66.73 (s, C_7), 49.00 (s, C_8), 35.79 (s, C_2, C_6), 31.08 (s, C_{11}), 30.97 (s, C_{10}), 25.69 (s, C_3, C_5), 21.31 (s, C_4).

IR (cm^{-1}) = 2934, 2857, 1738, 1454, 1384, 1238, 1149, 1080, 700.

ESI$^+$-MS: $[M+Na]^+$ = 276 m/z.

4-phenylbutyric acid

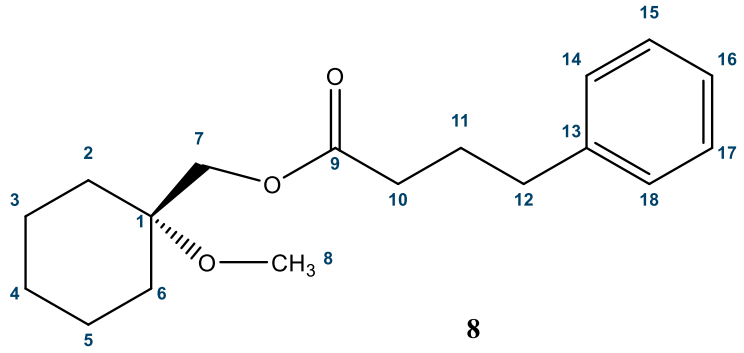

8

4-phenylbutyric acid (**8a**, 115 mg, 0.70 mmol), DCC (157 mg, 0.76 mmol) and DMAP (8.5 mg, 0.07 mmol) were dissolved in 20 mL of dichloromethane and the mixture was stirred on ice for 30 min. **5** (100 mg, 0.69 mmol) was added and the reaction was left going for 48 h at room temperature. The solvent was removed under vacuum and the residue was re-dissolved in 50 mL of ethyl acetate. The organic phase was washed with 50 mL of 5% aqueous solution of $NaHCO_3$, 50 mL of water, 50 mL of 10% aqueous solution of citric acid, 50 mL of water and 50 mL of brine, respectively. The organic phase was dried over Na_2SO_4 and the solvent was removed under vacuum. The residue was purified via flash chromatography using isocratic elution with a mobile phase of ethyl acetate and petroleum ether in ratio 1:1, giving **8** transparent oil (48%).[179]

R_f (petroleum ether to ethyl acetate 5:1**)** = 0.72, stained with aqueous permanganate solution.

^{1}NMR (400 MHz, $CDCl_3$, ppm) δ = 7.33-7.24 (m, 2H, H_{15}, H_{19}), 7.20-7.10 (m, 3H, H_{15}, H_{17}, H_{16}), 4.04 (s, 2H, H_7), 3.22 (s, 3H, H_8), 2.66 (t, 2H, J=7.6 Hz, H_{12}), 2.38 (t, 2H, J=7.4 Hz, H_{10}), 1.97 (q, 3H, J=7.6 Hz, H_{11}), 1.79-1.70 (m, 2H, H_2, H_6), 1.64-1.51 (m, 2H, H_2, H_6), 1.51-1.41 (m, 3H, H_3, H_5, H_4), 1.29-1.20 (m, 2H, H_3, H_5, H_4).

^{13}NMR (400 MHz, $CDCl_3$, ppm) δ = 173.40 (s, C_9), 141.36 (s, C_{13}), 128.49 (s, C_{14}, C_{18}), 128.37 (s, C_{15}, C_{17}), 125.97 (s, C_{16}), 74.02 (s, C_1), 66.21 (s, C_7), 48.99 (s, C_8), 35.13 (s, C_{12}), 33.61 (s, C_{10}), 31.14 (s, C_2, C_6), 26.60 (s, C_{11}), 25.72 (s, C_4), 21.32 (s, C_3, C_4).

IR (cm^{-1}) = 2934, 2858, 1735, 1454, 1385, 1147, 1082, 1032, 897, 746, 700.

ESI$^+$-MS: $[M+Na]^+$ = 313 m/z.

5-phenylvaleric acid

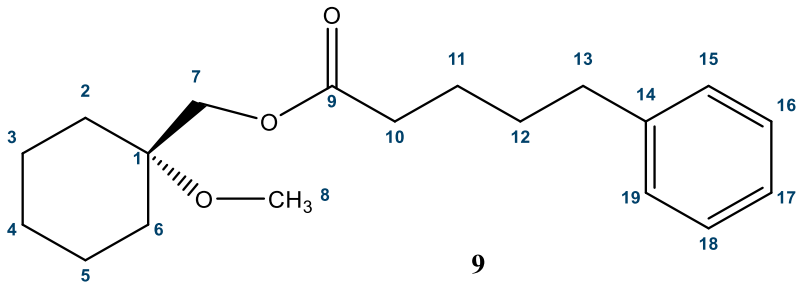

9

5-phenylvaleric acid (**9a**, 125 mg, 0.70 mmol), DCC (157 mg, 0.76 mmol) and DMAP (8.5 mg, 0.07 mmol) were dissolved in 20 mL of dichloromethane. The mixture was stirred on ice for 30 min. **5** (100 mg, 0.69 mmol) was added and the reaction was left going for 48 h at room temperature. The solvent was removed under vacuum and the residue was re-dissolved in 50 mL of ethyl acetate. The organic phase was washed with 50 mL of 5% aqueous solution of $NaHCO_3$, 50 mL of water, 50 mL of 10% aqueous solution of citric acid, 50 mL of water and 50 mL of brine, respectively. The organic phase was dried over Na_2SO_4 and the solvent was removed under vacuum. The residue was purified via flash chromatography using isocratic elution with a mobile phase of ethyl acetate and petroleum ether in ratio 1:1, giving **9** transparent oil (58%).[179]

R_f (petroleum ether to ethyl acetate 5:1**)** = 0.84, stained with aqueous permanganate solution.

^{1}H NMR (400 MHz, $CDCl_3$, ppm) δ = 7.33-7.24 (m, 2H, H_{15}, H_{19}), 7.20-7.10 (m, 3H, H_{18}, H_{18}, H_{17}), 4.03 (s, 2H, H_7), 3.21 (s, 3H, H_8), 2.63 (t, 2H, J=7.2 Hz, H_{13}), 2.39 (t, 2H, J=7.2 Hz, H_{10}), 1.81-1.63 (m, 6H, H_2, H_6, H_{12}, H_{11}), 1.63-1.50 (m, 2H, H_2, H_6), 1.50-1.41 (m, 2H, H_3, H_5), 1.36-1.20 (m, 4H, H_4, H_3, H_5).

^{13}C NMR (400 MHz, $CDCl_3$, ppm) δ = 173.54 (s, C_9), 142.10 (s, C_{14}), 128.36 (s, C_{16}, C_{18}), 128.29 (s, C_{15}, C_{19}), 125.75 (s, C_{17}), 74.01 (s, C_1), 66.27 (s, C_7), 49.01 (s, C_8), 35.57 (s, C_2, C_6), 34.14 (s, C_{13}), 31.13 (s, C_{10}), 30.89 (s, C_{12}), 25.72 (s, C_4), 24.64 (s, C_{11}), 21.32 (s, C_3, C_5).

IR (cm^{-1}) = 2917, 2850, 1736, 1603, 1496, 1453, 1177, 1082, 914, 817, 697, 665.

ESI$^+$-MS: $[M+Na]^+$ = 327 m/z.

^{1}H NMR Titration of 7 with in D_2O

11 mg of **7** were dissolved in 800 µL of $CDCl_3$, representing 40 µmol of the template and forming a 50 mM solution. After each addition of D_2O, a ^{1}H NMR spectrum was recorded. The shifts of the proton signals of the methoxy group of the (1-methoxycyclohexyl)methyl part of the molecule were observed after each addition and compared to their shift in the ^{1}H NMR spectrum of the template before the titration.

	2 eq	12 eq
	80 µmol	480 µmol
D_2O	1.4 µL	8.4 µL

Synthesis of the polymerizable derivative for 16-O-methylcafestol

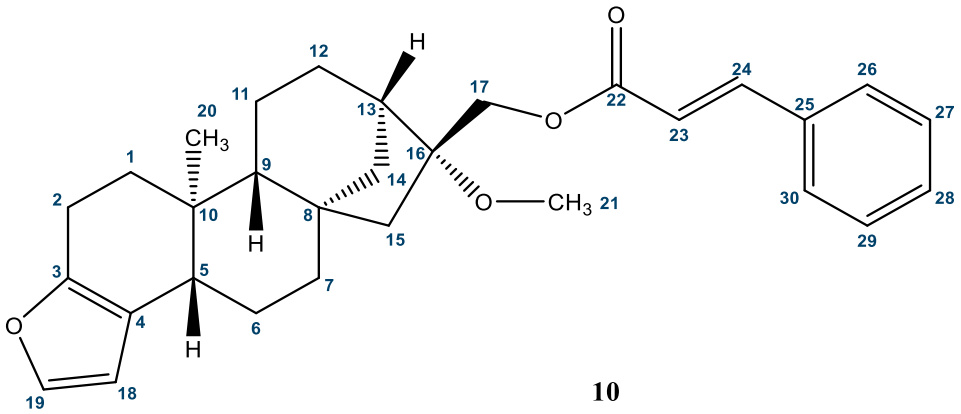

10

Trans-cinnamic acid (**10a**, 49.3 mg, 0.33 mmol) with DCC (75.5 mg, 0.36 mmol) and DMAP (4.5 mg, 0.04 mmol) were dissolved in 30 mL of dichloromethane, and the mixture was stirred on ice for 30 min. 16-OMC (100 mg, 0.30 mmol) was added and the reaction was left going for 48 h at room temperature. The solvent was removed under vacuum and the residue was re-dissolved in 50 mL of ethyl acetate. The organic phase and washed with 50 mL of 5% aqueous solution of $NaHCO_3$, 50 mL of water, 50 mL of 10% aqueous solution of citric acid, 50 mL of water and 50 mL of brine, respectively. The organic phase was dried over Na_2SO_4 and the solvent was removed under vacuum. The residue was purified via "flash" chromatography using isocratic elution with a mobile phase of ethyl acetate and petroleum ether in ratio 1:1, giving **10** as a transparent oil (46%).[179]

R_f (petroleum ether to ethyl acetate 5:1**)** = 0.62, stained with aqueous permanganate solution.

^{1}H NMR (400 MHz, $CDCl_3$, ppm) δ = 7.71 (d, 1H, J=16.02 Hz, H_{24}), 7.56-7.51 (m, 2H, H_{26}, H_{30}), 7.56-7.51 (m, 3H, H_{27}, H_{28}, H_{29}), 7.24 (d, 1H, J= 1.8 Hz, H_{19}), 6.51 (d, 1H, J=16.00, H_{23}), 6.20 (d, 1H, J=1.9 Hz, H_{18}), 4.61-4.31 (dd, 2H, J=12.53 Hz, H_{17}), 3.21 (s, 3H, H_{21}), 2.66-2.56 (m, 2H, H_2), 2.38-2.32 (m, 1H, J=12.6, 2.6 Hz, H_5), 2.27 (dd, 1H, J=12.6, 2.5 Hz, H_5), 2.05 (dt, 1H, J=8.9, 4.0 Hz, H_1), 2.00 (d, 1H, J=12.09 Hz, H_{14}), 1.83-1.78 (ddd, 1H, J=13.0, 6.3, 3.2, H_6), 1.71 (d, 1H, J=7.6 Hz, H_{11}), 1.67-1.48 (m, 9H, H_6, H_7, H_{11}, H_{12}, H_{14}, H_{15}), 1.33-1.24 (m, 1H, H_1), 1.22 (d, 1H, J=7.9 Hz, H_9), 0.84 (s, 3H, H_{20}).

^{13}C NMR (400 MHz, $CDCl_3$, ppm) δ = 167.17 (s, C_{22}), 148.72 (s, C_3), 145.06 (s, C_{24}), 140.54 (d, C_{19}), 134.36 (s, C_{25}), 130.31 (s, C_{28}), 128.86 (s, C_{27}, C_{29}), 128.12 (s, C_{26}, C_{30}), 120.09 (s, C_4), 117.95 (s, C_{23}), 108.28 (d, C_{18}), 84.79 (s, C_{16}), 62.80 (s, C_{17}), 52.15 (s, C_9), 49.75 (s, $C1_5$), 49.59 (s, C_{21}), 44.45 (s, C_8), 44.24 (s, C_5), 42.16 (s, C_{13}), 40.92 (s, C_7), 38.67 (s, C_{10}), 37.88 (t, C_{14}), 35.75 (s, C_1), 26.03 (s, C_{12}), 23.11 (s, C_6), 20.62 (s, C_2), 19.11 (s, C_{11}), 13.30 (s, C_{20}).

IR (cm^{-1}) = 2920, 2850, 1711, 1638, 1450, 1378, 1312, 1265, 1173, 1070, 868.

ESI^+-MS: $[M+Na]^+$ = 483 m/z.

6.5 MIPs for cafestol and 16-OMC

Several molecularly imprinted, non-imprinted and control polymers were synthesized in our attempts to develop optimal imprinted polymers for cafestol and 16-OMC. All the polymers were synthesized by radical polymerization in high dilution conditions. They were usually purified by dialysis against water, then freeze-dried and characterized by size, zeta potential and NMR measurements.

6.5.1 Re-crystallization of AIBN

Into a round-bottom flask with a stirring bar, 3 g of AIBN were placed, then 7.5 mL of anhydrous ethanol were added. The flask was attached to a condenser and the atmosphere was replaced with argon. The solution was stirred at 50-55°C for an hour. 1 mL of anhydrous ethanol was added, and heating continued for 5 more minutes. The solution was then rapidly filtered under vacuum. The filtrate was left to crystallize in an ice bath. The crystals were filtered off, dried and stored in the refrigerator.

6.5.2 Dialysis of polymers

All the polymers, whose polymerization product mixture was not analysed for incorporation of cafestol via HPLC-UV, were dialysed against water. The product mixtures were placed in pre-soaked dialysis tubes. Both ends of the tubes were well tied, and the dialysis lasted for 3 days with water being switched three times per day.

6.5.3 Freeze-drying of polymers

After dialysis, the contents of dialysis tubes were transferred into a round-bottom flask or a Falcon tube and frozen in liquid nitrogen. The flasks were attached to a freeze-drier and left to dry from 24 h to 48 h, depending on the volume of the solvent in the sample. Yields of polymerisations were always reported.

6.5.4 Dynamic light scattering (DLS)

Size of synthesized polymer particles was measured via dynamic light scattering. For the measurements 2 mg/mL solutions of polymers were prepared and left in an ultrasonic bath for 30 min. Upon filtration through 0.45 μm syringe filters into 1 mL disposable cuvettes, the samples were analysed in triplicates.

6.5.5 Zeta potential

0.25 mg/mL solutions of polymers in water were prepared and left in an ultrasonic bath for 30 min. The samples were then placed into folded capillary zeta cells and analysed in triplicates. If necessary, they were filtered through 0.45 μm syringe filters prior to analysis.

6.5.6 Molecularly imprinted polymers for cafestol

Imprinted and non-imprinted polymers were synthesized. In both cases, NIPAM was used as a monomer, MBA as a cross-linker, AIBN as the initiator and DMSO as the solvent. The only difference between the two types of the polymers was in the choice of the co-monomer. For the imprinted polymers the **3** was used, and for the non-imprinted polymers the **3b** acid was used.

The ratios monomer to crosslinker to co-monomer were 60:30:10 in imprinted polymer **Ca1** and non-imprinted polymer **Ca 1.1**, while 40:50:10 was used in the polymers of the series **Cb**. Those were prepared with either 1% of AIBN in the imprinted polymer **Cb1** and non-imprinted polymer **Cb 1.1**, 2% of AIBN in the imprinted polymer **Cb2** and non-imprinted polymer **Cb 2.1**, and 5% of AIBN in the imprinted polymer **Cb5** and non-imprinted polymer **Cb 5.1**. The amount of AIBN was calculated as percentage of moles of all double bonds in the reaction. The reaction times of polymerizations were 48 h.

	NIPAM (mg)	**MBA** (mg)	**Co-monomer** (mg)	**AIBN** (mg)	**DMSO** (mL)	**Time**	**Yield**
Ca 1.1	33.95	23.13	9.60 **Boronic A.**	1.07	6.00	48 h	57 %
Cb 1.1	22.63	38.54	9.60 **Boronic A.**	1.23	6.37	48 h	82 %
Cb 2.1	22.63	38.54	9.60 **Boronic A.**	2.46	6.37	48 h	40 %
Cb 5.1	22.63	38.54	9.60 **Boronic A.**	6.15	6.37	48 h	50 %

	NIPAM (mg)	MBA (mg)	Co-monomer (mg)	AIBN (mg)	DMSO (mL)	Time	Yield
Ca1	33.95	23.13	23.62 **Caf. Boronate**	1.07	7.26	48 h	13%
Cb1	22.63	38.54	23.62 **Caf. Boronate**	1.23	7.63	48 h	26%
Cb2	11.32	19.27	11.81 **Caf. Boronate**	1.23	9.82	48 h	22%
Cb5	11.32	19.72	11.81 **Caf. Boronate**	3.08	3.82	48 h	23%

Common polymerisation protocol

The co-monomer, NIPAM, MBA and AIBN were weighed into a clean and dry Wheaton flask. Anhydrous DMSO was added to form critical monomer concentration (c_M) of 1%. The flask was sealed with a rubber and a metal seal. While stirring the solution at room temperature, the solution was flushed with a stream of nitrogen for 10 minutes. The flask was checked for foreign and undissolved particles, then put into the oven at 70°C for 48 h. Upon termination of the reaction, the polymers were dialysed against water for 3 days and freeze-dried. They were characterized with size, zeta potential NMR measurements and HPLC-UV analysis.

Removal of cafestol from the MIPs

To 7 mg of the polymer **Cb1**, 20 mL of 1M aqueous solution of NaOH were added. The mixture was left stirring at room temperature for 1 h, then it was dialysed and freeze-dried. Removal of the template was monitored with ^{1}H NMR, observing the disappearance of peaks, significant for cafestol.

Incorporation of the boronic ester for cafestol in the MIPs

To define the degree of incorporation of cafestol in the MIPs, non-dialysed polymerisation product mixtures were used. The polymer was removed from the solutions with centrifugal filters. The incorporation of its polymerizable derivative was determined by HPLC quantification of cafestol, upon releasing it from the unreacted polymerizable derivative in the product mixute. Agilent's version of DIN 10779 method with an external standard of cafestol was used for quantification of cafestol, and the amount of the incorporated boronic ester was calculated from the results.

1. Preparation of external standards

1 mg/mL stock solutions of cafestol, **3b**, and **3** were prepared in DMSO and diluted to 50 µg/mL with the mobile phase.

2. Reliability of centrifugal filters

The stock solution of the external standard of the **3** was filtered through a centrifugal filter. 100 µL of the filtrate was then treated with 100 µL of 1M NaOH to release cafestol, then diluted to 1 mL with the mobile phase for HPLC analysis. From the deviation of the amount of the boronic ester from its expected concentration, the retention of the boronic ester on centrifugal filters was calculated.

3. Incorporation of the polymerizable derivative

100 µL of polymerization product mixtures of MIPs from the **Ca** and **Cb** series were filtered through centrifugal filters. The filtrates were then treated with 100 µL of 1M aqueous solution of NaOH to release cafestol. Upon dilution of the samples to 1 mL with the mobile phase, they were analysed via HPLC. By calculating the amount of **3b** it represents, the ratio between the amount of **3b** and the combined amounts of monomers during polymerization, % of incorporated boronic ester of the polymerizable derivative into the polymer was calculated.

4. Control of the incorporation studies

The polymers, remaining on the centrifugal filters after the previous experiment, were resuspended in 1M solution of NaOH. Upon filtration and HPLC analysis, the amount of **3** the quantified cafestol represents was compared with the results of the previous experiment. The sum of the results of the incorporation studies and control studies was expected to be the amount of **3** used during polymerisation per a polymer.

5. HPLC-UV analysis

Agilent's version of the DIN 10779 method for quantification of 16-O-methylcafestol in roasted coffee by HPLC-UV was used. The mobile phase in the study was a mixture of acetonitrile and water in ratio 60:40, the expected time of elution of cafestol was 15 min. The injection volume was 20 µL with the temperature of the column department at 25°C.

Re-binding studies

The studies were done for imprinted and non-imprinted polymers. For the experiment a 200 mM stock solution of cafestol in DMSO and a 200 μM stock solution of 16-OMC in DMSO were prepared. 1.5 mg samples of polymers were prepared in 2 parallels. To one parallel 1.5 mL of the stock solution of cafestol were added and to the other 1.5 mL of the stock solution of 16-OMC. While stirring, 250 μL of the solutions were sampled after 30 min, 60 min, 120 min, 240 min and 360 min. The aliquots were filtered through centrifugal filters. To the filtrates 250 μL of the HPLC mobile phase were added and the samples were analysed via HPLC-UV.

The HPLC analysis was performed using a Phenomenex Kinetex column with dimensions 250 x 4.6 mm and the size of particles 5 μm. The mobile phase consisted of acetonitrile and water in ratio 70:30, with 0.05% of trifluoroacetic acid. The flow was 0.75 mL/min and the temperature of the column compartment 25°C. The retention times of cafestol and 16-OMC were 5.8 min and 8.9 min, respectively.

Before the analysis, external standards were prepared for both stock solutions, by diluting 250 μL of each with 250 μL of the mobile phase. Based on the correlation between a known concentration of both diterpenes, their area under the curve and the area under the curve of the samples, concentrations of cafestol and 16-OMC were determined. Taking the dilution of the aliquots with the mobile phase in the account, the concentrations at each time-point were plotted to the time of sampling.

Competitive rebinding

The studies were done for imprinted and non-imprinted polymers. For the experiment a stock solution in DMSO, simultaneously containing 200 μM of cafestol and 200 μM of 16-OMC was prepared. To 1.5 mg samples of polymers 1.5 mL of the stock solution were added. While stirring, 250 μL of the solutions were sampled after 30 min, 60 min, 120 min, 240 min and 360 min. The aliquots were filtered through centrifugal filters. To the filtrates 250 μL of the HPLC mobile phase were added and the samples were analysed via HPLC-UV.

The HPLC analysis was performed using a Phenomenex Kinetex column with dimensions 250 x 4.6 mm and the size of particles 5 μm. The mobile phase consisted of acetonitrile and water in ratio 70:30, with 0.05% of trifluoroacetic acid. The flow was 0.75 mL/min and the temperature of the column compartment 25°C. The retention times of cafestol and 16-OMC were 5.8 min and 8.9 min, respectively.

Before the analysis, an external standard was prepared for the stock solution, by diluting 250 μL of it with 250 μL of the mobile phase. Based on the correlation between a known concentration of both diterpenes, their area under the curve and the area under the curve of the samples, concentrations of cafestol and 16-OMC were determined. Taking the dilution of the aliquots with the mobile phase in the account, the concentrations at each time-point were plotted to the time of sampling.

6.5.7 Synthesis of MIPs for 16-O-methylcafestol

Synthesis of MIPs for isoamyl cinnamate

Imprinted, non-imprinted and control polymers were synthesized. As a co-monomer for the imprinted polymers isoamyl cinnamate was used, for the non-imprinted ones trans-cinnamic acid, while in the synthesis of control polymers no co-polymer was present. As a monomer acrylamide or NIPAM were used, the cross-linker was always MBA, the initiator was AIBN, and the solvent was anhydrous DMSO. The ratios monomer to cross-linker to co-monomer are given for all polymers.

	Monomer (mg)	**MBA** (mg)	**Co-monomer** (µL)	**AIBN** (mg)	**DMSO** (mL)	**Time**	**Yield**
AA 50:30:20	35.54 **Acrylamide**	46.25	43.53 **i-amyl cinnamate**	2.13	11.29	24 h	59%
AA 30:50:20	21.32 **Acrylamide**	77.09	43.53 **i-amyl cinnamate**	2.46	12.79	24 h	31%
AA 60:30:10	42.65 **Acrylamide**	46.25	21.76 **i-amyl cinnamate**	2.13	9.97	24 h	51%
AA 40:50:10	28.43 **Acrylamide**	77.09	21.76 **i-amyl cinnamate**	2.46	11.46	24 h	55%
N24 50:30:20	28.29 **NIPAM**	23.13	21.76 **i-amyl cinnamate**	1.07	6.59	24 h	29 %
N24 30:50:20	16.97 **NIPAM**	38.54	21.76 **i-amyl cinnamate**	1.23	6.96	24 h	44 %
N24 60:30:10	33.95 **NIPAM**	23.13	10.88 **i-amyl cinnamate**	1.07	6.12	24 h	44 %
N24 40:50:10	22.63 **NIPAM**	38.54	10.88 **i-amyl cinnamate**	1.23	6.49	24 h	53 %
N48 50:30:20	28.29 **NIPAM**	23.13	21.76 **i-amyl cinnamate**	1.07	6.59	48 h	45 %
N48 30:50:20	16.97 **NIPAM**	38.54	21.76 **i-amyl cinnamate**	1.23	6.96	48 h	45 %
N48 60:30:10	33.95 **NIPAM**	23.13	10.88 **i-amyl cinnamate**	1.07	6.12	48 h	53 %
N48 40:50:10	22.63 **NIPAM**	38.54	10.88 **i-amyl cinnamate**	1.23	6.49	48 h	45 %

For the polymers on the basis of either acrylamide or NIPAM, the ratios of components were always 50:30:20, 30:50:20, 60:30:10 and 40:50:10. 1% of the initiator AIBN to the moles of all double bonds in the reaction was always used.

The monomer, co-monomer, MBA and AIBN were weighed into a clean and dry Wheaton flask, then anhydrous DMSO was added, forming a c_M of 1%. The flask was sealed with a rubber and a metal seal. The solution was flushed with a stream of nitrogen for 10 min while stirring at room temperature. The flask was checked for foreign and undissolved particles and put into the oven at 70 °C for 24 h or 48 h. Upon termination of the reaction, the polymers were dialysed against water and freeze-dried. They were characterized with size, zeta potential and NMR measurements.

Synthesis of control polymers

Polymers with acrylamide or NIPAM as monomers were synthesized in two parallels, with molar ratios of monomer to cross-linker of 50:50 in one parallel and 70:30 in the other. The monomer, MBA and AIBN were weighed into a clean and dry Wheaton flask, then anhydrous DMSO was added, forming a c_M of 1%. The flask was sealed with a rubber and a metal seal. While stirring at room temperature, the solution was flushed with a stream of nitrogen for 10 minutes. The flask was checked for foreign and undissolved particles and put into the oven at 70 °C for 48 h. Upon termination of the reaction, the polymers were dialysed against water for 3 days and freeze-dried. They were characterized with size and zeta potential measurements.

	Monomer (mg)	**MBA** (mg)	**AIBN** (mg)	**DMSO** (mL)	**Time**	**Yield**
Acrylamide 50:50	35.45 **Acrylamide**	77.09	2.46	10.14	24 h	69 %
Acrylamide 70:30	49.76 **Acrylamide**	46.25	2.13	8.64	24 h	53 %
NIPAM 50:50	28.29 **NIPAM**	38.54	1.23	6.01	24 h	83 %
NIPAM 70:30	28.29 **NIPAM**	38.54	1.23	6.01	24 h	84 %

Removal of the template from the MIPs

Removal of the template from the imprinted polymers for isoamyl cinnamate was attempted. Hydrolysis of the ester bond was performed by stirring 10 mg of each polymer with 20 mL of 0.1 M of aqueous NaOH solution for 24 h. The polymers were then dialysed against water for 3 days and freeze-dried. Removal of the template was monitored with ^{1}H NMR.

Isoamyl hydrocinnamate

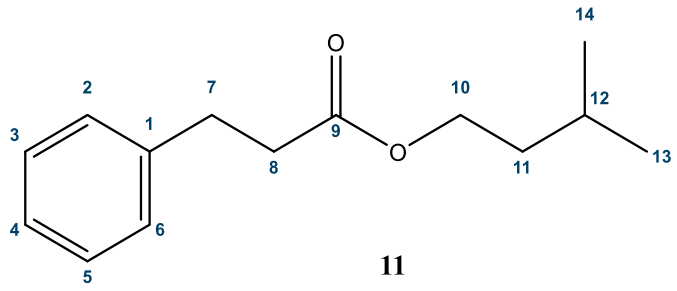

11

Pd/C (40 mg) was weighed into a flame-dried round-bottom flask. The flak was sealed, its atmosphere was switched to N_2, then anhydrous ethanol (10 mL) and isoamyl cinnamate (122 µL, 0.56 mmol) were added with a syringe. The solution was flushed with a stream of N_2 for 10 min. H_2 was gradually introduced and left to be absorbed into the solution for 6h. Upon completion, the atmosphere in the flask was brought back to N_2. The product mixture was filtered through a 1 cm layer of Celite, then the solvent was removed under vacuum, leaving behind **11** as a transparent oil (92%).[180]

R_f (petroleum ether to ethyl acetate 5:1**)** = 0.87

^{1}H NMR (400 MHz, $CDCl_3$, ppm) δ = 7.26-7.20 (m, 5H, H_2, H_3, H_4, H_5, H_6), 4.16 (t, 2H, J=6.85 Hz, H_{10}), 2.99 (t, 2H, J=7.82 Hz, H_7), 2.66 (t, 2H, J= 7.82 Hz, H_8), 1.68 (sp, 1H, J=6.71 Hz, 13,47 Hz, H_{12}), 1.53 (q, 2H, J=6.87 Hz, H_{11}), 0.95 (d, 6H, J=6.87 Hz, H_{13}, H_{14}).

^{13}C NMR (400 MHz, $CDCl_3$, ppm) δ = 173.06 (s, C_9), 140.51 (s, C_1), 128.43 (s, C_2, C_6), 128.3 (s, C_3, C_5), 126.19 (s, C_4), 63.13 (s, C_{10}), 37.27 (s, C_{11}), 35.93 (s, C_8), 30.91 (s, C_7), 25.20 (s, C_{12}), 22.50 (s, C_{13}, C_{14})

IR (cm^{-1}) = 2959, 2871, 1733, 1605, 1497, 1454, 1368, 1162, 699.

ESI$^+$-MS: $[M+Na]^+$ = 243 m/z.

Calibration curve for isoamyl hydrocinnamate

Three stock solutions of **11** in DMSO were prepared, with concentrations of 1 mg/mL, 2 mg/mL and 5 mg/mL. A calculated amount of each stock solution was further diluted with DMSO to 1 mL, to form samples with concentrations of 50 µg/mL, 100 µg/mL, 150 µg/mL, ..., 600 µg/mL. UV-VIS spectra of the samples were recorded from 200 nm to 400 nm at a constant temperature of 25°C with DMSO as a background sample. The absorbances at 264 nm were averaged for each concentration point and the readings were plotted to concentration. Via linear regression, a tendency line was determined, representing the calibration curve.

Incorporation of isoamyl cinnamate into MIPs

1 mg/mL solutions of all **AA** and **N** types of polymers, and Acrylamide and NIPAM types of control polymers in DMSO were left in the ultrasonic bath for 30 min. The samples were further diluted to 30 µg/mL with DMSO and their UV-Vis spectra were recorded from 200 nm to 400 nm at a constant temperature of 25°C with a background sample of DMSO. Intensities of absorbances at 264 nm were observed.

For the polymers with the same monomer and the same percentage of the cross-linker, the absorbance of the control polymer was deducted from the absorbance of the imprinted polymer. Thus, an absorbance value for the aromatic ring of the isoamyl cinnamate was obtained. From the calibration curve, this value was connected to the corresponding concentration of **11** in the calibration curve. Considering all the dilutions, the incorporation of isoamyl cinnamate in the polymers was calculated.

Re-binding studies

The studies were done for the imprinted polymers AA 30:50:20 and N48 50:30:20. For the experiment a 400 mM stock solution of isoamyl alcohol was prepared in deuterated DMSO. To 1.5 g of each polymer 1.5 mL of the stock solution were added. While stirring, 300 µL of the solutions were sampled after 60 min, 120 min, 240 min and 24h. The aliquots were filtered through centrifugal filters. To the filtrates 600 µL of deuterated DMSO and 6 µL of toluene as an external standard were added. The samples were well mixed and an ^{1}H NMR spectra for each time-point were recorded.

From the ratio of the integrations of the methyl group of toluene and the quartet next to the oxygen, belonging to isoamyl alcohol, the amount of non-rebound alcohol was calculated. By calculating the difference between the amount of isoamyl alcohol at each time-point and its amount at time zero, the amount of rebound isoamyl alcohol was calculated.

6.5.8 Synthesis of the MIPs for 16-O-methylcafestol

Imprinted and non-imprinted polymers were synthesized. For the imprinted polymers, **10** was used as a monomer and for the non-imprinted ones **10a**. The cross-linker was always MBA and the initiator 1% of AIBN, calculated to all double bonds in the reaction. The solvent was DMSO and the time of polymerizations 48 h. NIPs and MIPs with ratios monomer to cross-linker to co-monomer of 60:30:10 and 40:50:10 were synthesized. The ratio 60:30:10 was represented in the imprinted polymer **16a1** and in the non-imprinted polymer **16a 1.1**, while the ratio 40:50:10 was used in the imprinted polymer **16b1** and non-imprinted polymer **16b 1.1**. The c_M was always 1% in anhydrous DMSO and the times of polymerization 48h.

Common polymerisation protocol

The monomer, co-monomer, MBA and AIBN were weighed into a clean and dry Wheaton flask, then anhydrous DMSO was added. The flask was sealed with a rubber and a metal seal. While stirring at room temperature, the solution in the flask was flushed with a stream of nitrogen for 10 minutes. The flask was checked for foreign and undissolved particles and put into the oven at 70 °C for 48 h. Upon termination of the reaction, the product mixture was dialyzed and freeze-dried. Simultaneously, NIPs were synthesized, replacing **11** with **11a** as a monomer.

	NIPAM (mg)	**MBA** (mg)	**Co-polymer** (mg)	**AIBN** (mg)	**DMSO** (mL)	**Time**	**Yield**
16a 1.1	22.63	38.54	7.41 **Cinnamic acid**	1.23	7.43	48 h	41%
16b 1.1	22.63	38.54	7.41 **Cinnamic acid**	1.23	6.17	48 h	40%
16a1	33.95	23.13	21.33 **16-cinnamate**	1.07	7.06	48 h	57%
16b1	22.63	38.54	21.33 **16-cinnamate**	1.23	7.43	48 h	54%

Removal of the template

Removal of the template was attempted for both imprinted polymers, **16a1** and **16b1**. Hydrolysis of the ester bond was performed by stirring 10 mg of each polymer with 20 mL of 0.1 M aqueous NaOH solution for 24 h. The polymers were then dialysed against water for 3 days and freeze-dried. Removal of the template was monitored with ^{1}H NMR.

Calculation of incorporation

500 µL of the sample after hydrolysis following the previous point was fltered through a centrifugal filter at 5000 rpm for 5 min. The filtrate was analysed on HPLC using a Phenomenex Kinetex column with dimensions 250 x 4.6 mm and the size of particles 5 µm. The mobile phase consisted of acetonitrile and water in ratio 70:30, with 0.05% of trifluoroacetic acid. The flow was 0.75 mL/min and the temperature of the column compartment 25°C. The retention times of cafestol and 16-OMC were 5.8 min and 8.9 min, respectively.

The concentration of 16-OMC in the sample was calculated by using a external standard with the concentration 200 µM. The incorporation was presented as % of incorporated polymerizable derivative of 16-OMC.

Re-binding studies

The studies were done for imprinted and non-imprinted polymers. For the experiment a 200 μM stock solution of 16-OMC in DMSO and a 200 μM stock solution of cafestol in DMSO were prepared. 1.5 mg samples of polymers were prepared in 2 parallels. To one parallel 1.5 mL of the stock solution of 16-OMC were added and to the other 1.5 mL of the stock solution of cafestol. While stirring, 250 μL of the solutions were sampled after 30 min, 60 min, 120 min, 240 min and 360 min. The aliquots were filtered through centrifugal filters. To the filtrates 250 μL of the HPLC mobile phase were added and the samples were analysed via HPLC-UV.

The HPLC analysis was performed using a Phenomenex Kinetex column with dimensions 250 x 4.6 mm and the size of particles 5 μm. The mobile phase consisted of acetonitrile and water in ratio 70:30, with 0.05% of trifluoroacetic acid. The flow was 0.75 mL/min and the temperature of the column compartment 25°C. The retention times of cafestol and 16-OMC were 5.8 min and 8.9 min, respectively.

Before the analysis, external standards were prepared for both stock solutions, by diluting 250 μL of each with 250 μL of the mobile phase. Based on the correlation between a known concentration of both diterpenes, their area under the curve and the area under the curve of the samples, concentrations of 16-OMC and cafestol were determined. Taking the dilution of the aliquots with the mobile phase in the account, the concentrations at each time-point were plotted to the time of sampling.

Competitive rebinding

The studies were done for imprinted and non-imprinted polymers. For the experiment a stock solution in DMSO, simultaneously containing 200 μM of 16-OMC and 200 μM of cafestol was prepared. To 1.5 mg samples of polymers 1.5 mL of the stock solution were added. While stirring, 250 μL of the solutions were sampled after 30 min, 60 min, 120 min, 240 min and 360 min. The aliquots were filtered through centrifugal filters. To the filtrates 250 μL of the HPLC mobile phase were added and the samples were analysed via HPLC-UV.

The HPLC analysis was performed using a Phenomenex Kinetex column with dimensions 250 x 4.6 mm and the size of particles 5 μm. The mobile phase consisted of acetonitrile and water in ratio 70:30, with 0.05% of trifluoroacetic acid. The flow was 0.75 mL/min and the temperature of the column compartment 25°C. The retention times of cafestol and 16-OMC were 5.8 min and 8.9 min, respectively.

Before the analysis, an external standard was prepared for the stock solution, by diluting 250 μL of it with 250 μL of the mobile phase. Based on the correlation between a known concentration of both diterpenes, their area under the curve and the area under the curve of the samples, concentrations of 16-OMC and cafetol were determined. Taking the dilution of the aliquots with the mobile phase in the account, the concentrations at each time-point were plotted to the time of sampling.

6.6 Colorimetric assay for Arabica and Robusta

6.6.1 Preliminary tests on cafestol and 16-OMC

Solutions of cafestol and 16-O-methylcafestol were treated with a solution of antimony(III) chloride as it was reported in literature.[1]

Preparation of 30% solution of antimony(III) chloride

The 30% solution in chloroform was prepared in four parallels by dissolving 450 mg of antimony(III) chloride in 1500 µL of chloroform, forming reagents A, B, C and D (**Table 6.1**). Apart from reagent A, the original solution of antimony(III) chloride solely in chloroform, reagents B, C and D were solutions of antimony(III) chloride in chloroform with a drop of acetic acid, a drop of H_2SO_4 or a drop of HCl. The reagents were sonicated until all the antimony(III) chloride dissolved.

A: 30% antimony(III) chloride solution
B: 30% antimony(III) chloride solution with a drop of acetic acid
C: 30% antimony(III) chloride solution with a drop of H_2SO_4
D: 30% antimony(III) chloride solution with a drop of HCl

Table 6.1: Compositions of prepared antimony(III) chloride solutions.

Treatment of cafestol and 16-O-methylcafestol

2.5 mg of cafestol and 16-O-methylcafestol were weighed into their own Eppendorf vials, each diterpene in four parallels. To each parallel of the two diterpenes, 0.5 mL of the reagents A, B, C or D were added, the final concentration of cafestol and 16-O-methylcafestol in their respective Eppendorf vial in each solution was 5 mg/mL.

UV-VIS spectra were recorded for cafestol and 16-O-methylcafestol 10 min after the addition of the reagent B. The samples were diluted 1:10 with chloroform and the UV-Vis spectrum was recorded at a constant temperature of 25°C in baseline correction mode from 300 nm to 700 nm with a blank sample of chloroform.

6.6.2 Coffee extracts in various solvents

To prepare the coffee extracts, 1 g of ground roasted Arabica and Robusta coffee were weighted into separate flasks and for each species. 7 parallels for each species were prepared. To both one sample of Arabica and one sample of Robusta 5 mL of methanol, acetone, ethyl acetate, acetonitrile, diethyl ether, dichloromethane or chloroform were added. The vials were capped, wrapped in parafilm and left on a shaker for 1 h. The extracts were filtered through PTFE syringe filters with a pore size of 0.45 μm.

The composition of the antimony(III) chloride reagent was similar as the one of the reagent B in the previous paragraph, consisting of 300 mg of antimony(III) chloride, 1000 μL of chloroform and 20 μL of acetic acid. The mixture was sonicated until all antimony(III) chloride dissolved. 250 μL of a coffee extract were treated with 250 μL of the antimony(III) chloride solution and a photo was taken 5 min after the treatment.

UV-VIS measurements

UV-VIS spectra were recorded for the treated extracts in acetonitrile, dichloromethane and chloroform. The samples for measurements were 1:10 dilutions of the original samples in the corresponding solvent, diluted and measured 15 min after the treatment with the antimony(III) chloride solution. At a constant temperature of 25°C in baseline correction mode, the spectra for the extracts in chloroform were recorded from 300 nm to 700 nm, and the spectra for the extracts in acetonitrile and dichloromethane from 300 nm to 800 nm.

Diagnostic capability of the peak

Mixtures of the extracts of Arabica and Robusta in dichloromethane were prepared, in volumetric ratios 1:3, 1:1 and 3:1 of the Arabica extract to Robusta extract. The extracts of Arabica and Robusta alone were treated as well. To 250 μL of each extract mixture 250 μL of the antimony(III) chloride solution were added. The vials were capped and gently shaken. After 15 min their content was diluted 1:10 with dichloromethane. The spectra were recorded under the same conditions as before and still in the range of 300 nm to 800 nm. The peak at 726 nm was observed.

Analysis of other commercially available coffees

Extracts of several commercially available brands of coffee were tested: illycaffe's blend and Tesco Arabica as pure Arabica, Amigos as pure Robusta, and Lavazza Qualità Rossa, Co-op and Sainsbury's Italian Style Coffee as mixtures of Arabica and Robusta. The coffee extracts were prepared by stirring 1 g of ground roasted coffee sample with 5 mL of dichloromethane for 1 h. Coffee was filtered off with syringe filters and the solvent was removed with a stream of N_2, in an attempt to standardize the sample preparation and improve the redults. The residues were re-dissolved in dichloromethane to form 100 mg/mL stock extract solutions.

The antimony(III) chloride solution was prepared by dissolving 300 mg of antimony(III) chloride in 1000 µL of dichloromethane. To that, 20 µL of acetic acid were added and the solution was sonicated until all the antimony (III) chloride dissolved.

The samples for measurements were prepared by adding 25 µL of the antimony (III) chloride solution to 950 µL of dichloromethane, then adding 25 µL of the stock extract solution. 25 min after the addition, a UV-VIS spectrum was recorded at a constant temperature of 25°C from 300 nm to 900 nm in baseline correction mode, with a blank sample of dichloromethane. The spectra were then overlapped to better observe the behaviour of the peak at 726 nm and the absorbance readings were compared and assigned to the coffee sample.

6.6.3 Development of the extraction procedure

First attempts

Extracts of the coffee samples were usually prepared in glass vials with a ratio of 1 g of ground roasted coffee to 5 mL of dichloromethane. The vials were capped and wrapped in parafilm to prevent evaporation of the solvent, then placed on a shaker for 1 h. Coffee was then filtered off with the use of syringe filters and clear extracts were used immediately.

Standardization of the concentration of the extracts

A ratio of 1 g of ground roasted coffee to 5 mL of dichloromethane continued to be used. The glass vials were capped and wrapped in parafilm to prevent evaporation of the solvent, then placed on a shaker for 24 h. Coffee was then filtered off with the use of syringe filters, the solvent from the filtrate was evaporated at room temperature with a stream of N_2 and after weighting them, the residues were re-dissolved in dichloromethane to the concentration of 100 mg/mL.

Improved yield and filtration

To 1 g of coffee, 25 mL of dichloromethane were added. The round bottom flask was capped and wrapped in parafilm, then left on a magnetic stirrer for 24 h. Afterwards, the coffee was filtered off with a 1 to 2 cm layer of Celite® via vacuum filtration. The solvent was removed under vacuum; the residues were weighed into another glass vial and re-dissolved in dichloromethane to the concentration of 100 mg/mL.

6.6.4 Development of the antimony(III) chloride solution

In literature, solutions of antimony(III) chloride with or without colour developing catalysts have been found to give various colour reactions with diterpene, sterols and oils[1,2]. Descriptions of 30% solutions of antimony(III) chloride in dichloromethane with 1-3% of acids, alcohols or acetic anhydride are generally found.

Addition of acids, acetic anhydride

4 parallels of a 30% antimony(III) chloride solution in dichloromethane were prepared by adding 500 µL of dichloromethane to 150 mg of antimony(III) chloride. To each parallel, 10 µL of a different colour catalyst were added: acetic acid, acetic anhydride, 10% HCl or 5% H_2SO_4. The mixture was then sonicated until all antimony(III) chloride dissolved.

Residues from the extracts of Arabica and Robusta were re-dissolved to 100 mg/mL in dichloromethane. The samples for the measurements were prepared by adding 25 µL of the chosen antimony(III) solution to 950 µL of dichloromethane, then 25 µL of the re-dissolved stock extract solutions of Arabica and Robusta. The vials were gently shaken and left reacting for 30 min. At minute 30, UV-VIS spectra were recorded at a constant temperature of 25°C from 350 nm to 900 nm in baseline correction mode with a blank sample of dichloromethane. Differences in absorbance at 726 nm between the same way treated Arabica and Robusta were observed.

Addition of various degrees of acetic acid

2 parallels of the antimony(III) chloride solution were prepared, for both 150 mg of antimony(III) chloride were used. In the first case 410 µL of dichloromethane and 100 µL of acetic acid were added, and in the second case 510 µL of acetic acid was added. Both solutions were then sonicated until all antimony(III) chloride dissolved.

The coffee extracts of Arabica and Robusta were prepared by weighing 1 g of each coffee in separate vials and adding 5 mL of dichloromethane, then leaving both vials to stir overnight. After 24 h, the coffee was filtered off with the use of syringe filters and the solvent was evaporated with a stream of N_2 at room temperature.

The residues from the extracts of Arabica and Robusta were re-dissolved to form a stock extract solution in dichloromethane with a concentration of 100 mg/mL. The samples for the measurements were prepared by adding 25 µL of the chosen antimony(III) solution to 950 µL of dichloromethane, then 25 µL of the stock extract solution of Arabica and Robusta. The vials were gently shaken and left reacting for 30 min.

At minute 30, UV-VIS spectra were recorded at a constant temperature of 25°C from 350 nm to 900 nm in baseline correction mode with a blank sample of dichloromethane. Differences in absorbance at 726 nm between the same way treated Arabica and Robusta samples were observed.

Various ratios of the stock extract solution to antimony(III) chloride solution

The antimony(III) chloride reagent was prepared from 300 mg of antimony(III) chloride, 20 µL of acetic acid and 1000 µL of dichloromethane. The mixture was sonicated until all the antimony(III) chloride was dissolved and used fresh.

The coffee extracts of Arabica and Robusta were prepared by weighing 1 g of each coffee in separate vials and adding 5 mL of dichloro-methane, then leaving both vials to stir overnight. After 24 h the coffee was filtered off with syringe filters and the solvent was evaporated with a stream of N_2 at room temperature.

The residues were re-dissolved in dichloromethane to form a stock extract solution with a concentration of 100 mg/mL. 5 samples for UV-VIS measurements were prepared by adding first the antimony(III) chloride solution to dichloromethane, then the stock extract solution. The used combinations are presented in **Table 6.2**.

	DCM	Extract	$SbCl_3$
1	950 µL	15 µL	35 µL
2	950 µL	25 µL	25 µL
3	950 µL	35 µL	15 µL
4	950 µL	40 µL	10 µL
5	940 µL	30 µL	30 µL

Table 6.2: Volumes of Arabica and Robusta stock extract solutions to reach the final ratios.

The vials were gently shaken and left reacting for 30 min. At minute 30, UV-VIS spectra were recorded at a constant temperature of 25°C from 350 nm to 900 nm in baseline correction mode with a blank sample of dichloromethane. Differences in absorbance at 726 nm between the same way treated samples of Arabica and Robusta were observed.

6.6.5 Kinetic studies

To improve the stability of the antimony(III) chloride solution, addition of zinc dust was attempted.[50] Its efficiency was examined with kinetic UV-Vis studies. To explore a possible improvement, two preparations of the antimony(III) chloride were tested.

Preparation of antimony(III) chloride solutions

In two parallels, 300 mg of antimony(III) chloride were dissolved in 1000 µL of dichloromethane, then 20 µL of acetic acid were added. The first parallel was left as it was, forming the **solution I**, and to the second parallel, forming the **solution II**, 15 mg of zinc dust were added. Both solutions were sonicated until all antimony(III) chloride dissolved, then left standing for 5 min on dry ice until all zinc dust in the solution II settled.

Preparation of coffee extracts

The coffee extracts were prepared by weighing 5 g of Arabica and Robusta in separate vials and adding 25 mL of dichloromethane, then leaving both vials to stir overnight. After 24 h, the coffee was filtered off with the use of syringe filters and the solvent was evaporated with a stream of N_2 at room temperature. The residues were re-dissolved in dichloromethane to stock extract solutions with a concentration of 100 mg/mL.

Measurements

In the first round, changes of absorbance at 726 nm through time were monitored for samples of Arabica and samples of Robusta. The samples were prepared by adding first 50 µL of the antimony(III) chloride solution I to two cuvettes, filled with 900 µL of dichloromethane, then 50 µL of the solution II to two cuvettes, also filled with 900 µL of dichloromethane. To one cuvette containing the antimony(III) chloride solution II and one cuvette containing the antimony(III) chloride solution II, 50 µL of 100 mg/mL stock extract solution of Arabica were added. To the remaining two cuvettes with antimony(III) chloride solutions I and II 50 µL of the 100 mg/mL stock extract solution of Robusta were added.

In the second round, changes of absorbance at 819 nm through time were monitored. The samples were prepared by adding first 50 µL of the antimony(III) chloride solution II to two cuvettes, filled with 900 µL of dichloromethane. To one cuvette 50 µL of 100 mg/mL stock extract solution of Arabica were added, and to the other 50 µL of the 100 mg/mLmg/mL stock extract solution of Robusta. In both cases the experiment was initiated 2 min after the addition of the stock extract solution to its corresponding cuvette. The samples were recorded in Kinetics mode, with the temperature of the measurements constant at 25°C. Al the studies were left going for 4 h.

6.6.6 Linearity of responses for Arabica and Robusta

0%, 5%, 20%, 50%, 80% and 100% mixtures of ground roasted beans of Robusta in a mixture with Arabica were prepared, following the amounts of roasted ground coffee beans in **Table 6.3**.

% of Robusta	Robusta	Arabica
0	/	1 g
5	0.05 g	0.95 g
20	0.20 g	0.80 g
50	0.50 g	0.50 g
80	0.80 g	0.20 g
100	1 g	/

Table 6.3: Amounts of Arabica and Robusta used to reach the final m/m percentage of Robusta in the mixture of the ground roasted coffee beans.

1 g of each coffee mixture, 1 g of ground roasted beans of Arabica and 1 g of ground roasted beans of Robusta were stirred with 25 mL of dichloromethane in a capped and parafilmed glass vial for 24 h. After, the coffee was then filtered off through a 1 to 2 cm layer of Celite® on a vacuum filter and the solvent was removed under vacuum. The residues were dissolved in dichloromethane to form stock extract solutions with a concentration of 100 mg/mL.

The antimony(III) chloride solution was prepared by adding 1000 µL of dichloromethane to 300 mg of antimony(III) chloride and 15 mg of zinc dust. Finally, 20 µL of acetic acid were added. The mixture was sonicated until all the antimony(III) chloride dissolved and stored in a capped vial on dry ice for 5 min, until all zinc dust settled.

The samples for measurements were prepared by adding 50 µL of the antimony(III) chloride solution to 900 µL of dichloromethane. 50 µL of the chosen stock extract solution were added, the vial was gently shaken, and the samples were incubated at 25°C for 60 min. At minute 60, a UV-VIS spectrum was recorded at a constant temperature of 25°C in baseline correction mode from 650 nm to 900 nm with a blank sample of dichloromethane. Readings of absorbance at 726 nm and 819 nm were plotted to % of contamination of Arabica with Robusta and checked for linearity.

6.6.7 Experiments on different Arabicas and Robustas

For this experiment illy's Monoarabicas: Brazil, Ethiopia and Guatemala were used to represent Arabica, while Amigos, Marcafe Oro, and Lavazza Suerte were chosen to represent Robusta. All coffees are commercially available with a declared content of 100% Arabica for Arabicas and 100% Robusta for Robustas and were ground roasted coffees.

Their extracts were prepared by adding 25 mL of dichloromethane to 1 g of a coffee sample and stirring the mixture in a capped round-bottom flask for 24 h. The coffee was then filtered off with a 1 to 2 cm layer of Celite® and the solvent was evaporated under vacuum. The residues were dissolved in dichloromethane to form 100 mg/mL stock extract solutions and used immediately.

The antimony(III) chloride solution was prepared by adding 1000 µL of dichloromethane to 300 mg of antimony(III) chloride and 15 mg of zinc dust in a capped glass vial. To that, 20 µL of acetic acid were added. The mixture was sonicated until all the antimony(III) chloride dissolved and stored on dry ice until the zinc dust settled.

The samples for measurements were prepared by adding 50 µL of the antimony(III) chloride solution to 900 µL of dichloromethane. Next, 50 µL of a chosen stock extract solution was added and the samples were incubated at 25°C for 60 min. At minute 60, a UV-VIS spectrum was recorded at a constant temperature of 25°C in baseline correction mode from 350 nm to 900 nm, with a blank sample of dichloromethane. Readings of absorbance at 726 nm and 819 nm for Arabicas and Robustas were statistically evaluated.

6.6.8 Final protocol for determination of the degree of contamination of Arabica with Robusta

Following the experiments, a method protocol has been established:

Preparation of coffee extracts

1 g of ground roasted coffee beans
25 mL of dichloromethane

To ground roasted coffee beans, dichloromethane is added. The round bottom flask is capped, wrapped in parafilm and left stirring overnight. After 24 h the mixture is filtered through a 1 to 2 cm layer of Celite® on a vacuum filter. Clear filtrate is collected, and the solvent removed under vacuum. The residue is used immediately.

Preparation of stock extract solutions for UV-VIS measurements

10 mg of the oily dry coffee extract
100 µLof dichloromethane

To the oily residue, weighed into a glass vial, dichloromethane is added to form a 100 mg/mL stock extract solution. The solution is stored on dry ice in a capped vial to prevent excessive evaporation of dichloromethane from the sample.

Preparation of the antimony(III) chloride solution

150 mg of antimony(III) chloride
500 µLof dichloromethane
10 µL of acetic acid
7.5 mg of zinc dust

To antimony(III) chloride and zinc dust, first dichloromethane and then acetic acid are added. The container is capped, and the mixture is sonicated until all antimony(III) chloride dissolves, then stored capped on dry ice until the zinc dust settles.

Preparation of samples for UV-VIS measurements - per sample

900 µL of dichloromethane
50 µL of antimony(III) chloride reagent
50 µL of stock extract solution

To dichloromethane, the antimony(III) chloride solution is added, then the stock extract solution. The vial is capped, gently shaken and incubated at 25°C for 60 min. At minute 60, a UV-VIS spectrum is recorded at a constant temperature of 25°C from 650 nm to 900 nm in baseline correction mode with a blank sample of dichloromethane. The absorbance at 819 nm is read and correlated to the % of contamination of Arabica with Robusta via the calibration curve.

6.6.9 Fluorescence of coffee extracts

Due to a red to bright red shine noticed in the coffee extracts of mixtures of Arabica and Robusta after treatment with the antimony(III) chloride solution, the fluorescence was investigated further.

Fluorescence of treated coffee extracts

The coffee samples for the measurements were illy's blend representing Arabica, Amigos representing Robusta and Lavazza Qualità Rossa representing a 60 to 40 ratio of Arabica to Robusta mixture. The coffee extracts were prepared by adding 25 mL of dichloromethane to 1 g of ground roasted coffee. The round bottom flasks were capped, wrapped in parafilm and left stirring for 24 h. Next day the mixture was filtered through a 1 to 2 cm layer of Celite® on a vacuum filter. Clear filtrate was collected, and the solvent was removed under vacuum. 5 mg of the residue were weighed into a glass vial and re-dissolved to form a 100 mg/mL stock extract solution in dichloromethane.

The antimony(III) chloride solution was prepared by weighing 150 mg of antimony(III) chloride and 7.5 mg of zinc dust, then adding 500 µL of dichloromethane and 10 µL of acetic acid. The container was capped, and the mixture was sonicated until all antimony(III) chloride dissolved, then stored capped on dry ice until the zinc dust settled.

The samples for the fluorometric measurements were prepared by adding 50 µL of the antimony(III) chloride reagent to 900 µL of dichloromethane, and finally 50 µL of the chosen stock extract solution. The vial was capped, gently shaken and incubated at 25°C for 60 min, then left at room temperature overnight. The excitation wavelengths 355 nm, 400 nm and 410 nm were tested and were chosen based on the peaks in a pre-recorded UV-VIS spectra, then fine-tuned to 355 nm and 400 nm while recording the fluorescent spectra to get the best response.

Fluorescence of coffee extracts

The coffee samples for the measurements were illy's blend representing Arabica, Amigos representing Robusta, mixtures of Arabica and Robusta in ratios 9:1, 1:1 and 1:9 of ground roasted coffee beans, and Lavazza Qualità Rossa, commercially declared as a 60% to 40% mixture of Arabica to Robusta.

The coffee extracts were prepared by adding 25 mL of dichloromethane to 1 g of ground roasted coffee. The round bottom flasks were capped, wrapped in parafilm and left stirring for 24 h. Next day the mixture was filtered through a 1 to 2 cm layer of Celite® on a vacuum filter. Clear filtrate was collected, and the solvent was removed under vacuum. 5 mg of the residue were weighed into a glass vial and re-dissolved to form 3 mL of a 33 mg/mL solution in dichloromethane, corresponding to the concentration of the measured sample.

The excitation wavelengths of 355 nm and 400 nm and 410 nm were chosen based on the fluorometric spectra of the coffee samples, treated with the antimony(III) solution from the previous experiment, then fine-tuned to 410 nm while recording the fluorescent spectra to get the best response. From the readings of emissions at 671 nm, with the excitation wavelength of 410 nm, a calibration curve was formed.

6.6.10 Microscopy of coffee

After the initial success with the antimony(III) chloride method on coffee extracts in dichloromethane, we were curious to try to use the same reagent solution as a microscopical staining agent for coffee, hoping that it would allow us to differentiate Arabica from Robusta. Green coffee beans of Arabica Ethiopia, Robusta Vietnam and Robusta Brasil Conilon were used in the experiment, with the thickness of the cryo-sections of 12 μm.

Preparation of microscopical slides

The antimony(III) chloride solution II was used. It was prepared by adding 10 mL of dichloromethane to 3 g of antimony(III) chloride and 150 mg of zinc duct, then adding 200 μL of acetic acid. The container was capped, and the mixture was sonicated until all antimony(III) chloride dissolved, then left standing still until the zinc dust settled. Additionally, a 1:10 dilution of the reagent solution in dichloromethane was prepared. The antimony(III) chloride solutions were applied drop-wise to the slides, left reacting for 10 min, and observed by eye until analysing them under the microscope. Either directly after mounting, or after being washed with chloroform and mounted with resin DPX, the samples were then observed with light and fluorescent microscopy, using the filters H3, A and D.

Green coffee beans soaked in the antimony(III) chloride solution

Green coffee beans of Arabica and Robusta were soaked in the antimony(III) chloride solution overnight, cut into cryo-sections of 12 μm, mounted with the DPX resin and observed with fluorescent and light microscopy.

Hand-sliced green coffee beans

Additionally, the beans were hand-sliced with a razor and placed on the microscopic slide. They were then treated with 3 drops of the 1:10 diluted antimony(III) solution and left reacting for 5 min. Any changes were observed with light microscopy.

6.7 Acrylamide in Arabica and Robusta

For the preparation of coffee samples, to a medium degree roasted Robusta coffee was used, unless stated otherwise, due to the reports from literature, that in Robusta generally a higher degree of acrylamide is formed during roasting as in Arabica.[107]

6.7.1 Selection of chromatographic conditions

Selection of the mobile phase

Three mobile phases were tested with a 1 mg/mL sample of acrylamide:

MP1: 500 mL of water, 500 mL of acetonitrile, 500 µL of trifluoroacetic acid.
MP2: 800 mL of water, 200 mL of acetonitrile, 500 µL of trifluoroacetic acid.
MP3: 1000 mL of water, 500 µL of trifluoroacetic acid.

All the mobile phases were prepared by combining all the components in a 1 mL glass bottle, stirring them for 15 min on a magnetic stirrer and sonicating them for 15 min. they were tested using the column Phenomenex Gemini 150 x 2 mm, with the C18 filling, size of particles 4 µm, flow 0.2 mL/min, injection volume 50 µL, temperature of the column department 25°C and detection wavelength 210 nm.

Selection of the column

Two columns were tested with a 1 mg/mL sample of acrylamide:

Column 1: Phenomenex Gemini, 150 x 2 mm, C18, 4 µm size of particles.
Column 2: Agilent Poroshell 120, 150 x 4.6 mm, C18, 2.7 µm size of particles.

Both columns were tested with the mobile phase of water with 0.05% of trifluoroacetic acid, injection volume of 50 µL, temperature of the column department 25°C and detection wavelength 210 nm. The flow of the **Column 1** was 0.2 mL/min and the flow of the **Column 2** was 0.5 mL/min.

Selection of the flow

Chromatograms of a 0.5 mg/mL aqueous solution of acrylamide were recorded using **Column 2**, Agilent Poroshell 120. Three different flows were tested: 0.5 mL/min, 0.75 mL/min and 1 mL/min. The mobile phase used for the experiment was HPLC grade water with 0.5 % of trifluoroacetic acid, at an injection volume of 50 µL, temperature of the column department was 25°C and detection wavelength 210 nm.

Selection of the detection wavelength

Chromatograms of a 500 ng/mL aqueous solution of acrylamide were recorded using **Column 2**, Agilent Poroshell 120. Detection wavelengths 202 nm and 210 nm were tested by using the flow 0.5 mL/min and the mobile phase of HPLC grade water with 0.5 % of trifluoroacetic acid. The injection volume was 50 µL and temperature of the column department 25°C.

6.7.2 Sample preparation

Preparation of a sample according to the DemusLab GC-MS method

1 g of coffee was homogenized with 2 g of sorbent C18 for 2 min with a spatula. 8 mL of water were added, and the mixture was stirred for 30 min at room temperature. The sample was centrifuged at 4500 rpm for 15 min, then 5 mL of the supernatant were filtered through a preconditioned AccuCAT SPE column. The SPE column was conditioned with 3 mL of methanol and 3 mL of water, discarding the eluates. Upon filtration of the extract, all the filtrate was collected.

1 mL of the filtrate was analysed on HPLC, using the column Poroshell 120 (**Column 2**). Injection volume was 50 µL, temperature of the column department 25°C and the wavelength of detection 210 nm. The mobile phase consisted of HPLC grade water with 0.05 % of trifluoroacetic acid. The time of analysis of a sample of roasted coffee was 60 min.

Hindered extraction of polar compounds

Extraction in presence of NaCl

1 g of coffee was homogenized with 2 g of sorbent C18 for 2 min with a spatula. 8 mL of a 125 mg/mL NaCl solution were added and the mixture was stirred for 30 min at room temperature. The samples were centrifuged at 4500 rpm for 15 min. 5 mL of the supernatant were filtered through an AccuCAT SPE column.

1 mL of the eluate was analysed on HPLC, using the column Poroshell 120 (**Column 2**). Injection volume was 50 µL, temperature of the column department 25°C and the wavelength of detection 210 nm. The mobile phase consisted of HPLC grade water with 0.05 % of trifluoroacetic acid. The time of analysis of a sample of roasted coffee was 45 min.

Extraction in an acidic or basic medium

1 g of coffee was homogenized with 2 g of sorbent C18 for 2 min with a spatula in two parallels. To one parallel 8 mL of 1% acetic acid solution was added, and to the other 8 mL of 1% ammonia solution. The mixture was stirred for 30 min at room temperature. The samples were centrifuged at 4500 rpm for 15 min. 5 mL of the supernatants were filtered through an AccuCAT SPE column. The SPE column was conditioned with 3 mL of methanol and 3 mL of water, discarding the eluates. Upon filtration of the extract, all the filtrate was collected.

1 mL of the filtrate was analysed on HPLC, using the column Poroshell 120 (**Column 2**). Injection volume was 50 µL, temperature of the column department 25°C and the wavelength of detection 210 nm. The mobile phase consisted of HPLC grade water with 0.05 % of trifluoroacetic acid. The time of analysis of a sample of roasted coffee was 45 min.

Removal of interferences with salting out extractions

Salting out extractions were attempted from aqueous extracts of coffee and from extracts of coffee in polar organic solvents.

Water extracts

To 1 g of coffee in 4 parallels 8 mL of water were added. The mixtures were stirred for 30 min at room temperature, then the extracts were filtered onto 1 g of NaCl. To each mixture 5 mL of a polar organic solvent were added: methanol, acetonitrile, acetone or isopropanol. The samples were vigorously shaken to dissolve as much of NaCl as possible, then centrifuged for 15 min at 5000 rpm. In each sample each phase was sampled in two parallels. One was analysed as it was, while the other one was spiked with a 500 µg/mL aqueous solution of acrylamide.

Extracts in polar organic solvents

To 1 g of coffee in 4 parallels 8 mL of methanol, acetonitrile, acetone or isopropanol were added. The mixtures were stirred for 30 min at room temperature, then the extracts were filtered onto 1 g of NaCl. To each mixture 5 mL of water were added. The samples were vigorously shaken to dissolve as much of NaCl as possible, then centrifuged for 15 min at 5000 rpm. In each sample each phase was sampled in two parallels. One was analysed as it was, while the other one was spiked with a 500 µg/mL aqueous solution of acrylamide.

HPLC-UV analysis

The samples were analysed on HPLC, using the column Poroshell 120 (**Column 2**). Injection volume was 50 µL, temperature of the column department 25°C and the wavelength of detection 210 nm. The mobile phase consisted of HPLC grade water with 0.05 % of trifluoroacetic acid. The time of analysis of a sample of roasted coffee was 45 min.

Different treatments of acrylamide

To five samples of 10 mL of 500 µg/mL aqueous solution of acrylamide, one of the following was added:

1. 20 mg of active carbon
2. 100 mg of active carbon
3. 200 mg of MgO
4. 1000 mg of MgO
5. 100 mg of active carbon and 1000 mg of MgO

The samples were stirred for 30 min, then centrifuged. 1 mL of each sample was filtered through a 0.45 µm syringe filter into their own HPLC vial and analysed via HPLC-UV, using the column Poroshell 120 (**Column 2**). The injection volume was 50 µL, temperature of the column department 25°C and the wavelength of detection 210 nm. The mobile phase consisted of HPLC grade water with 0.05 % of trifluoroacetic acid. The time of analysis of a sample of roasted coffee was 15 min.

Testing of SPE columns

Discovery DSC MCAX, Isolute SAX/PSA and Biotage Isolute C18 SPE columns were tested. All were preconditioned with 3 mL of methanol and 3 mL of water, then dried completely, discarding the eluate. 1 mL of a 500 µg/mL aqueous solution of acrylamide was applied to each column and the eluate of all columns was collected in their own HPLC vials while drying the columns completely, creating the **Eluate** series of samples.

1 mL of water was applied to each column and the eluate of all was collected in their own HPLC vials while drying the columns completely again, creating the **1st wash** series of samples. 1 mL of water was then applied to each column once more and the eluate of all columns was collected in their own HPLC vials while drying the columns completely again, creating the **2nd wash** series of samples.

The samples, together with a 500 µg/mL standard sample, were analysed by using the column Poroshell 120 (**Column 2**). Injection volume was 50 µL, temperature of the column department 25°C and the wavelength of detection 210 nm. The mobile phase consisted of HPLC grade water with 0.05 % of trifluoroacetic acid. The time of analysis of a sample of roasted coffee was 15 min.

Calibration curve

The calibration curve was established in the interval of acrylamide concentrations from 0.2 ng/mL to 200 ng/mL, to include the expected concentrations in the coffee samples. First, a mother solution of acrylamide in water was formed, with a concentration of 10 µg/mL. From that dilutions of 2 ng/mL, 10 ng/mL, 40 ng/mL, 80 ng/mL, 100 ng/mL, 150 ng/mL and 200 ng/mL were prepared, filtered through 0.45 µm syringe filters and analysed on HPLC using the column Poroshell 120 (**Column 2**).

Injection volume was 50 µL, temperature of the column department 25°C and the wavelength of detection 210 nm. The mobile phase consisted of HPLC grade water with 0.05 % of trifluoroacetic acid. The time of analysis of a sample was 15 min. The areas under the curve were plotted to concentration and a calibration curve, most fitting to the data points, was determined automatically in Microsoft Excel via least squares method.

6.7.3 Improvements of the Demus Lab method

Samples of 1 g of coffee were prepared in two parallels. To the first parallel no adsorbent was added, while to the second one 1000 mg of magnesium oxide and 100 mg of active charcoal were added. The components in the second parallel were homogenized with a spatula first, then 10 mL of water was added to both parallels.

After 30 min of stirring, both mixtures were centrifuged for 15 min at 4500 rpm, then the supernatants were carefully collected. All supernatants were purified on an SPE system, composed of a Discovery DSC MCAX SPE column, connected to a Biotage Isolute C18 SPE column underneath. Both columns were preconditioned with 3 mL of methanol and 3 mL of water, discarding the eluate.

500 µL of the supernatants were applied to the upper, Discovery DSC MCAX, columns on top, and let running through both columns. Both columns were dried, and the eluate was discarded. 500 µL of water was applied to the upper column and let through both columns until they were dry again, collecting the eluate in their own HPLC vial.

The Discovery DSC MCAX columns were removed and the Isolute C18 columns were washed with 1 mL of water. The eluates were added to the previous ones in HPLC vials and the samples were analysed using the column Poroshell 120 column (**Column 2**). Injection volume was 50 µL, temperature of the column department 25°C and the wavelength of detection 202 nm. The mobile phase consisted of HPLC grade water with 0.05% of trifluoroacetic acid and the time of analysis per sample was 30 min.

Removal of lipids with hexane

5 g of coffee was stirred with 50 mL of hexane for 1 h. The coffee was then filtered off and washed with 10 mL of hexane. The filtrate was discarded, and the coffee was let to dry completely.

Samples of 1 g of coffee were prepared in two parallels. To the first parallel no adsorbent was added, while to the second one 1000 mg of magnesium oxide and 100 mg of active charcoal were added. The components in the second parallel were homogenized with a spatula first, then 10 mL of water was added to both parallels. After 30 min of stirring, both mixtures were centrifuged for 15 min at 4500 rpm, then the supernatants were carefully collected. All supernatants were purified on an SPE system, composed of a Discovery DSC MCAX SPE column, connected to a Biotage Isolute C18 SPE column underneath. Both columns were preconditioned with 3 mL of methanol and 3 mL of water, discarding the eluate.

500 µL of the supernatants were applied to the upper, Discovery DSC MCAX, columns on top, and let running through both columns. Both columns were dried, and the eluate was discarded. 500 µL of water was applied to the upper column and let through both columns until they were dry again, collecting the eluate in their own HPLC vial.

The Discovery DSC MCAX columns were removed and the Isolute C18 columns were washed with 1 mL of water. The eluates were added to the previous ones in HPLC vials and the samples were analysed using the column Poroshell 120 column (**Column 2**). Injection volume was 50 µL, temperature of the column department 25°C and the wavelength of detection 202 nm. The mobile phase consisted of HPLC grade water with 0.05% of trifluoroacetic acid and the time of analysis per sample was 30 min.

Shorter time of extraction

Extraction times 30 s and 5 min were used. For the extraction time of 30 s, 1 g of coffee was weighed in 2 parallels. One was left as it is, while to the other one 200 mg of MgO and 20 mg of active charcoal were added. The sample with the extraction time of 5 min consisted of 1 g of coffee. To all samples 10 mL of water were added, the samples were stirred for 30 s or 5 min, and then centrifuged at 4500 rpm for 15 min, then the supernatants were decanted.

Biotage Isolute C18 SPE columns were preconditioned with 3 mL of methanol and 3 mL of water, then dried completely with the eluate discarded. 500 µL of the supernatants were applied, and the eluates were discarded. Upon applying 200 µL of water, the eluates were discarded once again. Finally, 1 mL of water was applied to the columns and the eluates were collected into HPLC vials.

The samples were analysed using the column Agilent Poroshell 120 (**Column 2**). The injection volume was 50 µL, temperature of the column department 25°C and the wavelength of detection 202 nm. The mobile phase consisted of HPLC grade water with 0.05% of trifluoroacetic acid and the time of analysis per sample was 30 min.

Combination of sorbents and acetone

Green Robusta beans from Uganda were used as green, lightly roasted (colour 62.7, light+), medium roasted (colour 50.0, medium+) and dark roasted (colour 31.1, dark+) coffee beans. Roasting and determination of the colour of the beans were done in Demus Lab. Upon roasting, the coffee beans were cooled, ground and sifted.

To 1 g of coffee of each roasting degre, 200 mg of magnesium oxide were added. The mixtures were homogenized with a spatula for 2 min, then 2 mL of HPLC grade water were added. The samples were homogenised on a magnetic stirrer for another 2 min. Finally, 8 mL of acetone were added, and the samples were left stirring for 30 min. The samples were then centrifuged at 5000 rpm for 15 min. 5 mL of the supernatants were transferred to small beakers

decanted, and acetone was evaporated with a stream of compressed air until 1 mL of water remained in the flasks.

Bond Elut AccuCAT columns were conditioned with 3 mL of acetone and 3 mL of water and dried completely while discarding the eluate. 200 µL aliquots of the samples after evaporation of acetone were applied to the columns, discarding the eluate. The columns were then washed with 1 mL of water, collecting the eluates in HPLC vials, while drying the SPE columns completely once again.

The samples were analysed via HPLC-UV, using the column Poroshell 120 (**Column 2**). Injection volume was 50 µL, temperature of the column department 25°C and the wavelength of detection 210 nm. The mobile phase consisted of HPLC grade water with 0.05% of trifluoroacetic acid and the time of analysis per sample was 45 min.

6.7.4 Final method

Agilent Bond Elut QuEChERS Acrylamide Kit[176] was used for preparation of samples for measurement of acrylamide through extraction and dispersive SPE cleanup.

Extraction

1 g of coffee was placed into a 50-mL centrifuge tube from the Bond Elut QuEChERS Extraction kit. Samples were mixed with 9 mL of water. After shaking vigorously for 1 min, 10 mL of CH_3CN were added, followed by an addition of Agilent Bond Elut QuEChERS extraction salt mixture for acrylamide. 5 mL of hexane were then added to the extraction mixture. The sample tubes were hand-shaken vigorously for 1 min and then centrifuged at 4000 rpm for 5 min, forming three layers. The upper hexane layer was discarded prior to the SPE cleanup.

Dispersive SPE cleanup

A 6-mL aliquot of the remaining top CH_3CN layer was transferred into a Bond Elut QuEChERS EN Dispersive SPE 15 mL tube. The tube was then further centrifuged at 4000 rpm for 5 min. A 1000-µL amount of extract was placed in an autosampler vial for an HPLC-UV analysis.

HPLC-UV analysis

Agilent ZORBAX HILIC Plus column, with dimensions 4.6 × 50 mm and the size of particles of 3.5 µm was used in the isocratic elution. As a mobile phase a mixture of 3% of 5 mM acetic acid and 97% of acetonitrile was used. The column temperature was set at 30 °C and the flow rate at 0.2 mL/min. A sample with a known amount of acrylamide was used for the experiment (529 ng/g).

Bibliography

13. Naegele, E. Determination of Methylcafestol in Roasted Coffee Products According to DIN 10779. *Agil. Technol.* (2016).

148. Roy, C. D. & Brown, H. C. Stability of boronic esters - Structural effects on the relative rates of transesterification of 2-(phenyl)-1,3,2-dioxaborolane. *J. Organomet. Chem.* **692,** 784–790 (2007).

149. Bermand, C. Trimethylsulfonium and trimethylsulfoxonium as versatile epoxidation reagents. A comparative study. *Arkivoc* **2000,** 128–132 (2000).

177. WANG Xiao-li, Z. S. Synthesis of Ethylene Glycol Ether by Montmorillonite Solid Acid Catalysis. *J. Liaoning Univ. Pet. Chem. Technol.*

178. Singjunla, Y., Baudoux, J. & Rouden, J. Direct synthesis of β-hydroxy-α-amino acids via diastereoselective decarboxylative aldol reaction. *Org. Lett.* **15,** 5770–5773 (2013).

179. Sova, M. *et al.* Flavonoids and cinnamic acid esters as inhibitors of fungal 17β-hydroxysteroid dehydrogenase: A synthesis, QSAR and modelling study. *Bioorganic Med. Chem.* **14,** 7404–7418 (2006).

180. Zürcher, M. & Diederich, F. Structure-based drug design: Exploring the proper filling of apolar pockets at enzyme active sites. *J. Org. Chem.* **73,** 4345–4361 (2008).

7. Conclusions

Through the past years, we have attempted to develop several analytical methods, which could improve the monitoring of quality control of coffee in two aspects: by monitoring fraudulence with finding simpler ways of distinguishing between *C. Arabica* and *C. Canephora*, and monitoring the amount of acrylamide, a potential carcinogen, in coffee. As such, our contributions are:

1. Synthesis of molecularly imprinted polymers for selective recognition of 16-OMC and potential application into a sensing device in the future.
2. Development of a colorimetric assay for quantification of Robusta in a mixture with Arabica.
3. Development of an HPLC-UV method for quantification of acrylamide in roasted coffee.

Under the point **1.**, new data on the topic of modelling, synthesis and characterisation of MIPs for cafestol and 16-OMC was collected. Upon isolation of the diterpenes from *C. canephora*, functional monomers for both compounds were determined. 4-(trans-2-carboxyvinyl)phenylboronic acid was found suitable for cafestol and trans-cinnamic acid for 16-OMC. Polymerisable derivatives for both diterpenes were synthesized, and then used in preparation of covalently imprinted polymers. The polymers were characterised and tested with rebinding studies upon removal of their templates.

When a single diterpene was rebound to the polymers, it was concluded that in equilibrium the polymers for both diterpenes rebind cafestol in a greater degree than 16-OMC. Following competitive rebinding, however, it was found that in equilibrium 16-OMC is more prone to rebinding to all polymers than cafestol. This could be explained with the differences in the kinetic of the rebinding between the diterpenes.

As 16-OMC is essentially methylated cafestol, it forms hydrogen bonds and π-methyl interactions with the binding sites of all MIPs. Cafestol, on the other hand, forms boronic esters and hydrogen bonds upon rebinding in the imprinted polymers for cafestol and hydrogen bonds in the binding sites of MIPs for 16-OMC. The formation of boronic esters is kinetically slower than formation of hydrogen bonds. This is why the amount of rebound cafestol is high, when the rebinding experiment is done in a solution of solely cafestol, and lower when it is done in a solution containing both diterpenes. This information is crucial in potential further applications of the imprinted polymers to sensing instruments.

Additionally, colorimetric reactions of a 30% solution of antimony(III) chloride in chlorinated solvents, towards diterpenes, sterols, terpenoids and several types of oils proved to be interesting for our purpose of differentiation of roasted Arabica from Robusta beans (**2.**). It was found, that its addition to dichloromethane or chloroform extracts of Arabica and Robusta results in formation differently coloured samples of Arabica and Robusta. Upon examining UV-VIS spectra of the two samples, peaks at 726 nm and 819 nm were found, characteristic for Robusta and Arabica, respectively.

Both were diagnostic for different degrees of contamination of Arabica with Robusta, yet 819 nm was chosen as a working wavelength due to exhibiting a linear “absorbance to percentage of contamination of Arabica with Robusta” response. Optimising the extraction procedure, improving the composition of the antimony(III) chloride reagent and following the results of kinetic studies, a colorimetric method for quantification of the degree of

contamination of Arabica with Robusta was established and initially statistically evaluated, yet complete validation still needs to be performed. Due to novelty of the approach, the method is in a state of a patent pending.

Our last contribution to the improvement of quality control of coffee was focused on the development of an HPLC-UV method for quantification of acrylamide in coffee, suitable for the use in an industrial analytical laboratory (**3.**). Upon selection of a column with a proper stationary phase, adjusting the mobile phase, finding the optimal wavelength for detection of acrylamide and vastly improving the preparation of coffee samples, we were able to develop a reliable method for quantification of acrylamide. Compared to the previously established GC-MS method on the Demus Lab S.r.L., we were able to shorten the time of analysis per sample and avoid a health hazardous bromination step of sample preparation.

The output of the method still needs to be optimised to improve the separation of acrylamide from one interfering peak. When this will be resolved, the method will be validated, certified and incorporated in the routine itinerary of the laboratory.

Acknowledgements

Special thanks to:

Prof. Federico Berti and prof. Cristina Forzato (DSCF), for giving me the opportunity to work on this project, their patience, valuable insights and support through the past three years.

Dr. Luciano Navarini, Dr. Elena Guercia, Dr. Paola Crissafuli and the rest of the group (illycaffé, AromaLab), for a great introduction into the world of coffee, thousands of extractions of cafestol and 16-OMC and several days of microscopy.

Prof. Marina Resmini (School of Biological and Chemical Sciences at Queen Mary University of London), for allowing me to join her research group for 6 months and giving me a very intensive course on molecular imprinting.

Dr. Max Fabian and Dr. Elena Fragiacomo (Demus Lab S.r.l.), for allowing me to work in DemuLab and helping me in the quest to find acrylamide in coffee.

Dr. Paola Posocco (DIA, UNITS), for working with me on DLS and zeta potential measurements of the polymers and several indications on how to not get lost in the Department of Engineering.

The IPCOS dudes for sharing this incredible journey with me.

The QMUL dudes for sharing this incredible journey with me.

The DSCF dudes for sharing this incredible journey with me.

And, last but not least, to family, friends and a decent amount of stubbornness, for their unconditional love and support in times when the laws of nature went mad, science stopped working and I ran out of pizza or coffee.